2015

The efficacy of lignosulfonate in controlling the swell potential of expansive soil and its stabilization mechanisms

Dennis Pere Alazigha
University of Wollongong

Recommended Citation

UNIVERSITY OF WOLLONGONG

Department of Engineering and Information Sciences,

School of Civil, Mining and Environmental Engineering

The Efficacy of Lignosulfonate in Controlling the Swell Potential of Expansive Soil and its Stabilization Mechanisms

Dennis Pere Alazigha

(B.Eng, M.Eng, M.Sc)

This thesis is presented as part of the requirement for the

award of the Degree of Doctor of Philosophy

of the

University of Wollongong

August 2015

For what shall it profit a man, if he shall gain the whole world, and lose his own soul? For whatever a man soweth, that shall he also reap!

Mark 8: 36 (KJV), Galatians 6:7.

Lovingly dedicated to my earthly true rare treasures: my wife; Vera E. Alazigha and my ever vibrant son; Master Bryan Binapere Alazigha, and of course to my HEAVENLY FATHER; GOD ALMIGHTY.

CERTIFICATION

I, Dennis Pere Alazigha, declare that this thesis, submitted in fulfilment of the requirements for the award of Doctor of Philosophy, in the School of Civil, Mining, and Environmental Engineering, University of Wollongong, is wholly my own work unless otherwise referenced or acknowledged. The document has not been submitted for qualifications at any other academic institution.

Dennis Pere Alazigha

July 2015

ABSTRACT

Many techniques have been developed and applied to prevent and/or remediate infrastructural damage caused by expansive soils throughout the world. Of these techniques, traditional chemical (lime and cement) stabilization has gained world attention because of a good understanding of the underlying mechanisms, availability of technical guidelines, and years of demonstrated field experiences. However, despite the global acceptance of traditional additives for treating expansive soil, other environmentally benign alternatives have been an important subject of research due to the inherent health and safety concerns for traditional admixtures. One such alternative is from the paper industry that manufactures pulp from wood and in the process produces over 50 million tons annually of a waste substance known as lignosulfonate (LS). This substance has been disposed of as a waste product resulting in colossal disposal cost; however, it does have a potential application in geotechnical engineering under the concept of sustainable development.

This investigation into LS admixture consists of experimental and theoretical studies. The experimental investigation involved a laboratory evaluation of the efficacy of LS admixture in controlling the swell potential of a remoulded expansive soil. The swell potential was examined in terms of percent swell and swell pressure of the soil. In addition to these engineering properties, the Atterberg limits, unconfined compressive strength, durability (wet/dry and freeze/thaw), compaction characteristics, permeability, consolidation characteristics, and shrinkage behaviours were also investigated. Furthermore, the mechanism by which the remoulded soil was modified or altered by the LS admixture was probed and identified.

The optimum content of LS admixture was found to be about 2% by dry weight of the soil. Standard geotechnical laboratory tests performed on untreated and treated compacted soil specimens showed significant and consistent changes in the swell potential and other engineering properties such that the percent swell decreased by 22% while maintaining the soil's pH. In some instances, identical specimens treated with 2% cement were prepared and tested for comparison. Although the specimens treated with cement recorded a 33% reduction in the percent swell, the ductile

characteristics were replaced by brittleness and a significant increase in pH. Further analysis of the laboratory test data also suggested that LS admixture is a resourceful alternative for "low" swelling soils. This finding led to the formation of a "LS application chart" that will help geotechnical practitioners on admixture choice for a particular expansive soil deposits.

The physical-chemical analyses of untreated and 2% LS treated specimens were studied microstructurally after 7 days of curing. When LS was added into expansive soil, the stabilization mechanisms consisted of an insignificant exchange of interlayer cations due to the "cover-up-effect", basal/peripheral adsorption on mineral surfaces through hydrogen bonding (water bridging), direct bonding to dehydrated cations with the subsequent formation of flocculation-aggregates, initial expansion of diffuse double layer and water entrapment, and a waterproofing effect. An elemental analysis of untreated and treated specimens suggested inter-molecular interactions between soil minerals and the LS admixture as opposed to major chemical reactions. Thus, LS summarily altered the crystallographic characteristics of the soil minerals, and helped to reduce shrink-swell behaviour of the otherwise expansive soil.

The theoretical aspect of this research work involved the development of a robust mathematical model to predict the swell behaviour of expansive soil treated with LS. Relationships were proposed to estimate the suction behaviour of treated soil using laboratory data obtained experimentally. Suction behaviour was governed by a single constant (β), which depends on an input variable; the degree of saturation (S_d). A reasonable correlation was found between the percent swell determined experimentally and the predicted values.

A non-traditional admixture such as LS has the potential to become a technically and economically competitive alternative in the stabilization of expansive soils. With over 50 million tons being produced annually, the successful use of LS admixture as a new stabilization material for expansive soil appears to be one of many viable solutions to the sustainable use of a waste by-product, green construction, and as well as saving the disposal problems inherent in the paper manufacturing industry.

ACKNOWLEDGEMENTS

to acquire this immense knowledge from a reputable university like the University of Wollongong, New South Wales, Australia.

To my parents; Chief and Mrs Christo Alazigha, thanks a lot for your calls, prayers and your genes. My appreciation will be incomplete without recognizing my loving wife; Vera E. Alazigha. I appreciate your wisdom and perfect understanding throughout the past 3.6years, and to crown it all, thanks to Master Bryan Binapere Alazigha, your disturbances made me a better man. At just two years old, you were able to recognize and count the alphabets from A − Z. At age 3, you were able to spell over 40 words such as vase, medication, book, x-ray, watch, uncle, queen, radio, jacket, daddy, leaf, apple, oven, zebra, window, yellow, koala, green, igloo, ice, red, fish, kite, star, moon, door, pan, zero, dell, pig, dog, hat, net, pink, cup, jam, car, bus, tree, pan, girl, Bibi, egg, no, and yoyo. In addition, you were able to recognize and count the numbers from 1 − 100. Nothing else could make a dad happier. Thank you, Master Bibi, for your intelligence. To my uncles; Prince Wej Alazigha, Dr Tarilah Tebepah, and my brothers Hon. Bolou Alazigha and Dr Princewill Igbagara you are indeed precious.

Above all, thank you Heavenly Father for all that you have done in my life, for in Jesus name, Amen.

LIST OF PUBLICATIONS

The following publications are related with this PhD thesis.

Journal papers

1. Alazigha D.P., Indraratna B., and Vinod J.S. (2015) "The Swelling Behaviour of Lignosulfonate Treated Expansive Soil", Institute of Civil Engineers - *Journal of Ground Improvement* (Accepted for publication).

2. Alazigha, D.P., Indraratna, B., and Vinod, J.S. (2015). A mathematical model for predicting the swell behaviour of Lignosulfonate treated expansive soil, *Journal of Geomechanics, ASCE,* (under review).

3. Alazigha, D.P., Indraratna, B., Vinod, J.S., and Heitor, A. (2015). Mechanisms of stabilization of expansive soil with Lignosulfonate admixture, *Journal of Geotechnical and Geoenvironmental Engineering – ASCE,* (under review).

4. Alazigha, D.P., Indraratna, B., and Vinod, J.S. (2015). The potential use of Lignosulfonate; a waste by-product, for expansive soil stabilization (in preparation).

5. Consolidation and durability characteristics of Lignosulfonate treated expansive soil (in preparation).

LIST OF SYMBOLS

Letters

A	Cross-sectional area of specimen
$\mathring{A}$	Angstrom (10^{-10}m)
Al:Si	Aluminium and silica ratio
a_s	Cross-section area of standpipe
A_V	Avogadro's number = 6.02 x 10^{23}/mol
A_{MB}	Area covered by one molecule of MB
B	Base exchange capacity of clay
C	Clay content
CH	High plasticity clay
^{o}C	Degree Celsius
C_{mi}	Matrix suction index for layer i
C_{ti}	Effective stress index for layer i
cm	Centimetre
CuKα	X-ray radiation source
c/s	Counts per second
C	Moisture characteristics
C_m	A constant of proportionality
cm^{-1}	Inverse of centimetre
C_s	Swell index (slope of e – log P curve)
C_v	Coefficient of consolidation
d	*In*ter-planar spacing distance (as function of θ)
D_2O	Deuterated water
$d_{1/2}$	Half the distance between parallel platelets
D_{av}	Average diameter
e_o	Initial void ration
e	Void ratio
é	Elementary electrical charge
Δe	Change in void ratio
E_w	Shrink modulus
F	Load at failure
g	Gravitational force
G_s	Specific gravity of soil solids
g/mol	Gram/mole
h	Thickness of specimen
h	Thickness of layer under consideration
h_1	Initial head difference at $t = 0$,
h_2	Final head difference at $t = t_F$
h_f	Final height in the standpipe
Δh_i	Heave in a layer
h_i	Layer thickness
H	Height

H_s	Values of soil suction change
Hi	Initial height
$\overline{H}$	Average specimen thickness at each load increment
ΔH	Change in specimen height,
H_o	Height of original soil specimen
Hz	Hertz
Ib/ft^2	Pound square foot
I_{ps}	Shrinkage index of soil
I_p	Instability factor
I_{pt}	Instability index, in %/picofarads
kg	Kilogram
km^2	kilometre square
K$_m$*, K$_m$** and m	Regression functions
k_θ	Coefficient of permeability at test temperature
kN/m^3	Kilo Newton per metre cube
kN	Kilo Newton
kW	Kilowat
k	Boltzmann constant
kPa	KiloPascal
keV	Kilo-electron-volt
kJ/m^3	Kilojoule per metre cube
k$_s$	Coefficient of permeability for saturated soil
kV	Kilo volt
k$_{rw}$	Relative permeability
k$_w$	Coefficient of Permeability
L	Length of mould
L	Length of the specimen
Ls	Longitudinal shrinkage of the specimen
mA	Mili-ampere
^{0}/min	Scan speed
mm	Millimetre
meq	Milliequivalents
Δmc	Moisture change
M_{MB}	Mass of the adsorbed MB at end point
M_S	Mass of soil specimen
M$_v$	Coefficient of volumetric compressibility
m^2/g	metre square per gram
n	*N*umber of diffraction
N	Number of soil layers under consideration
nm	Nano-metre
p	Osmotic pressure or swelling pressure
Δp	Increase in pressure above the overburden pressure
P$_f$	Final stress state (i.e. swelling pressure of soil)
pF	Unit of suction (pF = 1.01 + kPa)
P$_0$	Initial stress state (P$_f$ = δy + Δδy - μ$_{wf}$)

r	*U*nsaturated permeability of LS treated expansive soil
S	Percent swell
S	Specific surface area of soil
SL	Linear shrinkage
S_r	Residual degree of saturation
S_e	Effective degree of saturation
S	Degree of saturation
s_o	Initial soil suction
t	Time interval
t_{90}	Time for 90 percent primary consolidation
T	Absolute temperature
u_a	Pore air pressure
u_w	Pore water pressure
μm	Micrometre
v	Ionic valence
V_s	The volumetric shrinkage
ΔV	Change in specimen volume
V_f	Final height of soil specimen after oven drying
w	Compaction water content
w	Water content
w_i	Initial water content
x	Distance from clay surface
y	Nondimensional potential at distance x from clay
y_s	Characteristic surface movement in millimetres
y_w	Unit weight of water
z	Depth from ground surface
z	Nondimensional potential at distance x from the clay
z_i	Thickness of layer i
%	Percentage

Greek alphabets

α	Lateral restraint factor
α	Fitting parameter
β	Diffusion coefficient of soil
$ɣ_d$	Dry density
Γ	Surface charge density
Δδy	Total stress due to excavation or placement of fill
$\Delta\varphi$	Change in soil suction within soil layer
$\overline{\Delta u}$	Average soil suction of soil thickness
δ	Chemical shift
δ	bending vibrations of water
ε	Dielectric constant of pore fluid,
ε_{sw}	Percent swell
θ	critical angle of incidence on the crystal plane

Φ	Diameter
λ	wavelength of the x-rays
λ	Pore size distribution index
μ	Nondimensional midplane potential
μ_{wf}	Predicted or estimated final pore-water pressure
$2\nu_\omega$	H-O-H molecules involved in strong hydrogen bonds
$\left(u_a - u_b\right)_b$	Air entry value
$u_a - u_w$	Soil suction
ν_{OH}	stretching vibrations of water
$\nu_{OH} + \delta_{AlFeOH}$	stretching and bending combinations
ξ	Distance function
ρ	Total density
ρ_d	Dry density of soil
ρ_B	Bulk density of soil
ρ_w	Density of water
$\sigma\text{-}u_a$	Applied pressure
σ_v	Vertical stress
σ	Total stress
φ_m	Matric suction component
φ_o	Osmotic suction component
φ_t	Total suction component

Abbreviations

A	No surface movement
AASHO	American Society of State Highway Officials
AMG	Australian Map Grid
ASTM	American Society for Testing and Materials
AS	Australian Standard
BET	Brunauer, Emmett and Teller
C-A-H	Calcium aluminate hydrate
C-A-S-H	Calcium aluminosilicate hydrate
C-S-H	Calcium silicate hydrate
CaLS	Calcium Lignosulfonate
CO_2	Carbon dioxide
CEC	Cation exchange capacity
CT SCAN	Computed tomography
DDL	Diffuse double layer
DTA	Differential thermal analysis
EDS	Energy dispersive spectroscopy
E	Extremely reactive
FHA	Federal Housing Authority
FOV	Field of view
FTIR	Fourier transform infrared spectroscopy
G	Gibbsite

GPC	Gel permeation chromatography
GPS	Global positioning system
hrs	hours
H1	Highly reactive
H2	very highly reactive
^{1}H-NMR	Protons nuclear magnetic resonance spectroscopy
HPLC	High-performance liquid chromatography
I	Illite
IC	Ion chromatography
JECFA	Joint FAO/WHO Expert Committee on Food Additives
K	Kaolinite
KLS	Potassium Lignosulfonate
LS	Lignosulfonate
LL	Liquid limit
M	Moderately reactive
M	Montmorillonite
MB	Methylene blue
MBI	Methylene blue index
MDUW	Maximum dry unit weight
MGA	Map Grid of Australia
mL	Millilitre
MIR	Mid infrared
Min	Minute
MPa	Mega Pascal
MS	Mass spectroscopy
Mt	Mountain
Na	Sodium Lignosulfonate
NIR	Near infrared
NMR	Nuclear magnetic resonance spectroscopy
OMC	Optimum moisture content
OPC	Ordinary Portland cement
P	Made-Ground
pH	$Log_{10}(H^+$ concentration)
PI	Plasticity index
PL	Plastic limit
ppm	Parts per million
PVC	Potential volume change
Q	Quartz
S	Slightly reactive
SA-44/LS-40 or DRP	Liquid comprising sulfuric acid and LS admixture
SEM	Scanning electron microscope
SSA	Specific surface area
TMS	tetramethylsilan
UCS (q_u)	Unconfined compressive strength
USBR	United State Bureau of Reclamation
UVs	Ultraviolet spectroscopy
XRD	X-ray diffractometer

TABLE OF CONTENTS

LIST OF FIGURES

LIST OF TABLES

CHAPTER ONE

1 INTRODUCTION

1.1 GENERAL BACKGROUND OF THE STUDY

The stability and integrity of any superstructure depends on the performance of the foundation materials (e.g. soil or rock). These materials are known to have several inabilities in terms of geotechnical requirements such as the potential to change volume in response to variations in moisture. When expansive soil minerals are exposed to moisture, the suction changes as water molecules are adsorbed between interlayer lattices, resulting in the development of the energy of hydration known as the swell pressure. This pressure prompts the soil to heave and cause damage to associated infrastructure that ranges from minor cracking to irreparable destruction.

The presence of these soil deposits have been reported in every part of the globe (Chen 1988; Gourley et al. 1993; McManus et al. 2004; Fityus et al. 2009; Jones and Jefferson 2012). In Australia, many populated areas such as the western suburbs of Sydney, Brisbane, the western and northern suburbs of Melbourne, the foothills of Perth, Adelaide and many regional areas are underlain by expansive soils (Richards et al.1983; Kapitzke and Reeves 2000). Each year in Australia, expansive soils cause billions of dollars of damage to buildings, roads, pipelines, and other structures (Richards 1990; McManus et al. 2004). Expansive soils are not an isolated curiosity because in the US for example, it is estimated that more than twice as much is spent on damage due to swelling soils as is spent on damages due to flood, tornadoes, earthquakes, tsunami, landslides, and hurricanes put together (Jones and Holtz 1973; Nelson and Miller 1992). Although not life threatening or calamitous when juxtaposed with other natural events, expansive soils are certainly a natural hazard. In fact, Snethan (1986) called expansive soils the "hidden disaster," because damage caused by these soils are not as dramatic as hurricanes or earthquake and since they only cause damage to property, not loss of life.

Engineers have developed several techniques to minimize the effects of expansive soils on infrastructure. The literature on stabilization techniques of such soils reveals that the use of traditional chemical additives (lime and cement) has had global acceptance for decades, and while they can be very effective, though not without inherent health and safety concerns, hence, the clamour for environmentally benign admixtures is growing exponentially. The use of waste materials in civil engineering continues to gain attention under the concept of sustainable development. A lot of industrial co-products such as fly ash, coal wash, and granulated blast furnace slag have been used as a stabilizing agent for soil. Of interest in this study, is the use of a waste by-product from the paper manufacturing industry commonly known as Lignosulfonate (LS) to stabilize expansive soil. With an annual production of LS estimated at 50 million tons (Gandini and Belgacem 2008) coupled with the huge cost of disposing of this enormous quantity of material by the manufacturing industries, it is envisaged that the successful use of this waste product as soil admixture will be a viable solution.

1.2 DESCRIPTION/MAGNITUDE OF THE PROBLEM

Expansive (reactive or swelling or black earth or vertosol) soils are clayey soils that experience a significant change in volume in response to changes in their moisture content; essentially these soils shrink upon drying and swell upon wetting. Their mineralogical composition (intrinsic property) enables them to adsorb and absorb moisture to cause changes in their volume. During the last eight decades there has been an increasing interest in research towards the behaviour of expansive soil. According to the American Society of Civil Engineers, one of the most common and least recognised problems causing severe structural damage to houses and lightly-loaded wood framed structures stems from expansive soils. Light weight infrastructures are more susceptible to swelling/shrinkage because their shallow foundations are located within the active zone; so the degree of damage could arrange from a simple hair-like crack, to severe cracks, and total collapse (Mitchell 1980). Deposits of expansive soil are the most common types in Southern Australia,

Queensland, Victoria, and New South Wales, and cause most of the failure problems in light infrastructures (Fityus et al. 2004).

During the dry season, moisture moves from the perimeter to the centre of a building causing the soil to shrink at the perimeter and swell at the centre (dome heave). The symptoms of dome heaving include vertical cracks that are narrow at the bottom and widen up the height of the wall (Fig 1.1a). During the wet season, moisture moves from the centre to the perimeter of a structure resulting in edge heaving (dish heaving) that is synonymous with soil sagging, which places the foundation and lower walls in tension. The indicator of centre dishing includes vertical crack that are wider at the bottom and narrower up the height of the wall (Mitchell 1980) (Fig 1.1b).

Vertosols (as they are commonly called in Australia) are the most common types of soil in Australia with a large belt running from the New South Wales border to Charters Towers—corresponding with Brigalow forests (McKenzie and Anderson 1998). Several authors have reported damage from expansive soil ranging from minor cracking to the irreparable destruction of buildings in Australia's largest cities (Cameron et al. 1987). Many towns, cities, transport routes, and buildings in Australia are founded on expansive clays. Appraisals in Victoria have suggested that about 30,000 new homes are expected to be affected annually, increasing the building costs by AU$ 60–90 million (McManus et al. 2004). Considine (1984) reported that more than 50,000 houses cracked each year due to deposits of expansive soil, and accounted for approximately 80% of all housing insurance claims.
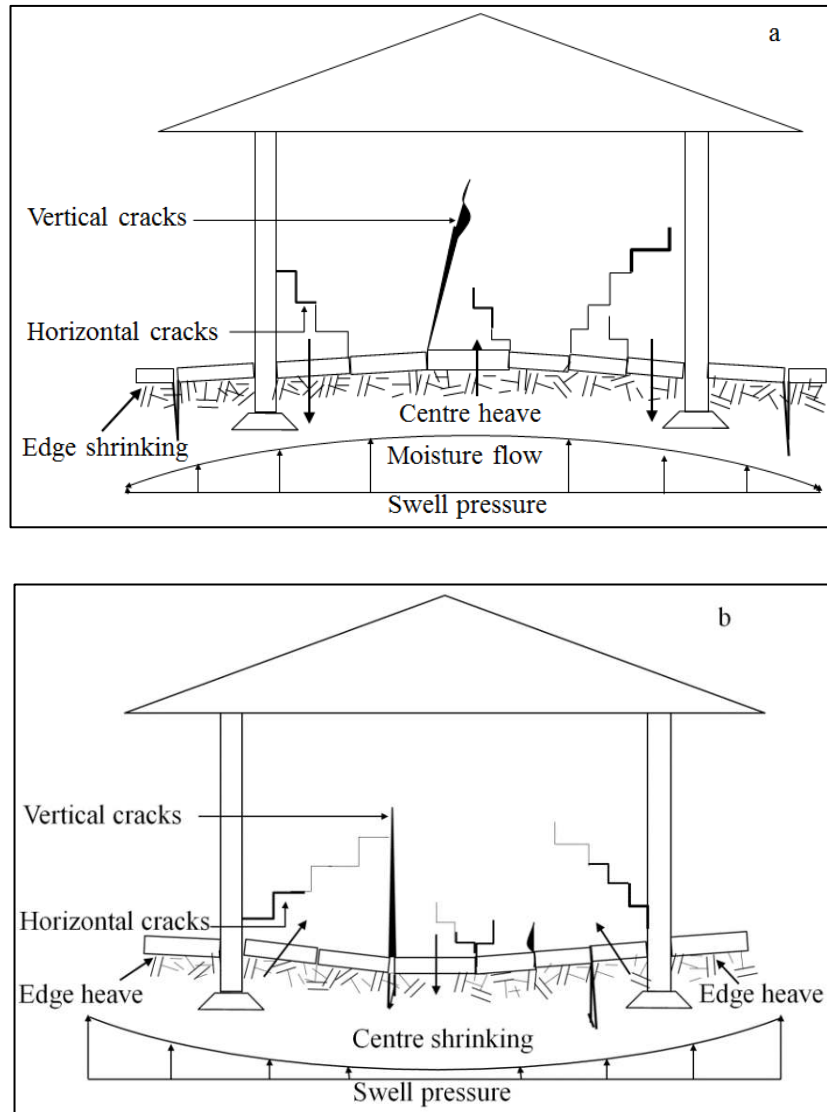
Figure 1.1: a) Crack patterns and centre heave (dome) during a dry season, b) Crack patterns and edge heave (dishing) during a wet season (modified after Mitchell 1980).

In Queensland, Australia, there is evidence of damaged culverts that appear to rise above their original level and deform at the soil-culvert interfaces. Fig 1.2a is typical of structures founded on expansive soil formations in Australia. Reeves (2001) reported the magnitude of pavement failure on roads managed by the Queensland Department of Main Roads at about $10 million per year. Fig 1.2b is a common example of longitudinal cracking due to expansive material on the Bruce Highway north of Brisbane. This phenomenon is indeed not peculiar to Australia, it is a global problem. Estimates in the United States of America show that one in five Americans

are affected by damage due to expansive soil while only one in ten are affected by major floods. Fig 1.3 shows a longitudinal crack on an abandoned home in the US. The estimated average annual loss due to shrink-swell phenomena is about $7 billion (Krohn and Slosson 1980; Jones 1981). Expansive soils are certainly a costly natural hazard in the USA, accounting for as much as twice the cost of repairs from all other natural disasters combined (Jones and Holtz 1973).

Figure 1.2 a): Cracked culvert wing wall of the drainage structure over Jingi Jingi Creek due to shrink-swell of the foundation soil on the Warrego Highway west of Brisbane, b): Longitudinal cracking due to expansive embankment material on the Cooroy exit off ramp, on the Bruce Highway north of Brisbane (© Queensland Department of Main Roads)

Figure 1.3: Cracked floor of a building founded on expansive soil (© of Arredondo Group)

The use of "Standard" or "traditional" or "calcium based" admixtures (lime and cement) are the most common techniques used by geotechnical engineers to treat expansive soil globally, but these traditional admixtures present certain concerns. For example, the pH of the soil increases as the content of admixture increases and this high alkaline environment could be detrimental to flora and fauna (Rollings et al. 1999). Moreover the high pH could also affect the longevity of reinforced concrete and steel frame structures (Perry 1977), they show poor performance in sulfate rich soils (Puppala et al. 2004), while the manufacturing processes contribute significantly to "greenhouse" gas emissions. Within this framework, it is pertinent to scout for an environmentally friendly alternative to traditional admixtures.

In recent times the literature has been inundated with non-traditional chemical admixtures and claims and counter-claims of for their soil stabilization potential. While the performance records of these admixtures coupled with lack of reports on their stabilizing mechanisms are mixed, an understanding of the different properties and behaviour of stabilised soil, including the stabilizing mechanisms, is of vital importance for a non-traditional admixture to be accepted globally. This research therefore seeks to assess the effectiveness of spent sulfite liquor (LS), by performing

standard geotechnical laboratory tests on samples of soil. In some case the effectiveness of the non-traditional admixture was compared with traditionally (cement) treated samples whose stabilization reactions are understood and documented.

In spite of the potential advantages offered by various non-traditional soil additives, geotechnical engineers are still reluctant to specify their use because:

1   Kota et al. (1996) argued that the principal concern is the lack of published, independent studies of non-calcium-based admixtures.

2   The secrecy surrounding the chemical composition of these admixtures further hinders an independent evaluation of the supplier's claims (Rauch et al. 2003).

3   The lack of comprehensive understanding and documentation of the stabilising mechanisms makes it difficult to assess their limitations and appropriate applications (Rauch et al. 2003).

This research work attempts to answer all the above concerns.

1.3   OBJECTIVES OF THE STUDY

The stabilization of expansive soil has traditionally been accomplished using lime, cement, and fly ash (Chen 1988), but due to the inherent problems, alternative materials should be investigated, and LS is a potential candidate. In this research the potential use of LS to stabilize remoulded expansive soil has been studied in detail. The specific objectives of this research are as follows:

1   To investigate the efficacy of a non-traditional waste admixture (LS) in controlling the swell potential of a remoulded expansive soil in the laboratory and compare data obtained from samples treated with cement (in some cases).

2   To study how other engineering properties (e.g. Atterberg limits, soil gradation, unconfined compressive strength, durability, compaction, consolidation, and permeability) of remoulded soil are affected by the LS admixture.

3   To investigate and identify the mechanisms by which remoulded expansive soil is modified or altered by the LS admixture using analytical techniques such as x-ray diffraction (XRD), scanning electron microscope (SEM), SEM coupled with energy dispersive spectroscopy (SEM/EDX), fourier transform infrared spectroscopy (FTIR), nuclear magnetic resonance (NMR), and x-ray computed tomography (CT Scan), specific surface area (SSA), and as well as cation exchange capacity (CEC) tests.

4   To develop a robust mathematical model and consecutively to study and evaluate the performance of such a model. Hence, predict the swell behaviour of LS treated expansive soil

The pulp and paper manufacturing industry generates a considerable amount of spent sulphite liquor (LS) annually and are experiencing major disposal problems. It is usually disposed as landfill but that is becoming more expensive due to tighter regulations, and moreover, the runoff can potentially pollute the groundwater. Another common technique is to burn the liquid with wood but that generates "greenhouse" gases. Thus, a successful use of LS could set the stage for green construction and save substantial amounts of money for the pulping industries.

1.4   RESEARCH WORK-PLAN

This project was planned and executed in 5 steps as described below.

1.4.1   Step 1: Selection of most suitable type of LS admixture

Three commercial types of LS liquids [sodium-LS (NaLS), potassium-LS (KLS), and calcium-LS (CaLS)] were available at the University of Wollongong, Geotechnical Research Laboratory for examination. The efficacy of these admixtures in terms of

reductions in the percent swell in a remoulded expansive soil was investigated via a one dimensional laboratory swell test. Moreover, the appropriateness of the LS admixtures was tested by measuring its effect on the Atterberg limits of the soil in accordance with Grim (1968). The LS that exhibited the most significant effect on the percent swell and the Atterberg limits of the remoulded expansive soil was then used throughout this research project.

1.4.2 Step 2: Characterization of selected LS admixture

The chemical properties of the selected LS admixture were characterized to identify their major constituents and to formulate the chemical structure of an otherwise proprietary chemical. This characterisation was accomplished using instrumental analytical techniques such as fourier transform infrared (FTIR), nuclear magnetic resonance (NMR), and scanning electron microscope coupled with energy dispersive spectroscopy (SEM/EDS).

1.4.3 Step 3: Soil characterization

The baseline properties of the remoulded expansive soil were characterized prior to any reaction with the LS admixture. Tests were conducted to measure their physical and chemical properties. This macro-characterization study included measuring the grain size distribution, compaction characteristics, freeze/thaw and wet/dry durability, Atterberg limits, permeability, shrinkage, consolidation, unconfined comprehensive strength, and swell potential tests using Australian or American Standards (AS 1289; ASTM). These micro-characterization analyses were achieved using XRD, FTIR, SEM/EDS, SSA, and CEC techniques.

1.4.4 Step 4: Identify mechanisms of reaction between the soil minerals and the functional groups of LS admixture

The mechanism identification techniques involved a detailed physico-chemical study of the untreated and LS treated specimens using the above analytical techniques (steps 2 and 4). Identifying the existence and significance of trends in untreated and LS treated samples at microscopic level provided an insight into the possible mechanisms of stabilization. The physical properties (as in step 3) of untreated and

LS treated samples were also evaluated to study how much of the mechanisms identified translated to changes in the physical properties of the soil.

1.4.5 *Step 5: Evaluation of laboratory findings to assist in the development of a robust swell predictive model for LS treated expansive soil*

The impact of LS admixture on the swelling properties of the remoulded soil was evaluated for any significance, and these findings helped to develop the mathematical relations that aided the modelling of the suction behaviour of LS treated soil specimen using fundamental concepts of unsaturated soil mechanics. With the knowledge of variations in suction with time under laboratory conditions, the percent swell of the soil was determined using a pre-developed empirical relationship based on experimental data.

1.5 THESIS ORGANIZATION

Chapter 1 is an introductory chapter providing preliminary information about expansive soils and its distribution in Australia. This chapter also describes the use of traditional admixtures and the need for resourceful alternatives. The magnitude of the research problem along with the objectives and structure of the thesis are also presented. **Chapter 2** discusses the existing literature to justify the need for the research objectives. The review consisted of the mineralogy and general properties of expansive soils, distribution, classification, identification, and the problems associated with this type of soil. The stabilization of such soils using traditional admixtures (e.g. lime and cement), including their environmental and safety concerns, are also discussed and presented to rationalize the need for a more environmentally sustainable admixtures. The physical and chemical characterization methods for the materials used in this research project are discussed in chapter 3. Moreover, the various standard geotechnical laboratory test methods are also described in this chapter. **Chapter 4** covers an analysis of the effectiveness of LS admixtures s in controlling the swell potential and other engineering properties of remoulded expansive soil. A comprehensive parametric study of the test data obtained from untreated, LS, and cement treated samples are presented followed by a

critical discussion explaining the possible reasons behind the observed behaviours. The stabilization mechanisms of LS admixture on expansive soil were identified through microstructural characterization characterisation, and are reported in **Chapter 5.** This chapter covers a series of analytical test (XRD, SEM/EDS, FTIR, NMR, CT, SSA, and CEC) results for untreated and LS stabilized specimens. It explains the changes in the micro-fabrics of the materials, giving an insight into the stabilizing mechanisms of LS admixtures. Based on data obtained from Chapters 4 and 5, a number of mathematical relations, incorporating the effect of LS admixture on the observed mechanical behaviours are developed and presented in **Chapter 6**. Consequently, a robust mathematical model capable of predicting the suction behaviour of LS treated remoulded soil is proposed, leading to a simple swell predictive model which was validated based on the experimental data. **Chapter 7** presents the major conclusions drawn from this work, along with recommendations for further related studies.

1.6   SUMMARY

The substantial loss of properties and financial costs in combating the threat of expansive soils around the world contributes a great deal to the burden that natural hazards place on the economy of every affected nation. Thus, an appropriate, cost effective technique to minimize the impact that these soils have on infrastructure could be of great benefit to home owners, geotechnical engineers, and the government at large. As the threat to infrastructural stability grows exponentially as cities around the world expand, the pulp and paper manufacturing industry is also faced with increasing problems of disposing of a waste by-product known as LS. The pulping industries get rid of this waste through incineration but this in itself generates anthropogenic carbon dioxide (CO_2) while simultaneously producing large quantities of residuals such as fly ash and bottom ash that become formidable problems in their own right. Therefore, a successful use of this product in geotechnical engineering will serve as solution to several problems in society.

CHAPTER TWO

2 LITERATURE REVIEW

2.1   INTRODUCTION

Expansive soil is recognized as a clayey soil which shrinks and swells in response to change in moisture content or suction. The engineering properties of such soils are known to be influenced significantly by moisture; as the moisture content increases the soil swells and shrinks with decreasing moisture content. Such soils contain smectite mineral derived from certain sedimentary strata and basic igneous rocks (Donaldson 1969). In cases where such volume change is restrained, a pressure known as swell pressure develops and acts on the existing structures resulting in damage.

It is estimated that up to 20% of ground surface is covered by reactive (expansive) soils in Australia (Cameron and Walsh 1984). In the state of Queensland alone, expansive soils are estimated to cover up to one third of the surface with the greatest distribution occurring in western Queensland and the Darling Downs Region. Failure to correctly identify these soils and adopt appropriate sustainable engineering design solutions could lead to severe operational and maintenance cost which could result in colossal economic losses. Currently, the available methods at managing such problems include soil replacement, applying adequate surcharge, stiffening of the super structure, moisture control, physical and chemical alteration of the soil among others. Considering the environmental and engineering credentials, LS is considered a good candidate material among the chemical alteration scheme.

The aim of this chapter is to analyse the current state of research related to expansive soils to provide a basic platform for better understanding of how and why such soils shrink and swell. Also reviewed in this Chapter are the systemic problems associated with infrastructures founded on such soils and evaluation of existing treatment

methods with emphasis on chemical stabilization. It begins by defining basic expansive soil terminologies and the basic clay units because expansive clay minerals are a part of an ensembly of soils in an evolutionary continuum. The germane literature on swell mechanisms, factors influencing shrink/swell phenomenon, and global distribution of these soils are also discussed. In addition, the damages caused by such soils together with recognition and classification techniques are also explained. Besides, the review also placed an important emphasis on the limitations of the traditional (calcium-based) additives to justify the need for this research. Furthermore, the environmentally benign non-traditional admixture (LS) is reviewed and proposed as alternative candidate. To better understand the fundamentals of expansive soil, examination of existing swell predictive models were also undertaken and the deficiencies were identified. The understanding acquired from the reviewed literature is then summarized.

2.2   DESCRIPTION OF EXPANSIVE SOIL TERMINOLOGIES

In the course of reviewing the literature, it is evident that authors have used numerous terms in describing the expansive behaviour of clayey soils. In order to clarify the presentation of information, the terms as presented below are used in this thesis henceforth as explained.

2.2.1   Intrinsic expansiveness of soil

The intrinsic (integral) expansiveness of a soil is defined as that soil property resulting from its mineralogical composition, the gradation and its interaction with water. However, no procedure has been developed to measure this soil property (Oloo et al 1987). Oloo et al. (1987) defined intrinsic expansiveness as that property which relates change in volume to the suction change (or change in moisture) of a clayey soil. This means that for a given suction change, a soil of high intrinsic expansiveness will adsorb greater amount of moisture hence, larger volume change, compared to a soil with low intrinsic expansiveness.

2.2.2 *Percent swell of soil*

In this research, percent swell of an intrinsically expansive soil is described as the value of the axial strain that result from a change in moisture content or suction during inundation of specimen at maximum dry unit weight (MDUW) and optimum moisture content (OMC) under a seating load of 7kPa in the one-dimensional swell test. Authors have proposed techniques of measuring percent swell of expandable clays (e.g. Seed et al. 1962; Chen 1988; Nelson and Miller 1992).

The percent swell of a soil is typically presented as illustrated in Fig 2.1. The swell-time curve typically consists of three regions; an initial swell region, primary swell region, and secondary swell region. The minor initial swell is due to the closing of macro-pore spaces, and destruction and disorientation of large clay aggregates whereas the major primary swell and minor secondary swell has been attributed to microstructural swelling (Al-Rawas and Goosen 2006). The secondary swell continues until a diffuse double layer (DDL) is fully developed.

$$s = \left(\frac{H_1 - H_o}{H_0}\right) \times 100$$

H_1 = final height,
H_o = initial height
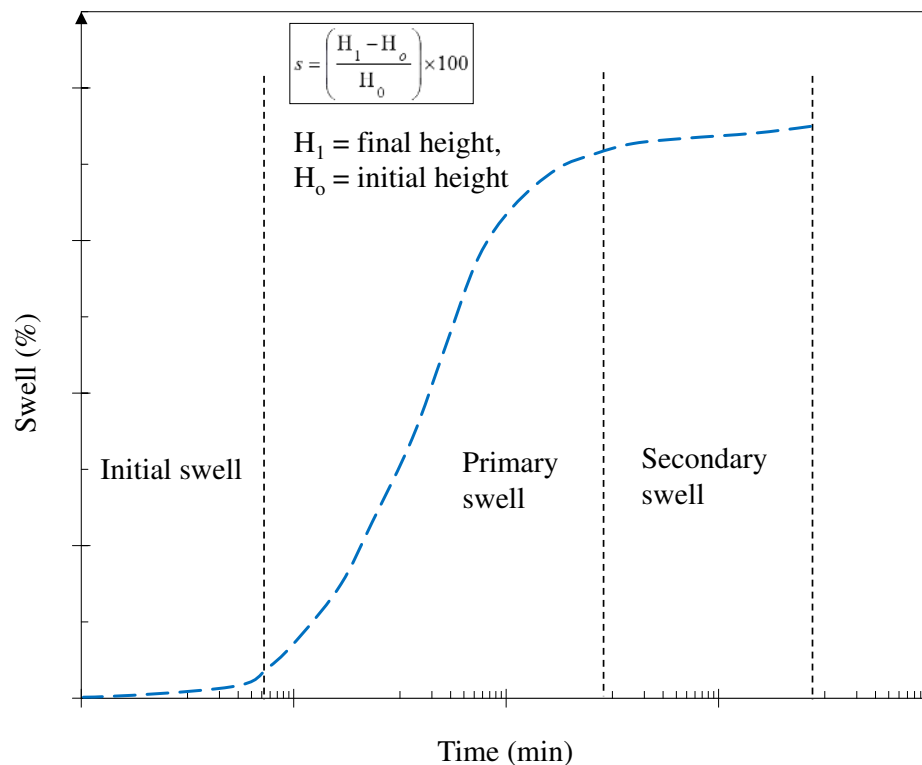
Figure 2.1: Swell-time behaviour of compacted expansive soil (After Al-Rawas et al. 2006)

2.2.3 *Swell pressure of soil*

The Swell pressure indicates the trouble potential of an expansive soil. This pressure is the maximum force per unit area that needs to be applied over a swelling soil to prevent volume increase. Al-Rawas and Goosen (2006) suggested that a swell pressure of less than 20kPa may be ignored in practice. It is common practice to determine the swell pressure of expansive soil using the constant volume test method that relates void ratio to effective stress (Fig 2.2). The swell pressure according to this test is the averaged maximum applied stress required to preventing the specimens from swelling (ASTM 4546). However, Fredlund (1983) proposed a correction factor procedure for swell pressures obtained from this technique due to equipment deformation as demonstrated in Fig 2.2.
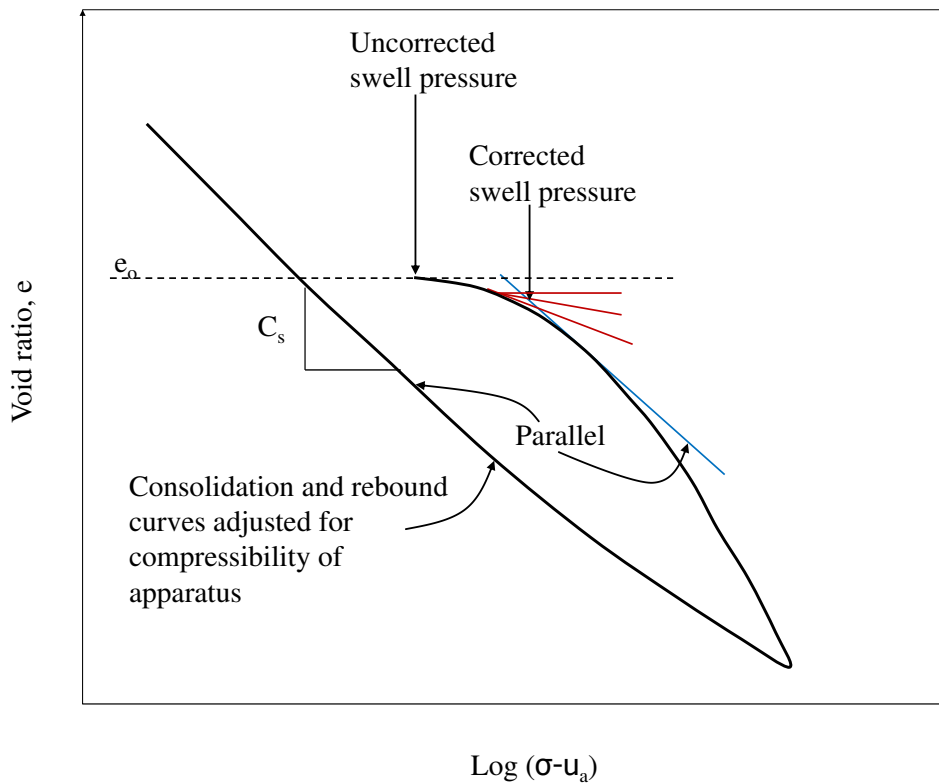
Figure 2.2: Construction procedure to correct the effect of sample disturbance and equipment deformation (After Fredlund 1983)

15

2.2.4   Swell potential of soil

The two components describing the expansive behaviour of soil as described above; namely the percent swell and swell pressure, are herein referred to as the swell potential of the soil.

2.2.5   Soil heave

Heave is the displacement of a point in the soil due to suction and stress changes as water interact with the intrinsic expansiveness of the soil. Heave is not a soil property (Lytton 1977). Heave occurs because the moisture increases in the expansive soil (Fig 2.3). Because water is incompressible, the clay particles are forced apart, causing soil heave (Kelm and Wylie 2008).
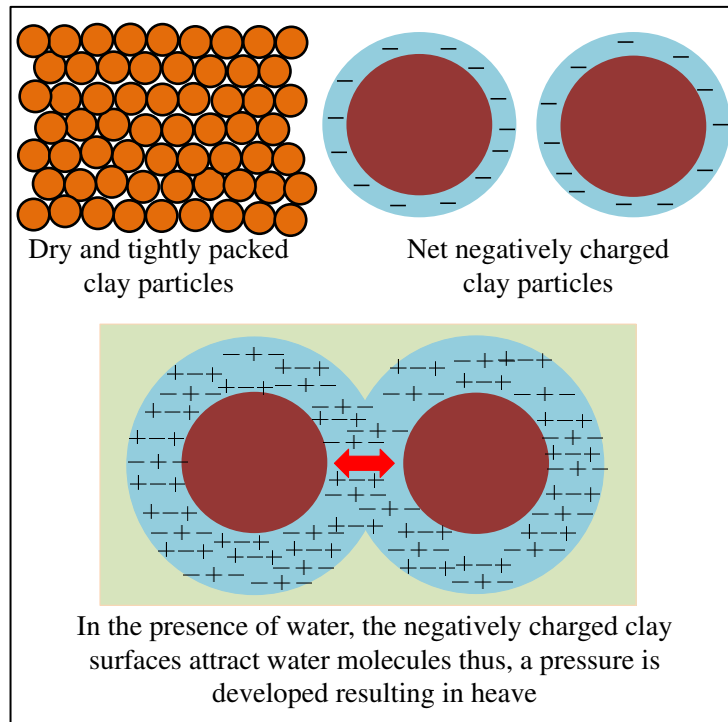
Figure 2.3: Graphical demonstration of heave (Kelm and Wylie 2008)

2.2.6   Soil suction

The fundamental ability of a soil to attract and retain water is traditionally described in mechanical terms as total suction (φ_t); i.e. negative stress in the pore water. The mechanisms responsible for this attraction are attributed to capillary (matric; φ_m) and

16

osmotic (φ_o) components. The total suction is considered as the algebraic sum of the two suction components as shown in equation (2.1).

$$\varphi_t = \varphi_m + \varphi_o \qquad (2.1)$$

Matric suction (φ_m) originates from physical interactive forces between air-water-solid interfaces of an unsaturated soil system whereas, the osmotic suction (φ_o) in a soil arises from the forces exerted on water molecules as a result of the chemical potential causing dissimilar dissolution of solute concentrations in a soil fluid (Fredlund and Rahardjo 1993).

2.3   ORIGIN OF EXPANSIVE SOILS

The origin of expansive soil has been concisely summarized by several authors (Chen 1988; and Al-Rawas et al. 2006). The geneses of these soils are regarded as a complex combination of processes and conditions. These conditions and processes include the composition of the parent materials and the degree of physical and chemical weathering encountered by the parent rocks which in turn dictates the mineralogy of the soils (Chen 1988). However, Borchardt (1989) argues that the polygenetic nature of these soils makes it difficult to determine if smectite rich soils originated from transformation of other minerals or through precipitation as smectite.

Another school of thought postulate that mica minerals are the major source of smectite rich soils as depotassication of mica is believed to form smectite minerals (Jackson 1965). Through pedogenic transformation processes of depotassication, dealumination of the tetrahedral sheet and silication of the tetrahedral sheet, it has been reported by Fanning et al. (1989) that mica could be transformed to a smectite group member; vermiculite. However, it has been widely reported that certain environmental conditions must be fulfilled to favour mica transformation to smectite minerals. Jackson (1965) reported that the following factors are vital in the transformation processes.

17

1) The prevailing temperature and pressure should be low enough to destabilize Al in mica minerals

2) Low aluminium ion concentration

3) Low potassium ion concentration

4) High silica concentration

The formation of vermiculite and other smectite minerals from mica transformation has been reported in the United States of America (Reid et al. 1996). High-charged smectite minerals, identified as beidellite, were observed in surface horizons and proposed to have developed from the weathering of mica.

Another school of thought believes that smectite minerals are widely distributed in areas of volcanic deposits or origins with arid or semi-arid and in tropical climates. In tropical volcanic settings, alumina rich volcanic ash gets deposited in general over a wide area. Part of which could be concentrated in depressions or low areas which are almost always inundated with water. This regular inundation tends to leach the alumina and concentrate it at about 0.1 meter to 4.0 meters depth to form expansive minerals in the soil. This explains the sporadic occurrence of expansive soils as alumina is the primary source of the expansive tendency and most often are shallow in occurrence due to the poor levelling effects (Eswaran 1979).

Another complimentary theory on the origin of expansive soils is reported by Borchardt (1989). He argues that basic rocks containing high Fe and low Al often weather to a Fe-smectite. Magnesium rich rocks such as serpentine have been reported to form Fe-rich smectite. Borchardt (1989) is of the opinion that smectite minerals do not form in-situ. That their presence in basin environments is due to reduced leaching which simply protect smectite from weathering. He further argued that the occurrence of smectite minerals in well drained basin environments are rather due to the very high concentration potentials of Si, Al and Mg to preserve smectite rather than providing conditions for its formation.

18

2.4 CLAY–MINERAL STRUCTURE AND CHEMICAL COMPOSITION

Clay soils are made of very fine particles with less than 0.002mm in diameter packed together. Grim (1968) analysed clay soils using X-Ray, optical microscope, and dehydration methods and reported that clays generally are aggregates of extremely minute particles of one or more species of small groups of minerals known as the clay minerals [kaolinite, illite and smectite (montmorillonite)], all of which are in crystalline form and tend to be of flat, platy shapes (Snethan et al. 1977), and that each clay crystal is made up of simple building units.

2.4.1   The clay building units

A "unit or block" is a basic repeating structural element of clay minerals. The different clay minerals are made up of various combinations of the basic building units of mineral otherwise known as sheets. There are two types of sheets: tetrahedral (silicate) and octahedral (Grim 1968). Tetrahedral sheets are made up of silicon (Si^{4+}) and oxygen (O_2^-), whereas, Octahedral sheets are of hydroxide (OH^-) and either aluminium (Al^{3+}) or magnesium (Mg^{2+}). An octahedral sheet is referred to as dioctahedral if it is made up of aluminium whereas, if it is made up of magnesium it is referred to as trioctahedral (Fig 2.4a) (Knappett and Craig 2012). The basic building blocks of clay minerals (i.e. silicon-oxygen tetrahedral, aluminium-oxygen octahedra and magnesium or aluminium octahedral) form the major clay mineral groups; Kaolinite, Illite and Smectite (montmorillonite) causing variation in the physical and chemical properties. For example, kaolinite is made up of one tetrahedral sheet plus one octahedral sheet (1:1 layer mineral), while smectite and illite is made up of two tetrahedral sheets and one octahedral sheet (2:1 layer mineral).

2.4.2   The structure of clay mineral groups

2.4.2.1   Kaolinite group

This group of clay minerals consist of one silica tetrahedral sheet and one alumina octahedral sheet (gibbsite; Al-OH) (Fig 2.4b). This structure is often referred to as the 1:1 lattice type with typical basal spacing of about 7.2Å (Mitchell and Soga

19

2005). They are derived from the weathering of alkali feldspars under acidic conditions and contain no exchangeable cations. The virtual absence of ionic substitution in either the tetra- or octahedral layers results in a more or less complete electrical neutrality. Thus, the hydrogen bonding between the tetrahedral and octahedral layers is significant. This bonding holds the 1:1 layers tightly together leaving little to no interlayer space for absorption of water or cations, thus shrink/swell phenomenon is virtually non-existence (Dixon 1989). There is high degree of regularity in the stacking of well crystallized kaolinite units, with crystal diameter ranging from 0.5 - 4μm and with specific surface area of 10 - 20 m²/g (Chen 1988). The theoretical formula of kaolinite is given as $Si_4Al_4O_{10}(OH)_8$. It is the least active clay mineral with the lowest plasticity and lowest capacity for adsorbing cations among the three clay mineral groups.

2.4.2.2 Illite group

The structure of illite is of two silica tetrahedral sheets with a central alumina octahedral sheet (gibbsite or brucite) (Fig 2.4c). The illite group is also referred to as the 2:1 lattice type (i.e. similar to montmorillonite structure). Illites are derived from weathering of silicates including micas and alkali feldspars under alkaline conditions (Mitchell and Soga 2005). It has a relatively low plasticity and swell potential in comparison to smectite minerals due to its higher particle diameter of 0.5 - 10μm and lower specific surface area of 60 - 180m²/g (Chen 1988). They have a general formula of $[(K,H_3O)(Al,Mg,Fe)_2(Si,Al)_4O_{10}[(OH)_2,(H_2O)]]$ with a non-exchangeable cation inner layer potassium ion (K^+). The K^+ satisfies charge deficiencies residing mainly on the tetrahedral layers of the mineral thus; the sheets are fairly tightly packed (Borchardt 1989). This effectively preclude the admission of significant amounts of water between the unit layers, thus illite minerals exhibit shrink/swell potential a little more than kaolinite, but significantly less than the smectite group minerals.

2.4.2.3 Smectite (Montmorillonite) group

Smectite is the generic name given to all expanding 2:1 phyllosilicates minerals (Fig 2.4d). The smectite structure is composed of two silica tetrahedral sheets with a

central alumina octahedral sheet (gibbsite; Al-OH or brucite; Mg-OH) with typical basal spacing of 9.6 – 17.1Å (or more) (Mitchell and Soga 2005). Unlike kaolinite, the charge distribution within the lattice is unbalanced due to isomorphous substitutions within the octahedral sheet of fe^{3+}, and/or Mg^{2+} for Al^{3+} and a limited substitution by Al^{3+} for Si^{4+} in the tetrahedral sheet. These substitutions results in positive charge deficiency which is partially neutralized by the adsorption of ions (Ca^{2+}, Mg^{2+}, H^{-}, Na^{+} etc) between unit layers of the minerals with relatively small proportion located at the external crystal surfaces (Knappett and Craig 2012).

In smectites, cation substitutions occur in the octahedral sheet, the tetrahedral sheet, or both. These substitutions determine the properties and chemical composition of the smectite minerals. Dioctahedral smecties — montmorillonite (Mg-rich), beidellite (Al-rich), and nontronite (Fe-rich) — generally form as a result of geochemical and pedochemical weathering. Trioctahedral smectites — hectorite (Li-rich), saponite (Mg-rich), and sauconite (Zn-rich). However, in general terms, smectites are commonly referred to as montmorillonites even though significant tetrahedral Al substitution and Fe octahedral substitution can occur (Borchardt 1989).

Smectite minerals show extensive inner layer expansion on hydration. The particle diameter ranges from 0.05 - 10μm with large active surface area of about 700 – 800m^2/g exposed, allowing enormous range of guest molecules (e.g. water) to intercalate because inter-sheet bonding is mainly due to weak Van Der Waal's forces (Chen 1988). Chemically, it is an hydrated sodium calcium aluminium magnesium silicate hydroxide, with a chemical formula; $(Na,Ca)_{0.33}(Al,Mg)_2(Si_4O_{10})(OH)_2 \cdot nH_2O$.

2.5   THE MECHANISMS OF CLAY SWELLING

Although all clays shrink and swell upon change in moisture content, smectite minerals exhibit a very high magnitude of this volume change phenomenon. The very small lattice size, the large surface area, and the diffuse layer charge allow smectite minerals to absorb water several times over other clay mineral groups (Borchardt 1989). The fundamental concept of clay swelling is the balancing of the

forces of interaction between the clay surface ions, and water molecules (McBride 1989); however, there is no common consensus about the most appropriate theory of clay expansion. The mechanisms presented in Table 2.1 are some of the many theories described in the literature. The mechanism of swelling in expansive soil is complex and is influenced by a number of factors. Snethan et al. (1975) posited that the major portion of volume change is caused by four out of six possible mechanisms; i.e. osmotic repulsion, cation hydration, clay particle repulsion and capillary imbibition. The influence of these four major mechanisms is generally combined and described by Fredlund and Rachardjo (1993) as the total soil suction.
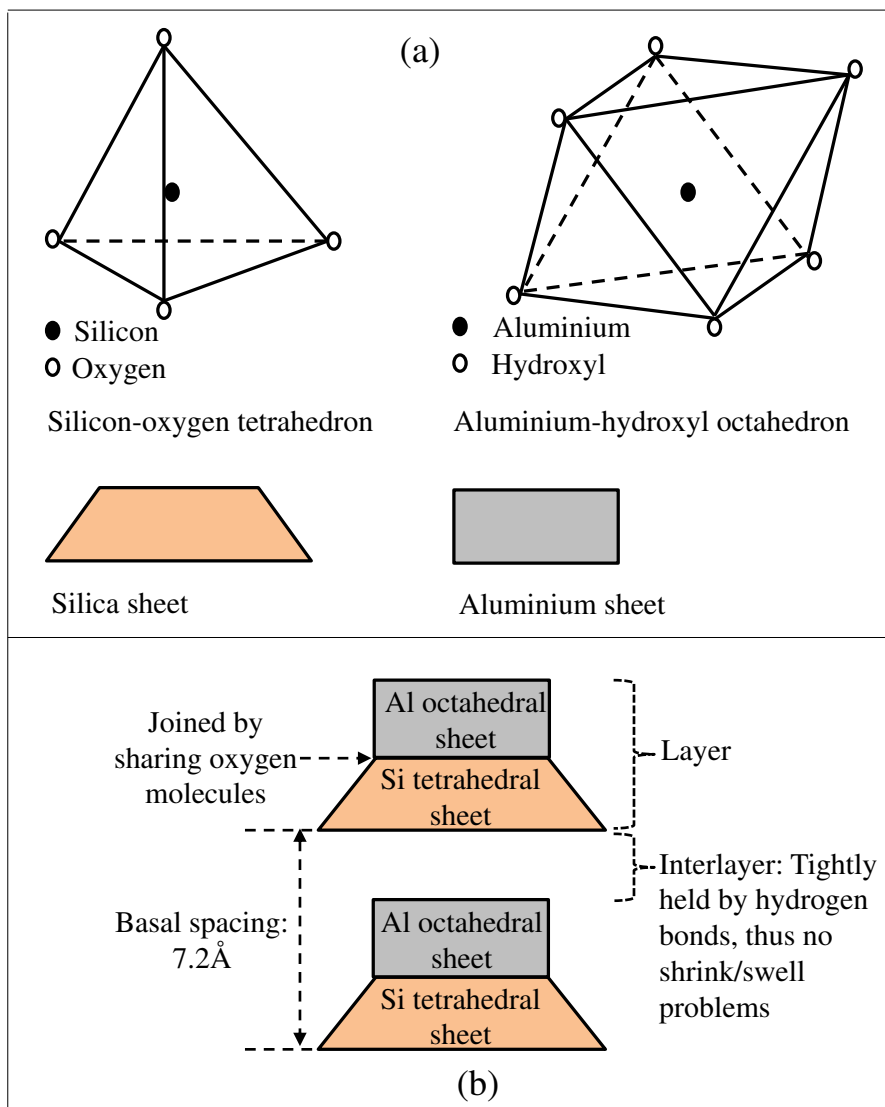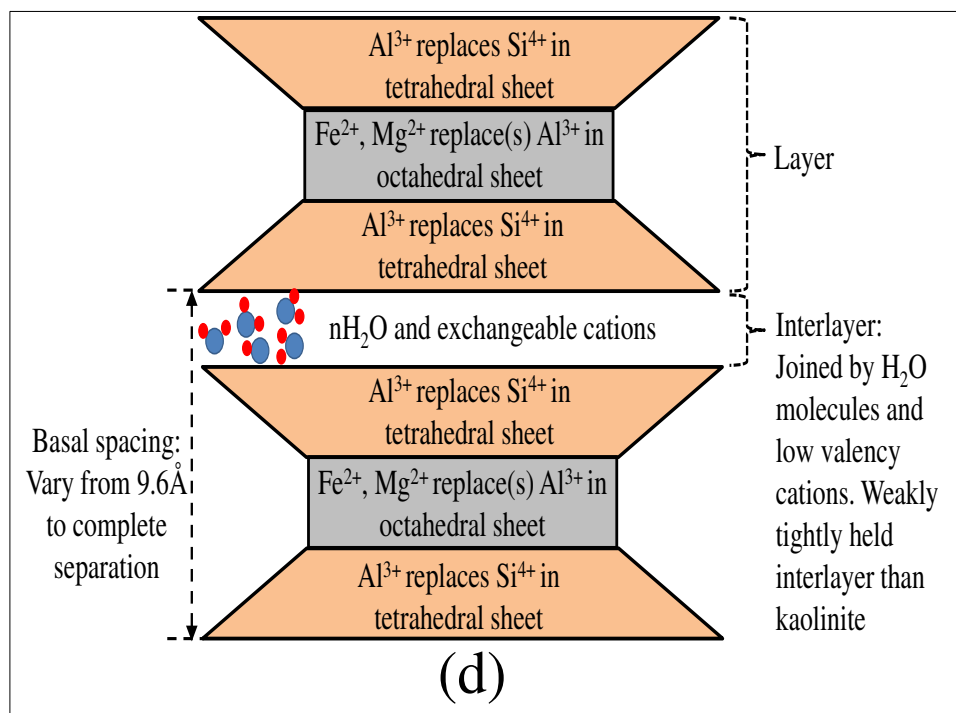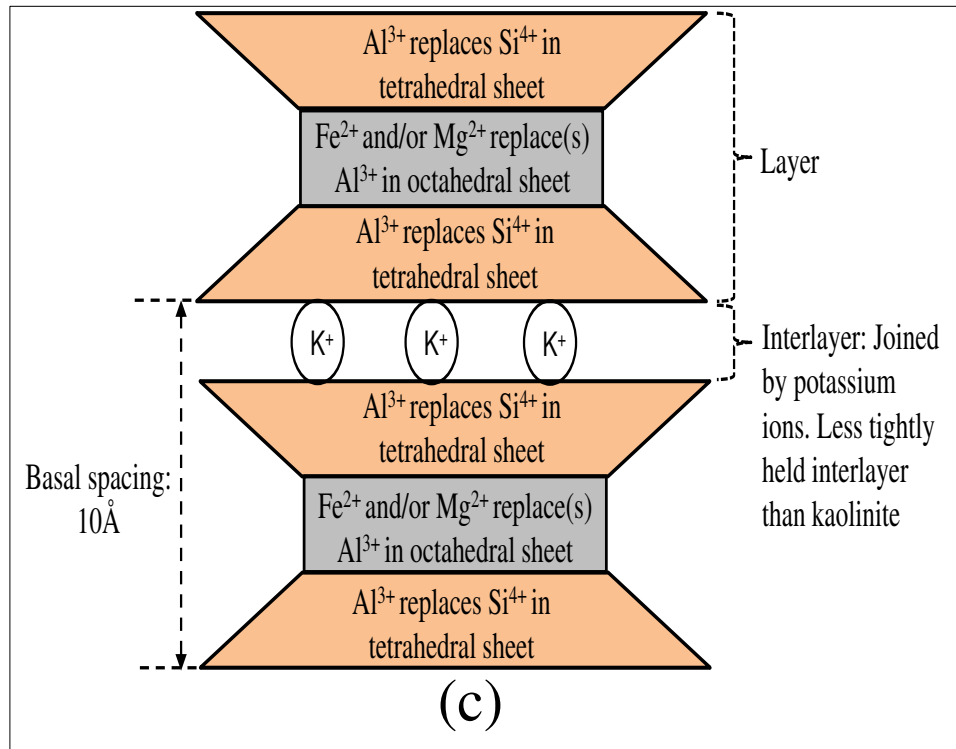
Figure 2.4: a) Clay minerals: basic units (After Knappett and Craig, 2012), b) General structural arrangements of kaolinite clay mineral, c) General structural arrangements of illite clay minerals, d) General structural arrangements of smectite (montmorillonite) clay mineral (After Mitchell and Soga 2005).

Despite the nebulous concept of clay swelling mechanisms, a generally accepted clay swelling mechanisms has been posited by several authors (e.g. Van Olphen 1977). It is accepted widely that due to ion concentration imbalance between the diffuse double layer (DDL) and pore fluid, an osmotic pressure is generated within the soil system. Hence, water permeates through a semi-permeable membrane to hydrate cations in the DDL, thus generating hydration energy. This energy otherwise known as the swell pressure causes the distance between two parallel smectite mineral platelets to increase, resulting in clay swelling (Fig 2.5).
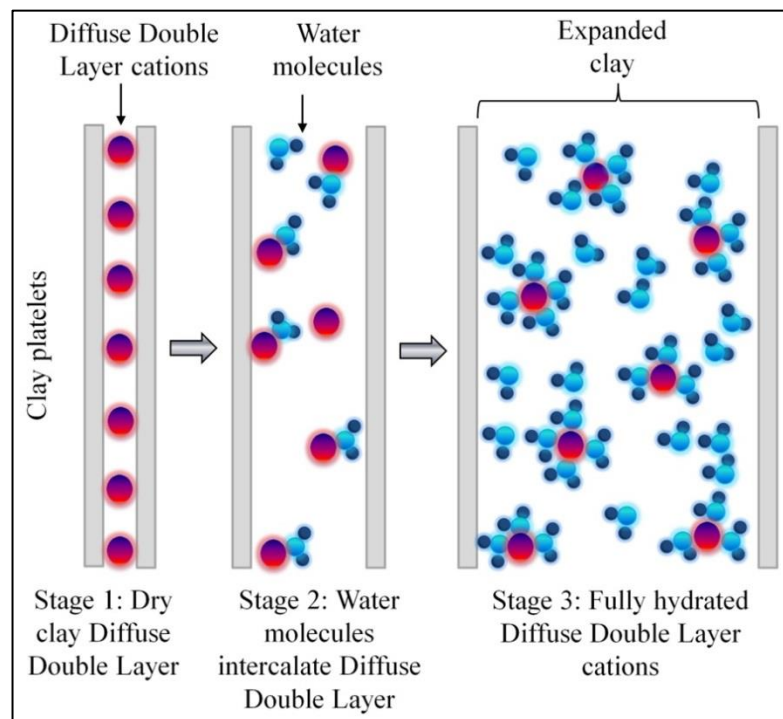
Figure 2.5: Crystalline swelling mechanism of clay (Illustrated after Snethan et al. 1975)

2.5.1 *Clay swelling and the concept of diffuse double layer (DDL) theory*

Several researchers have proposed theories to explain the basic mechanisms of soil expansion. One such study is the diffuse double layer theory proposed by Gouy (1910) and improved upon by Chapman (1913, cited in Mitchell and Soga 2005) thus, also referred to as the Gouy-Chapman theory. Stern (1924); Derjaguin and Landau (1941); and Verwey and Overbeek (1948) as cited in Mitchell and Soga

(2005) have extended the Gouy-Chapman theory to describe the ionic distribution in the immediate vicinity of the surface of a unit layer. The theory has been useful for understanding several aspects of physico-chemical forces of attraction, aggregation, flocculation, dispersion and deflocculation and the relationships of these processes to formation of soil structure and clay swelling and compression.

Due to the negatively charged interlayer surfaces of clay particles, cations could be held tightly onto dry clay surfaces. On addition of water, these tightly adsorbed cations diffuse away in order to equalize concentrations throughout the soil-water system. This diffusing tendency is however, opposed by the attractive force between the cations and the negatively charged clay surfaces. The end result of this phenomenon is an ion distribution in the vicinity of the clay surfaces (Fig 2.6). This charged surface and the distributed charges in the adjacent phases are together termed the DDL. The DDL is a result of electrostatic attraction of positive ions in the pores by the negatively charged clay particle surfaces whose overlapping generate inter-particle repulsive forces that bring about swelling (Mitchell and Songa 2005). The DDL theory of volume change in expansive soil is attributed to osmotic pressure generated by chemical potential gradients between free water and water in the inner layer, forming around the clay mineral surfaces.
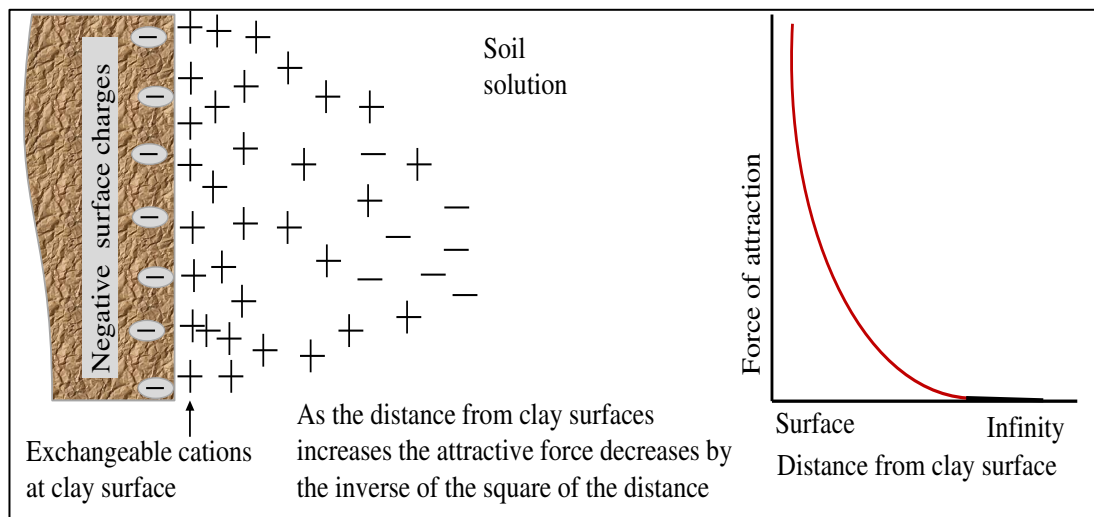
Figure 2.6: The concept of the diffuse double layer at the surface of a clay particle (Das 1997)

Table 2:1: Natural microscale mechanisms causing volume change in expansive soils
(Reproduced after Snethan et al. 1975)

Mechanisms	Explanation	Influence on volume change
Osmotic repulsion	Pressure gradients developed in the double-layer water due to variations in the ionic concentration in the double layer. The greatest concentration occurs near the clay particle and decreases outward to the boundary of the double layer	The double-layer boundary acts as an osmotic membrane when exposed to an external source of free water; that is, it tries to draw the water into the double layer to reduce the ionic concentration. The result is an increase in the double-layer water volume and the development of repulsive forces between interacting double layers. The net result is an increase in the volume of the soil mass
Clay particle attraction	Clay particles possess a net negative charge on their surfaces and edges which result in attractive forces for various cations and in particular for dipolar molecules such as water. This makes up the major "holding" force for the double-layer water	In an effort to satisfy the charge imbalance, the volume of water in the double layer will continue to increase until a volume change of the soil mass occurs
Cation hydration	The physical hydration of cations substituted into or attached to the clay particle	As the cations hydrate, their ionic radii increase, resulting in a net volume change of the soil mass
London-van der Waal forces	Secondary valence forces arising from the interlocking of electrical fields of molecule associated with movements of electrons in their orbits. The phenomenon frequents molecules in which the electron shells are not completely filled	The interlocking of electrical fields causes a charge imbalance which creates an attractive force for molecules such as water

Capillary imbibition	Movement of water into a mass of clay particles resulting from surface tension effects of water and air mixtures in the pores of the clay mass. Compressive forces are applied to the clay particles by the menisci of the water in the pores	As free water .becomes available to the clay mass, the pore water menisci begin to enlarge and the compressive forces are relaxed. The capillary film will enlarge and result in a volume change or supply water for one of the other mechanisms
Elastic relaxation	A readjustment of clay particles due to some change in the diagenetic factors	Volume change results from particle reorientation and/or changes in soil structure due to changes in the diagenetic factors

2.6 PHYSICAL PROPERTIES OF EXPANSIVE SOILS

Due to the complexity involved in swelling mechanisms of soils, a large number of factors in multiple publications have been identified to affect volume change behaviour of these soils (e.g. El-Sohby and Rabba 1981). From the literature, attempts to single-out a property or combining certain soil properties to explain the behaviour also exist (e.g. Chen 1988). Nonetheless, Snethan et al. (1975) postulated that the actual behaviour is a function of combinations and interrelationships among several factors. They grouped these factors in two folds:

1   Intrinsic soil properties which contribute to the actual volume change and
2   Environmental conditions which enhance the probability and magnitude of expansivity

2.6.1   Intrinsic properties

Composition of soil: It is common knowledge that the swelling of a clayey soil is a function of its clay mineral composition (Fig 2.7). Thus, the type of clay mineral within a soil, the amount, the size, and specific surface area of the clay minerals could dictate the soil expansive behaviour. The type and amount of clay minerals are the intrinsic factors which determine whether or not a soil will expand (Snethan et al. 1975).

The clay mineral size in expansive soils affects volume change by controlling the development of DDL in mineral lattices. It is reported widely that small particle sizes result in large effective surface areas which permit considerable development of DDL water within individual particles. For example, kaolinite mineral sizes are of the order of fine silts whereas, smectite minerals occur in extremely small particles which may be considered as colloid hence, smectite minerals does possess higher swell potential than the kaolinite counterpart (El-Sohby and Rabba 1981).
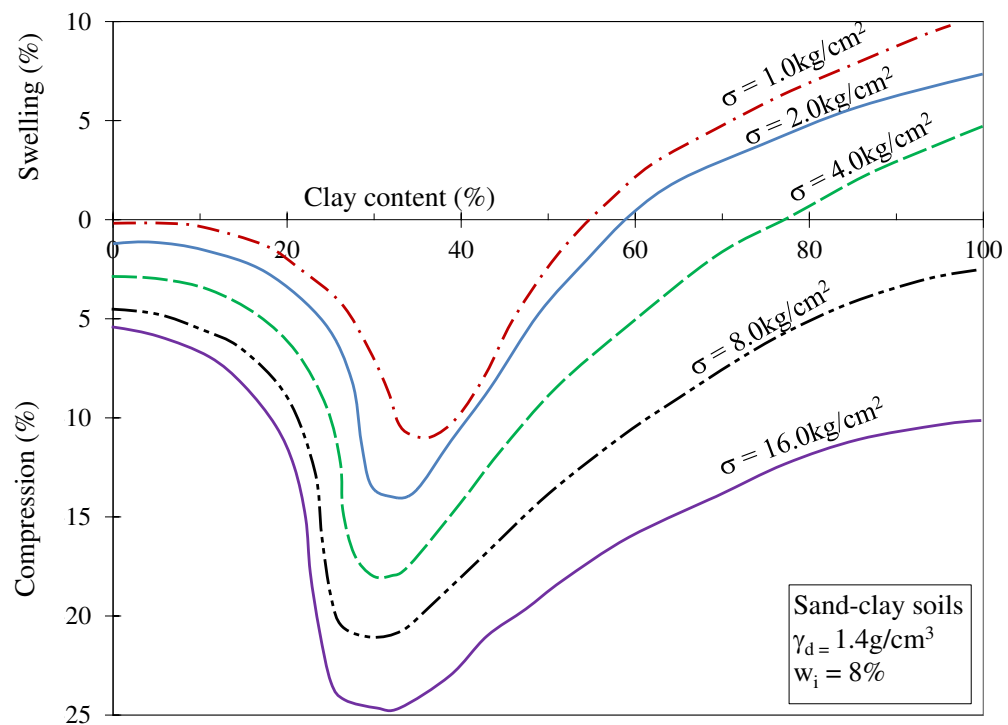
Figure 2.7: The effect of clay content on swell percent of soil (After El-Sobhy and Rabba 1981)

Dry density: Variation in initial dry density or void ratio is known to significantly affect swelling of clayey soils (Fig 2.8). At a constant moisture supply, the swell potential increases with increasing dry density though with a much slower rate. El-shobhy and Rabba (1981) has demonstrated this phenomenon by observing percent swell of soils compacted at different initial dry density. The report suggests that samples with higher dry density exhibited higher swell potentials than those with lower density. The reason is that increasing sample density quantitatively increases the expansive minerals in a sample thus, on inundation, the DDL-water interaction

28

increases which results in higher osmotic repulsive forces causing significant volume change (Snethan et al. 1975). Though the swell rate decreases with increasing initial dry density due to improved particle packing which is likely to impede permeating water molecules.
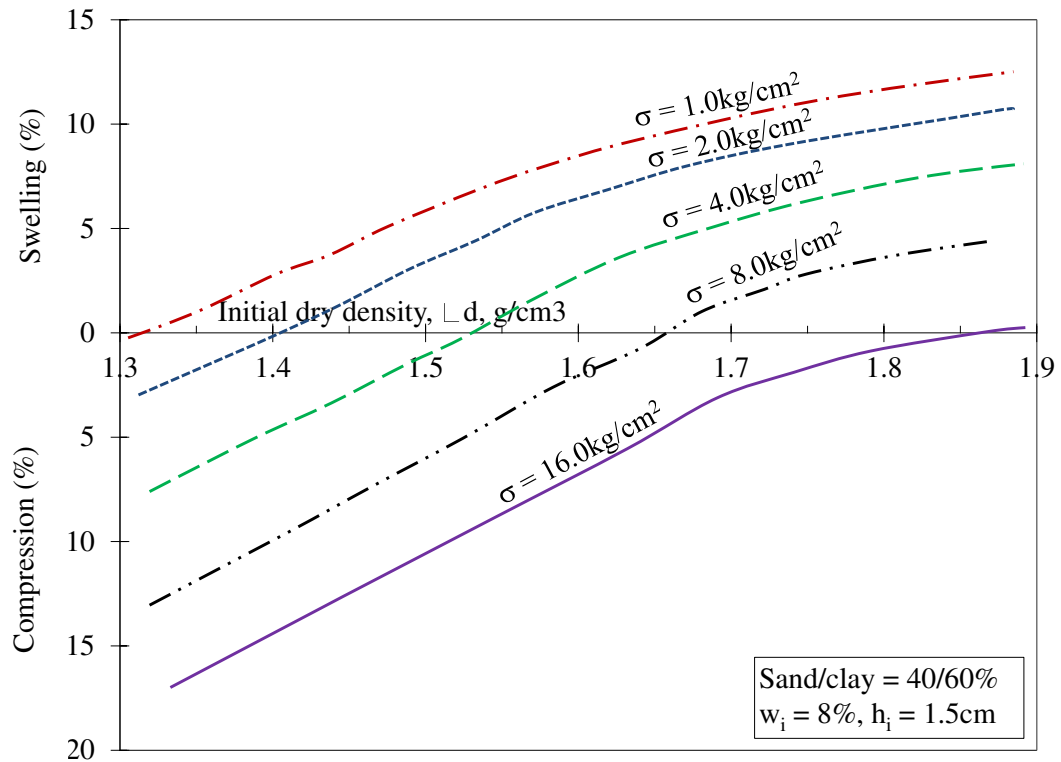
Figure 2.8: The effect of dry on swell percent of soil (After El-Sohby and Rabba, 1981)

Orientation of clay particles: Though there is no universally accepted theory on the influence of particle arrangement on swell behaviour of soils, some authors (e.g. Yong and Warkentin 1966) are of the opinion that clay particle orientation or arrangement seems to affect their accessibility to moisture and thus swell characteristics. They argued that the percent swell recorded for sodium montmorillonite clay with parallel particle orientation is greater than other forms of particle arrangements. However, Pacey (1956, cited in Snethan et al. 1975) posited that the greatest percent swell is obtained with randomly arranged soil particles and minimal with parallel orientation of particles. For a given compaction effort, a less

oriented fabric is obtained at low initial moisture contents but as the initial moisture content increases, the soil fabric become more oriented (Fig 2.9).
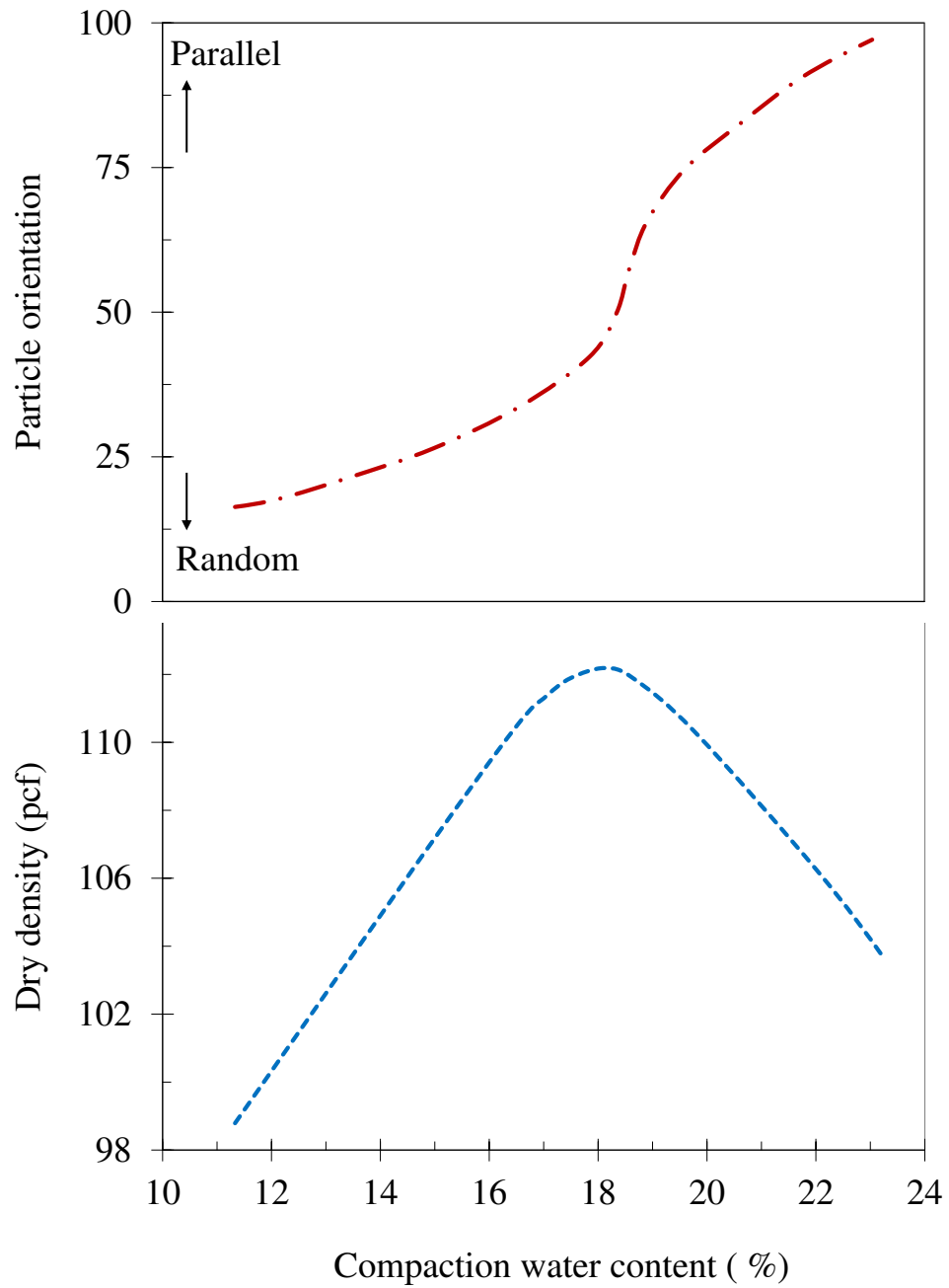
Figure 2.9: Compaction water content of Boston blue clay versus dry density and particle orientation (After Pacey 1956, cited in Snethan et al. 1975)

On the contrary, Day (1994) discussed the complexity and the difficulty involved in observing the nature of expansive soil fabrics and its relation with volume change. Individual clay mineral platelets occur in either agglomerated arrangements which consist of independent groups of platelets, or non-agglomerated arrangements (dispersed) which are void of definitive clay mineral patterns. An agglomerated group may consist of individual units which might be aggregated face-to-face. This orientation of soil particles suggest that percent swell is less significant due to the poor development of DDLs. In some case, the individual units could exist in a dispersed state i.e. the units exist with little or no points of contact with other units and thus, surrounded by well-developed DDLs in the presence of water, and exhibit greater percent swell (Fig 2.10) (Johnson and Snethan 1978). The swell potential reported by Seed and Chan (1959) is greatest for random particle arrangement. Olson (1964) reported higher swell pressure with samples of higher compaction pressure. He believes that as compaction pressure increases, it produces more oriented soil particles.

Compaction method used in specimen preparation: Seed and Chan (1959) demonstrated that the method of soil compaction induced different structures at given moisture contents and densities and thus significantly affect the swell potential of soil. However, Oloo (1987) argued that insignificant effects on swell potential exist between specimens prepared by static or dynamic compaction methods except at low moisture contents. Contrary to Oloo's argument, Yong and Warkentin (1975) posited that at moisture contents greater than optimum, static compaction produces a flocculated orientation whereas dynamic compaction produces a dispersed orientation. The dispersed sample was reported to exhibit a greater percent swell due to the increase in inter-particle spacing in the presence of water. In a similar study, Attom et al. (2001) reported a greater percent swell with the use of dynamic compaction technique followed by static, and kneading techniques as a result of fabric orientations (Fig 2.11).
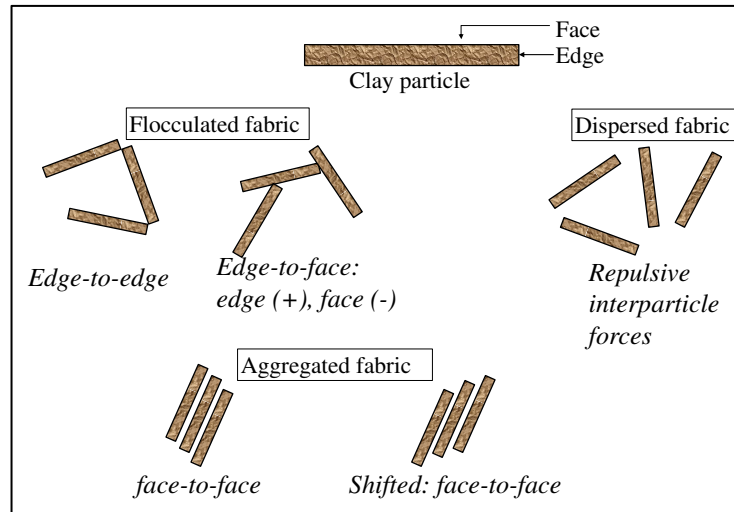
Figure 2.10: Soil fabric and volume change (After Van Olphen 1977).
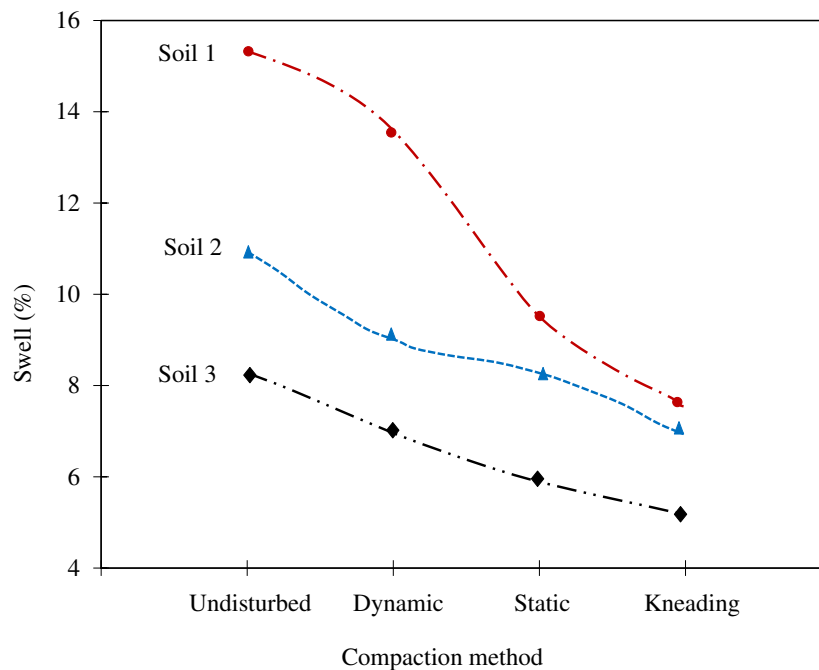
Figure 2.11: Percent swell versus compaction method for expansive soils (After Attom et al. 2001)

Pore-water chemistry: The volume change of an expansive soil is greatly influenced by the adsorbed ions (basal and peripheral) and the variability of the pore fluid. Nelson and Miller (1992) opined that the degree of hydration of soil particle is swayed by the amount and type of ions on the particle surfaces and the amount and

32

valency of ions in the pore fluids (Johnson and Snethan 1978). The reason is that the valency of exchangeable cations governs the thickness of the DDL in soils. The higher the valency of the dominant exchangeable cation, the thinner the DDL layer thickness. For instance, the presence of trivalent cations (e.g. Al^{3+}) in soil solution will reduce DDL thickness (reduced swelling) more than divalent cation (e.g. Ca^{2+}) and in turn, the percent swell in divalent cations dominated soil fluid will be more significant than when dominated with monovalent cation (e.g. Na^+) (McKenzie and Anderson 1998; Xie et al. 2007). Xie et al. (2007) demonstrated this phenomenon by varying pore-water chemistry in bentonite. Compacted bentonite was treated with NaCl solutions at different concentrations and they reported that with the increase in the ionic strength, the measured swell pressure decreased significantly (Fig 2.12).

Applied pressure: The application of a surcharge to an expansive material alters the amount of volume change that is likely to occur. Surcharge pressure has its greatest influence on expansive soils in terms of swell pressure development (Chen 1988). At pressures greater than the swell pressure, deformations in expansive soils could be contained. In other words, the greater the applied pressure the greater the counteracting stress and thus, the smaller the deformation (Fig 2.13). It is believed that light weight structures founded on expansive soils fail because the applied load is far less than that required to maintain minimal deformation.

Soil plasticity (PI): Nelson and Miller (1992) reported that soil plasticity is a good indicator of percent swell of expansive soil. A soil with significant plastic behaviour over a wide range of moisture content coupled with high liquid limit exhibit great potential to shrinking/swelling. In a similar study carried out by Chen (1988). He reported that PI is a good indicator of shrink/swell behaviour of soil; the lower the PI the lower the shrink/swell behaviour and vice versa (Fig 2.14).

 Soil suction: Soil suction has been related to volume change in expansive soils. At a given initial dry density and initial moisture content of a sample, Cokca and Birand (2000) demonstrated that a linear relationship exist between initial soil suction and swell pressure with a very high coefficient of correlation (Fig 2.15).
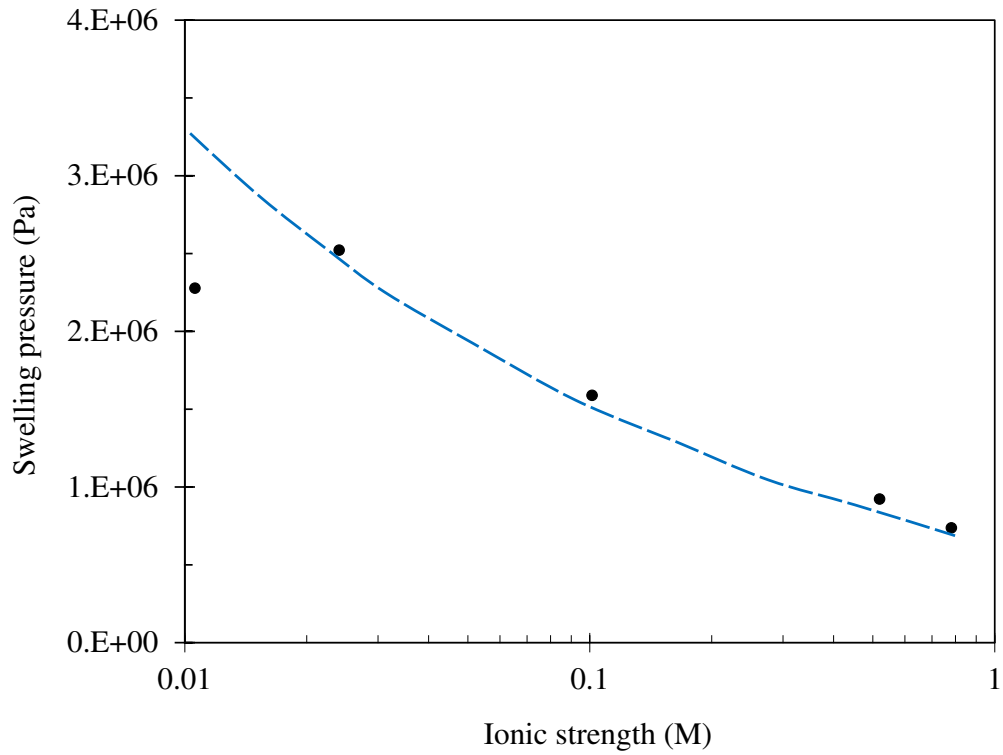
Figure 2.12: Swelling pressure of bentonite and its dependence on ionic strength of NaCl (After Xie et al. 2007)
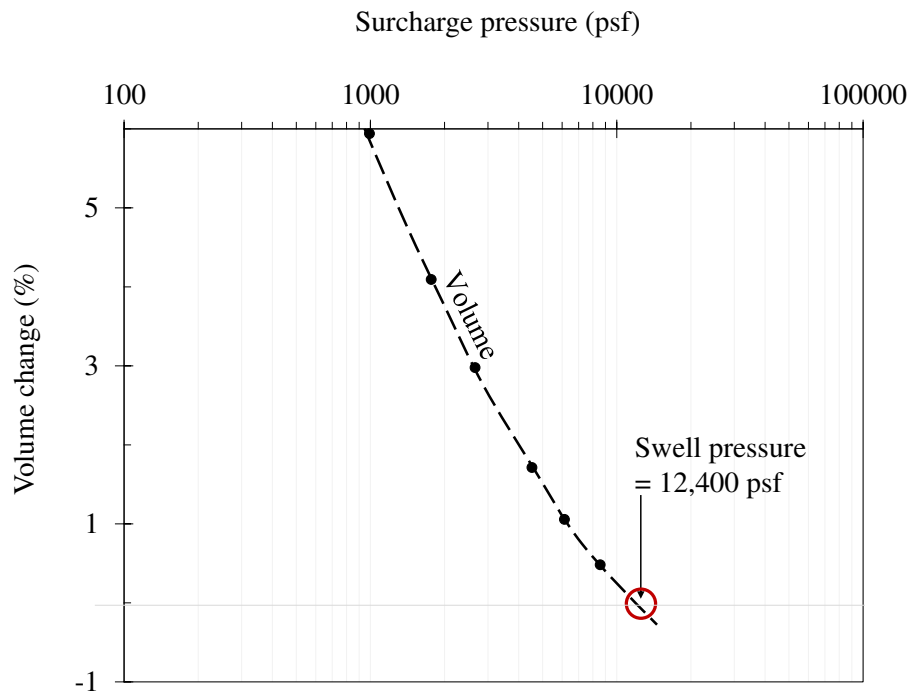
Figure 2.13: Effect of varying pressure on volume change for constant density and moisture content sample (After Chan 1988).
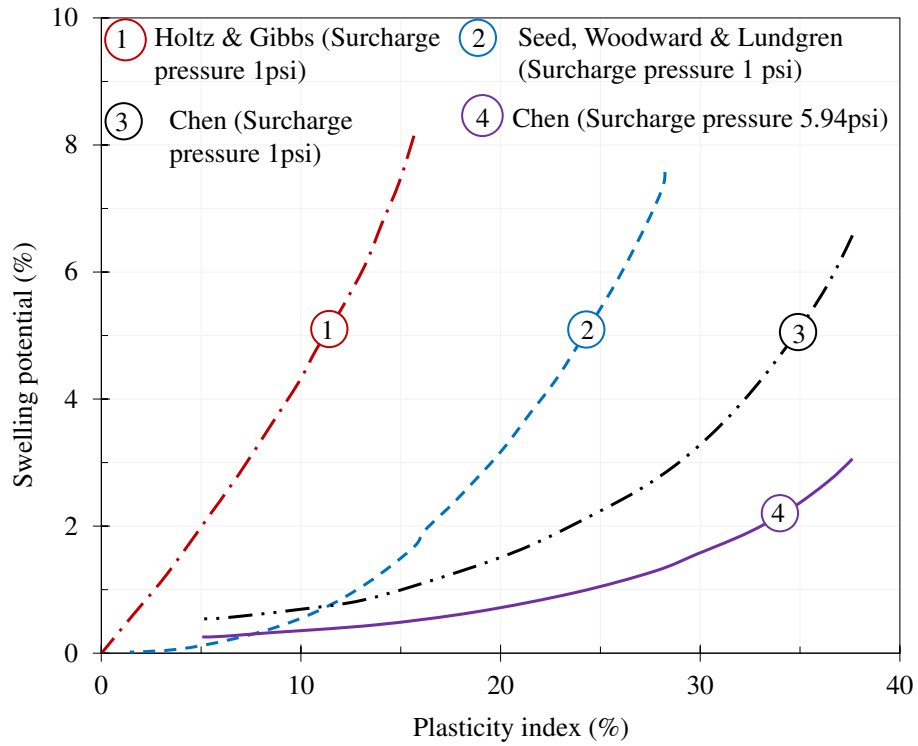
Figure 2.14: Correlations between percent swell and plasticity index (Reproduced after Chen 1988)
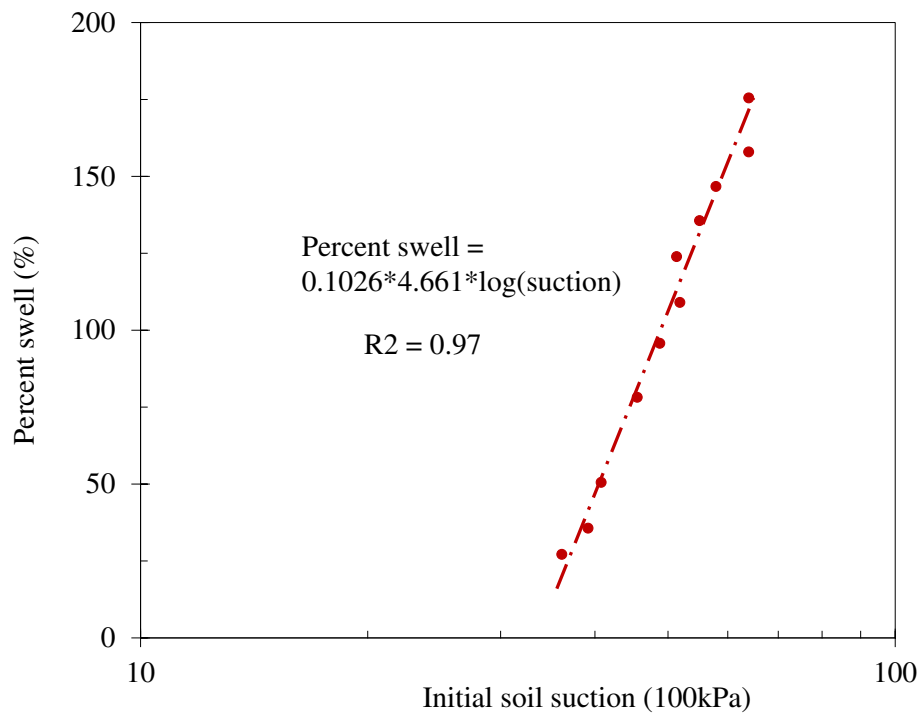
Figure 2.15: Relationship between percent swell and matric suction (After Cokca and Birand 2000).

2.6.2 Environmental conditions:

The environmental factors that influence the volume change behaviour of intrinsic expansive soils are illustrated in Fig 2.16 as defined from literature. Also included in the pictorial diagram is the intrinsic factors discussed above. In the absence of the intrinsic factors, expansive minerals will not undergo volume change thus; the intrinsic and environmental factors complement each other for a change of volume to occur in soils (Nelson and Miller 1992; Snethan et al. 1975).

2.7 PHYSICOCHEMICAL PROPERTIES OF EXPANSIVE SOILS

Adsorbed/pore fluid ions and cation exchange capacity have been identified as a major physicochemical properties influencing expansive soil behaviour.

Adsorbed ions: The process of soil heaving is mainly caused by the intercalation of water molecules into the inner layers of smectitic clay minerals (McKenzie and Anderson 1998) thus, the nature of adsorbed ions play a vital role. Clay minerals have a net negative surface charge due to isomorphous substitutions in the mineral lattices. These negative surface charges are balanced by counterions (opposite charge ions). The type of countertions adsorbed on to the negative surface of clay influences their hydration properties thus, the swell potential of soil. The counterions commonly
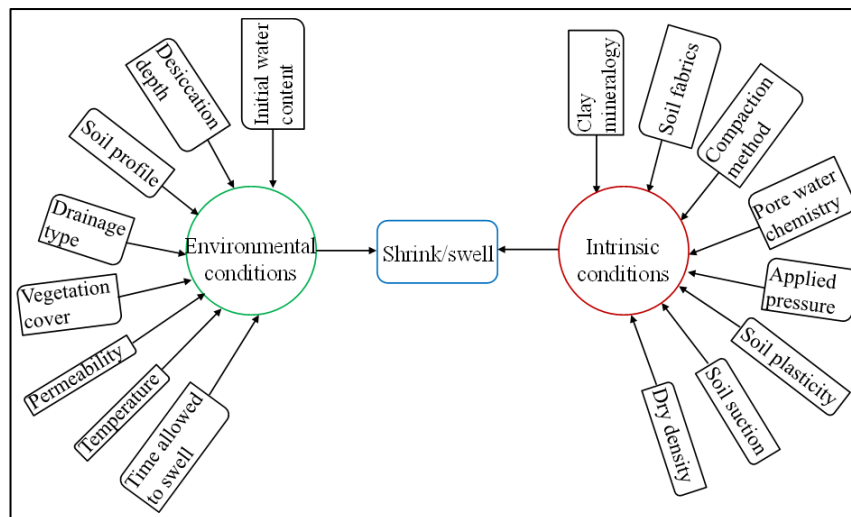
Figure 2.16: A pictorial representation of the intrinsic and environmental factors influencing the swell behaviour of expansive soils

present in pore fluid of expansive soils in order of increasing ionic radii are Li^+, Na^+, H^+, K^+, Mg^{2+}, Ca^{2+} among others (Grim 1968). In the presence of water, these ions hydrate and increase in size. The smaller the ionic radius, the greater the amount of hydration thus, a greater volume change phenomenon (McKenzie and Anderson 1998). This is the basic mechanism why sodium smectite undergo greater volume change than a smectite saturated with calcium, for example (Fig 2.17 and 2.18).
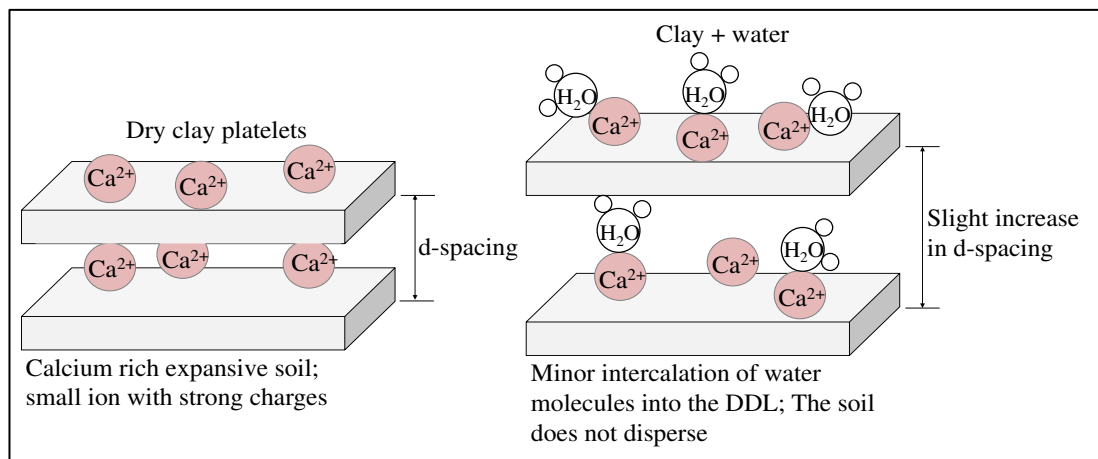
Figure 2.17: The reaction of calcium rich clay to the addition of water (After McKenzie and Anderson 1998)

Cation exchange capacity: The quantity of exchangeable cations in a soil is termed the cation exchangeable capacity (CEC) and is usually expressed in milliequivalents (meq) per 100 grams of dry soil. Typical CEC values of clay minerals are illustrated in Table 2.2. Due to isomorphous substitutions in the lattices of clay minerals, clay surfaces are negatively charged. These negatively charged surfaces are neutralized by counterions. These counterions are not firmly held on clay surfaces in the presence of a fluid (e.g. water) and are subject to exchange by ions in the soil solution. The ease of cation replacement depends on the followings (Israelachvili 1991).

1)   Primarily on the valency (higher valency cations replaces cations of lower valency)

2)   Ion size (cations with larger non-hydrated radii or smaller hydrated radii have greater replacement power) and

3)   Relative amount (high concentration of Na^+ can replace Al^{3+} at low concentration).

For example, the monovalent cations (Na^+, K^+, H^+ etc) could be replaced by the divalent cations (e.g. Ca^{2+}) from soil solution (Fig 2.19). This result in the modification of the DDL (reduction in DDL thickness) and allow improved attraction between particles which stick together in floccs − a process known as flocculation. Generally, the expansive properties of clay minerals increase with increasing CEC. The replacing capacity of cations is in accordance with the Lyotropic Series, $Li^+ < Na^+ < H^+ < K^+ < NH_4^+ < Mg^{2+} < Ca^{2+} < Ba^{2+} < Al^{3+} < Fe^{3+} < Th^{4+}$ (Mitchell and Soga 2005). In other words, any cation will tend to replace cations towards the left and also monovalent cations are generally replaced by multivalent cations.
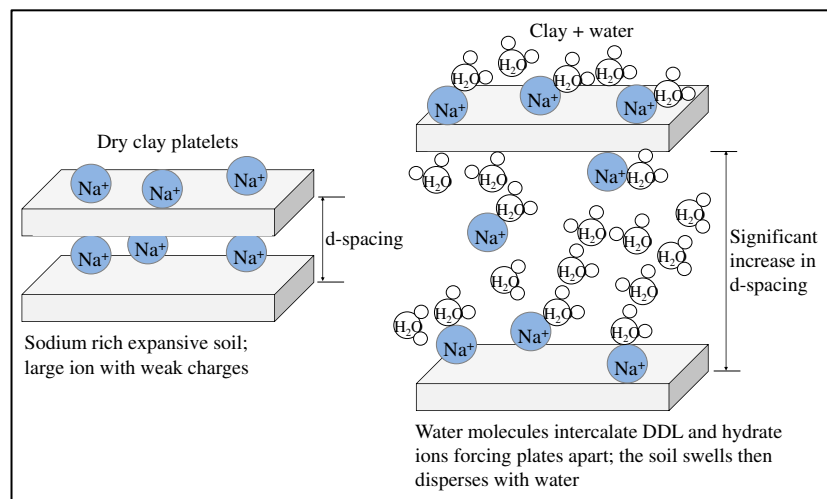
Figure 2.18: The reaction of sodium rich clay to the addition of water (After McKenzie and Anderson 1998)
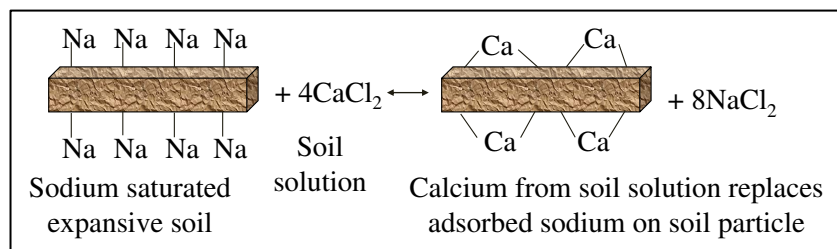
Figure 2.19: Cation replaceability capacity of sodium dominated soil (After Mitchell and Soga 2005)

Table 2:2: Ranges of cation exchange capacities of various clay minerals (After Chen 1988)

Soil parameters	Kaolinite	Illite	Montmorillonite
Particle thickness	0.5-2 μm	0.003-0.1 μm	Less than 9.5Å
Particle diameter	0.5-4 μm	0.5-10 μm	0.05-10 μm
Specific surface (sq. meter/gram)	10-20	65-180	50-840
Cation exchange capacity (milliequivalents per 100g)	3-15	10-40	70-80

2.8   GLOBAL DISTRIBUTION OF EXPANSIVE SOILS

It is estimated that more than 2.4 million km^2 of expansive soils are distributed throughout the world. Extensive deposits of such soils have been reported in Australia ($800000km^2$), India ($730000km^2$), and Sudan ($500000km^2$) among others (Buol et al. 1997). In the United States, the largest deposits are found in the southern states where over $100000km^2$ of the Houston Black clay (Ustic Pellustert) dominates the landscape. In addition, over $28000km^2$ of smectitic rich soils have been reported in the western parts of the U.S including $10000km^2$ in California (Buol et al. 1997). More than half of the soils in the desert and semi-arid areas around the world are dominated by smectite rich soils. Such environments contain high Si and basic cations with minimal leaching; conditions favourable for smectite mineral formation and/or preservation (Jackson and Sherman 1953). In regions of expansive soil deposits, the evaporation/evapotranspiration rate is higher than the annual precipitation so there is usually a moisture deficiency in the soil. The deficiency in rainfall leading to the lack of leaching processes is believed to have aided the formation of smectite minerals in semi-arid zones of the world (Chen 1988). Chen (1988) noted that expansive soil deposits could be found in almost all underdeveloped countries of the world if only research could be conducted.

These soil deposits are not an isolated curiosity as demonstrated in Fig 2.20 (Donaldson 1969). However, after 1969, several other countries have reported occurrence of such soils and some devastating effects on infrastructure thus; Fig 2.20 is modified to suite present day situations. The literature is inundated with documented problems from Australia, UK, USA, Canada, Canada, France, China, Japan, Argentina, Burma, Cuba, Ethiopia, Nigeria, Ghana, India, Isreal, Iran, Mexico, Morocco, South Africa, Spain, Brazil, Turkey, Venezuela, Cyprus, Jordan, Saudi Arabia, Oman, Sudan, Botswana, Kenya, Tanzania, Chad, Puerto Rico, Indonesia, Taiwan, and Zimbabwe (e.g. Krohn and Slosson 1980; Snethan et al. 1975; Chen 1988; Donaldson 1969; Buol et al. 1997).

2.8.1 *Distribution of expansive soils in Australia*

In Australia, expansive soils are located discontinuously within eastern longitudes of 112.76^0-122.08^0 and 133.12^0-152.45^0 and are notorious for posing a wide range of problems on infrastructure. Hubble (1972) estimated that expansive soils in Australia include some $750000km^2$ of "grey and brown soil of heavy structure" and $330000km^2$ of "black earth". In a similar study, Cameron et al. (1987) opined that about 20% of the Australian ground surface could be classified by moderately to highly expansive soil (Fig 2.21) with related damages ranging from minor cracking to irreparable destruction of buildings in cities and region al areas.

Expansive soils are commonly referred to as Vertosols in Australia (Australian Soil Classification terminology) or Vertisols in the United States. Vertosols are the most common soil types in Queensland, Victoria, Southern Australia, and New South Wales (Hubble 1972). A large belt of such soils run from the New South Wales border to Charters Towers—corresponding with Brigalow forests (McKenzie and Anderson 1998). In Victoria, Jenken (1999) reported the occurrence of expansive soils at the Murray basin plains, the central highlands, the western district plains, and the southern uplands and lowlands. According to Rankin and Fairweather (1978) there is overwhelming occurrence of such soils at the Darling Downs, Queensland and the deposit extend within the 250-1000mm isohyets, covering the North-Western states through the eastern states and into the South-East.
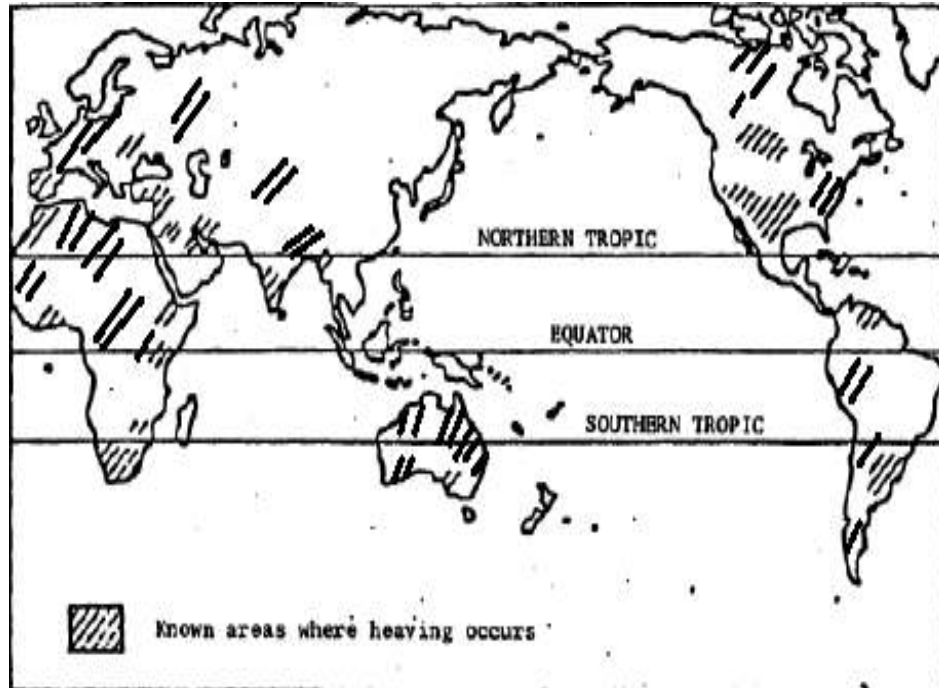
Figure 2.20: Global distribution of expansive soils (Modified after Donaldson 1969)

2.9   EXPANSIVE SOIL CHALLENGES

Damage on infrastructure (e.g. roads, parking lots, homes, tunnels, service pipelines, industrial/commercial buildings, and swimming pools) founded in/on expansive soil has been extensively reported by several authors around the world. For example, in Canada - (Fredlund and Rehardjo 1993), USA - (Jones and Holtz 1973; Krohn and Slosson 1980); Australia - (McManus et al. 1983; 2003; 2004; Richard et al. 1983; McManus and De Marco 1996; Cameron 2001; Walsh et al. 1998; Fityus et al. 2009), India - (Chaudhary 2011), South Africa - (Williams et al. 1985); UK - (Jones and Jefferson 2012); Other parts of Europe - (Entwisle and Kemp 2003), Nigeria – (Ola and Omange 1987), Middle East - (Al-Rawas and Goosen 2006), South America – (Furtado 2010).
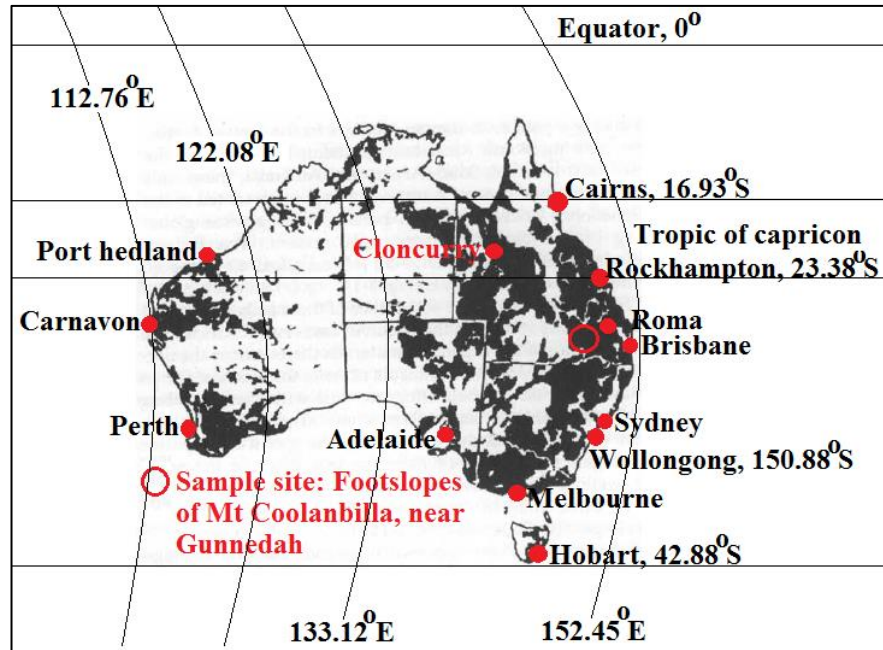
Figure 2.21: Australia map of expansive soils (Not drawn to scale; modified after Steinberg 1998)

There are reports of damage to a Saudi Arabian King's palace in the Middle East (Steinberg 1998) due to differential soil surface movement. A review of the literature gives a global concern of the challenges these soils present. Expansive soils are known in every US state (Fig 2.22a). Much of this soil is located in highly populated regions of both California and Texas and there are reports of damage to private homes in the Texas Gulf coast to the Imperial Valley of California (Steinberg 1998). The American Society of Civil Engineers estimates that 1/4 of all homes in the United States have some damage caused by expansive soils.

According to Krohn and Slosson, (1980) the annual cost of expansive soil damage in the US is about $7.0 billion. Wray (1995) conducted a damage survey in Dallas County, Texas, and identified 8,470 residential foundation failures in only one year, 98% of which occurred in expansive soils. Structural damage caused by expansive clay soils in the United States annually exceeds that caused by earthquakes, hurricanes, and floods combined (Jones and Holtz 1973). In fact, Krohn and Slosson (1980) argued that shrink-swell problems were the second most likely problem a homeowner would encounter, after insects.

In Canada, expansive clay problems are strongly evident in the interior plains of the prairie provinces of Saskatchewan, Manitoba, and Alberta states (Fig 2.22b). Though there areal extent is limited (less than 1% of the land area of Canada), their impact is greatly felt (Chen 1988). Hamilton (1965) reported a 6 inches basement floor movement of shallow foundation buildings in 18 months due to differential uplift pressures. In Saskatchewan, Ching and Fredlund (1984) reported on the impact of swelling clays on a small town; Eston. Their investigation showed that the soil in Eston is extremely expansive and that a school building experienced approximately one meter of heave during its history. Expansive soils constitute a significant hazard to engineering construction in terms of their ability to swell or shrink in the United Kingdom (Fig 2.23a) (Jones and Jefferson 2012).

According to Williams et al. (1985), expansive clays are widely found in South Africa (Fig 2.23b). The hazard these expansive soils create can be significant, except they are recognized and mitigated. They have been reported to disrupt supply lines (i.e. roads, power lines, railways, and bridges) and damage structures. Serious problems associated with heaving of such soils have been reported in various areas such as Johannesburg, Leeuhof, Vereeniging, and Pretoria in Transvaal on fluvio-lacustrine deposits.

2.10 RECOGNITION AND CLASSIFICATION OF EXPANSIVE SOILS

It is important that expansive soil deposits are recognized prior to construction in order to take proactive measures in minimizing associated threats to infrastructure. Snethan et al. (1975) discussed two main methods of recognition of potentially expansive soils. These methods include;

- ➢ Direct identification and
- ➢ Indirect measurement methods
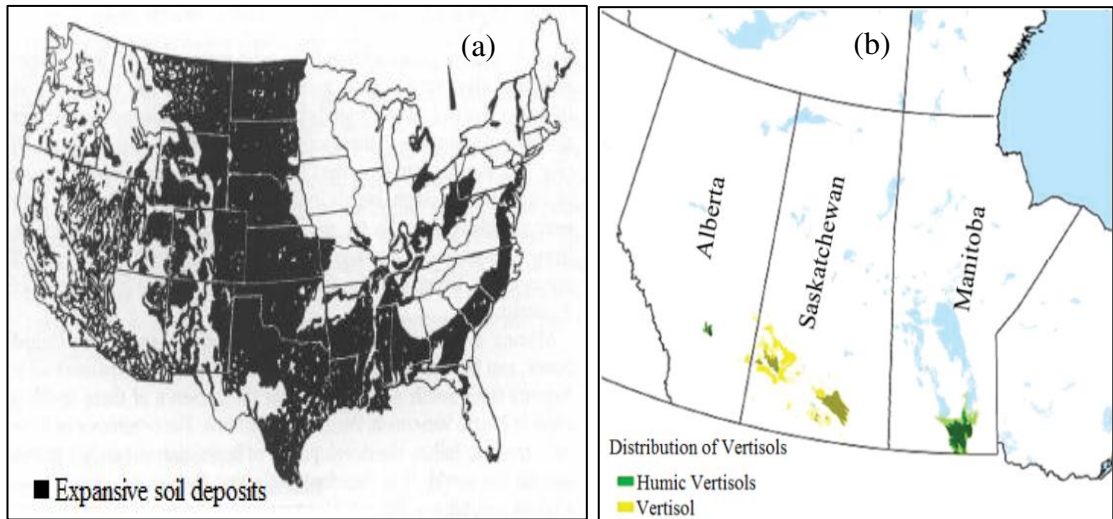
Figure 2.22: a) Expansive soils in the United States (After Steinberg 1998), and b) Expansive soils in Canada (After Brierley et al. 2011)
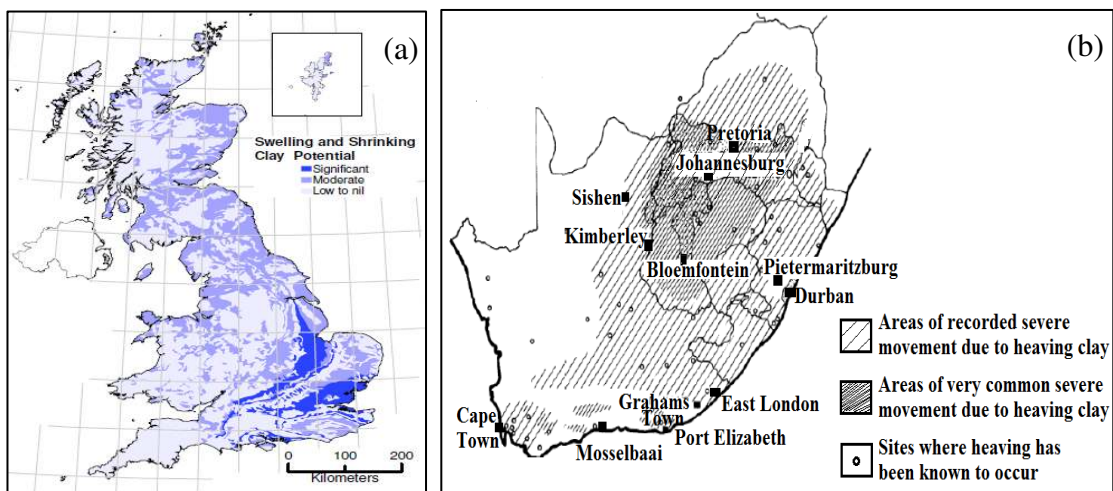
Figure 2.23: a) Shrink/swell potential map of the UK (After Jones & Hobbs 2004), and b) Expansive soils in South Africa (After Williams et a. 1985)

2.10.1 *Direct technique*

This method includes the quantitative evaluation of the swelling characteristics of a soil sample. In other words, it involves the actual measurement of swell potential using the conventional one-dimensional oedometer test apparatus or field measurements. Table 2.3 (reproduced after Snethan et al. 1975) defines and describes some of the direct measurement procedures for percent swell and swell pressure determination of both undisturbed and remoulded soils.

44

Table 2:3: Direct techniques for quantitatively measuring volume change in expansive soils (Reproduced after Snethan et al. 1975)

Method	Description	Reference
Navy method	Odometer test on remolded or undisturbed samples in which deformations under various surcharges are measured to develop a surcharge versus percent swell curve. The surcharge versus percent swell curve is related to the depth of clay versus percent swell curve from which the magnitude of volume change is calculated as the area under the curve	Dept. of the Navy, Design Manual DM-7, (1971)
Potential vertical rise (PVR)	The correlation of measured volumetric swell of a triaxial specimen (all around pressure of 1 psi) with classification test data (LL, PI, SR, and percent soil binder) to determine the Family Number (predetermined correlations) for the soil. The vertical pressures at the midpoints of strata are calculated and used in conjunction with Family Curves to obtain percent volumetric swell under actual loading conditions in each strata. The linear swell is take" as one-third of the volumetric swell which is cumulatively summed to calculate the potential vertical rise	McDowell (1959)
Noble method	Odometer test on statically compacted samples (total four, two initial moisture contents under two surcharge pressures) measuring deformation. Previously correlated data are consulted to determine the magnitude of volume change with changing loading and initial moisture conditions	Noble (1966)
Double oedometer	Odometer test in which two adjacent undisturbed samples are subjected to differing loading conditions. One sample is inundated and allowed to swell to equilibrium, then consolidation-tested using routine procedures. The second sample is consolidated-tested using routine procedures at its natural moisture content (NMC). The virgin portion of the NMC curve is adjusted to coincide with the swell consolidation curve, and relationships from consolidation theory are used to estimate volume change	Jennings (1961)
Simple oedomeer	Odometer test using one undisturbed sample which is loaded to its in situ overburden pressure the" unloaded to & seating load, inundated, and allowed to swell to equilibrium, the" consolidation-tested using routine procedures. Analytical procedures are Same as double odometer method	Jennings (1973)

Sampson et al.	Odometer test in which two undisturbed or remoulded samples are subjected to different loading conditions. One sample is loaded to the testing machine capacity (32 tsf reported) and consolidated to equilibrium, inundated, unloaded to 0.1 tsf, and allowed to swell to equilibrium. The second sample is loaded to its in situ overburden pressure, inundated, unloaded to the planned structure load, and allowed to swell to-equilibrium. The swelling index and changes in void ratio and consolidation theory are used to determine amount of volume change	Sampson et al. (1965)
Lambe and Whitman	Odometer test in which undisturbed or remoulded samples are consolidation-tested using routine procedures including rebound. Effective stresses are calculated before and after testing, and the associated void ratio changes are determined. From this $\Delta e/L+e_o$ or AH/H^* versus depth curves are plotted. Magnitude of volume change is equal to area under the curve (NOTE: A = height)	Lambe and Whitman (1959)
Sullivan and McClelland	Odometer test in which a" undisturbed sample is loaded to its in situ overburden pressure, inundated, and swell pressure measured by maintaining constant volume, then unloaded to a light seating load and the swell measured. Changes in void ratio are taken from the curve corresponding to the initial and final effective stress conditions of the in situ soil. Consolidation theory is used to estimate volume change	Jennings (1969)
Komornik et al.	Odometer test on undisturbed samples in which swell is measured under corresponding overburden pressures to develop depth versus percent swell curve. Magnitude of volume change is equal to area under curve	Komornik et al. (1969)
Wong and Yong	Same as previous procedure except that a "additional surcharge equal to the pore water suction at hydrostatic conditions is added. Same analytical procedures	Wong and Yong (1973)
Expansion Index (Orange county)	Odometer test on compacted samples measuring volume change under l-psi surcharge	Krazynski (1973)
Third cycle expansion pressure test	Used in conjunction with standard R-value test. Swelling pressure is measured at the end of the third cycle of volume change development (i.e., swell pressure is developed and relieved twice, then measured after developing the third time)	California Dept. of Highway, 354-B

2.10.2 Indirect identification

Research has demonstrated that the strength of the inner layer bonding, the exchange capacity, and the negative charges on clay surfaces contribute significantly to swell potential of soil. Thus, it is believed that the swell potential of any clay could be estimated by identifying the mineralogical composition of the soil (Chen 1988). Different methods have been developed to identify mineralogical content in clays. The most common techniques include.

- ✓ X-ray diffraction
- ✓ Differential thermal analysis
- ✓ Dye adsorption
- ✓ Chemical analysis
- ✓ Electron microscopy

According to Chen (1988), these methods require specialised expensive equipment as well as an expert for data interpretation thus; it is uncommon in many civil engineering laboratories. The variety of other indirect techniques for qualifying potential volume change in soil is just as numerous and varied as the proponents. The possibility of indirect estimation of the degree of expansiveness from the intrinsic properties of expansive clay is widely reported. For example, the Atterberg limits (plasticity index) tests indicates that the higher the plasticity index, the greater the quantum of water absorbed by the clay soil and hence the greater the percent swell (Chen 1988). Other commonly used correlation parameters include liquid limit, shrinkage limit, colloidal content, and activity. However, in some cases prediction equations are obtained from statistical comparison of measured properties. The most common indirect techniques as proposed by Snethan et al. (1975) are reproduced with additional data in Table 2.4.

Table 2:4: Indirect techniques for recognition/classification of expansive soils (Reproduced after Snethan et al. 1975).

Indicator group property and/or method		Description	Reference
Soil composition	Clay mineralogy by X-ray diffraction	Measure of diffraction characteristics of clay minerals when exposed to x-radiation. Procedure permits qualitative and semi-quantitative identification of clay mineral components based on structural differences between the clay minerals. Solvation techniques identify expansive clay minerals	Hardy (1965)
	Clay mineralogy by differential thermal analysis (DTA)	Identification is based upon exothermic and/or endothermic reactions which occur at particular temperatures. The type of reaction and temperature are functions of mineralogy. Heating rates, grain size, and sample size influence results. Multicomponent samples we difficult to analyze	Machenzie (1957)
	Clay mineralogy by X-ray diffraction	Measure of selective absorption of infrared radiation by hydroxyls in clay minerals. Fair indicator, but not conclusive	Rich and Kunze (1964)
	Clay mineralogy by X-ray diffraction	Qualitative indicator based on selective adsorption of different types of dyes by different clay minerals. Accuracy decreases if more than one mineral is present	Kacker and Gupta (1966)
	Clay mineralogy by X-ray diffraction	Measure of the radiofrequency electric properties of clay-water systems. Dispersion is the measure of the dielectric constant at two frequencies. Good indicator of type and amount of clay minerals. Some problems evolve when mixtures of different expandable	Basu and Arulanandan (1993)

		minerals are present in the soil	
Physico-chemical	Cation exchange capacity	Measure of the ion adsorption properties of clay minerals. CEC increases from a minimum for keolinite to a maximum for montmo~illonite. Good indicator of hydration properties of clay minerals	Gupta et al. (1967)
	Exchange cations	Measure of the type of cations adsorbed on the clay minera1s. Does not directly relate to swell potential but rather to the expected degree of swell from ion hydration	Diamong and Kinter (1958)
Physical	Colloidal content from hydrometer analysis	Measure of percent by dry weight basis of particles less than 1 micron in size. Indicator of amount of clay but no reference to type of mineral. Not conclusive	Millot (1970)
	Specific surface area of clay particles	Measure of available clay mineral surface area for hydration. Fair indicator of amount of clay mineral and to some extent the type, since montmorillonite minerals are very fine and result in large specific surface areas for given samples	Johnson (1969)
	Soil fabric by electron microscopy	No direct measure of swell potential. Primarily used for studies of the influence of soil fabric on volume change	Seed and Chan (1959)
	Structure by X-radiography	Good for determining the extent of cracks and fractures of undisturbed materials which will influence moisture movement. NO direct measure of swell potential	Krinitzsky (1970)
Index properties	Atterberg limits	Measures of the plasticity and shrinkage characteristics of cohesive soils. Liquid limit (LL) and plastic index (PI) correlate reasonably well with swell potential primarily because there 8re good correlations between them and the type and amount of clay	Holtz and Gibbs (1956)

		minerals present. For shrinkage limit and shrinkage index (LL-SL) the property of volume reduction is correlated with swell potential because of similarities between the phenomena. Some of the published classifications based bn Atterberg limits	
	Linear shrinkage	Measure of shrinkage from a given moisture content. Reasonably good indication of swell potential	Altmeyer (1955)
Soil activity	Soil activity	Active clays provide the most potential for expansion. The three classes of clay according to activity are inactive for activity less than 0.75; normal for activity between 0.75-1.25; and active for activity greater than 1.25.	Skempton (1953)
Soil classification system	AASHO	A-6 and A-7 and borderline soils to A-4, A-6, and A-7 generally have high swell potentials	ASSHTO (1974)
	SCC	Pedological classification system in which the vertisol order is by expansive soils	SCC (1970)

Nayak and Christensen Method

$$S_P = \left(2.29 \times 10^{-10}\right)\left(PI\right)^{1.45} \frac{C}{W_1} + 6.38$$

Where; S_p = predicted swell percent; PI = plasticity index; C = clay content; and W_1= initial moisture content

$$P_p = \left(3.5817 \times 10^{-2}\right)\left(PI\right)^{1.12} \frac{C}{2} + 3.7912$$ Where; P_p = predicted swelling pressure

Seed et al. (1962) Method

$$S = KC^X$$

Where, S = percent swell (%) under 1psi surcharge, C = clay content, X = an exponent depending on clay type, and K = coefficient depending on clay type

2.11 EXPANSIVE SOIL CLASSIFICATION METHODS

Several research workers have used the outcomes of indirect and direct identification procedures to provide classification schemes with regards to severity of volume change in soils. However, a universal standard procedure is yet to evolve hence, classification schemes are usually based on locations (Nelson and Miller 1992). Depending on the proponent, the severity of volume change or quantitative estimates of volume change are described as either low, medium, high, very high, extremely high or CH or A6 among others. The proceeding paragraphs are dedicated to the widely published classification schemes.

2.11.1 *Seed et al. (1962) and Hotz/Gibbs (1956) methods:*

Based on oedometer test, Hotz and Gibbs (1956) and Seed et al. (1962) classified the relative expansivity of swelling soils as illustrated in Table 2.5.

Table 2:5: Classification of expansive soil

Degree of expansivity	Holtz and Gibbs' classification of swell percent (undisturbed soil under 6.9kPa surcharge)	Seed et al., classification of swell percent (remoulded and compacted soil at OMC and MDD, under 6.9kPa)
Low	0 – 10	0 – 0.15
Medium	10 – 20	1.5 – 5
High	20 – 35	5 – 25
Very high	>35	>25

2.11.2 *Bureau of reclamation (Holtz 1959) and Altmeyer (1955) methods:*

The Bureau of reclamation method was developed by Holtz and Gibbs (1956). It involved a direct correlation between soil volume change and several soil properties (i.e. clay content, plasticity index and shrinkage limit). The **Altmeyer's technique** used linear shrinkage and shrinkage limits to quantify possible percent swell of soil (Table 2.6).

2.11.3 Federal Housing Administration (PVC; 1960) and Chen (1965) methods:

Lambe (1960) developed the PVC technique for the Federal Housing Administration (FHA) for the determination of volume change in remoulded samples. This technique is widely used by the FHA and the Colorado State Highway Department (Chen 1988). **Chen (1965)** improved on the USBR method with undisturbed soil samples under a surcharge of 54kPa. The degree of expansion related to Chen's rating is illustrated in Table 2.7.

Table 2:6: Expansive soil classification systems (After USBR 1959 and Altmeyer 1955)

United State Bureau of Reclamation (USBR) Method				
Colloid content (<1μm) (%)	Plasticity index (%)	Shrinkage limit (%)	Probable expansion (under 6.9kPa) (%) for air-dry specimen	Degree of Expansion
<15	<18	>15	<10	Low
13 – 23	15 – 28	10 – 16	10 – 20	Medium
20 – 31	25 – 41	7 – 12	20 – 30	High
>28	>35	<11	>30	Very high
Altmeyer Method				
Linear Shrinkage (%)		Shrinkage limit (%)	Probable Swell (under 31kPa) (%)	Degree of expansion
<5		>12	<0.5	Non-critical
5 – 8		10 – 12	0.5 – 1.5	Marginal
>8		<10	>1.5	Critical

2.11.4 Ladd/Lambe (1961) and Sorochank (1965) methods

Ladd and Lambe (1961) improved on the PVC method by correlating swell index with additional factors such as plasticity index, volume change occurring between field moisture equivalent and the shrinkage limit, moisture content at 100%

humidity, and the volume change occurring between the field moisture equivalent and the shrinkage limit. The researchers then developed a combined PVC rating to measure the degree of expansion of a soil (Table 2.8).

Table 2:7: Expansive soil classification systems (After Lambe 1960 and Chen 1965)

PVC (Federal Housing Administration)	
PVC rating	Degree of expansion
0 – 2	Non-critical
2 – 4	Marginal
4 – 6	Critical
>6	Very critical
Chen Method				

Percent < No. 200 sieve	Liquid limit (%)	Standard penetration blows/foot	Probable expansion (under 54kPa) (%)	Degree of expansion
<30	<30	<10	<1.0	Low
30 – 60	30 – 40	10 – 20	1 – 5	Medium
60 -095	40 – 60	20 – 30	3 – 10	High
>95	>60	>30	>10	Very high

Sorochank (1965) classified the expansiveness of soils by correlating the parameter void ratio at end of swell divided by initial void ratio i.e. e/e_o (or swell index) with plasticity index of soil. A classification scheme was developed as illustrated in Table 2.8.

2.11.5 *Vijayvergiya and Ghazzaly (1973) method*

The method regarded swell index as the ratio of natural moisture content (w) and the liquid limit (LL) of the soil under 11kPa and correlated it with swell pressure. The resulting classification of the degree of expansion is illustrated in Table 2.9

2.11.6 Activity methods:

Skempton (1953) correlated plasticity index and percentage clay content of soil and referred to the parameter as "Activity". He defined this term as follows:

$$\text{Activity} \ = \ \frac{\text{plasticity index}}{\text{\% by weight finner than 3microns}}$$

The resulting classification of the degree of soil expansiveness according to Skempton (1953) is as illustrated in Table 2.10.

2.11.7 Van Der Merwe method (or the South African method):

Van Der Merwe (1964) introduced a classification scheme by grouping the percent swell into "very high and low potential expansiveness" (Fig 2.24). This method is widely used in South Africa to determine the amount of heave in soils perhaps due to the fact that the method was developed locally.

2.11.8 The Australian method

The Australian method assigns a single "site classification" to a soil deposit. The classification gives an indication of the expected amount of surface movement of the soil, which indicates the reactivity of the soil in that particular location. AS2870-2011 (i.e. equation 2.3) is the Australian Standard that deals with Site Classification estimation. It designates a Site Classification that is appropriate to the expected amount of movement at the surface under normal conditions (Table 2.11). It also designates a "P" Classification under abnormal site conditions.

$$y_s = \frac{1}{100} \sum_{n=1}^{N} \left(I_{pt} \overline{\Delta u h} \right)_n \qquad (2.3)$$

Where,

y_s = surface movement, I_p = instability factor, $\Delta \varphi$ = change in soil suction within soil layer, h = height of soil layer.

54

Table 2:8: Expansive soil classification systems (After Ladd/Lambe 1961 and Sorochank 1965)

Ladd/Lambe Method (Surcharge = 9.6kPa)

Combined PVC	Degree of expansion
<2	Noncritical
2-4	Marginal
3-6	Critical
>6	Very critical

Sorochank Method

15<PI<20	20<PI<25	25<PI<30	30<PI<35	35<PI<40	Degree of expansion
<1.12	<1.11	<1..09	<1.08	<1.07	Non swelling
1.12-1.23	1.11-1.21	1.09-1.19	1.08-1.17	1.07-1.15	Slight
1.23-1.39	1.21-1.30	1.19-1.28	1.17-1.25	1.15-1.22	Medium
>1.39	>1.30	>1.28	>1.25	>1.22	High

Table 2:9: Expansive soil classification scheme (After Vijayvergiya and Ghazzaly 1973)

Ratio of w and LL(Surcharge = 11kPa)	Probable swell pressure (kPa)	Probable swell (%)
>0.5	<0.3	<1
0.37-0.5	0.3-1.25	1-4
0.25-0.37	1.25-3.0	4-10
<0.25	>3.0	>10

Table 2:10: Classification of clays according to activity and activity values for clay
minerals (Skempton 1953)

Clay type	Activity
Inactive	<0.75
Normal	0.75-1.25
Active	>1.25

Clay minerals	Activity
Kaolinite	0.33-0.46
Illite	0.9
Montmorillonite (Ca)	1.5
Monntmorillonite (Na)	7.2
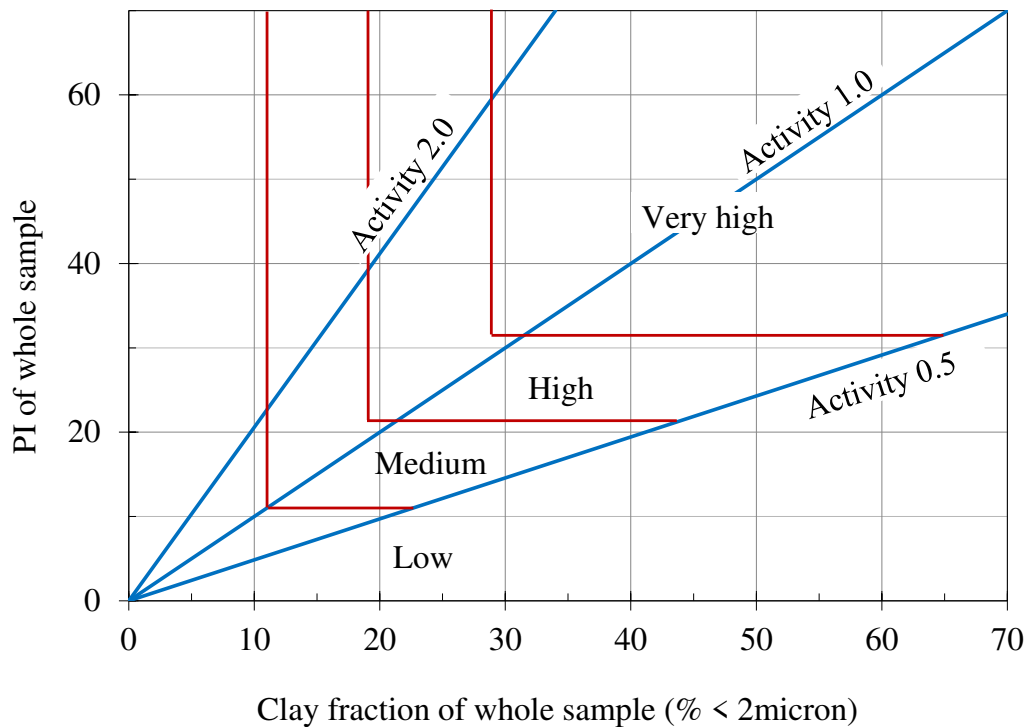
Figure 2.24: Determination of potential expansiveness of soils (After Van der
Merwe, 1964)

2.12 EXPANSIVE SOIL TREATMENT OPTIONS

Soil stabilization is defined as "chemical or mechanical treatment designed to increase or maintain the stability of a mass of soil or otherwise to improve its engineering properties" (ASTM D 653-11). Global research efforts have enabled the engineering community to devise certain chemical and mechanical treatment methods in dealing with expansive soils before and after construction. The treatment procedures that have gained global attention include: soil removal and replacement (Nelson and Miller 1992), surcharge loading (Chen 1988), prewetting (Teng *et al.* 1972), stiffening the super structure (Nelson and Miller 1992), moisture control (Kassiff and Wiseman 1966), remoulding and compacting (Chen 1988), use of soil cushion (Murty and Praveen 2008), Heat treatment (Arioz *et al.* 2008), use of cohesive non-swelling soils (Katti 1978), use of piles (Chen 1988), avoidance of expandable soil deposits (Nelson and Miller 1992), mat foundation (Coduto and Prentice-Hall 1994), and chemical stabilization (Puppala *et al.* 1999; 2003; 2004; Vinod 2010). Among these treatment techniques, chemical stabilization has a very long history in view of its effectiveness and adoptability. Details of these treatment techniques are available as referenced. The intention here is limited to chemical stabilization with traditional admixtures with the aim of establishing the need for a sustainable alternative non-traditional admixture.

2.12.1 *Chemical stabilization of expansive soils*

Chemical stabilization has been used as a method for altering the clay structure in order to prevent or minimize swelling of expansive clays for quite some time now. Huang (1954) compiled a bibliography on expansive soil stabilization and literally hundreds of additives have been tried. Each additive have been proposed to act through various mechanisms such as cation exchange, cation fixation in expanding lattice clays, deactivation of sulfates, waterproofing, cementation, and or alteration in soil permeability (Snethan et al. 1975). The literature suggests that expansive soil properties could be altered by adding other minerals.

The chemical agents used so far include lime, cement, salt, polymers, surfactants, acid, enzymes, fly ash, and alkali-activated blast furnace slag among others. Among

several chemical techniques adopted to overcome the menace of these soils, lime admixture continues to be the most effective and widely used additive (Al-Rawas and Goosen 2006) followed by cement. The cache of previous studies covering cement and LS admixtures are reviewed in the following pages.

Table 2:11: Classification by characteristic surface movement (y_s) (After AS 2870-2011)

Characteristic surface movement (ys) mm	Site classification	Foundation
$y_s = 0$	A	Most sand, gravel and rock sites. These sites have no expected movement with moisture variation
$0 < y_s \leq 20$	S	Slightly reactive sites which exhibit only slight ground movement with moisture variation
$20 < y_s \leq 40$	M	Moderately reactive clay or silt sites, exhibit moderate ground movement with moisture variation.
$40 < y_s \leq 60$	H_1	Highly reactive sites exhibit high amounts of ground movement with moisture variation.
$60 < y_s \leq 75$	H_2	Highly reactive sites exhibit very high amounts of ground movement with moisture variation.
$y_s > 75$	E	Extremely reactive sites which exhibit greater than 75mm of surface movement. These sites typically demand quite expensive footing systems.
	P	A "P" classification does not indicate a specific Ys value and is described as a "Problem" site. It could be a sight that might experience abnormal moisture conditions with growth or removal of trees, sites prone to ponding, sites prone to collapse or very low bearing capacity, sites prone to mine subsidence, and sites that cannot be classified as normal sites for one reason or another.

2.12.1.1 Cement stabilization of expansive clayey soil

Portland cement is regarded as the "workhorse" of the construction industry. It is a heterogeneous substance comprising four compounds as listed in Table 2.12 (Bergado et al. 1996). On hydration, Portland cement produces calcium aluminate

58

hydrates, calcium silicate hydrate, and large amount of hydrated lime. The effect of Portland cement on clay minerals is to reduce the liquid limit, potential volume change, increased shrinkage limit, increased shear strength, and increased plastic limit thus, the reduction in the plasticity index of the soil (Chen 1988).

Table 2:12: Major mineral constituents of Portland cement (After Bergado et al. 1996)

Compound	Abbreviation	Chemical formula	Conc. %
Tricalcium silicate	C_3S	$3CaO.SiO_2$	$60 - 70$
Dicalcium silicate	C_2S	$2CaO.SiO_2$	$10 - 20$
Tricalcium aluminate	C_3A	$3CaO.Al_2O_3$	$5 - 10$
Tetracalcium alumino-ferrate	C_4AF	$4CaO.Al_2O_3.Fe_2O_3$	$3 - 8$

Mechanisms of soil cement stabilization

The fundamental mechanisms of soil-cement stabilization has been reported by several authors (e.g. Mitchell and Songa 2005; Berdago et al. 1996). The mechanisms are grouped into primary and secondary reactions as discussed below.

Primary reactions (Hydraxtion)

On addition of cement into a soil, pore water comes into contact with the cement and initiates hydration reaction. Hydration reaction in cement occur rapidly and primary cementitous products such as hydrated calcium silicates (C_2SH_x, $C_3S_2H_x$), hydrated calcium aluminates (C_3AH_x, C_4AH_x) and hydrated lime $Ca(OH)_2$ are formed (Lea 1956, cited in Bergado et al. 1996). Hydrated calcium silicates and calcium aluminates are the two primary cementitious products whereas; the hydrated lime is deposited as a separate crystalline solid phase. During these processes, the dissolution of alkalis and corresponding initial heat-evolution occurs within minutes,

during which time, a semi-permeable film of hydration products coat the surface of the cement grains and bind adjacent cement grains together during hardening and form a hardened skeletal matrix which is believed to enclose unaltered soil particles (Broms 1984, cited in Bergado et al. 1996). Due to the heterogeneous nature of cement (Table 2.12), these major four strength producing compounds react at different pace. The stoichiometry of the reactivity of anhydrous phases of cement with water is in the following general order (Cocke and Mollah 1993, cited in Bergado et al. 1996):

$$C_3A > C_3S > C_2S > C_4AF$$
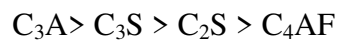
However, the setting of cement can be divided into four stages involving a series of overlapping reactions as the anhydrous phases hydrate.
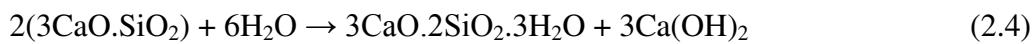
$$2(3CaO.SiO_2) + 6H_2O \rightarrow 3CaO.2SiO_2.3H_2O + 3Ca(OH)_2 \qquad (2.4)$$

(tricalcium silicate + water) $\longrightarrow$ (tobermorite gel + calcium hydroxide)

$$2(2CaO.SiO_2) + 4H_2O \rightarrow 3CaO.2SiO_2.3H_2O + Ca(OH)_2 \qquad (2.5)$$

(bicalcium silicate + water) $\longrightarrow$ (tobermorite gel + calcium hydroxide)

$$4CaO.Al_2O_3.Fe2O_3 + 10H_2O + 2Ca(OH)_2 \rightarrow 6CaO.Al2O_3.Fe2O_3.12H_2O \quad (2.6)$$
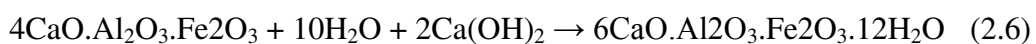
(tetracalciumaluminoferite + water + calcium hydroxide) $\longrightarrow$ (calcium aluminoferrite hydrate)

$$3CaO.Al_2O_3 + 12H_2O + Ca(OH)_2 \rightarrow 3CaO.Al_2O_3.Ca(OH)_2.12H_2O \qquad (2.7)$$

(tricalcium aluminate + water + calcium hydroxide) $\longrightarrow$ (tetracalcium aluminate hydrate)

$$3CaO.Al_2O_3 + 10H_2O + CaSO_4.H_2O \rightarrow 3CaO.Al_2O_3 .CaSO_4.12H_2O \qquad (2.8)$$
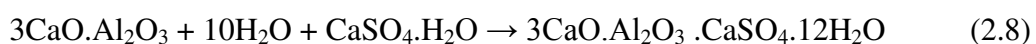
(tricalcium aluminate + hydrogen + gypsum) $\longrightarrow$ (calcium monosulfoaluminate)

It has been reported that the substances in equations 2.4 and 2.8 constitute about 75% of Portland cement (Lea 1956, cited in Bergado et al. 1996). Therefore, the hydration of calcium silicate (C_3S) produces the binding agents of tobermorite gel and hydrated lime. The reaction given below is for tricalcium silicate (C_3S) only, because it is the most important constituent of Portland cement (Bergado et al. 1996).

$$C_3S + H_2O = C_3S_2H_x \text{ (hydrated gel)} + Ca(OH)_2 \text{ (hydrated lime)} \qquad (2.9)$$
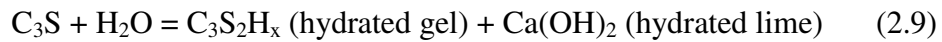
<div align="center">Primary cementitious product</div>

Secondary Reactions (Pozzolanic reactions)

During hydration of cement, the production of C-S-H is accompanied by a rise in pH level of pore water to a range of 12-13, caused by the dissociation of the hydrated lime. This high pH dissolves the silica and alumina from clay and other sources (e.g. quartz). The hydrous silica and alumina so formed slowly react with the calcium ions liberated from the hydrolysis of cement to form insoluble compounds i.e. secondary cementitious products, which hardens with time (Diamond and Kinter 1965, cited in Bergado et al. 1996). The reaction that forms secondary cementitious products that harden when cured to stabilize the soil is known as the pozzolanic reaction (Cocke and Mollah 1993, cited in Bergado et al. 1996). The stochiometry of these reactions are illustrated in equations 2.10 – 2.12 and these reactions can last for months and years after mixing.

$$Ca(OH)_2 = Ca^{++} + 2(OH)^- \qquad (2.10)$$

$$Ca^{++} + 2(OH)^- + SiO_2 \text{ (soil silica)} = CSH \text{ (secondary cementitious product)} \quad (2.11)$$

$$Ca^{++} + 2(OH)^- + Al_2O_3 \text{ (soil alumina)} = CAH \text{ (secondary cementitious product)}$$
$$(2.12)$$
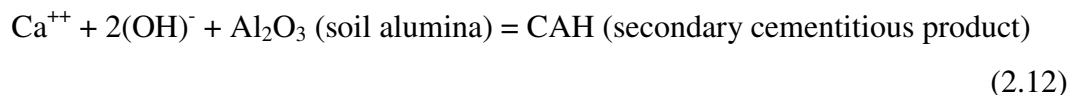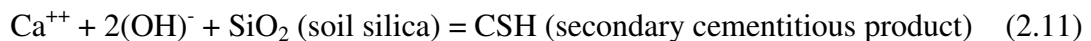
Kamaluddin (1995, cited in Bergado et al. 1996) demonstrated that the unconfined comprehensive strength of a soil increased with increasing curing time due to pozzolanic reactions between $Ca(OH)_2$ in pore fluid and the liberated pozzolans (SiO_2, AlO_2) (Fig 2.25). Based on gradient, the curve was divided into three zones.

The zonal demarcations show the effectiveness of cement stabilization as pozzolanic reactions occur gradually. In a similar study, Saitoh et al. (1985, cited in Bergado et al. 1996) schematically illustrated the conditions of hardening in a cohesive soil when mixed with agent slurry (Fig 2.26a and b). It has been reported that even if a cohesive soil is thoroughly mixed with hardening agent slurry, clay particles will form a cluster, which will be surrounded by the slurry (Bergado et al. 1996). (Fig 2.26a) shows the immediate soil condition after mixing with hardening agent slurry whereas; Fig 2.26b shows the same cohesive soil after pozzolanic reactions has occurred, believed to be responsible in forming hardened cement bodies with subsequent strength improvement.

Factors that control the hardening characteristics of cement treated soils

The literature identified the following factors (Table 2.13) as responsible for controlling the hardening characteristics of cement treated soils. The effectiveness of Portland cement in stabilizing volume change in expansive soils is less in terms of magnitude compared to lime admixture. Chen (1988) argued that the less soluble nature of cement makes it difficult to mix homogenously with fine-soil grains hence, the reduced effectiveness compared to a more soluble lime.
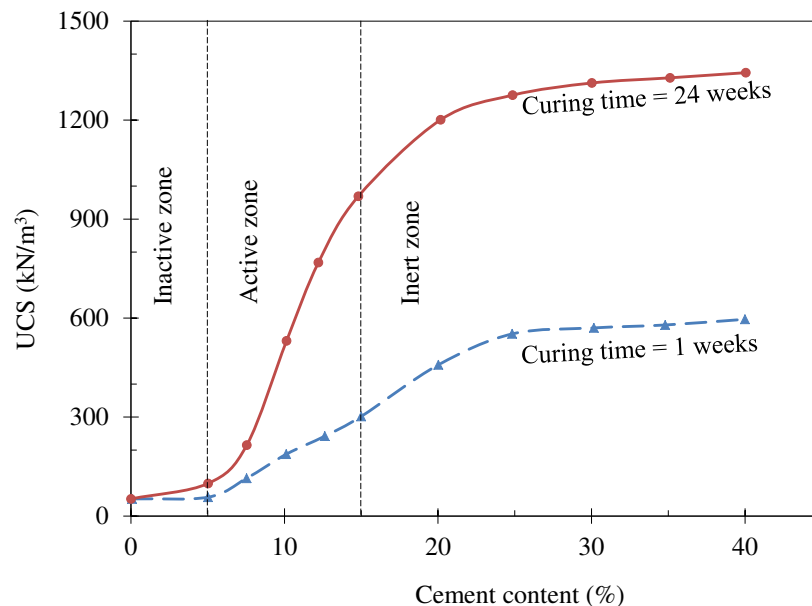
Figure 2.25: Influence of cement content on unconfined compressive strength (After Kamaluddin 1995, cited in Bergado et al. 1996)

62

(a) Immediately after mixing

(b) After hardening

☐ Cement slurry

Cluster of clay particles

▨ Hardened cement body

☐ Hardened soil body
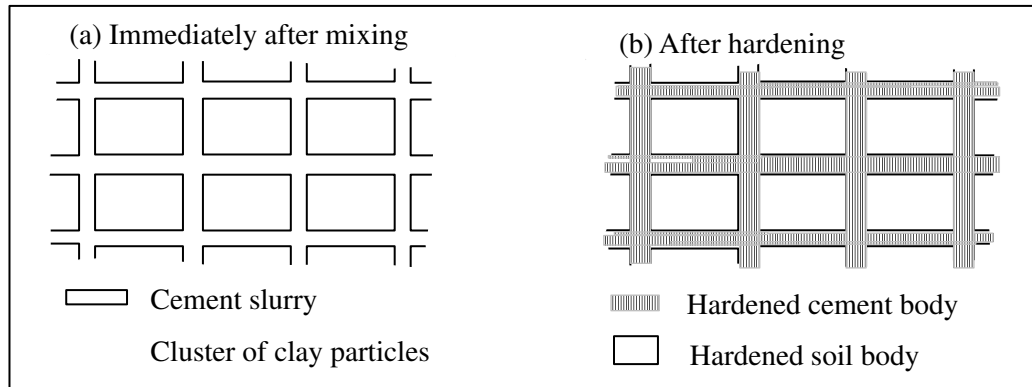
Figure 2.26: a) and b) Schematic illustrations of improved soil (After Saitoh et al. 1985, cited in Bergado et al. 1996)

Jones (1958, cited in Chen 1988) investigated the effect of 2-6% Portland cement content on expansive Porterville clay of California and reported substantial decrease in the volume change characteristics of the soil. Results with lime admixture in the same investigation were reported to be similar with Portland cement treatment. However, it was reported that Portland cement reduced the shrinkage of the air-dried specimens at about 25-50% more than did the lime.

Table 2:13: Factors that affect the hardening characteristics of cement treated clays

Factor	Remarks	Reference
Type of cement	Type III Portland cement has been reported to be more effective in soil stabilization than type I cement, however, type I cement is widely used in soil stabilization.	Bergado et al. (1996)
Cement content	The higher the cement content, the higher the strength growth	Broms 1984
Curing time	The strength of cement treated clays increases with time. The rate of increase in rapid during the early stage of curing. Therefore, the rate of strength increase decreases with time.	Bergado et al. (1996)
Soil type	The effectiveness of cement decreases with increasing water content and organic matter. The improvement decreases with increasing plasticity index of the clay	(Woo1971; Broms 1986).

Curing temperature	Increase in temperature accelerates chemical reactions and solubility of the silicates and aluminantes, thus increasing the rate of strength gain in cement treated soil.	Bergado et al. (1996)
Soil material	The mineral type present in soils affects the pozzolanic reactivity of the chemically treated soils. For example, montmorillonite clay minerals will more active in pozzolanic reactions than kaolinites, illites, chlorides and vermiculite. In general, if improvement conditions are equal, greater strength is obtained from the soil with higher pozzolanic reactivity.	(Hilt and Davidson 1960; Wissa et al. 1965)
Soil pH	Long term pozzolanic reactions are favoured by high pH values, since higher rates of reaction is obtained due to the increased solubility of the silicates and aluminates of the clay particles with soil pH maintained at about 12.6.	Bergado et al. (1996)

2.13 METHODS OF STABILIZATION IDENTIFICATION IN CHEMICALLY TREATED SOILS

Several authors have demonstrated the use of instrumental analytical techniques (e.g. SEM/EDS, XRD, FTIR, CT, NMR, and CEC) in investigating changes in soil mineralogy and fabrics of traditionally treated expansive clays (e.g. Abduljauwad 1995, Al-Rawas and Goosen 2006). Abduljauwad (1995) using X-ray diffractometer reported mineralogical changes and identifiable reaction products on addition of lime to clay soils. It was found that new reflections (new minerals) were visible with d-spacings of 3.87, 3.67, 3.035, 1.619, and 1.582 Å (1Å = 0.1nm), which appeared to be indicative of calcite, feldspars, kaolinite, and chlorite, respectively. Abduljauwad, showed that the major peaks of the clay minerals (i.e., smectite, palygorskite, and illite) of untreated soils were significantly altered upon lime treatment.

Bishop et al. (1994) investigated the nature of water in smectite minerals using infrared spectroscopic analysis technique. The absorptions due to water molecule was studied in smectite exchanged with H^+, Na^+, Ca^{2+}, Mg^{2+}, and Fe^{3+} interlayer cations under varying moisture conditions. They reported changes in absorption

energies due to H_2O stretching vibrations as sample dehydrates. They assigned the absorption bands near 3620cm^{-1} and 3350cm^{-1} to water bonding directly to inner layer cations and surface bonded H_2O whereas, absorption bands near 3450cm^{-1} and 3350cm^{-1} were assigned to additional adsorbed water molecules.

Parfitt and Greenland (1970) investigated the adsorption of water by montmorillonite-polyethylene glycol adsorption products using instrumental analytical techniques such as FTIR and XRD. They reported that when organic compounds are adsorbed by montmorillonite from aqueous solutions, the adsorption products usually contain the organic compound and water in the inner layers of the soil enabling the association with the exchangeable cations. As the organic compound wedged into the inner layers, the mineral lattices swells to accommodate the intercalated polymer admixture. They reported that the intercalation of the polymer initiated the development of weak hydrogen bond between polymer and adsorbed water and inner layer cations. It was concluded that the presence of the polymer did not prevent excessive swelling of the sodium montmorillonite as a result of the weak hydrogen bond that was formed.

In a comprehensive study, Rauch et al. (2003) investigated the mode of stabilization of three representative non-standard admixtures on three reference clays (kaolinite, illite, and montmorillonite) and two native Texas clays (from Bryan and Mesquite, Texas). The microstructural study involved the use of instrumental and chemical analytical tests such as SEM/EDS, XRD, NMR, FTIR, ultraviolet spectroscopy (UVs), ion chromatography (IC), potentiometric titrations, high-performance liquid chromatography/mass spectroscopy (HPLC/MS), and gel permeation chromatography (GPC). These techniques were used for detailed physical-chemical study of the untreated and chemically treated soils to characterize the modes of product reactivity at microstructural level. The interpretation of data obtained from the above techniques enabled the authors to identify the stabilizing mechanisms of each chemical admixture used in each soil.

2.13.1 *Schematic representation of reaction mechanisms of traditional admixtures*

Åhnberg and Johansson (2005) illustrated a rough outline of the chemical processes taking place and the main reaction products formed when mixing common binders such as quicklime, cement, slag and fly ash with soil (Fig 2.27). As expected, the cementing products are all similar because the binders are calcium based.

2.14 HEALTH AND SAFETY CONCERNS IN LIME AND CEMENT (TRADITIONAL) TREATED SOILS

Lime and cement basically make up what is known today as the "standard" or "traditional" or "calcium based" admixtures for expansive soil treatment. However, these traditional admixtures possess intrinsic health and safety concerns. For example, for effective lime or cement stabilization of soil, the soil pH must be greater or equal to at least 10.5 (Eades and Grim 1966, cited in Bergado et al. 1996). Such high alkaline environment is detrimental to fauna and flora (Rollings et al. 1999). The high pH could also affect the longevity of reinforced concrete and steel frame structures founded on such treated soils as it could be prone to corrosion problems (Perry 1977). In engineering practice, brittle mode of failure of any structure is most undesirable. However, cement and lime stabilized soils often exhibit brittle behaviour upon cyclic loading which could greatly affect roadways and aircraft runways (Sariosseiri and Muhunthan 2009).

Industry experience with these traditional admixtures over the years, supported by well documented applications in engineering works have propelled acceptance of this technique by soil engineers' world over. However, if sulphates which are quite common in clay soils are present, calcium reacts with sulphate to form an additional product of hydration known as ettringite ($Ca_6[Al(OH)_6]_2.(SO_4)_3.26H_2O$). In addition, at low temperatures ($<15^0C$) where carbonate is present, thaumasite mineral is also formed (Puppala et al. 2004; Harris et al. 2006).
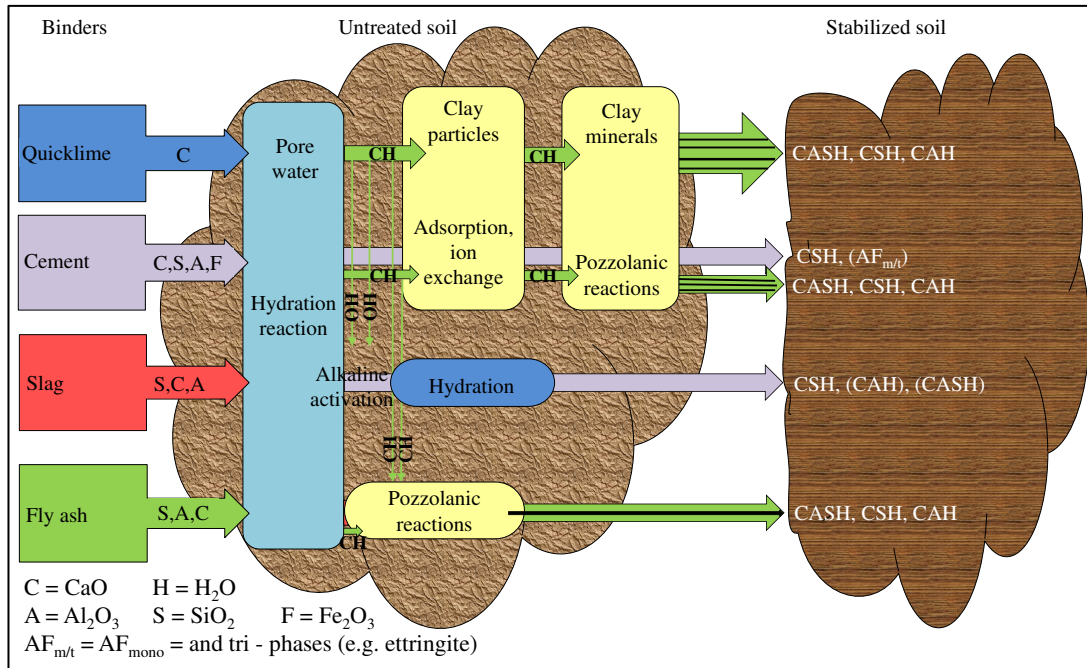
Figure 2.27: An outline of the principal chemical reactions and reaction products formed by different types of binders in a soil (After Åhnberg and Johansson 2005)

Ettringite and thaumasite show very high affinity for water, thus their expansion could cause severe disruption and ultimate failure of infrastructure (Harris et al. 2006). The stoichiometry of the ettringite formation reaction (equation 2.13) is as follows:

$$6Ca^{2+} + 2Al(OH)_4^- + 4OH^- + 3SO_4^{2-} + 26H_2O \rightarrow Ca_6[Al(OH)_6]_2.(SO_4)_3.26H_2O \quad (2.13)$$
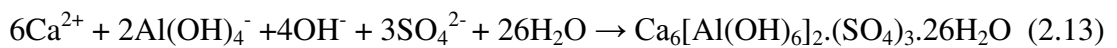
This is a major setback in the use of traditional admixtures in stabilization of sulphate rich soils. Harris et al. (2006) and Cerato and Miller (2014) reported severe damage on infrastructure due to ettringite formation with time in cement and lime treated sulphate rich expansive soil (Fig 2.28 and 2.29), respectively.

Figure 2.28: Vertical heave due to ettringite formation in sulphate bearing soil treated with cement in Texas, USA (After Harris et al. 2006)
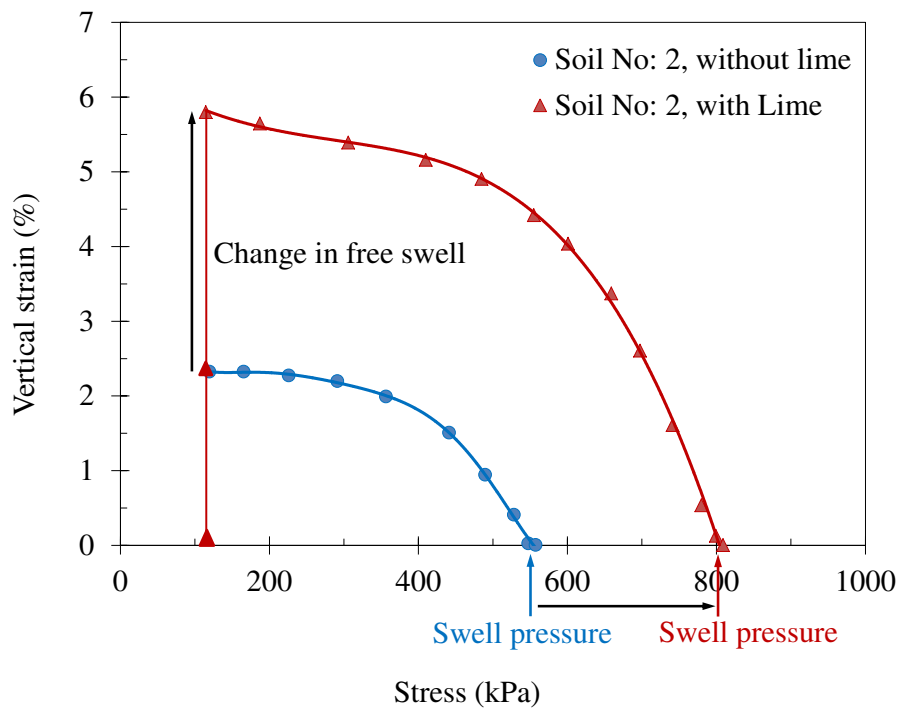
Figure 2.29: A soil rich in sulfate evidencing ettringite formation and induced swelling after lime treatment (After Cerato and Miller 2014).

As per energy and environmental concerns of these traditional stabilizers, WEC (1995) argued that certain intrinsic features of cement manufacturing cause serious problems in modern society. Cement production is a highly energy intensive process, consuming about 2% of the global energy production. The production of one tonne of cement accounts for 0.55 tonnes of carbon (IV) dioxide (greenhouse gas) released into the atmosphere and requires additional 0.39 tonnes of CO_2 in fuel emissions, accounting for a total of 0.94 tonnes of CO_2. Thus, the calcination process contributes about 5% of global anthropogenic CO_2 emissions (Albino et al. (2011).

Another limitation with traditional admixtures is reported by Chen (1988). The less soluble nature of cement makes it difficult to uniformly mix with very fine-grained soils. Larger particles of cement never completely hydrate, thus maximum outcome is never achieved. Additional demerits include the possibility of corrosion problems of the soil is crack formations at low temperatures. Furthermore, cement admixture is poor in stabilizing soils with organic content greater than 2% or soils with pH lower than 5.3 (ACI 230.1R-901990).

It has been reported that lime is highly susceptible to leaching. In a field study, Bhattacharja et al. (2003) reported that percent swell and plasticity index reverted almost to those of untreated soil due to leaching of lime. Thus, lime leaching from surface runoff could wash lime into surrounding areas and damage adjacent vegetation due to the high alkalinity or could pollute groundwater. Callister and Petry (1992) studied the leaching properties of a lime stabilized soil in the laboratory with leach-cells to measure changes in permeability, pH and leachate calcium cation concentration over a period of 90 days. They found that the leachate pH was increased significantly after 90 days of leaching and contained very high calcium content. Increased soil permeability was also reported by the authors upon lime addition. In Civil engineering practice, significant soil permeability is usually undesirable in order to limit internal piping and subsequent soil erosion susceptibility.

2.15 LIGNIN CHEMISTRY

Lignin (derived from the Latin word "Lignum") is one of the principal constituents of wood along with cellulose and hemicellulose. It is a naturally occurring three-dimensional amorphous polymeric material consisting of phenyl propane units along with hydroxyl, methoxyl, carbonyl, and other substitutions (Pearl 1967). Though structural details of the lignin molecule are unknown, it is generally accepted that three alcoholic monomers form the basic building blocks of lignin polymer i.e. coniferyl alcohol, sinapyl alcohol, and *p*-coumaryl alcohol (Fig 2.30) (Lebo 2002). The abundance of functional groups on surfaces of lignin, its susceptibility to chemical modification, cost competiveness, natural stability, and biodegradability are some of the reasons lignin have gained applications in various industries (Harkin 1966). Lignin content in wood stems has been reported at 17 to 32 percent of the weight of moisture-free wood (Heitner 2010). It is considered the second most abundant organic material available on earth behind cellulose. Among other functions, Lignin is known to give the stems their well-known rigidity and resistance to impact, compression, and bending deformations (Theng 1979). Its specific chemical makeup is highly complex. There are several reasons for its complexity. Lignin varies with tree species, climatic conditions, method of production, and locality of growth. Another reason is the difficulty in isolating pure lignin from wood into the free-state (Pearl 1967).

Because it is not possible to isolate native lignin from wood without degradation, the true molecular structure of lignin is unknown (Pearl 1967). It is important to keep in mind however; that the term "lignin" normally refers to a mixture of substances having similar chemical composition but with structural differences (Harkin 1969). For example, Meier et al. (1993) described lignin as a highly cross-linked polymer formed from different sulfonate, hydroxyl, phenolic and carboxyl groups. Some researchers (e.g. Harkin 1969; Cornel University 1951) believe that lignin is a giant polymer molecule with aliphatic and aromatic portions, whose basic unit is derived from phenylpropane; a six carbon benzene ring attached to a straight side chain of three carbon atoms. These units are interconnected in a large variety of ways by carbon-carbon or carbon-oxygen-carbon (ether) bonds (e.g Fig 2.31).

70
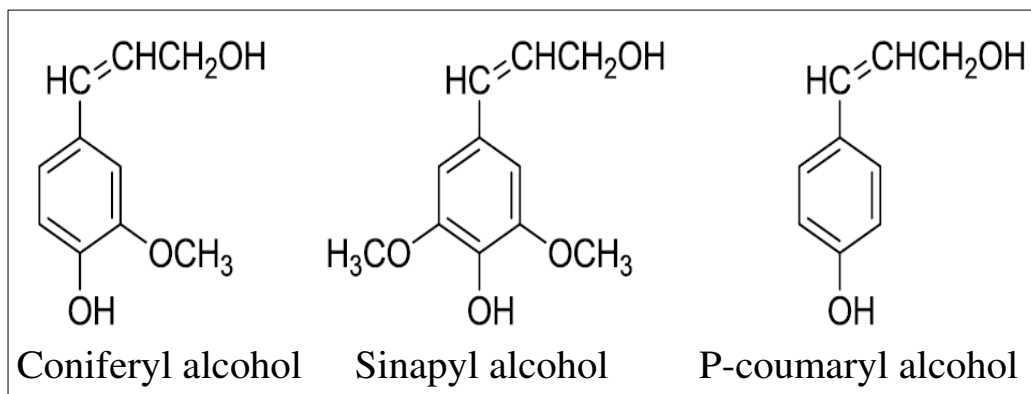
Figure 2.30: Lignin monomeric building blocks (After Lebo 2002)
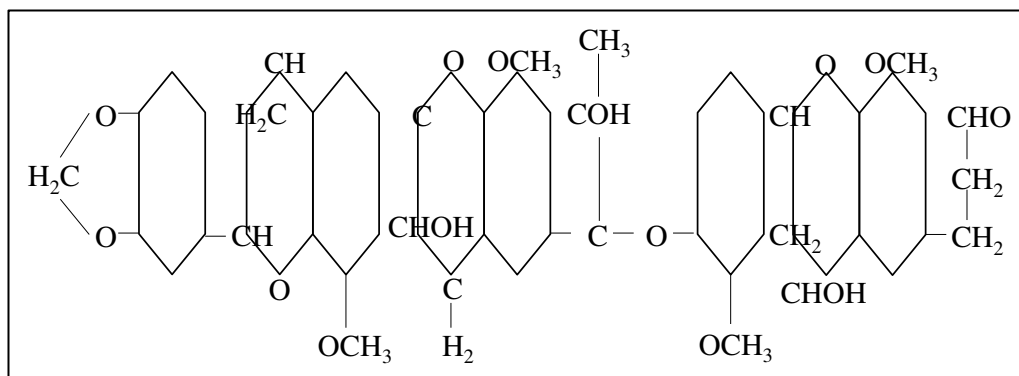
Figure 2.31: A proposed structure of lignin molecule (After Cornel University 1951)

2.15.1 *Preparation of LS during the pulping reaction and its structural properties*

The two principal components of wood are lignin and cellulose. The chemistry of wood pulping primarily involves dissolution of the lignin and isolation of the cellulose. The process is essentially the digestion of wood chips at temperatures between 125-145^{0}C in an aqueous solution of sulphur (IV) oxide and a salt of sulphurous acid such as calcium bisulphite (Pearl 1967).

In course of this cooking (digestion) process, the lignin polymer of the wood reacts with the liquor [sulphur (IV) oxide and a salt of sulphurous acid] to form soluble lignosulfonate in the cooking liquor. However, it has been reported that all water soluble products removed from the wood during pulping are contained in the spent sulphite liquor (a clear fluid that looks like freshly brewed coffee). But the major

71

constituents of these dissolved solids are high molecular weight lignosulfonates (Rydholm 1965, cited in Theng 1979). The dissolved lignosulfonate from the cooking liquor is then isolated from the residual cellulosic pulp by filtration and washing techniques such as ion exchange chromatography, solvent extraction, precipitation by calcium hydroxide, by dialysis, precipitation by quaternary ammonium salts, or salting out method (Forss and Fremer 1965, cited in Theng 1979). It is estimated that the amount of lignin obtained after delignification has an annual industrial output of 50 million tons (Gandini and Belgacem 2008).

LS is water soluble and highly acidic due to the strongly disassociated sulfonic acid groups present in their molecules (Pearl 1967). Its pH value is usually within the range of 2 - 4 and is capable of forming complexes with cations such as Ca, Na and Mg, enabling it to compete for adsorption sites in clays (Sulphite Pulp Manufacturers' Research League (1963). Despite the nebulous concept of LS, a number of structural formulae have been proposed. LS chemical structure as proposed by JECFA (2008) is illustrated in Fig 2.33 whereas; Fig 2.33a and b shows structures proposed by the Sulphite Pulp Manufacturers' Research League (1963) and Vinod et al. (2010), respectively. The surface of a LS molecule contains both negative (hydrophilic sulphite, hydroxyl, carboxyl, and phenolic groups) and positive (hydrophobic aromatic structure) potentials (Adams 1988), but its net potential is negative (Theng 1979). Due to the potential for both negative and positive charges, LS may be able to adsorb both negative and positive ions in soil solution. In addition, LS contain intra-molecular hydrogen bonds which may react with divalent or multivalent metal ions to form covalent coordinate bonds (Pearl 1967).

2.15.2 LS as a soil admixture

As the second most abundant natural polymer in the world, lignin based compounds have often tempted researchers to study their potential for use in novel applications (Indraratna et al. 2008, 2010; 2013; Sinha et al. 1957; Palmer et al. 1995; Vinod et.al 2010; Puppala and Hanchanloet 1999; Bolander 1999; Nicholls and Davidson 1958; Tingle et al. 2007; Athukorala 2013). Its abundance, renewable nature, and environmentally friendliness seem to make it ideally suited for the rising interest in

this waste by-product. However, despite some successes in the use of LS in geotechnical engineering, it is still currently a work in progress.
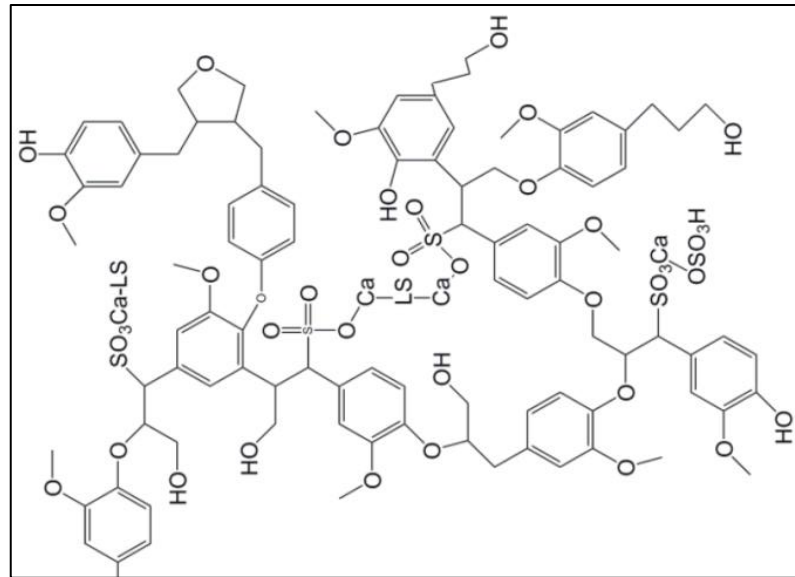
Figure 2.32: Representative structure of calcium lignosulfonate (Redrawn after JECFA 2008)
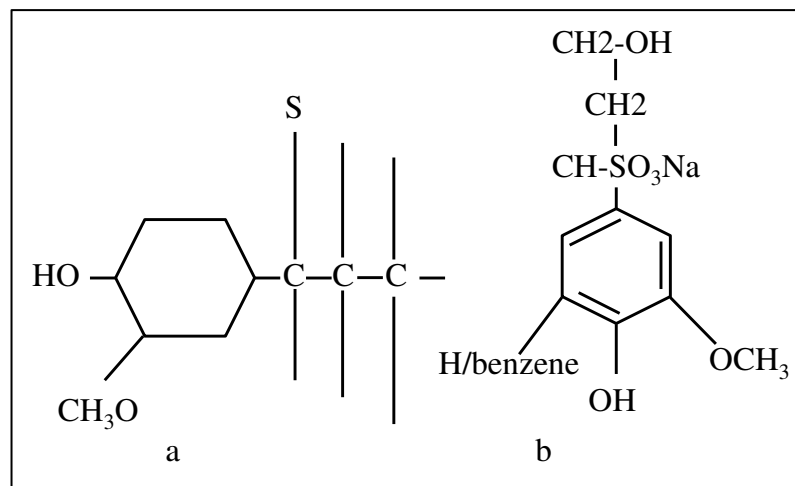
Figure 2.33: a) Binding Units of the LS molecule (After Sulphite Pulp manufacturers' Research League 1963); b) Chemical Structure of LS (After Vinod et al. 2009).

LS is used extensively in the concrete industry. When mixed with concrete it reduces the amount of water required for processing, quicken strength development, and ultimately give the concrete higher strength (Khalil and Ward 1973). In the

petroleum industry, LS is used for the manufacture of oil drilling muds. The LS component reduces the viscosity of a mud thus reducing the energy requirements needed for drilling (Orszulik 2013). The use of LS in agricultural practice has been demonstrated by Gargulak and Lebo (2000) when large scale quantities were used as binders for dust control. In civil engineering practice, road dust is often controlled by spraying LS solutions on road surfaces. Athukorala et al. (2013) also demonstrated that LS is a potential alternative in controlling erosion behaviour of erodible silty soil.

Documented research at the University of Wollongong, Australia, has demonstrated that LS could stabilize erodible soils by binding soil particles together. For example, Indraratna et al. (2010) reported that LS admixture reduced the coefficient of soil erosion and significantly increased the critical shear stress of a silt clay soil (Fig 2.34 and 2.35). They posited that the erosion parameters; critical shear stress and coefficient of soil erosion were better improved by LS admixture than did Portland cement.
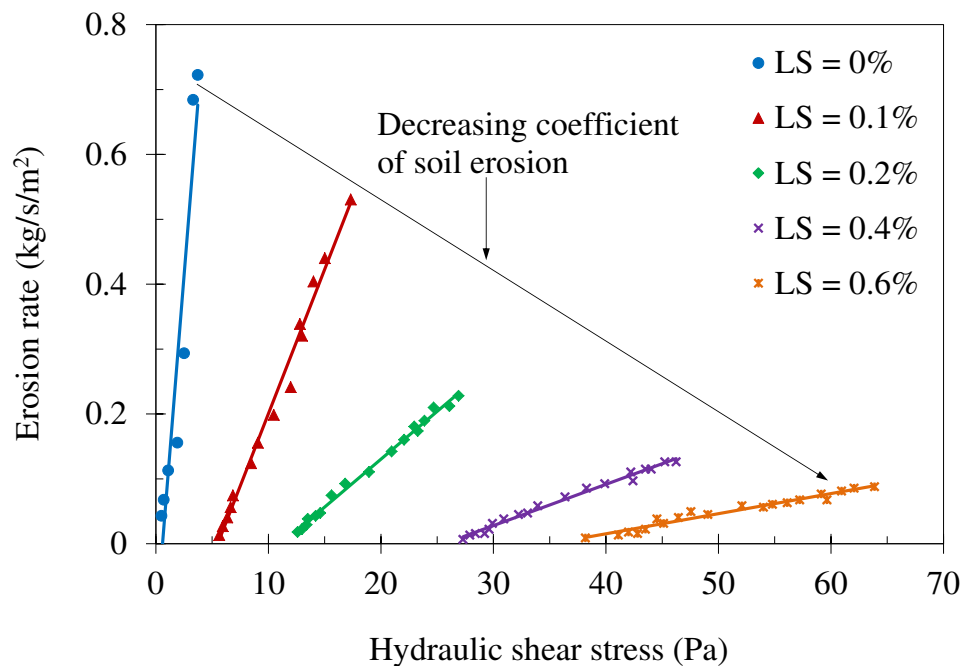
Figure 2.34: Erosion rate versus hydraulic shear stress of LS treated/untreated and cement treated/untreated silty sand (After Indraratna et al. 2010).

74
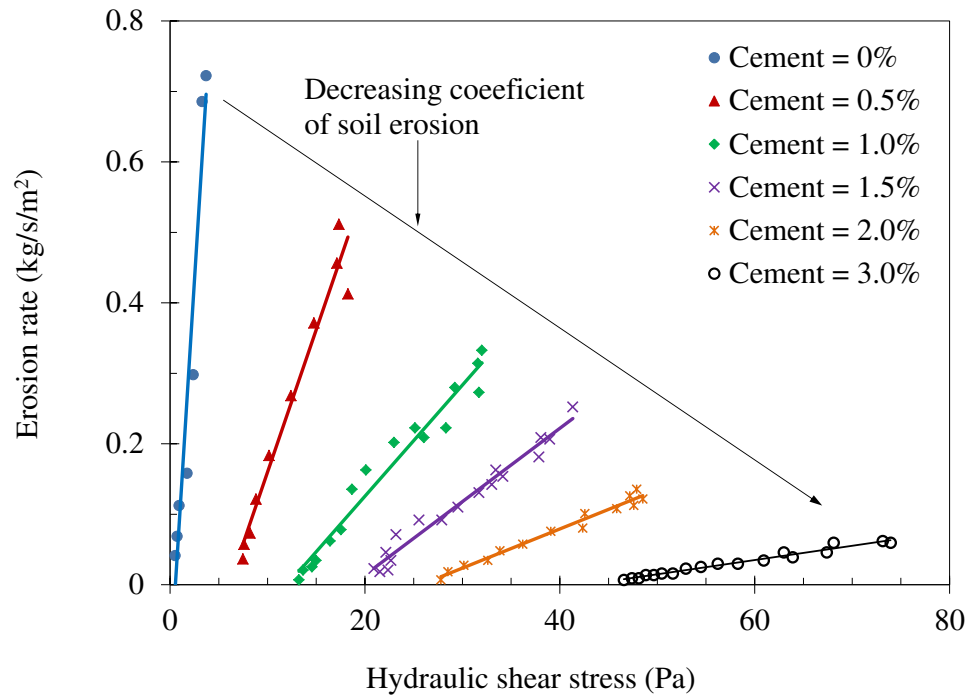
Figure 2.35: Erosion rate versus hydraulic shear stress of LS treated/untreated and cement treated/untreated dispersive clay (After Indraratna et al. 2010).

Laboratory and in-situ soil testing have been carried out to quantify soil stabilization using numerous chemical additives from time immemorial, including lignosulfonate. In one such study, Sinha et al. (1957) investigated the strength behaviour of Iowa loess (silty clay loam) treated with serious LS admixtures and reported that LS alone as admixtures showed little or no growth in strength in the amended silty clay soil. However, they concluded that LS could be much more effective for granular soils or soil aggregate mixtures. In a similarly invetigation, Bolander (1999) investigated the stabilization effects of several soil admixtures including LS. He reported that LS leached out of the material and exhibited low strength gain. On the contrary, Nicholls and Davidson (1958) reported that LS stabilizers contributed to a rapid increase in the strength of soil with an increase in the length of air curing.

Palmer et al. (1995) investigated the strength and density modification of unpaved road soils in the laboratory. The admixtures used in the investigation were LS, $CaCl_2$, and $MgCl_2$ at different concentrations. The admixtures were mixed with three different classes of soil materials obtained from a low-volume road. For each of the

soils tested, LS provided the highest increase in strength, as determined by the unconfined compression tests after seven-day air-curing of samples (Fig 2.36).
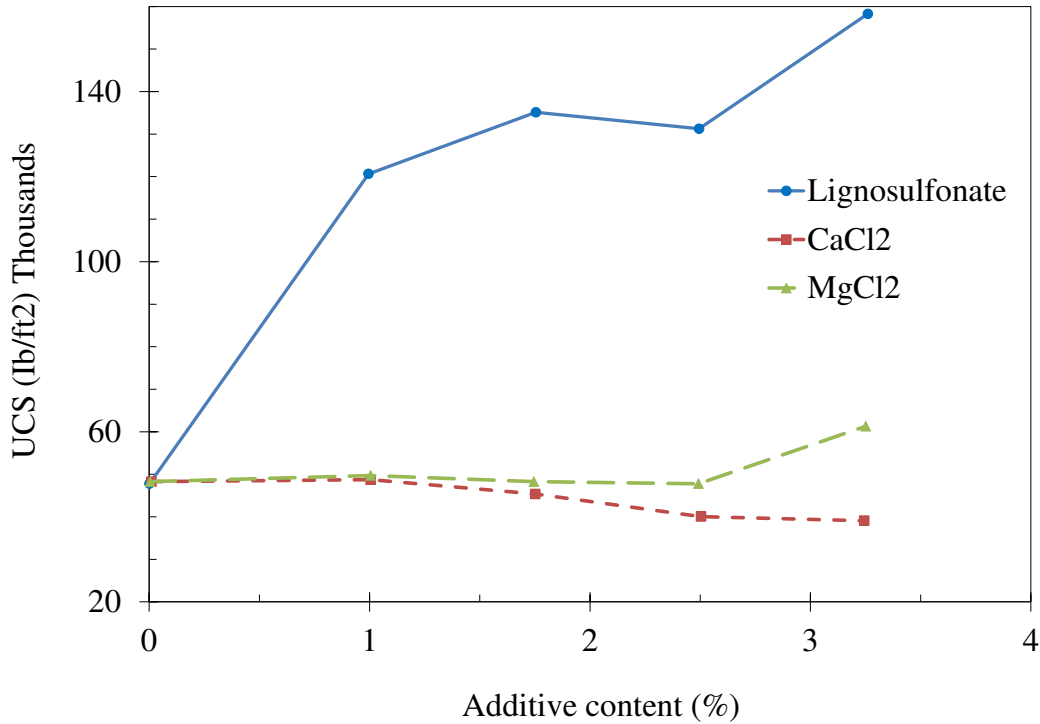
Figure 2.36: Average peak UCS for specimens tested dry (After Palmer et al. 1995)

At the U.S. Army Engineer Research and Development Centre, Tingle et al. (2007) conducted laboratory experiments to evaluate the stabilization of clay soils and silty-sand with non-traditional chemical admixtures (acid, enzymes, LS, a petroleum emulsion, polymers, and a tree resin) and traditional admixtures (Type I Portland cement and hydrated lime) under the same mixing, compaction, and curing conditions. Wet and dry UCS tests data for each soil treated with the additives were conducted and finally compared with a series of control specimens that were not stabilized. The report shows that LS provided excellent waterproofing for clay soils and silty-sand than did the rest stabilizers after 28 days of curing. It is thus, envisaged that the waterproofing characteristics of LS could minimize the intake of water by treated expansive soils hence, the likely reduction in percent swell magnitude.

Puppala and Hanchanloet (1999) combined LS with other chemicals to achieve maximum stabilizing effect on the strength of expansive soil. They studied the effect of a new liquid comprising sulfuric acid and LS admixture (SA-44/LS-40 or DRP) on the strength and plasticity characteristics of soils. The percent increase in UCS with the SA-44/LS-40 treatment ranged between 30% - 130% with similar increases in cohesion intercept and friction angles. The increase in strength properties were attributed to the formation of chemical bonds between soil particles upon LS addition. The LS admixture also increased the resilient moduli of the soils.

LS – Soil Reaction Mechanisms

A handful of research have been dedicated to the identification of the stabilizing mechanism(s) of non-traditional admixtures despite the numerous research conducted on non-traditional admixtures. In reviewing the literature, it is interesting to note that most of the proposed mechanisms for these admixtures are based on intuition (Addo et al. 2004; Gow et al. 1961; Puppala and Hanchanloet 1999). For instance, Addo et al. (2004) believe that the increase in stability of clay soils upon LS addition is caused by dispersion of the clay fractions. According to Gow, the dispersed clay causes the following four conditions in the soil which benefit the stability of the soil-aggregate mix.

(1) Plugging voids and consequently improving water tightness and reducing frost susceptibility
(2) Filling voids with fines, thus increasing density
(3) Increase in the effective surface area of the soil particles, which results in greater contribution to strength
(4) Eliminating soft spots caused by local concentrations of binder soil.

However, Tingle et al. (2007) investigated soil additives with the objective of advancing current understanding of the stabilization mechanisms associated with selected non-traditional admixtures including LS. The research consisted of conducting qualitative analyses of hypothesized stabilization mechanisms. Laboratory experiments included image analyses, physical/chemical characterization of untreated and chemically treated soil samples. They reported that LS coated

individual soil particles with thin adhesive-like film that physically bind soil particles together (Fig 2.37) and show inconsequential chemical reactions though depending on their chemical composition. They are of the opinion that LS could undergo cation exchange with certain soils minerals because of the presence of ions in the admixture. The particle coating and subsequent binding mechanisms of soil particles by LS admixture reduced moisture susceptibility exhibited during wet strength testing.
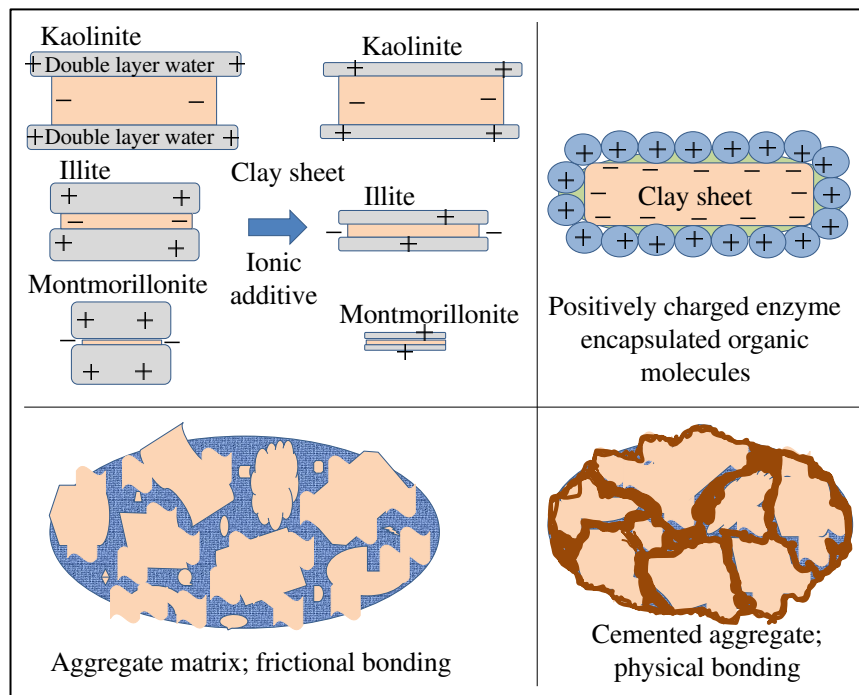
Figure 2.37: Proposed stabilization mechanisms of LS admixture (Reproduced after Tingle et al. 2007)

In a comprehensive study by Scholen (1992; 1995) several non-traditional admixtures were identified and grouped into biocatalysts (enzymes), electrolytes (ionic), acrylic polymer, and mineral pitches in order to describe the stabilizing mechanisms of the admixtures. He hypothesized that non-traditional admixtures could function as catalysts to accelerate the weathering process of individual clay minerals by altering the electrolyte concentration of the pore fluid and initiates cation exchange between pore fluid cations and cations on clay surfaces and flocculation of the clay minerals. The cation exchange and subsequent particle flocculation is as a result of the collapse of the clay structure into a more stable configuration expelling

excess DDL water in the process. Scholen also hypothesized additional mechanisms by which these additives could stabilize clay materials. He proposed possible breakdown of clay minerals with expulsion of water from the DDL, peripheral and basal adsorption on clay layers preventing water absorption, the binding of clay particles by aggregation, and/or interlayer expansion with subsequent moisture entrapment.

Vinod et al. (2010) investigated an erodible silty soil and examined the mechanisms through which it was stabilized by LS admixture. They studied the physico-chemical and microstructural changes in LS amended samples using analytical techniques such as XRD, FTIR, SEM, and SEM/EDX. They posited that on addition of LS in the presence of water, LS first undergo hydrolysis and then disintegrate into hydrogen (H^+) and hydroxyl (OH^-) ions, which causes the protonation of the LS admixture. The protonated LS thus, releases water and form a positively charged compound. This positively charged LS then neutralizes the negative charges of clay minerals due to electrostatic attraction which lead to the reduction of the double-layer thickness (Fig 2.38). They concluded that the improved engineering properties in treated soil were as a result of the reduction in the DDL thickness through the neutralization reaction and subsequent binding of the soil particles together to form flocs.
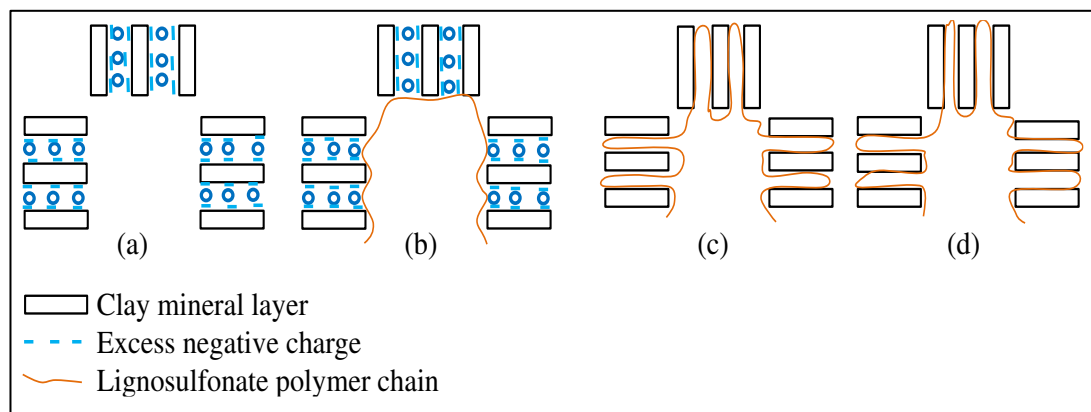
Figure 2.38: Stabilization mechanisms of LS amended silty sand (After Vinod et al. 2010)

2.16 ENVIRONMENTAL CONCERNS OF LS TREATED SOIL

Lignosulfonate is considered biodegradable; therefore, its presence in the environment could be considered harmless compared to other industrial by-products (e.g. fly-ash) or traditional admixtures. Adams (1988) argued that the application of LS as a soil additive has negligible impact on the environment and that it is safer to use for stabilization and dust control than any competing class of chemicals. Like Adams, ILI (1992) reported that LS has never been responsibly suggested to have any negative impacts on the environment and/or human health. It is considered nontoxic, non-hazardous, noncorrosive, and generally environmentally benign polymeric compound (Adam 1988). The pH of the soil practically remains unchanged upon LS addition unlike the traditional admixtures that considerably increase pH of treated soil.

2.17 MATHEMATICAL MODELLING OF THE SWELLING BEHAVIOUR OF EXPANSIVE SOILS

Several models for the prediction of swell behaviour of soils have been developed globally. These models are either purely theoretical, semi-empirical or purely empirical in nature.

Empirical model: Empirical models for swell behaviour of expansive soils are as numerous as the proponent. These models are drawn from relations derived from experimental data thus; it does not apply to all soil types but location specific. Simple soil properties such as liquid limit, plasticity index, activity, initial water content, and clay content are employed in the development of such models (e.g. Seed at al. 1962; Chen 1988; Buzzi 2010). Buzzi (2010) introduced dimensionless modelling into swell behaviour of expansive soils by relating percent swell with initial void ratio, applied surcharge, and initial suction (equation 2.14).

$$\varepsilon_{sw} = 3.90 \ln\left[\left(\frac{1}{e_o}\right)^3 \cdot \left(\frac{s_o}{\sigma_v}\right)\right] - 15.15 \qquad (2.14)$$

Where; e_o = initial void ration, s_o = initial soil suction, σ_v = vertical stress

Semi-empirical model: Using a semi-empirical approach, Nayak and Christensen (1970) developed a model of swell behaviour, leading to an equation relating percent swell of a compacted soil to its plasticity index, clay content and initial moulding water content. The model is based on the concepts of DDL theory, modified by introducing empirical constants to account for swelling effects and other limitations involved in the direct application of DDL theory to real soils. The equation (2.15) they proposed for percent swell, S, is of the form:

$$S = k_m^* \frac{E^m C}{w} + k_m^{**}$$
(2.15)

Where; K_m^*, K_m^{**} and m are regression functions, C = clay content, W = water content

Fredlund, (1983) used the results of oedometer test data to predict the total heave of expansive soil. The heave in an individual layer of soil is given as:

$$\Delta h_i = h_i \left(\frac{\Delta e}{1 + e_0} \right)$$

Where; Δh_i = heave in a layer, h_i = layer thickness, Δe = change in void ratio, e_0 = initial void ratio.

Total heave $\Delta h = \Sigma \Delta h_i$ is represented in equation 2.16.

$$\Delta h_i = h_i \left(\frac{C_s}{1 + e_0} \right) \log \frac{p_f}{p_0}$$
(2.16)

Where; C_s = Swell index (slope of e − log P curve), P_f = final stress state (i.e. corrected swelling pressure of soil), P_0 = initial stress state ($P_f = \delta y + \Delta \delta y - \mu_{wf}$); $\Delta \delta y$ is total stress due to excavation or placement of fill and μ_{wf} is predicted or estimated as final pore-water pressure.

Nelson and Miller (1992) developed heave predictive model based on soil suction test data. They correlated void ratio and matric suction to the compression index or swelling index determined from oedometer tests. They modelled heave using equations similar to the reverse consolidation equations. Total heave due to change in both the effective stress and the matrix suction is given as equation 2.17.

$$\rho = \sum_{i=1}^{n} \frac{z_i (\Delta e)}{(1+e_0)_i} = \sum_{i=1}^{n} \frac{z_i (\Delta e)}{(1+e_0)_i} \left[C_{mi} \Delta \log(u_a - u_w) + C_{ti} \Delta \log(\sigma - u_a) \right]_i \quad (2.17)$$

Where; ρ = total heave, z_i = thickness of layer i, $\Delta e_i = (e_f - e_0)_i = C_{mi} \log[u_a - u_w)_f/(u_a - u_w)_0]_i$, C_{mi} = matrix suction index for layer i, C_{ti} = effective stress index for layer i, σ = total stress, u_a = pore air pressure, u_w = pore water pressure.

The Australian model: The estimation of the characteristic surface movement is governed by the recommendations of the AS 2870-2011 Standard, which stipulate that for soil classification purposes, the characteristic surface movement (y_s) shall be determined by estimating the movement of each layer of soil 1 to N within design depth and summing the movement in all layers. The surface movement (y_s) is given as equation 2.18.

$$y_s = \frac{1}{100} \sum_{n=1}^{N} \left(I_{pt} \overline{\Delta u} h \right)_n \quad (2.18)$$

Where,

y_s = characteristic surface movement in millimetres, I_{pt} = instability index, in %/picofarads (pF), $\overline{\Delta u}$ = average soil suction of soil thickness under consideration, in picofarads (pF), h = thickness of layer under consideration, in millimetres, N = number of soil layers under consideration.

The Australian Standard (AS 2870-2011) define the instability index (I_{pt}) as the percent vertical strain per unit change in suction, considering the applied stress, degree of lateral restraint, and soil suction range. Thus, I_{pt} is not a constant for

particular clay but its determination is based on a correlation with shrinkage index of the soil as follows (equation 2.19):

$$I_{pt} = \alpha \times I_{ps}$$
(2.19)

Where,

I_{ps} = shrinkage index of soil and α is the lateral restraint factor

For the determination of "α", AS 2870 − 2011 recommended the following conditions:

In the cracked zone (unrestrained)

$$\alpha = 1.0$$

In the uncracked zone (restrained laterally by soil and vertically by soil weight)

$$\alpha = 2.0 - \frac{z}{5}$$

Where,

z = depth from ground surface, in metres, to the centroid of the area defined by the suction change profile and the thickness of the soil layer under consideration in the uncracked zone.

Surface movement occur due to changes in the suction of a soil profile. For determination of soil surface movement, the Australian Standard requires that the suction within the depth of the soil under considerations be estimated (see equation 2.18). Values of such suction change (H_s) in various Australian locations in Australia are provided in AS 2870 - 2011 (see Table 2.14).

The measurement of soil suction is a common practice in geotechnical engineering laboratories around the world. The most common techniques employed are the filter paper method, suction probe technique, psychrometer method, chilled − mirror hygrometer technique, time domain reflectometry, electrical conductivity sensors,

thermal conductivity sensors, tensiometer method, relative humidity sensor method, and axis-translation technique among others (Fredlund and Rehardjo 1993). Several authors (e.g. Vanapalli et al. 1999; Heitor 2013) have employed the axis-translation technique (Fig 2.39) in the determination of suction profiles, suction-saturation relationships and/or suction-moisture content relations. Such data enable the estimation of suction at a particular time and depth for any given soil for the estimation of surface movement prediction using equation 2.18.

Table 2:14: Soil suction change profiles for certain locations (Reproduced After: AS 2870 – 2011)

Location	Change in suction at the soil surface ($\overline{\Delta u}$) pF	Depth of design soil suction change (H_s) m
Adelaide	1.2	4.0
Albury/Wodonga	1.2	3.0
Brisbane/Ipswich	1.2	1.5-2.3
Gosford	1.2	1.5-1.8
Hobart	1.2	2.3-3.0
Hunter Valley	1.2	1.8-2.3
Launceston	1.2	2.3-3.0
Melbourne	1.2	1.8-2.3
Newcastle	1.2	1.5-1.8
Perth	1.2	1.8
Sydney	1.2	1.5-1.8
Toowoomba	1.2	1.8-2.3

NOTE: The variation in H_s depends largely on climate variation

It is common knowledge that suction tends to equilibrate at a moisture source within a soil mass. Mitchell (1980) demonstrated suction profile behaviour of various cities in Australia under certain boundary conditions of moisture change. For example, the

suction profile under well-watered garden is presented in Fig 2.40. From this relationship, the surface movement of such soil could be calculated using equation 2.18.
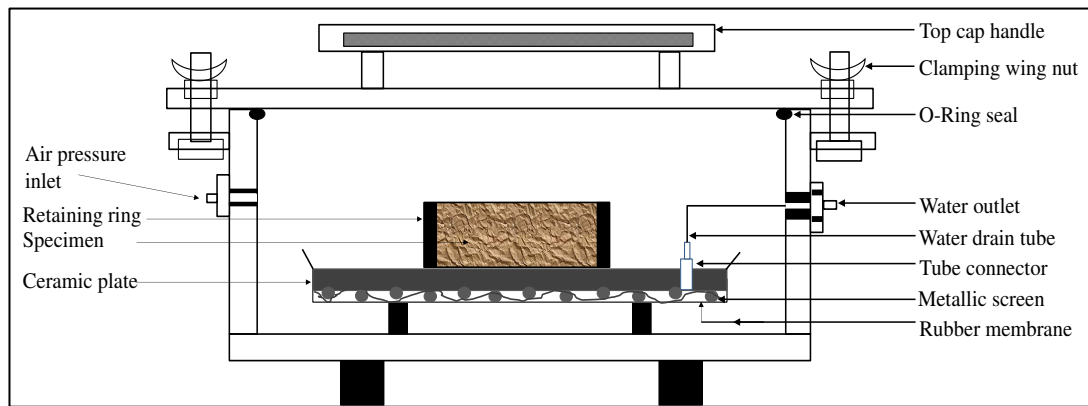
Figure 2.39: Schematic representation of the axis-translation equipment (Modified after Fredlund and Rahardjo 1993)
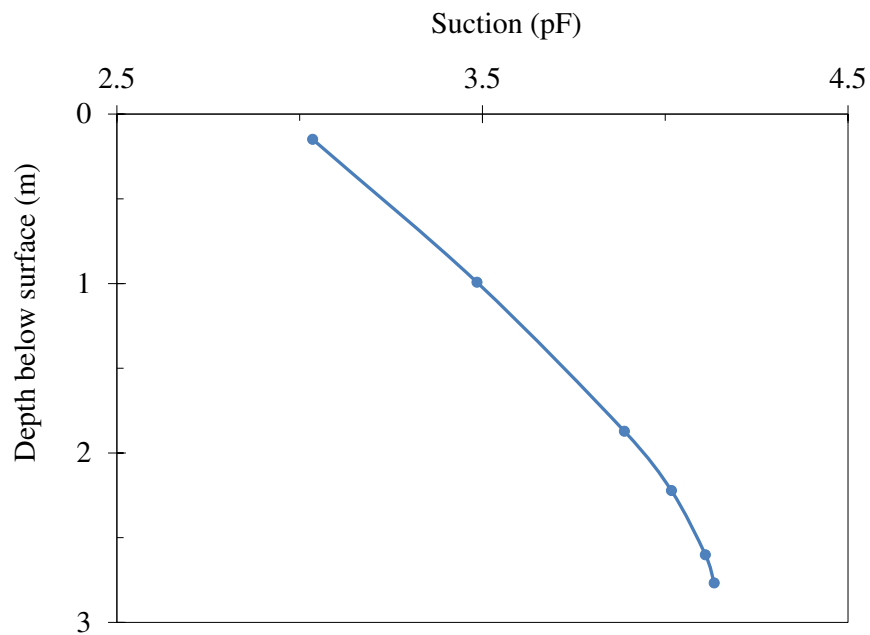
Figure 2.40: Suction under well-watered garden (After Mitchell 1980)

Theoretical model: A very common modelling technique for swell pressure prediction is the famous DDL theory originally proposed by Gouy (1910) and Chapman (1913, incited in Mitchell and Soga 2005). Several modifications from

different authors have been made on the original model (e.g. Komine and Ogata 1996) to capture parameters of interest. The modified models have given better credibility to some bogus assumptions made in the original model. Thus, the DDL theory is very useful in understanding several physicochemical forces of interaction, repulsion, aggregation, deflocculation and how these processes interact to form soil structure which affect clay swelling and compression behaviour (Mitchell and Soga 2005).

Bolt (1956, cited in Mitchell and Soga 2005) demonstrated that the swell pressure of clays is the difference between the osmotic pressure in the central plane between clay platelets and the osmotic pressure in the equilibrium solution. Bolt showed that the osmotic pressure at the central plane between the clay platelets for a given bulk chemistry and known properties of clay could be calculated from the Gouy-Chapman DDL theory. Sridharan and Jayadeva, (1982) improved on the DDL equation of Bolt (1956) for calculating the swell pressure in a clay-water-electrolyte system. Their equation for swell pressure of clay is as follows (equation 2.20).

$$e = G\gamma_w S d_{1/2}$$

$$\int_z^\mu \frac{1}{\sqrt{(2\cosh z - 2\cosh \mu)}} \, dy = \int_0^d d_{1/2}\xi = -Kd_{1/2}$$

$$-\left(\frac{dy}{d\xi}\right)_{x=0} = \sqrt{(2\cosh z - 2\cosh \mu)}$$

$$= \Gamma \sqrt{\left(\frac{2\pi}{\varepsilon n k T}\right)_{X=0, y=z}}$$

$$= \left(\frac{B}{S}\right)\sqrt{\left(\frac{2\pi}{\varepsilon n k T}\right)}$$

$$p = 2nkT(\cosh \mu - 1) \tag{2.20}$$

$$where, \qquad K = \sqrt{\dfrac{8\pi e^2 v^2 n}{\varepsilon kT}}$$

Where; G = specific gravity of soil solids, yw = unit weight of water, S = specific surface area of soil, e = void ratio, T = absolute temperature, v = ionic valence, é = elementary electrical charge, ξ = distance function, x = distance from clay surface, k = Boltzmann constant, ε = dielectric constant of pore fluid, $d_{1/2}$ = half the distance between parallel platelets, μ = nondimensional midplane potential, B = base exchange capacity of clay, p = osmotic pressure or swelling pressure, y = nondimensional potential at distance x from the clay surface, Γ = surface charge density (base exchange capacity/specific surface), z = nondimensional potential at distance x from the clay surface.

2.18 SUMMARY

Based on the reviewed literature, expansive soil deposits represent an economic saboteur of every nation plagued by such soils. The challenges on how best to deal with such soils are enormous as geotechnical engineers attempt to minimum its impact on infrastructure globally. Thus, failure to correctly identify these soils and adopt appropriate sustainable engineering treatment solutions could lead to severe operational and maintenance cost which could result in colossal economic losses. Some novel treatment techniques have been proposed and used globally. Among these numerous techniques, chemical stabilization with traditional admixtures (lime and cement) date back over 5,000 years. The efficacy of these admixtures is well documented and supported with numerous field applications/standardized test methods. However, the use of traditional admixtures has prompted health and safety concerns despite their international acceptance. There are documented evidences of vegetation attack on traditionally treated soil due to increased pH value, groundwater pollution, brittle behaviour under cyclic loading, crack formation, corrosion problems on steel frame structures among others.

It is interesting to realize that, in addition to traditional additives which have been used since time immemorial, many other products, sometimes considered as wastes, can be used for soil improvement, particularly for expansive soils. It is rational that products with chemical compositions which could initiate reactions in expansive soil be investigated; LS is one of such admixtures that require extensive engineering investigation considering the volume of annual global production of over 50 million tons. Previous engineering tests results suggest that LS admixture is a promising admixture considering its environmental credentials.

In this research project, attempt is been made to control the swell behaviour of a remoulded expansive soil using LS admixture and in addition, investigate the behavioural effect of LS on other engineering properties of the remoulded expansive soil. Another major objective is to define the stabilizing mechanisms of the LS admixture. Unlike the traditional admixtures, attempts to define the stabilizing mechanisms of LS admixture have been limited. Most laboratory and field research with LS has focussed on performance evaluation in terms of strength growth without recourse for stabilizing mechanism identification. So far, little or no comprehensive research has been conducted on the fundamental physico-chemical and microstructural behaviour of LS treated expansive soil using analytical methods such as XRD, CT, SEM, EDS, FTIR, NMR, CEC, and SSA.

To better understand the rudiments of expansive soil as well as damage to light weight infrastructures, examinations of existing models were undertaken. This included existing models in predicting soil movement due to changes in the influencing factors. It was interest to establish the dearth of research into swell predictive models of chemically treated expansive soils. Swell predictive models in the literature are developed based on data obtained from natural or artificial soils thus; this research seeks to find answers to the above deficiencies.

CHAPTER THREE

3 MATERIALS AND EXPERIMENTAL TESTING PROGRAMME

3.1   INTRODUCTION

It has been widely reported (e.g. Tingle et al. 2003, 2007; Indraratna et al. 2013) that LS could be a sustainable admixture to improve the strength and erosion resistance in soils. This research seeks to evaluate how LS admixture altered the swell potential and other relevant engineering properties of a remoulded expansive soil, and also attempt to explain the mode of reactions between the remoulded soil and the admixture using analytical techniques such as x-ray diffractometer (XRD), scanning electron microscope (SEM), energy dispersive spectroscopy (EDS), cation exchange capacity (CEC), computed tomography (CT-scan), fourier transform infrared (FTIR) and specific surface area (SSA). The need to develop a mathematical model to predict the change in volume in chemically treated expansive soil is also proposed in course of this research. Based on the above, this chapter discusses the methodologies adopted for this study including the characterisation of materials used and laboratory work plan as summarized in Fig 3.1.
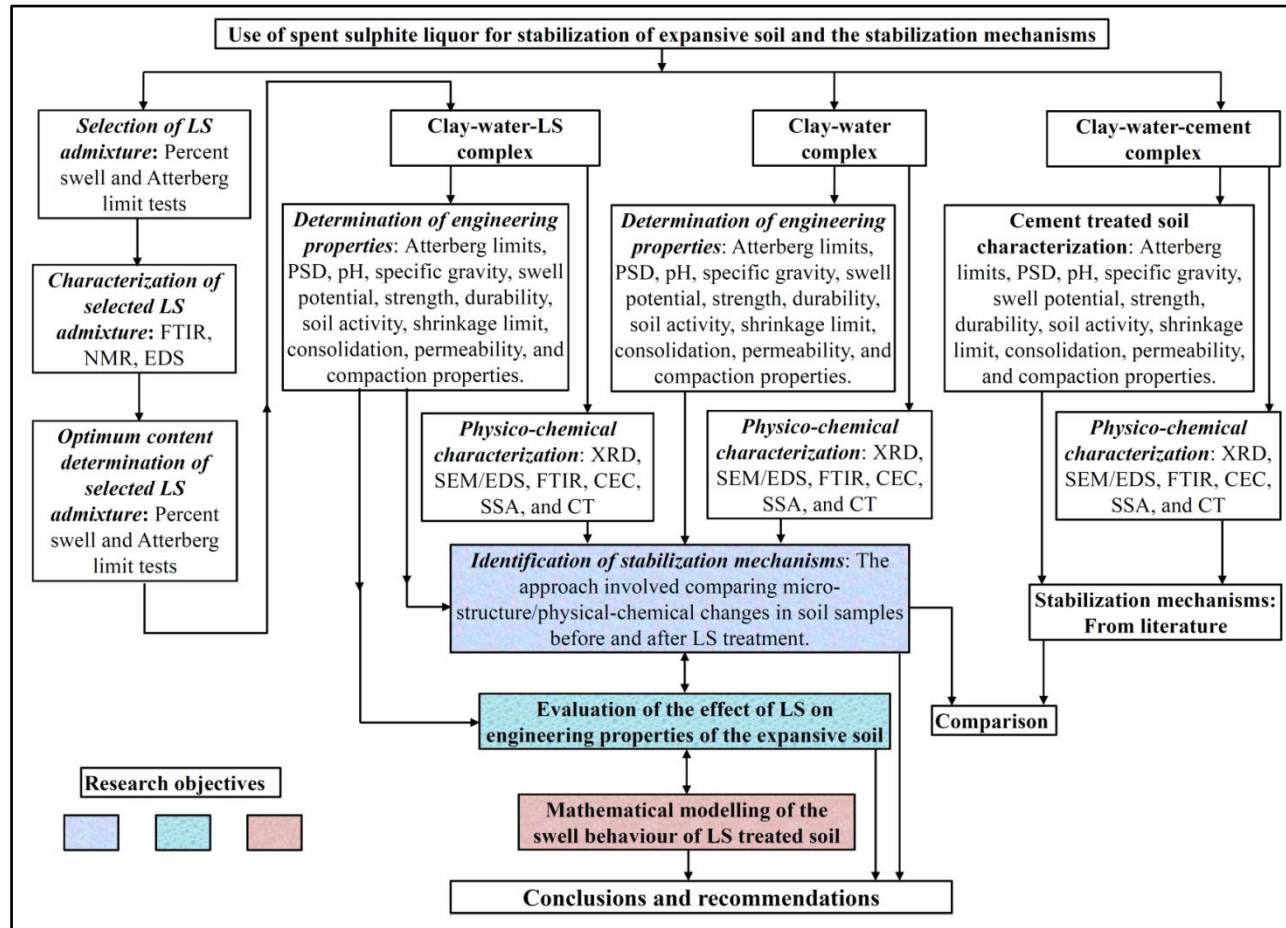
Figure 3.1: Diagrammatic illustration of research programme

To organise the research proceedings efficiently, the project was further divided into 8 phases to address the above issues. These phases are as described below:

3.2 PHASE 1: SELECTION PROCEDURE FOR THE MOST EFFECTIVE LS ADMIXTURE

Three liquid LS admixtures (sodium (Na), potassium (K), and calcium (Ca) Lignosulfonates) were available for examination. The procedure used to select the appropriate LS admixture involved assessing how much the percentage of swell and Atterberg limits were reduced after being treated with each of the three LS admixtures following ASTM D4546 and AS 1289 3.2.1 Standards, respectively. After identifying the most effective LS admixture the optimum product application rate was determined by following the recommendations of ASTM D4546 and by varying the LS contents from 0-7% by dry weight of soil.

3.3 PHASE 2: SOIL DESCRIPTION AND CHARACTERIZATION

The soil was sampled by hand after removing 25cm of top soil over an 8m radius with a sampling depth of 25-70cm. The site was on a Jurassic Basalt foot slope of Mt Coolanbilla, on the south side of Goran Lake near Gunnedah. This area is mapped as Noojee soil landscape in the "Soil Landscapes of the Curlewis 1:100 000 Sheet" (Banks, 1995). The soil is a giant Self-Mulching Black vertosol. The sampling location was taken using a hand held Garmin GPS 76 with a positional accuracy of about 5m. The coordinates are AMG Zone 56, MGA grid reference 227513E, 6533327N. The site was in the middle of a paddock managed under a no-till tramline system and was in fallow at the time of sampling (Fig 3.2).

Figure 3.2: Soil sampling site at the south side of Goran Lake near Gunnedah, Queensland, Australia, inset; is a magnified view of the in-situ soil (Courtesy of Bank Robert).

The sampled soil was placed in plastic container, sealed, and then transported to the laboratory for preparation and testing. Extensive laboratory tests were carried out to classify the soil (Table 3.1). The soil could be classified as expansive on the basis of its plasticity, percent swell, shrinkage limit, and activity. The high liquid limit (>50%) and high plasticity index (51%) support the typical characteristics of a montmorillonitic expansive soil (Holtz and Gibbs 1956; Chen 1988). The percent swell of approximately 6% classified it as "high" expansive following the classification scheme proposed by Seed et al. (1962) (i.e. percent swell = 5 - 25% under 7kPa surcharge). The soil shrinkage limit was 9% which was also in agreement with the same class of expansiveness (7 − 12%) in accordance with Holtz and Gibbs (1956). Furthermore, the soil activity was 1.42 which was also in concordance with the soil expansiveness (Skempton, 1953).

Table 3.1 also highlights the averaged oxides of the major elements present in the remoulded expansive soil, as obtained from EDS analysis. The presence of Si, Al,

Mg, Ca, Fe, and Na indicate the existence of montmorillonite minerals in the soil. This supports the XRD data, which indicated the presence of montmorillonite, illite, kaolinite and quartz minerals (Table 3.2). The EDS and XRD data were consistent with the degree of expansive classification based on the physical index properties of the soil.

3.3.1 *Methods of soil characterization*

The aim of characterizing the remoulded expansive soil was to establish the baseline properties prior to LS treatment. The physical properties measured included the swell potential, the Atterberg limit, soil gradation, cation exchange capacity, specific surface area, standard compaction characteristics, uniaxial compressive strength, durability (freeze-thaw and wet-dry) durability, consolidation characteristics, permeability parameters, and shrinkage. All the tests were carried out as detailed in either the Australian or American test Standards (AS 1289; ASTM). Instrumental analytical techniques such as x-ray diffractometer (XRD), fourier transform infrared (FTIR), scanning electron microscope coupled with energy dispersive spectroscopy (SEM/EDS), nuclear magnetic resonance (NMR), computed tomography (CT), cation exchange capacity (CEC), and specific surface area (SSA) were used to micro-characterize the remoulded soil.

3.3.1.1 Swell potential test method:

The swell test specimen was generally prepared in accordance with ASTM 4546. The field soil was oven dried at 105^{0}C to a constant mass, and then crushed and sieved through a 1.18mm sieve. An aliquot of the materials passing the 1.18mm sieve was collected and mixed with the optimum moisture content, and then sealed in plastic bags for 24hrs prior to compaction. A predetermined mass of soil-water material was statically compacted directly into consolidometer rings 50mm in diameter by 20mm high using a specially designed mould at a rate of 1mm/min, until the desired density was reached. These compacted specimens were then sealed and stored for 7 days prior to the one dimensional oedometer swell test. After the 7 day curing period, specimen was placed into the oedometer equipment, inundated with deionized water and allowed to swell for 10-14 days while data was acquired through a previously

installed data logger. To determine the swell pressure of the remoulded expansive soil, the constant volume method as described in ASTM D4546 was followed. This method involved inundating the specimen in an oedometer while preventing it from swelling by repeatedly increasing the vertical load. The swelling pressure was reported as the averaged maximum applied stress required to preventing the specimens from swelling. A method proposed by Fredlund (1983) was used to correct the swell pressure of the remoulded soil.

3.3.1.2 Atterberg limit test method:

The Atterberg limits (liquid limit and plastic limit) were determined in strict adherence to Australian Standards; AS 1289.3.9.1-2002 and AS 1289.3.2.1-2009 respectively. The dry soil materials passing through the 425um sieve was mixed with water at 5mL increments until a thick homogenous paste was formed. The paste was then sealed in plastic bags and stored overnight prior to determining the liquid limit using the cone penetration technique (Fig 3.3). To determine the plastic limit of the remoulded soil, an aliquot of thick homogeneous paste was allowed to dry in air until it become plastic enough to be shaped into a ball. The soil was later sealed in plastic bags and stored for 24hrs for water equilibration. The soil was then rolled to crumble at 3mm diameter (Fig 3.4). The plastic limit was reported as the moisture content at which the soil begins to crumble at 3mm diameter.

Figure 3.3: Cone penetration apparatus for liquid limit determination (Courtesy: UOW)
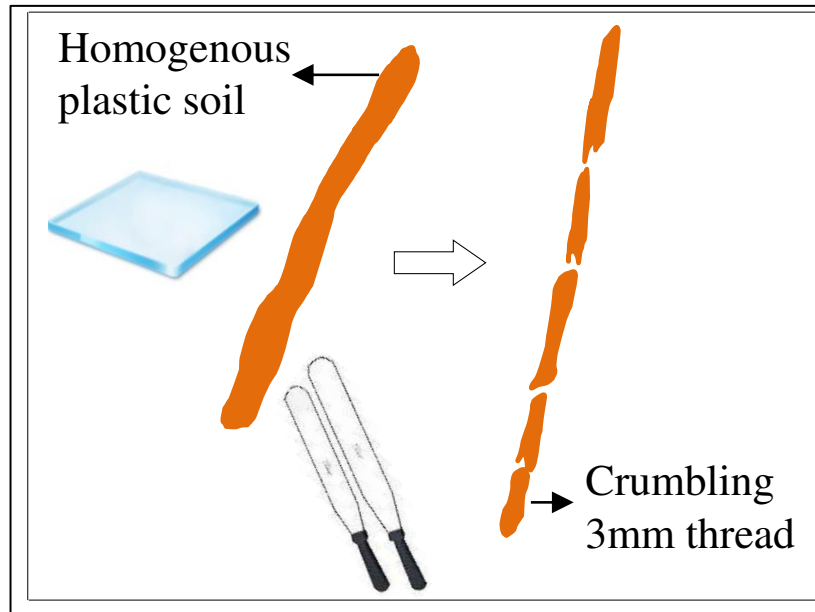
Figure 3.4: Pictorial illustration of plastic limit determination

3.3.1.3　X-RD test method:

Oriented specimens were prepared on a glass slide as suggested by Whittig and Allardice (1986). About 2g of soil was collected and placed in a mortar and crushed with a pestle to a fine homogeneous powder. Then 0.5mL of deionized water was added and the mixture was stirred thoroughly. About 0.1g of the clay suspension was transferred onto a 2.5cm diameter glass slide and allowed to air dry before being examined with an XRD diffractometer. A GBC MMA X-Ray diffractometer was used to scan samples with the following generator settings: 35kV, 28.5mA, 1.00kW, and CuKα radiation (Fig 3.5). Other settings included the wavelength (λ) = 1.54056Å, an angle scan (2θ): 2°-60° using a 0.02° step size, and a dwelling time (speed) of 1^{0}/min at each step. The data acquired provided qualitative information about mineralogical composition, phase identification, d-spacing and the crystallite size of remoulded expansive soil. For a quantitative analysis of the remoulded expansive soil, a Siroquant analysis was carried out on XRD diffractograms and the result is presented in Table 3.2.

Figure 3.5: X-ray diffractometer (XRD) (Courtsey: UOW)

3.3.1.4   SEM/EDS test methods:

An appropriate soil mass from a compacted swell test specimen was collected and placed onto a 2cm diameter SEM sample holder exposing the "undisturbed fresh" surface. The specimen was then inserted into a JEOL JSM-840A SEM (Fig 3.6), equipped with EDS to study morphological and elemental composition of the untreated soil and 2% LS treated soil. SEM micrographs were obtained at x2500 magnification for proper examination of the soil fabrics. The EDS tests were conducted on the entire soil surface at 20kV, 10mm working distance, and with a spot size of 52. No surface coating was involved during specimen preparation. EDS micrographs display the results of elemental intensities (counts/sec) versus energy (KeV). The energy levels were used to identify the elements present in the sample while the intensity generally corresponded to the concentration of corresponding elements (Cullity 1979). Moreover, an SEM micrograph of the remoulded expansive soil shows the "corn-flake" like texture typical of montmorillonite aggregates.

Table 3:1: Physical/chemical properties of the soil (Corrected Swell pressure; after Fredlund (1983).

Physical properties		References
Depth of sampling (m)	0.25–0.75	-
Specific gravity	2.7	AS 1289.
Natural moisture content (%)	38	AS 1289.2.1.1-2005
Liquid limit (%)	91	AS 1289.3.9.1-2002
Plastic limit (%)	40	AS 1289.3.2.1-2009
Plasticity index (%)	51	AS 1289.3.9.1-2002
Shrinkage limit (%)	9	AS 1289.7.1.1-1992
Maximum dry unit weight (MDUW), (kN/m^3)	13.1	AS 1289.5.1.1-2003
Optimum moisture content (OMC), %	37	AS 1289.5.1.1-2003
Soil classification	CH	AS 1289.
Clay content (%)	35.6	Malvern analysis
Silt content (%)	53.8	"
Sand content (%)	8.8	"
Soil activity	1.42	Skempton (1953)
% Swell of soil at OMC and MDUW under 7kPa	6	*ASTM D4546*
Corrected swell pressure (kPa) of remoulded soil at OMC and MDUW	220	*ASTM D4546-2008*
Natural soil pH	7.43	AS 1289.4.3.1-1997
Chemical properties (EDS analysis) Mass (%)		
SiO_2	55.1	EDS
Al_2O_3	19.49	"

Fe$_2$O$_3$	13.33	"
CaO	2.69	"
MgO	3.56	"
TiO$_2$	0.16	"
Na$_2$O	0.21	"
LOI	5.45	"
Cation exchange capacity (CEC)	57.5meq/100g	ASTM C837-2014
Specific surface area (SSA) of soil	61.75m2/g	ASTM C837-2014

Table 3:2: Analysis of XRD diffractogram for quantitative determination of soil mineralogical (Siroquant analysis).

Soil mineralogical	Mass (%)
Clay content in soil	36.0
Montmorillonite content in clay fraction	10.4
Montmorillonite-illite content in clay fraction	0.6
Montmorillonite-chlorite content in clay fraction	8.5
Illite content in clay fraction	4.4
Kaolinte content in clay	12.7
Quartz	25.3

3.3.1.5   CT scan test method:

The very small specimen sizes commonly used in analytical techniques (e.g. XRD) may not be a good representation of bulk samples. A combination of advances in experimental techniques has made it possible to characterize the pore geometry or micro-fabrics of bulk samples using a non-destructive X-ray computed tomographic (CT) technique (Fig 3.8). For this reason, a CT scan was used in this study to probe the microstructure, including the porosity, particle, and void space properties of

compacted free swell specimens before and after one-dimensional swell test. CT imaging of samples were carried out using a Toshiba Asteion S4 X-ray CT scanner with the following settings: The X-ray tube voltage: 135kV, current: 200mA, X-ray beam (slice thickness): 20mm, exposure time: 1second, and the field of view (FOV): 21cm with a zooming factor of four.

The acquired images were processed as suggested by Puech et al. (2007); using medical radiology software DicomWorks v. 1.3.5., including post-processing filtering (i.e. sharpness and inversion filters). The spatial resolution of each image was adjusted until a substantial arrangement of the soil structure could be seen.
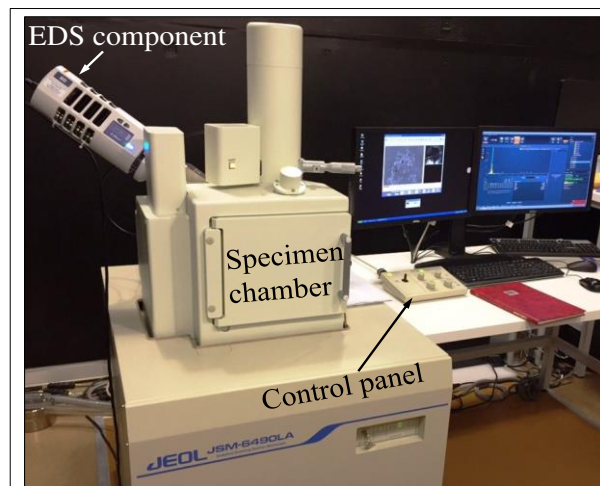
Figure 3.6: Scanning electron microscope coupled with energy dispersive spectroscopy (SEM/EDS) (Courtsey: UOW)
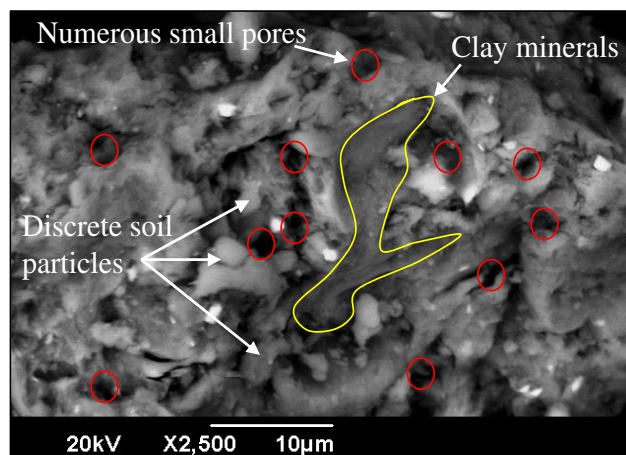
Figure 3.7: SEM image of remould natural expansive soil

Figure 3.8: Computed tomography (CT scan) (Courtsey: UOW)

3.3.1.6 FTIR test method:

FTIR identifies the chemical bonds by measuring the frequencies at which the bonds in a sample absorb infrared radiation (Santagata et al. 2008). Determining these frequencies allows identification of the specimen's organic functional groups or for identity testing of specimens and/or the concentrations of molecules in specimens (Coates 2000). FTIR was performed for optimally compacted samples using a Shimadzu IRAffinity-1 C 8984 model (Fig 3.9). About 2g of the compacted specimen was placed on the diamond specimen holder to measure absorbance at characteristic wavenumbers of 7000-400cm^{-1}. At all times, 100 scans were recorded with a 4cm^{-1} resolution. The FTIR pattern of the soil (Fig 3.10) indicated the presence of OH and H$_2$O vibrational modes which will play a vital role in identifying the stabilization mechanisms of the admixture.
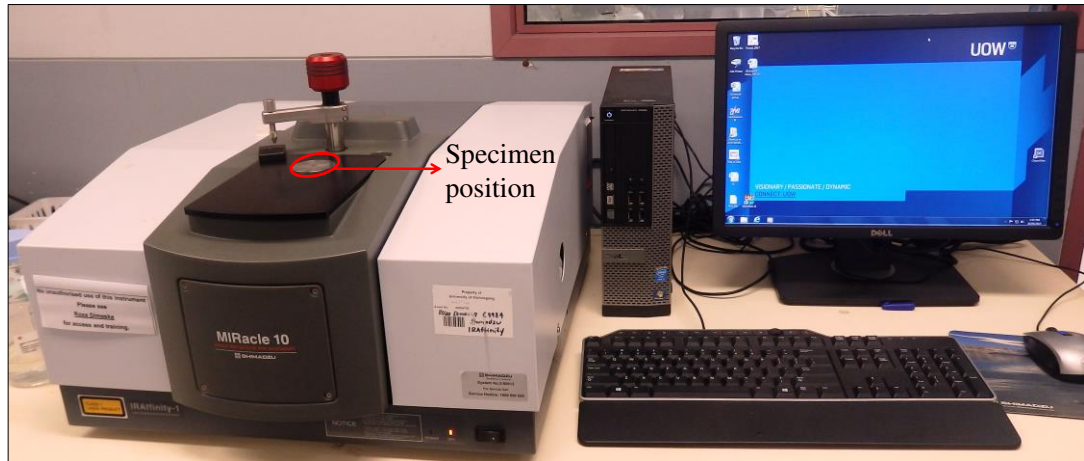
Figure 3.9: Fourier transform infrared (FTIR) spectroscopy (Courtsey: UOW)

3.3.1.7 CEC test method:

CEC was determined for samples of compacted untreated and 2% CaLS treated soil in accordance with ASTM C837. The method involved mixing 2g of dried soil with 300mL of deionized water in a 600mL beaker and stirring it to homogeneity with a shaker. The pH was then lowered to 2.6 by gradually adding sulphuric acid while stirring for 15mins. A litre of stuck solution of methylene blue (1mL = 0.01meq)[3] was added to the acidic complex in 5mL increments and then stirred for 2mins after each addition. A drop of the soil-acid-methylene blue solution was then placed at the edge of a piece of Whitman No. 1 filter paper. This procedure was repeated until the end point was reached, which was indicated by the formation of a light blue halo around the "drop" (Fig 3.11).

When the end point was reached the amount of adsorbed methylene blue was calculated which equal to the CEC of the remoulded expansive soil using equation (3.1)

$$CEC = \frac{E \times V}{W} \times 100 \qquad (3.1)$$

Where,

E = milliequivalent of methylene blue per millilitre, V = millilitres of methylene blue solution required for the titration and W = grams of dry soil.
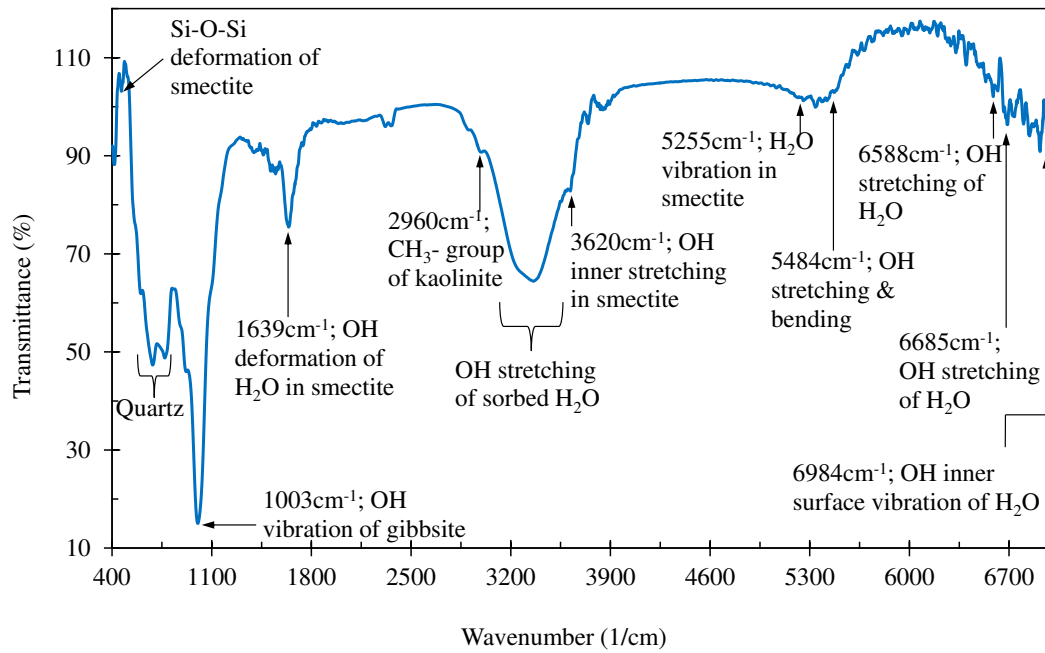
Figure 3.10: The FTIR pattern of remoulded expansive soil

3.3.1.8 Specific surface area (SSA) method:

With knowledge of the amount of adsorbed MB solution from the CEC test data, the SSA of the soil was computed using the Santamarina et al. (2002) equation (3.2).

$$SSA = \frac{M_{MB}}{319.89} A_V A_{MB} \frac{1}{M_S} \qquad (3.2)$$

Where

SSA = the specific surface area of soil particles, M_{MB} = mass of the adsorbed MB at the point of complete cation replacement, A_V = Avogadro's number = 6.02 x 10^{23}/mol, A_{MB} = the area covered by one molecule of MB (typically assumed to be 130Å^2) and M_S = mass of soil specimen.

102
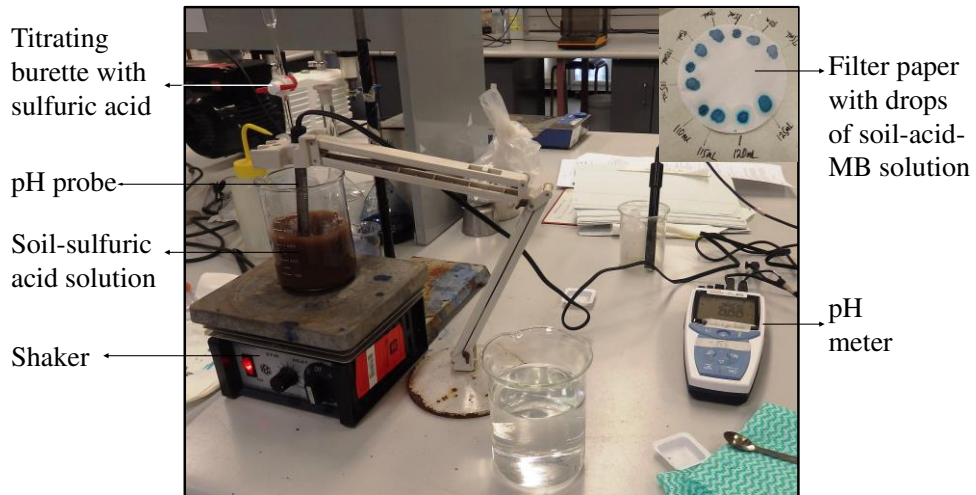
Figure 3.11: Pictorial view of the CEC test setup (Courtesy: UOW)

3.3.1.9   pH measurement:

An Orion 4 star portable pH meter was used to measure soil fluid pH in this study (Fig 3.12). About 30g of remoulded dry soil was put into a 100mL measuring beaker containing 75mL of deionized water. The solution was then stirred for 5minutes and allowed to stand overnight. The pH probe was then inserted into the soil-water solution without making contact with the beaker, while on a shaker. Readings were taken and averaged. Prior to each use, the probe was standardized using a pH buffer of pH 7.

Figure 3.12: Orion pH meter

3.4 PHASE 3: DESCRIPTION OF LS ADMIXTURE AND METHODS OF CHEMICAL CHARACTERIZATION OF THE SELECTED LS ADMIXTURE

The chemical agent (LS) used in this investigation was supplied by *Chemstab Consulting Pty Ltd,* Australia. It was supplied in three different varieties; NaLS, KLS, and CaLS, each consisting of 50% solid and 50% water.

LS is a by-product of the sulphite pulping process in paper manufacturing. It belongs to a family of lignin based organic polymers, and is considered to be a waste by-product that is usually disposed of by dumping into marine environments in enormous quantities. It is water soluble and contains a hydrophilic sulphate group and a hydrophobic aromatic structure, so it exhibits amphiphilic properties. It is a non-corrosive, non-toxic, amorphous, and environmental friendly surfactant capable of forming complexes with cations such as Na^+, K^+, Mg^{2+}, Ca^{2+}, Cr^{3+}, and Fe^{3+}.

3.4.1 *Methods of LS characterization*

The primary chemical constituents of the selected LS stabilizer were characterized using analytical techniques which enabled the identification of the chemical structure of this otherwise proprietary product. The analytical tests included FTIR, NMR, EDS, and a pH measurement.

3.4.1.1 FTIR test:

This method is similar to the test described for soil characterisation in "Phase 2" above, but the instrument was set to measure absorbance at characteristic wavenumbers of 700-4000cm^{-1} (Fig 3.13). In other words, only the mid-infrared region was used to define the structural groups in the LS admixture. The most likely functional groups of the admixture were identified and tabulated (Table 3.3).

3.4.1.2 NMR test:

Further analysis of possible function groups in LS was achieved using protons nuclear magnetic resonance (^{1}H-NMR) spectroscopy. The chemical shifts were identified (Fig 3.14) and assigned to specific functional groups in the organic

compound, as suggested by Klute (1986). Table 3.4 illustrates these chemical shifts in detail.

The spectrum was recorded with a Varian Gemini 300-Hz apparatus. The following conditions were used: a sweep width of 4000Hz, a pulse width of 7.2 ms, and a temperature of 297K. About 10 to 20mg LS was dissolved in 0.5 to 0.6mL deuterated water (D_2O) and tetramethylsilan [TMS; $(CH_3)_4Si$] was used as an internal standard whose chemical shift (δ_{TMS}) was taken as zero (0.00ppm).
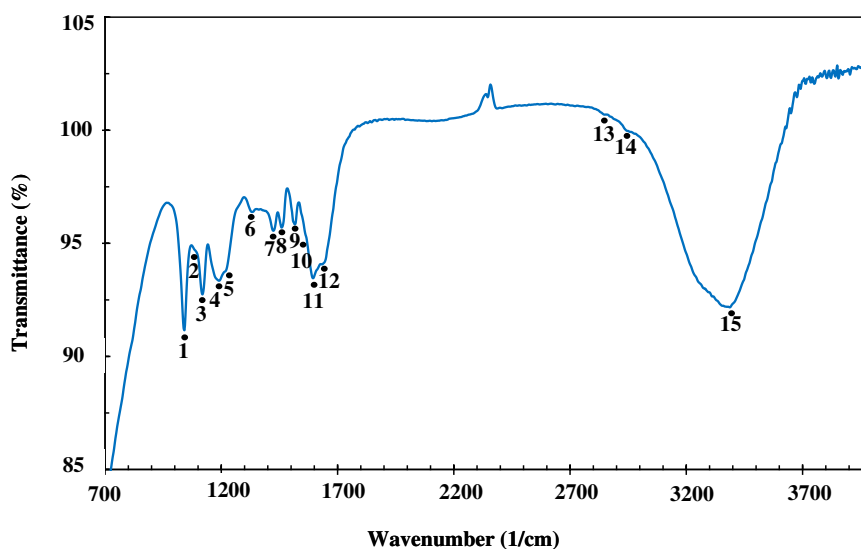
Figure 3.13: FTIR pattern of calcium Lignosulfonate
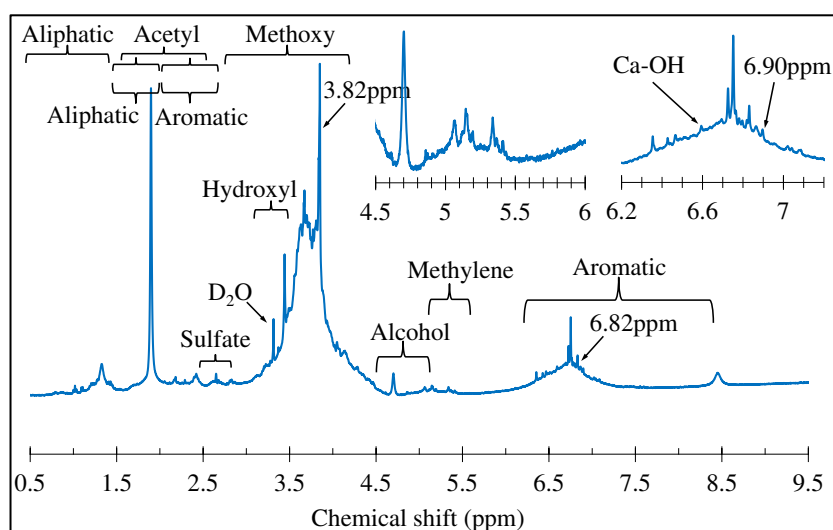
Figure 3.14: ^{1}H-NMR spectra of calcium Lignosulfonate

105

Table 3:3: Interpretation of FTIR bands of calcium Lignosulfonate admixture

Serial no.	Band position (cm-1)	Origin	Assignments
1	1041	C-O-C	Stretching vibration
2	1220	C-O	Phenol stretching
3	1221	C-C, C-O	Stretching vibration
4	1190	S-O	Sulfonic group
5	1334	O-H	Binding vibration
6	1423	C-C, C-H	Aromatic skeleton, C-H in-plane deformation
7	1460	C-H	Deformation (asymmetric in methyl and methylene group
10	1553	Ca^{2+}	Calcium-bound state
11	1508, 15517, 1594	C=C	Aromatic skeletal vibration
12	1600	C-H	Vibration of aromatic ring
13	2845	$O-CH^3$	stretching (methoxyl group)
14	2930	C-H	stretching (methyl and methylene group)
15	3396	O-H	Hydroxy group, H-bonded OH stretch (phenolic and aliphatic hydroxyl group)

3.4.1.3 EDS test:

The major elemental constituents of LS were determined using the EDS technique (Fig 3.15) and the quantitative elemental averages are illustrated in Table 3.5. The test method was similar to that discussed in "Phase 2" for soil characterization. The oxide of calcium cation quantitatively superseded other cations oxides present in the admixture, implying that calcium is the dominant salt present, thus the LS is a CaLS.

Based on the data obtained from the above analytical techniques (i.e. FTIR, NMR and EDS), a chemical structure of the LS was proposed and is presented in Fig 3.16.
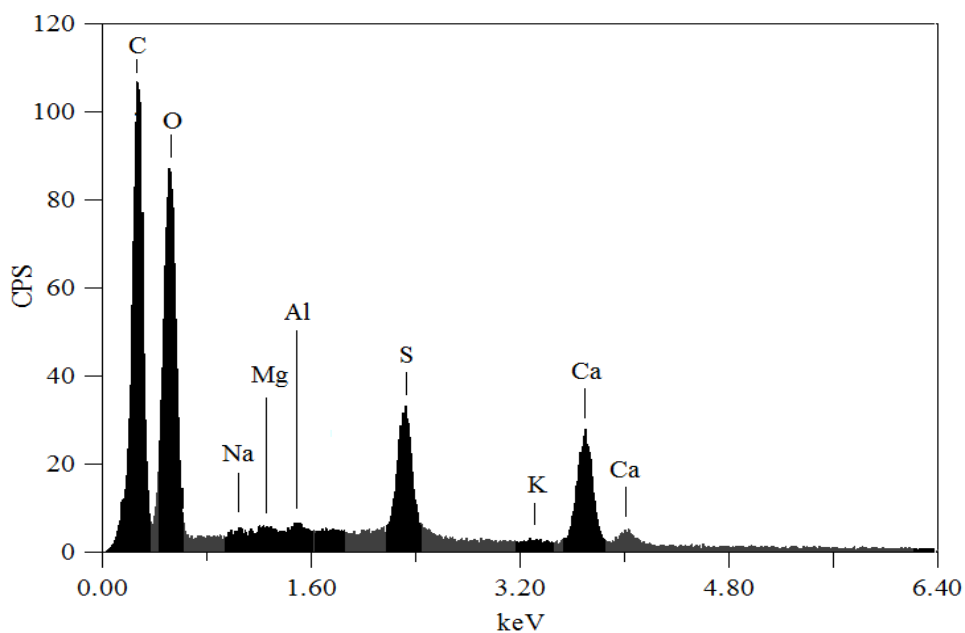
Figure 3.15: EDS spectra of calcium Lignosulfonate admixture

2,2-dihydroxy-1-(4-hydroxy-3-methoxyphenyl)ethanesulfonic acid
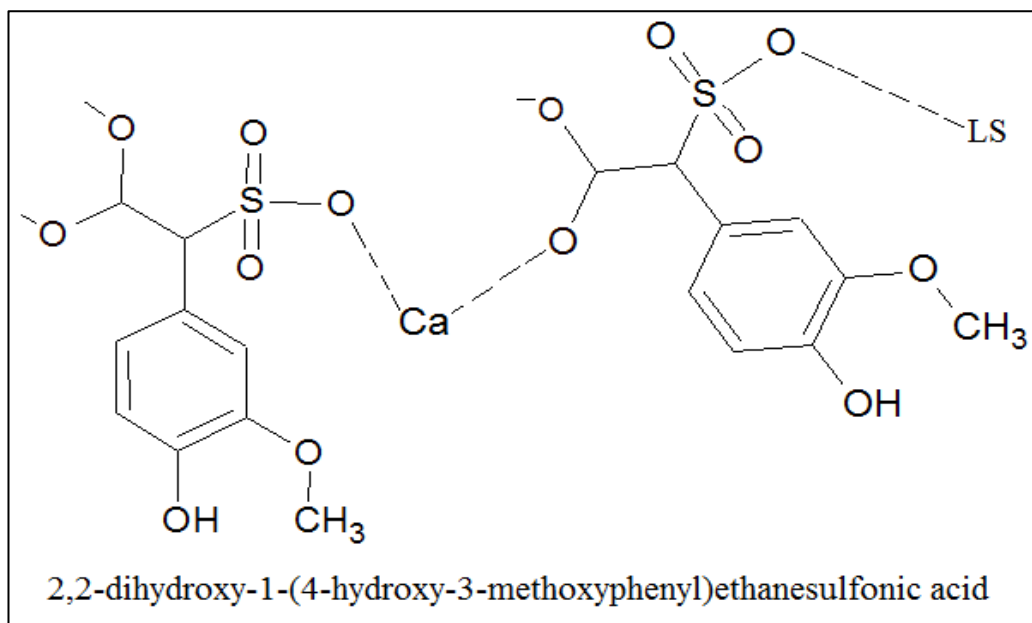
Figure 3.16: Proposed chemical structure of calcium Lignosulfonate admixture

Table 3:4: Assignment and chemical shifts in the ^{1}H NMR spectrum of LS using deuterated water (D_2O) as solvent

Serial no.	Chemical shift (ppm)	Assignment
1	0.9	Aliphatic protons
2	0.9-1.3	Methyl group of protons of highly branched aliphatic structure and terminal methyl groups of methylene chains
3	2.6-4.0	C-O-C (OCH_3)
4	2.58	Methanesulfonate acid
5	3.2, 3.5	OH group proton
6	3.6-3.75	C-H (CH_2) attached to side chain
7	3.3	Deuterated water
8	4.7, 5.0-5.2	C-O (alcohol)
9	6.6, 6.7	Ca-OH
10	3.82, 6.82, 6.92	Aromatic H in Guaiacol structure
11	8.5	Proton of phenolic hydroxyl

3.4.1.4 pH measurement:

The same model of pH meter that was discussed in "Phase 2" was used to determine the pH of the liquid admixture. About 10mL of the concentrate (as supplied) was put into a 25mL measuring cylinder and the pH probe was inserted to measure the pH of the admixture. It recorded a pH of 2.9. After dilution to OMC, the pH reading was found to have increased from 2.9 to about 6.4, attaining close to a neutral value.

Table 3:5: Elemental composition of LS using EDS technique

Compound	Mass (%)
Carbon (C)	60.98
Sulfur oxide (SO_3)	19.77
Calcium oxide (CaO)	17.37
Aluminium oxide (Al_2O_3)	0.72
Magnesium oxide (MgO)	0.47
Potassium oxide (K_2O)	0.29
Sodium oxide (Na_2O)	0.12

3.5   PHASE 4: METHODS OF CHARACTERIZATION ON THE EFFECT OF LS ON THE SWELL POTENTIAL AND OTHER ENGINEERING PROPERTIES OF THE REMOULDED EXPANSIVE SOIL

Conventional geotechnical laboratory tests were conducted to assess how much of the swell potential and other relevant engineering properties of the soil had changed after LS addition. The untreated and samples treated with LS were tested in order to compare changes in the engineering properties. Specimen preparation for each of these standard laboratory tests differed significantly so the techniques are discussed under each test method. The following engineering properties of the soil were assessed:

  ➢ Swell potential of untreated and LS treated samples using conventional one dimensional swell tests

  ➢ The Atterberg limits of the soil before and after LS treatment

  ➢ Soil gradation analysis before and after LS treatment

  ➢ Freezing and thawing durability test before and after LS addition

  ➢ Uniaxial compressive strength test of soil before and after LS treatment

➢ Compaction characteristics of soil before and after LS treatment

➢ Consolidation behaviour before and after LS treatment

➢ Soil permeability before and after LS treatment

3.5.1 Specimen Preparation

A rational procedure was developed for preparing the *"stock sample"* soil from which the different test specimens were prepared. The procedure for preparing the *"stock sample"* and percent swell test specimen are described in five steps below:

Step 1: Determine the optimum moisture content (OMC) and maximum dry unit weight (MDUW) of the soil in accordance with AS 1289.5.1.1-2003.

Step 2: Mix an aliquot of dry soil with OMC and mellow for 24hrs to ensure uniform distribution of moisture throughout the sample. *NOTE:* At the end of step 2, the soil is then referred to as the *"stock sample"*.

Step 3: From the *"stock sample",* determine the soil mass required for compaction into a given mould (e.g. Φ50 x 20mm high oedometer ring) using equations 3.3 and 3.4. Compact the soil mass into the mould to achieve the required density. In this investigation, the static compaction method at a rate of 1mm/min was used.

$$\rho_d = \frac{\rho_B}{1+w} \qquad (3.3)$$

$$\rho_B = \frac{m}{V} \qquad (3.4)$$

Where

ρ_d = dry density of soil (as obtained from Standard Proctor compaction test), ρ_B = bulk density of soil, w = compaction water content, m = soil mass required for compaction into a given mould, V = volume of the given mould.

Step 4:   Seal the compacted soil in plastic bags and cure for 7 days at constant humidity.

Step 5:   Carefully un-wrap the specimen for swell test.

NOTE: The same procedure was followed for specimens treated with LS except in step 2 where the dry soil was mixed with OMC and the predetermined amount of LS by dry weight of soil. A pictorial illustration of the specimen of treated soil and the test setup is shown in Fig 3.17

3.5.2   *Methods of characterization*

3.5.2.1   **Determination of percent swell and volumetric/linear shrinkage:**

The ASTM D4546 "Standard Test Methods for One-Dimensional Swell or Settlement Potential of Cohesive Soils" was used to measure the swell potential of untreated and LS treated specimens. Specimens measuring 50mm in diameter by 20mm high were prepared and tested in conventional one dimensional oedometer apparatus (Fig 3.17). A seating load of 7kPa was applied in accordance with Seed et al. (1962) recommendations. The test specimens were placed into the oedometer, inundated with deionized water, and allowed to swell for 10-14 days, as the case may be. The change in volume data was acquired using a data logger set at 5 minute intervals until a defined linear secondary swell response was observed. The magnitude of the percent swell (S) was determined using equation 3.5 and the values were plotted against elapsed time (min) in logarithmic scale.

$$S = \frac{\Delta H}{H_o} \times 100 \qquad\qquad (3.5)$$

Where

ΔH = change in specimen height, H_o = height of original soil specimen

111
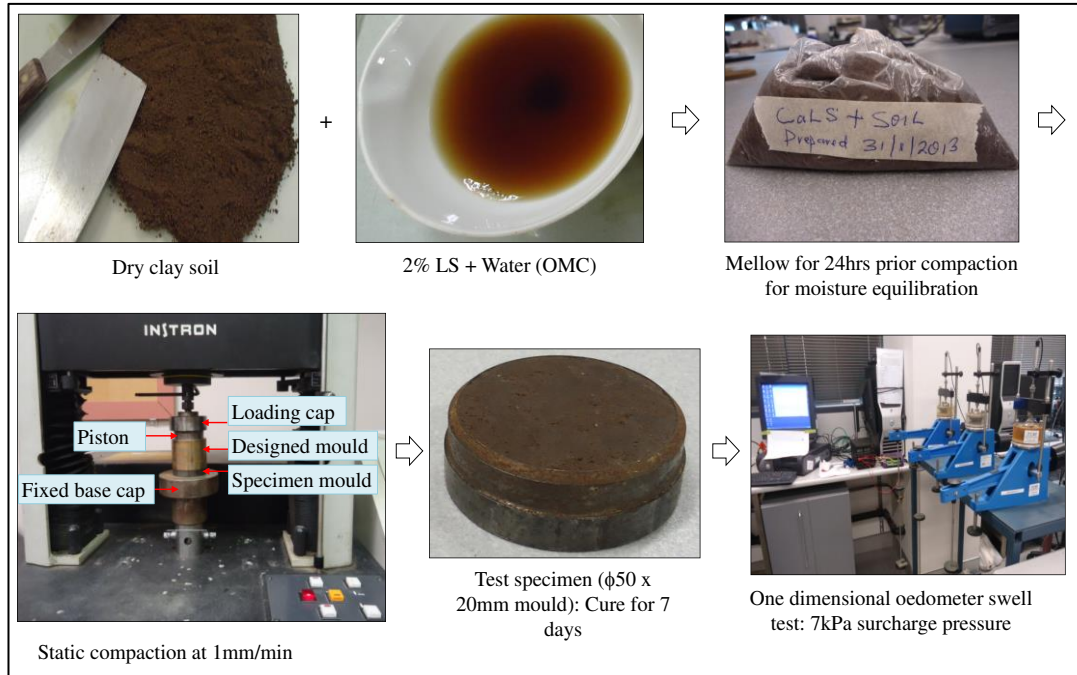
Figure 3.17: Specimen preparation for CaLS treated soil and percent swell test setup

At the end of the one dimensional swell tests the specimens were removed from the equipment and placed in containers at room temperature to determine the volumetric shrinkage. The procedure followed was in accordance with Braiud's (1998) recommendations. The dimensions and weights of the expanded specimens were measured, recorded, and monitored at 6 hourly intervals as the specimens dried to a constant mass. The specimens were then placed into an oven set at 105^0C to obtain the final weight and dimensions. The volumetric shrinkage (V_s) was calculated using equation 3.6.

$$V_s = \frac{\Delta V}{V_f} \times 100 \qquad (3.6)$$

Where ΔV = change in specimen volume, V_f = final height of soil specimen after oven drying.

Linear shrinkage of the untreated and LS treated samples was determined by following the Australian Standards (AS 1289.3.4.1). Soil materials passing the 425um sieve was used for this test. The amount of deionized water added to the dry

soil was equal the water content that would permit a cone penetration of 20mm in a liquid limit test. The shrinkage test was carried out by placing the clay-water complex into a linear semi-circular moulds (Fig 3.18) and allowed to dry at room temperature, and then in an oven set at 105^{0}C. The linear shrinkage (SL) of the specimens was calculated from equation 3.7.
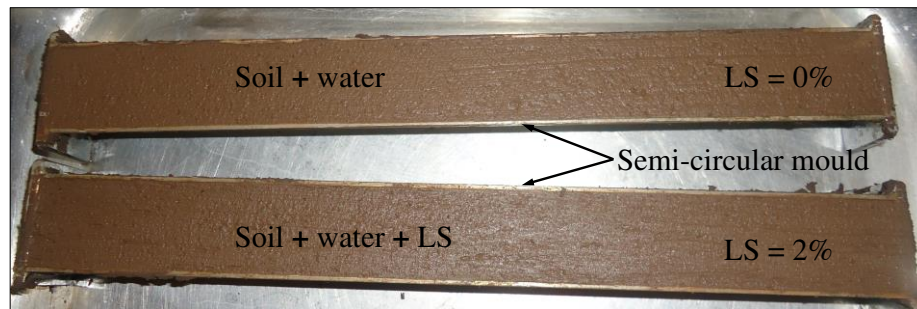
Figure 3.18: Linear shrinkage test setup

$$SL = \frac{L_s}{L} \times 100 \qquad (3.7)$$

Where

Ls = longitudinal shrinkage of the specimen (mm) and L = length of mould (mm)

To determine the swell pressure of untreated and LS treated samples, the ASTM D4546 method "A" i.e. *wetting-after-loading tests on multiple specimens* was adopted. Seven identical specimens were assembled in oedometer units under different seating loads and inundated and allowed to swell or undergo hydro-compression. The amount of swell or hydro-compression was measured and recorded in each seating load. The data from this test was used to estimate the magnitude of swell pressure of the samples which equals the minimum vertical stress required for preventing swell.

3.5.2.2 Determination of Atterberg limits:

The Atterberg limits of the untreated and LS treated samples were determined in accordance with Australian Standards. These samples were mixed with deionized water and stored in sealed plastic bags for 24hrs prior to testing. The liquid limit of

the samples was determined using the cone penetration technique (AS 1289.3.1.9), while the conventional method of rolling moist soil to crumble at 3mm diameter threads was used for the plastic limit test of these samples (AS 1289.3.2.1-2009). The moisture content at which 3mm diameter soil crumbled was reported as the plastic limit.

3.5.2.3   Determination of particle size distribution:

The gradation of untreated and LS treated samples was determined using a Malvern Laser Radiation Class 3B Master-sizer. About 2g from each of the samples was placed into a 50mL beaker containing 25mL of deionized water. The clay-water mix was stirred for about 5 minutes and then poured into the Master-sizer bath (Fig 3.19). The Master-sizer is equipped with a device that automatically generates the soil particle distribution data and curves.

Figure 3.19: Soil gradation analyser: Malvern 3B Master-sizer (Courtesy: UOW)

3.5.2.4   Determination of freezing and thawing durability characteristics:

Freeze-thaw durability tests were carried out to simulate the effect of seasonal temperature on the percentage of soil mass lost, percentage of soil moisture variation, and percentage of soil volume change. It was carried out in accordance with ASTM D560 but with slight modifications. In this investigation the application of a wire stretch brush as prescribed in the standard test method was avoided because the samples had very low resistance. The samples were prepared at the optimum moisture content and compacted at a rate of 1mm/min into a 105mm diameter by 115mm high mould until desired density was achieved. Each specimen was compacted in three layers. The top surface of each preceding layer was marked with a sharp object in regular patterns to ensure seamlessness between the layers of soil.

114

Fig 3.20 shows the specimens prepared for the freeze-thaw durability test after 7 days of curing in a temperature controlled room.

A freezing-and-thawing cycle for this test consisted of freezing the specimens at -4^{0}C for 24 hours and then thawing them for 24 hours at room temperature (20^{0}C) with a relative humidity of 98%. Freezing a specimen for 24hours and thawing it for another 24 hours represents one cycle; and these samples were predetermined to undergo 12 cycles of freezing and thawing in 24 days.
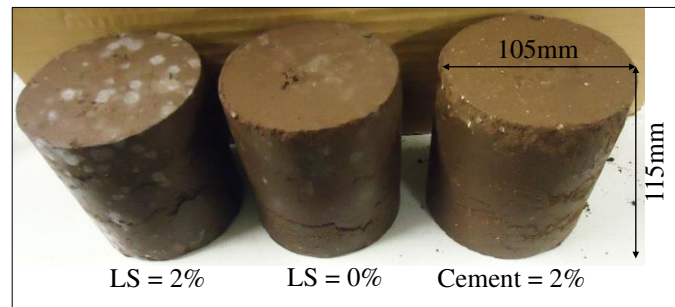
Figure 3.20: Freeze-thaw durability test specimens

3.5.2.5   Determination of wetting and drying durability characteristics:

Specimens identical to freeze-thaw were prepared for the wet-dry tests from the untreated and LS treated soil samples. The test procedure was a slight modification of ASTM D559. The application of wire scratch brush, as prescribed in the standard test method was avoided because the samples had very low resistance to such pressure. This test was carried out on untreated and LS treated specimens to determine the loss of soil mass, variation in moisture, and changes in volume produced by repeated wetting and drying. The weight and dimensions of each specimen were measured and recorded prior to commencing the test. The specimens were submerged in a water bath for 1 hour, their weight and dimensions were measured and recorded, and then they were placed inside an oven set at 25^{0}C for 42hours. Twelve such cycles of wetting and drying are recommended by the ASTM Standard Method for Wet-Dry testing of compacted soil-binder mix. The durability of the samples was measured by correlating the number of wet-dry cycles with moisture variation, mass lost, and change in volume.

3.5.2.6 Determination of uniaxial compressive strength (UCS) characteristics:

The purpose of the UCS test was to examine the unconfined compressive strength behaviour and the mode of failure of soil sample upon LS addition. The methods for preparing and testing compacted materials for unconfined compressive strength as recommended in AS 5101.4 were followed. An appropriate mass of soil was collected and mixed with OMC and cured for 24hrs prior to compaction. A pre-determined mass of soil was statically compacted into a 38mm diameter by 78mm high mould at a rate of 1mm/min to achieve MDUW. The specimen was then extruded and sealed in plastic bags for 7 days prior to testing. The UCS of the specimens was calculated using the following equation (3.8):

$$UCS = \frac{F \times 1273}{(D_{av})^2} \qquad (3.8)$$

Where

UCS = unconfined compressive strength (MPa), F = load at failure (kN), D_{av} = average diameter (mm), *NOTE:* $1273 = \pi/4 \times 1000$, $\pi/4$ = constant in the formula for the surface area of the specimens

3.5.2.7 Determination of compaction characteristics:

Standard Proctor compaction tests were carried out on the untreated and LS treated soils in accordance with AS 1289.5.1.1 using a compaction effort of 596kJ/m^3. The soil was compacted in a 105mm diameter by 115mm high mould (Fig 3.21), extruded with a mechanically operated hydraulic jack and split longitudinally, from which a representative sample was then taken to determine the water content. To evaluate the potential effects of the LS admixture on the compaction parameters; the OMC and MDUW of untreated and treated data was evaluated and compared.

Figure 3.21: Standard Proctor compaction apparatus

3.5.2.8 Determination of consolidation characteristics of soil:

The consolidation behaviour of untreated soil, soil treated with 2% LS and cement was investigated using conventional one dimensional oedometer test equipment. The samples were remoulded at a water content of about 1.1 times the liquid limit. Consolidation tests were performed as per ASTM D2435, with gradual load increments from 100, 150, 200, 400, 800, 1500, 2500, to 3500kPa. At each load increment, a 4 day time period was allowed to ensure that primary consolidation was complete. The consolidation parameters, i.e. the coefficient of consolidation (c_v), and coefficient of volume change (m_v) (equations 3.9-3.10) were evaluated to determine how LS and cement affected these parameters of the remoulded expansive soil.

$$C_v = \frac{0.111\overline{H}^2}{t_{90}} \qquad (3.9)$$

$$M_v = \frac{\Delta e}{\Delta p} \times \frac{1}{1+e} \qquad (3.10)$$

Where

$\overline{H}$ = average thickness of the specimen for the load increment, in millimetres; t_{90} = time for 90 per cent primary consolidation, in minutes; Δe = change in void ratio of the laboratory specimen; Δp = increase in pressure, in kilopascals, above the present overburden pressure; e = void ratio of the laboratory specimen.

117

3.5.2.9   Determination of soil permeability characteristics:

The Falling Head Permeability apparatus was used to measure the permeability of untreated, LS, and cement treated samples. The apparatus and testing procedures for the "Falling Head Permeability" are detailed in Das, (1997). Water from a standpipe flows through the sample with recorded initial head difference h_1 at time t = 0. Water is then allowed to flow through the saturated specimen such that the final head difference at time t = t_2 is h_2 (Fig 3.22).
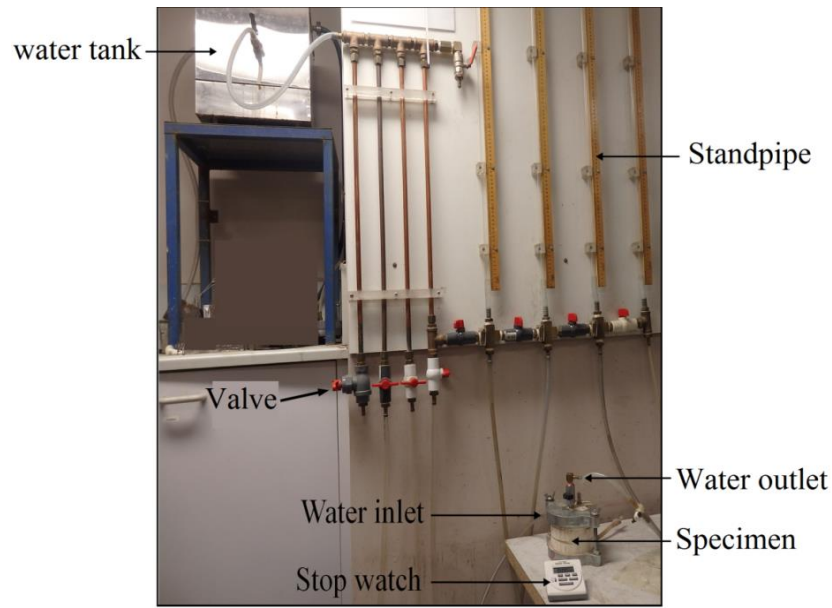
Figure 3.22: Falling Head Permeability equipment (Courtesy: UOW)

The coefficient of water permeability (k_w) through the specimen was calculated according to a predefined equation (3.11).

$$k_w = \frac{2.3 a_s h}{(6 \times 10)^4 \times At} \times \log_{10}\left[\frac{h_i}{h_f}\right] \qquad (3.11)$$

Where

k_w = coefficient of permeability in metres per second; a_s = cross-section area of standpipe in square millimetres; h = thickness of specimen, in millimetres; A = cross-sectional area of specimen in square millimetres; t = time interval for

measurement, in seconds; h_i = initial height in the standpipe, in millimetres; h_f = final height in the standpipe after time interval (t), in millimetres; θ = temperature of outflow water, in degrees Celsius.

3.6 PHASE 5: METHODS OF IDENTIFICATION OF STABILIZATION MECHANISMS OF LS ADMIXTURE

A micro-characterization study and subsequent identification of the stabilizing mechanisms of LS admixture on expansive soil was achieved by using a number of instrumental analytical techniques. The physical/chemical changes before and after LS addition was evaluated and compared to give an insight into the possible reaction mechanisms. To achieve this objective, analytical techniques such as XRD, SEM/EDS, FTIR, CT, CEC, and as well as SSA, were used. In every case the tests were repeated at least 3 times to characterize the variability and significance of the observed changes. These mechanisms were then correlated to changes in the properties of the compacted soil samples.

3.7 PHASE 6: METHOD FOR SOIL SUCTION DETERMINATION

To develop a mathematically predictive model for the percent swell behaviour of LS, it was imperative to experimentally determine the suction behaviour of soil after treatment. To achieve this objective, the "Standard Test Method for Determination of the Soil Water Characteristics Curve for Desorption" using pressure extractor (ASTM D 6836) was used (Fig 3.23). Multiple but identical specimens (at least 3) were prepared and tested to minimize variations in the acquired data due to experimental errors. At each stage of pressure increment, about 14-18 days was allowed to enable the specimens to attain equilibrium. The water content at each applied pressure was measured gravimetrically by weighing the specimen after removal from the apparatus.

119
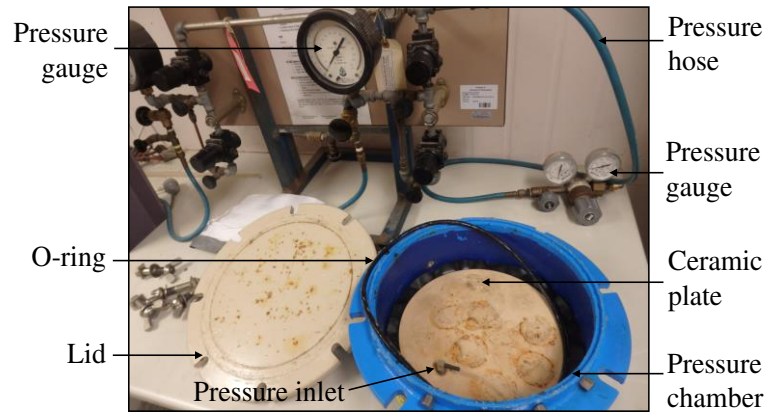
Figure 3.23: Photograph of a multiple-specimen pressure chamber (Courtesy: UOW)

3.8 PHASE 7: EVALUATION OF LABORATORY DATA FOR THE DEVELOPMENT OF A ROBUST MATHEMATICAL MODEL CAPABLE OF PREDICTING THE SUCTION BEHAVIOUR OF CALS TREATED EXPANSIVE SOIL.

The vertical strain of a soil is a function of the rate of moisture diffusing into the interlayers and inter-particle pores of clay minerals, but the flow of moisture in unsaturated soils depends on suction variation within the soil. Thus, if the flow of moisture through a body of soil has been determined, the suction within a defined space and time can be specified using modified Darcy's law (Lytton 1977).

To measure the change in suction, the rate of moisture diffusing into the soil was estimated mathematically, so by knowing the suction behaviour in LS treated soil, an empirically developed equation (3.12) based on test data could be used to model the movement of the surface of treated soil.

$$S = C_w \left[- A(\varphi_{Nor}) + B \right] \tag{3.12}$$

Where

φ_{Nor} = normalized soil suction, C_w = coefficient depending on the amount of adsorbed moisture with time, A and B are fitting parameters equal to -0.86 and 0.93, respectively.

3.9   PHASE 8: SUMMARY

The test methods used in this research program sufficiently met the aims of the investigation. The materials used in the investigation were thoroughly investigated and characterized. The laboratory test provided ample data on the swell behaviour of the remoulded expansive soil before and after LS treatment and on other engineering properties such as durability, strength, consolidation, and permeability. The instrumental analytical techniques provided in-depth technical information on the stabilization mechanisms of LS admixture on a remoulded expansive soil. The approach used in the development of suction and swell models of LS treated expansive soil was robust to the extent required in the study.

CHAPTER 4

4 THE SWELL BEHAVIOUR OF CALCIUM LIGNOSULFONATE TREATED EXPANSIVE SOIL

4.1 INTRODUCTION

The efficacy of LS to alter the swell potential (i.e percent swell and swell pressure) of remoulded expansive soil was assessed using standard geotechnical laboratory test methods. These tests were carried out on samples of soil before and after treatment with LS in order to measure by how much the percent swell was affected by the admixture. Three liquid LS admixtures [sodium (Na), potassium (K), and calcium (Ca)] were available for examination. The admixtures were assessed based on a one dimensional swell test. After identifying the most effective LS admixture, the optimum application rate was then determined. This chapter discusses the tasks outlined above. Furthermore, additional engineering properties were also investigated after samples were treated with the selected LS admixture. These properties included:

1   Volumetric/linear shrinkage

2   Atterberg limits (Liquid limit, plastic limit and plasticity index)

3   Soil durability in terms of freezing-thawing and wetting-drying

4   Uniaxial compressive strength (UCS)

5   Compaction characteristics

6   Consolidation characteristics

7   Permeability and Soil pH

4.2 SELECTION OF APPROPRIATE LS ADMIXTURE

In this research project the procedure for selecting the admixture involved assessing how much reduction in the percent swell was achieved after treatment with each of the three LS admixtures (Fig 4.1a-c). Conventional one dimensional swell tests were carried out in accordance with ASTM D4546. The contents of the admixtures were varied from $0 - 3\%$ by dry weight of soil based on suggestions from the reviewed literature. Fig 4.1a shows the influence of a NaLS admixture on the percent swell of the remoulded soil. The percent swell increased as the content of NaLS increased, probably due to the ease with which the sodium cations in LS were hydrated (section 2.7), whereas the KLS improved the expansiveness of soil slightly (Fig 4.1b). This marginal decrease could be ascribed to the relatively low hydration energy of potassium cations present in the LS ligand. CaLS reduced the percent swell of the soil from 6% to 4.7%, which is approximately a 22% reduction. The comparatively low hydration energy of calcium cations coupled with the cation exchange capability of the CaLS ligand and its susceptibility to adsorption by soil minerals are the likely reasons for this remarkable reduction in soil expansiveness.

For NaLS treated soil, the most effective application rate in terms of percent swell reduction is 0.5% by dry weight of soil, whereas this amounts corresponded to 1% and 2%, respectively for the KLS and CaLS admixtures. Plotting these LS contents with their corresponding maximum reductions (Fig 4.1d) indicated that the CaLS admixture was best suited for this particular soil, so calcium lignosulfonate was used throughout this research project.
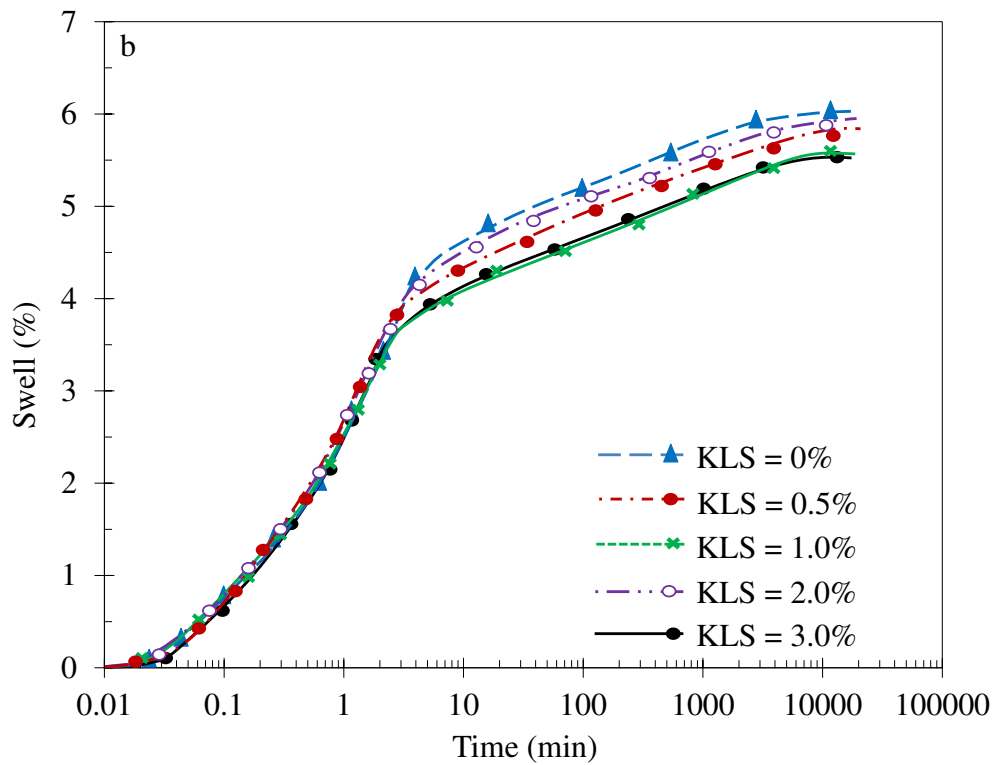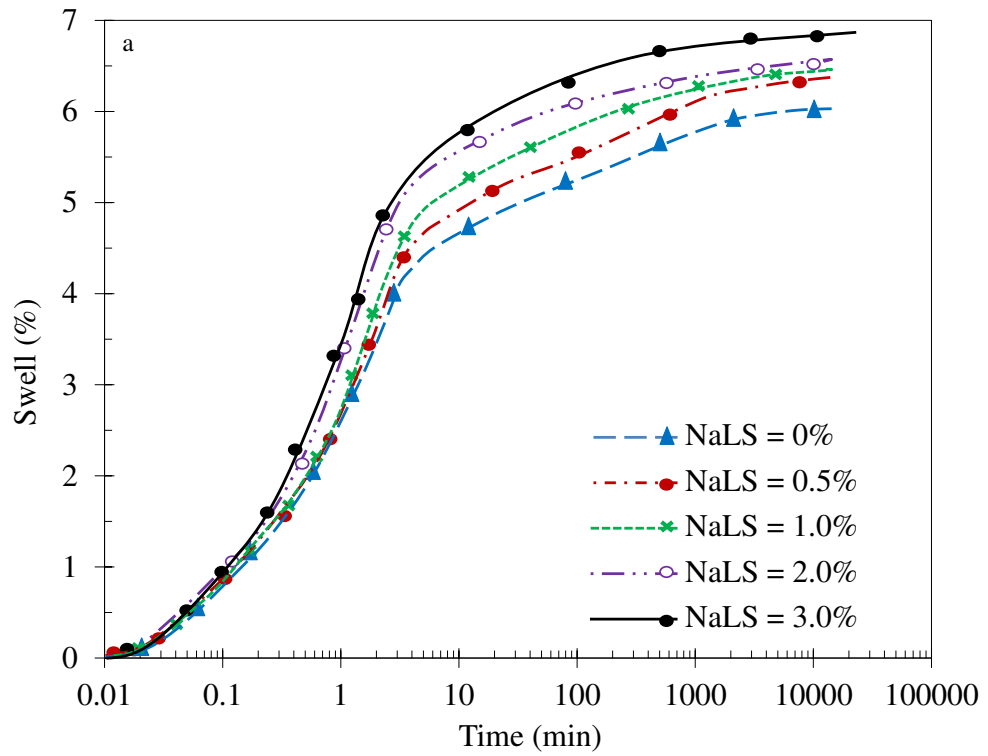
Figure 4.1: a) Effect of sodium LS (NaLS), b) potassium LS (KLS) on the percent swell of expansive soil
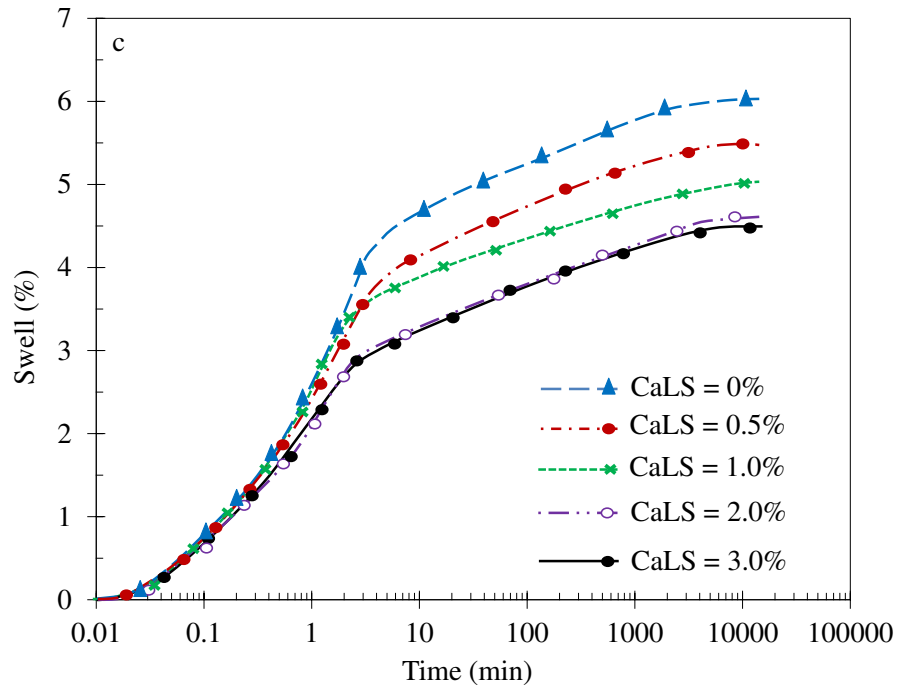
Figure 4.2: c) Effect of calcium LS (CaLS) content on percent swell of expansive soil
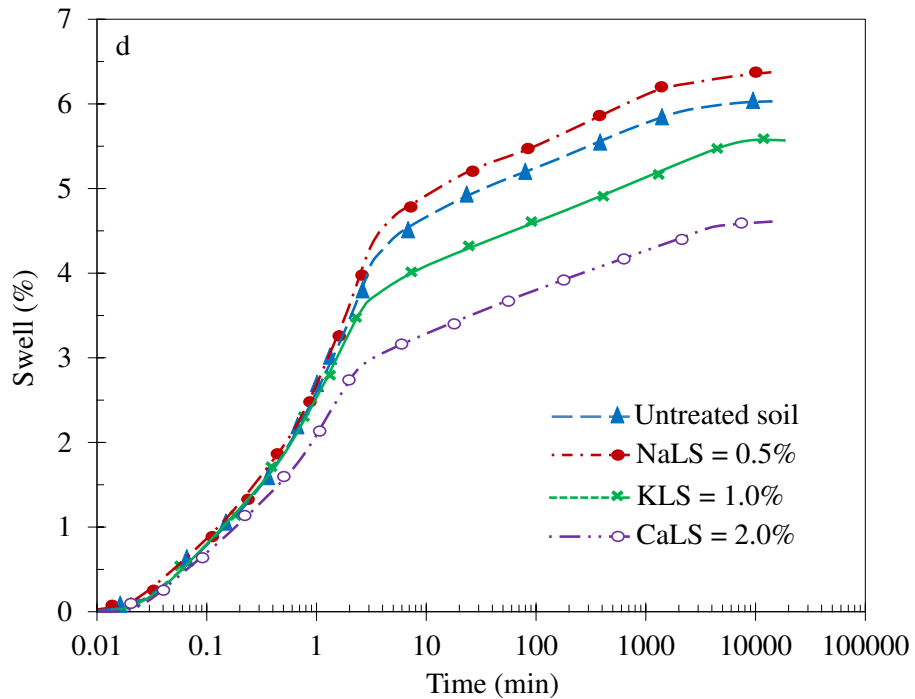
Figure 4.3: d) Determination of the most appropriate LS admixtures; LS contents corresponding to the maximum reduction in percent swell of the three admixtures (Fig 4.1a-c) were selected and plotted against time (CaLS admixture is most appropriate for the soil).

4.3 DETERMINING THE OPTIMUM CONTENT OF THE SELECTED LS ADMIXTURE (CALCIUM LIGNOSULFONATE)

Preliminary laboratory tests were carried out to determine the optimum content of CaLS needed to effectively stabilise the remoulded expansive soil. The test methods consisted of the conventional one dimensional swell test for samples of soil before and after treatment with CaLS and determining the Atterberg limit of the samples before and after treatment. The content of CaLS was varied from 0-7%. The most significant reduction (4.7%) occurred at 2% by dry weight of soil, which suggested that the optimum content of the admixture for this particular soil was about 2% (Fig 4.2). Applying 4% and 7% of CaLS the percent swell is was 5.4% and 5.7%, respectively. Sarkanen and Ludwig (1971) reported that LS can behave like an expanding polyelectrolyte because it carries a strong negative charge in neutral solutions. These negative charges are balanced by positively charged cations dispersed in the DDL of clay so when the application rates exceed the threshold value, the excess molecules of the polyelectrolyte (CaLS) which did not participate in the stabilization process due to spent ions in the clay result in mutually repulsive forces between the charged sections of the LS chain, causing the molecules to expand. This is possibly why beyond the threshold of 2% CaLS there was an abnormal increase in the percent swell of the soil.

A follow up test to determine the optimum content of CaLS for the soil was also conducted by measuring the effect that the admixture had on the Atterberg limits, as recommended by Grim (1968). The plasticity index and liquid limit of the soil decreased as the content of CaLS increased until about 2% by dry weight of soil was reached (Fig 4.3). Beyond this the liquid limit and plasticity index increased, which suggested that 2% was the optimum amount for the soil. This is in agreement with the one dimensional swell test data.
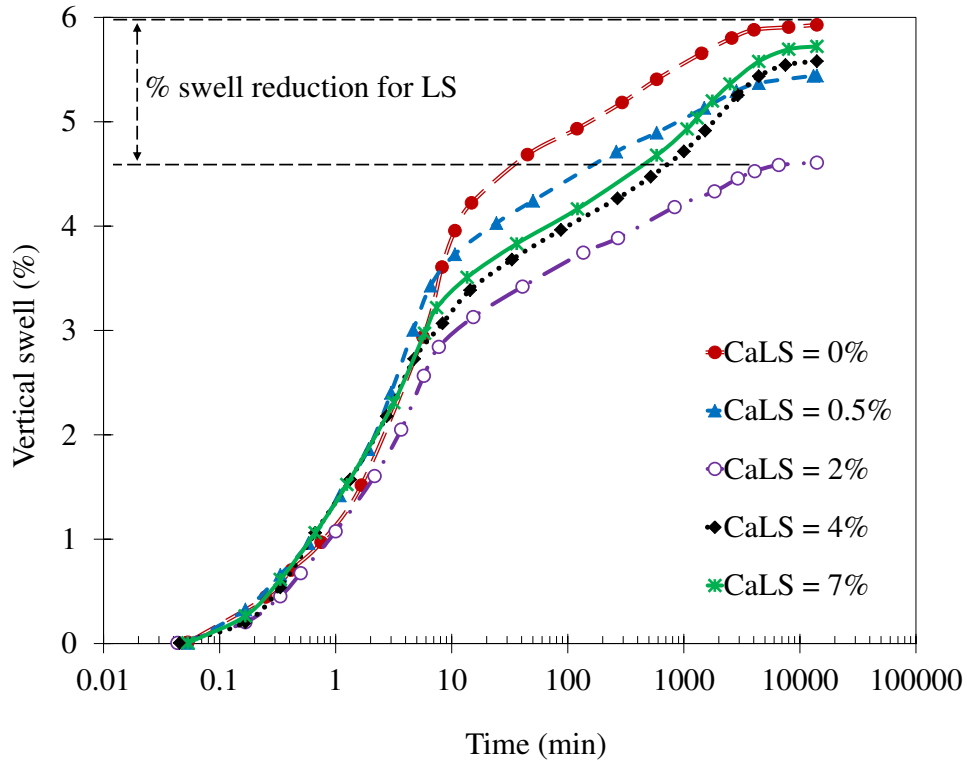
Figure 4.4: Method of determination of optimum application rate of CaLS admixture
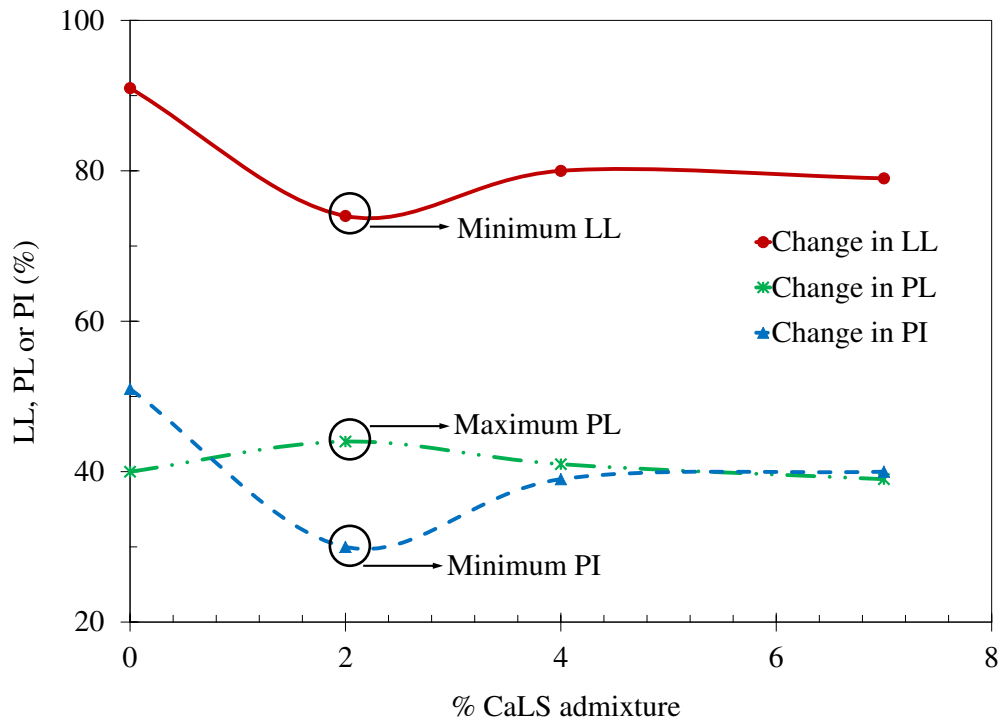
Figure 4.5: Another approach for the determination of the optimum CaLS content;
effect of CaLS on the Atterberg limits of the remoulded soil

4.4 EFFECT OF CALCIUM LIGNOSULFONATE ON THE SWELL BEHAVIOUR OF REMOULDED EXPANSIVE SOIL

The effects of 2% CaLS and cement on the percent swell of the remoulded expansive soil are illustrated in Fig 4.4. The test results varied despite the fact that the untreated and chemically treated specimens were prepared identically. Untreated clay can swell vertically by almost 6%, but when treated with 2% CaLS, the maximum vertical swell was about 4.7%, (Fig 4.4), accounting for a 22% reduction. This is a significant improvement in the percent swell, particularly for "low" formations of expansive soils. This reduction in the magnitude of swell was not unrelated to the effect that the admixture had on the index properties of the test soil. At 2% LS application, the plasticity index improved from 51% to 32% (see Fig 4.3), implying that the wettability of the soil decreased and the magnitude of the percent swell decreased. According to Saride et al. (2013), PI is a good indicator of the shrink/swell behaviour of soil, such that the lower the PI the lower the shrink/swell behaviour. For the sake of comparison, the specimen treated with 2% cement is shown in Fig 4.4 and indicates that the magnitude of swell decreased from 6% to 4%, which is a 33% reduction. Although the PI and percentage of swell reduction in soil treated with cement was much lower than the sample treated with LS, LS prompted a 37% reduction of plasticity in the soil. This means that LS could effectively improve the plasticity of a "low" expansive soil.

For soil treated with cement, the LL and PI decreased as the content of cement increased. The LL (91%) of untreated soil decreased to 60% while the plastic limit increased from 40% to 46% at 7% application; this resulted in reduction in PI from 51% to 14% (see Fig 4.3).

4.4.1 Effect of curing time on the swell behaviour of chemically treated soil

The effect of curing time on the percent swell of soil was investigated by conducting swell tests on compacted specimens treated with 2% CaLS and 2% cement and cured for 7, 14, 54, and 180 days. All the samples were prepared at optimum moisture content (OMC) and maximum dry unit weight (MDUW). The effect of curing time on swell behaviour of the soil treated with CaLS is presented in Fig 4.5, and shows

that the rate of swell depended on curing time in respect of the fact that the magnitude at the end of the swell regime was independent of the curing time. The rate of swell decreased as the curing period increased; for instance, after 10 minutes the untreated soil would have almost completed its primary swell (at 4%), whereas the percent swell of the sample cured for 180 days was significantly low at 0.4%, within the same time frame. The swell rate dependency on curing time could mean that the stabilization mechanisms of adsorption, coating, and subsequent aggregation of particles by the CaLS admixture is time-dependant, that is, under laboratory conditions a swell rate of soil treated with 2% CaLS would continue to improve over time.

What was significant was the reduction in the affinity of the soil treated with CaLS for water with the curing time. The percent swell is a function of the volume of moisture adsorbed in expansive soil, the percent swell reduced with reducing volume of adsorbed moisture. Theorganic molecules of CaLS inhibited water from wedging into the inner layers of expansive soil minerals with curing time, meaning there was less change in the rate of volume over time. In a similar study, Rosauer *et al.* (1961) treated bentonite with a dialkyl dimethyl ammonium salt (long unsaturated hydrocarbon chains) and reported that the test specimens resisted the uptake of water on inundation and actually waterproofed the clay fractions. They posited that this waterproofing action by the organic chemical was due to organic coatings around the bentonite aggregates, causing individual molecules to lie close enough together to keep out water.
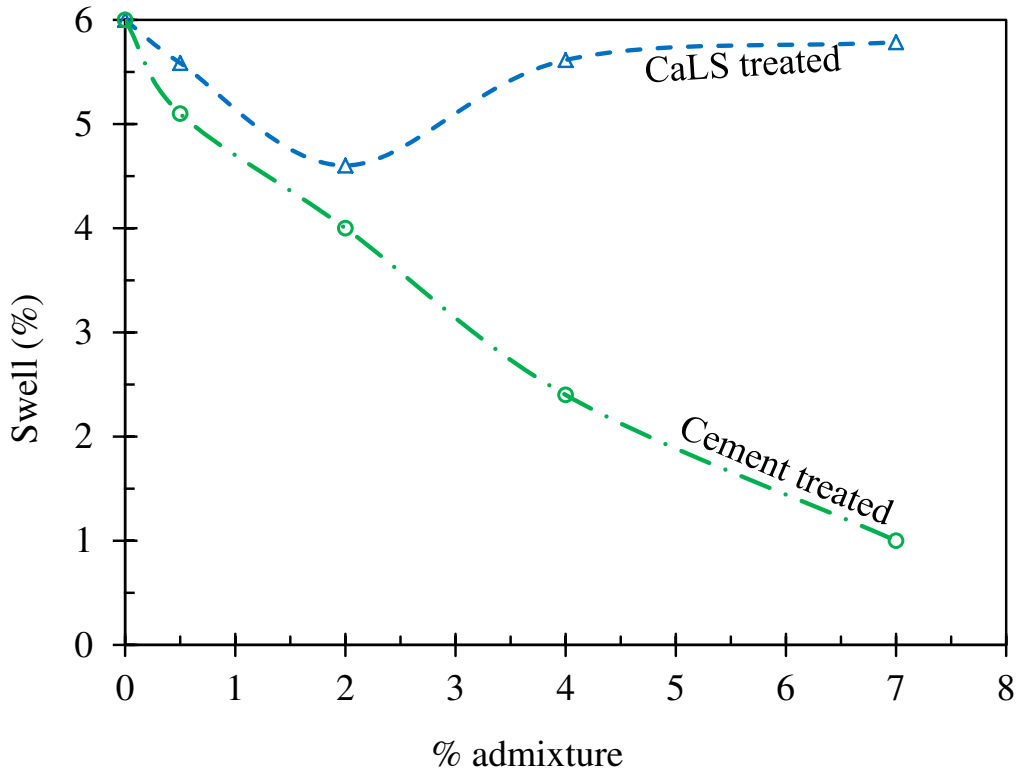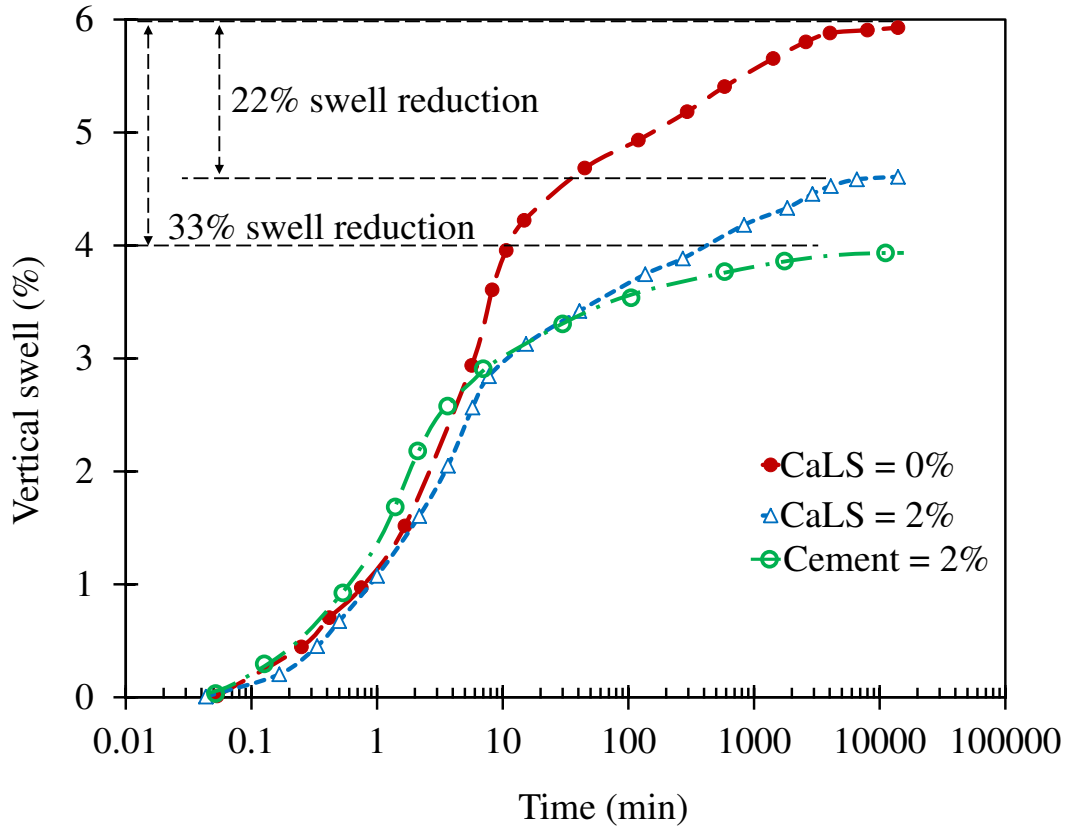
Figure 4.6: Effect of LS content on the percent swell with time,
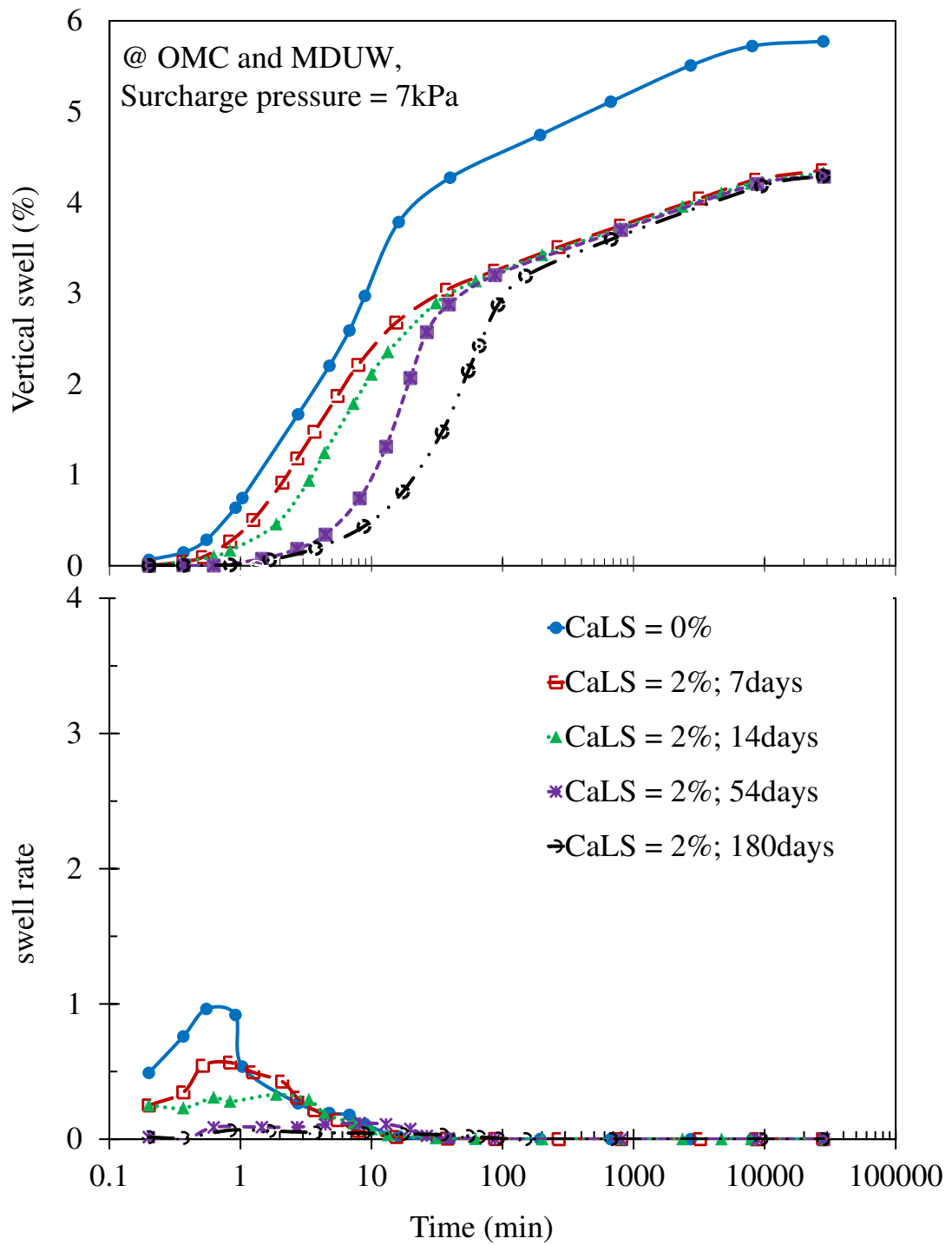
Figure 4.7: Time dependent swell behaviour of CaLS treated expansive soil showing the swell rate of the soil

On the other hand the specimens treated with cement showed no variation in the swell rates regardless of the curing time, although the reduction in percent swell was greater, i.e. from 6.0% to 4.0%, accounting for a 33% reduction (Fig 4.6). Moreover, the initial swell rate was higher than the untreated soil, possibly due to the high hydration energy of calcium ions present in the cement admixture. The independent behaviour of the rate of swell with curing time with 2% of cement implies that stabilization of cement in expansive minerals was completed within 7 days of treatment. Although at higher application rates such as 6% to 8%, the soil pH could increase to 12.4 to initiate pozzolanic reactions, in which case the above statement might not be valid.

4.4.2   *Effect of CaLS on the compaction moisture-dry unit weight and percent swell*

To determine the moisture-dry unit weight-percent of swell relationship of soil and to evaluate the behaviour of this relationship after LS addition, the untreated specimens and those treated with 2% CaLS were subjected to a Standard Proctor compaction test, and five specimens of each were prepared for a one dimensional swell test. These five specimens were replicas of specimens that were obtained from points 1-5 in Fig 4.7. This figure also includes the compacted conditions and the corresponding percent swell for specimens at different initial water contents.

The essence of compaction is to minimise the adverse effects of undesirable geotechnical properties in the soil. Laboratory practice and field compaction data has shown that most construction projects must achieve a compacted field dry unit weight of 90-95% of the maximum dry unit weight determined in a laboratory. The water content affects the extent of compaction operations because water added to the soil during compaction acts as a lubricating agent on the particles. It is common practice in geotechnical engineering that the moisture content lays between ± 2% of OMC.

Fig 4.7 shows such a moisture range and the conventional 95% of the maximum dry unit weight limit; and the various reasons why construction sites are compacted are satisfied within this range of OMC and the dry unit weight, represented by the shaded area. This compaction range gives a relatively satisfactory degree of soil

132

swelling as well because as the initial moisture content decreases, the percent swell increases. However, this progressive increase in the percent swell due to decreasing the initial moisture content is counter balanced by the decreasing density of the soil. In other words, as the dry density of the soil decreases, the amount of intrinsic expandable minerals also decreases and hence the percent swell decreases and creates an opposing sensation with the soil's tendency to swell due to the decreasing initial moisture content. This tendency to swell due to a decreasing initial moisture and the tendency to decrease the magnitude of the percent swell due to a decreasing initial dry density continue until a point referred to herein as the equilibrium point is reached. At this point the opposing phenomena are believed to be equal in magnitude and thus the slope of the swell curve tends to zero. It is expected that beyond the equilibrium point, the percent swell will decrease with decreasing initial moisture content.

4.4.3   *Effect of initial dry density on the shrink-swell behaviour of soil*

Fig 4.8 illustrates the shrink-swell behaviour of untreated expansive soil and that treated with CaLS. The percent swell decreased with as the content of admixture increased to 2%, thus forming a shape referred to herein as the cone of stabilization. This cone is divided into three sections based on the magnitude of the percent swell. The segments suggest that within a low compaction regime, the application of CaLS barely alters the magnitude of swelling, but as the dry unit weight of soil increases so the percent swell decreases. Within the medium compaction region, there is an appreciable reduction in the magnitude of swell, but a further increase in the dry unit weight of soil, i.e. within the high compaction regime, leads to a reduction in the percent swell such that 1% of CaLS equals the reduction experienced by 2% of CaLS within the low compaction range. The practical implication of these findings is that the efficacy of CaLS to stabilise expansive soils improves with the increasing initial dry unit weight of soil. It is therefore suggested that soil treated with CaLS should be compacted at OMC/MDUW in order to maximise its potential.

133
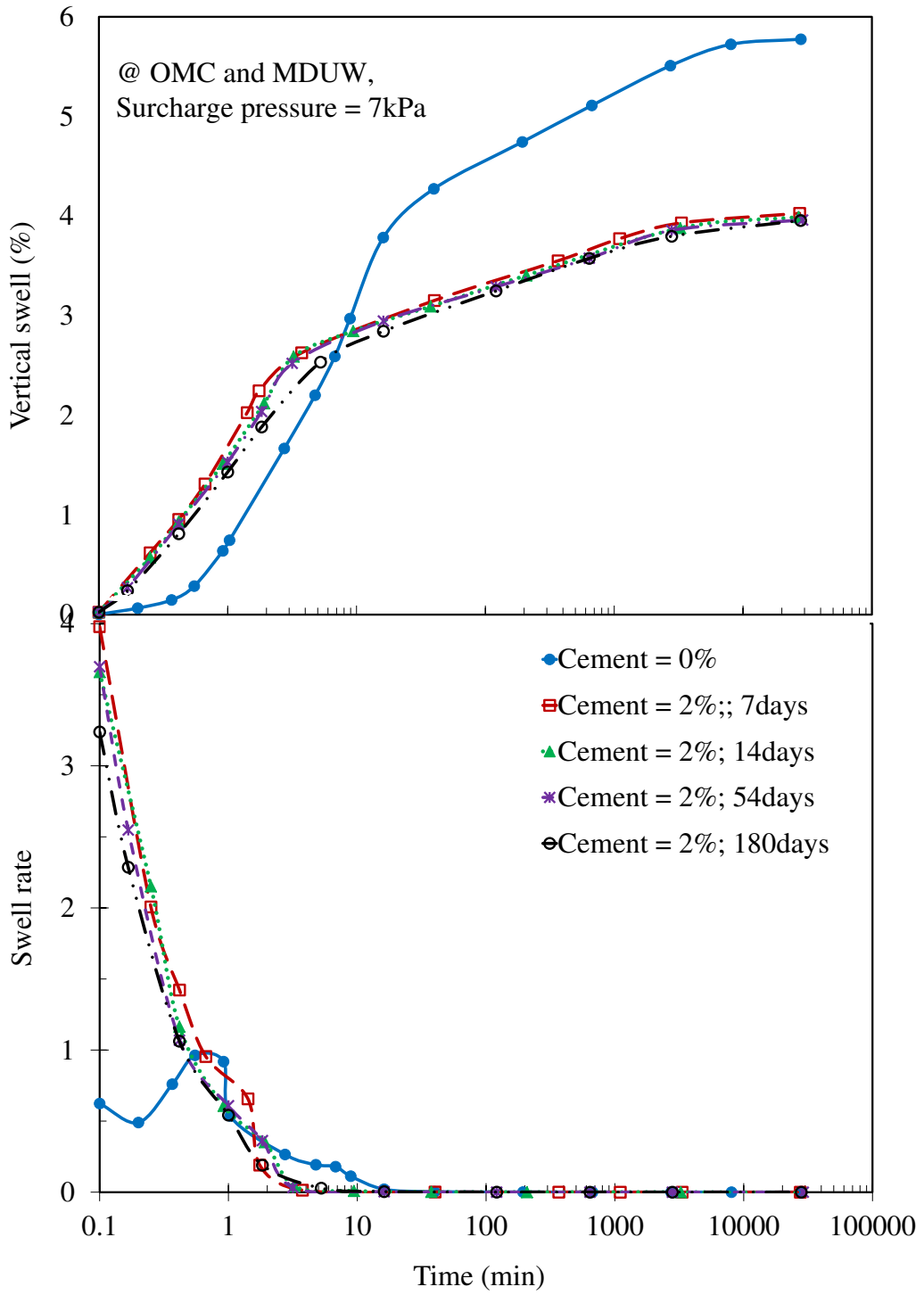
Figure 4.8: Time dependent swell behaviour of cement treated expansive soil showing the swell rate of the soil
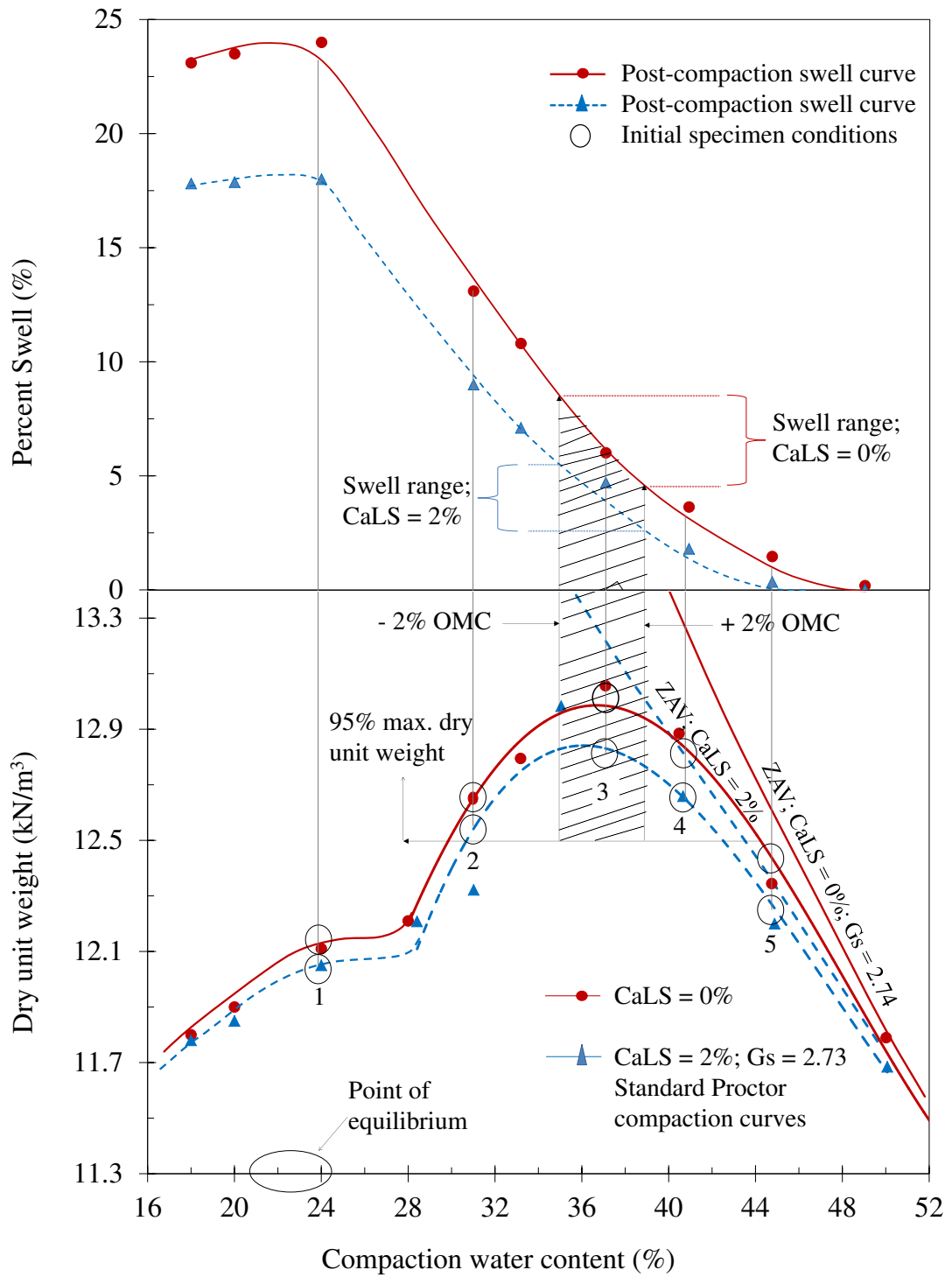
Figure 4.9: Relationship between compaction soil moisture-dry unit weigh and percent swell

Similarly, the magnitude of soil shrinkage decreased with an increasing initial dry weight of soil, while the incremental addition of CaLS showed a continual decrease in shrinkage. After 2% was added the soil's potential to shrink was almost non-existent, an effect that was more pronounced within the high compaction regime. The effective packing together of soil particles within the "high compaction region" coupled with the stabilization effect introduced by the CaLS admixture prevented the soil from shrinking. Although the effect of CaLS on shrinkage was less significant when juxtaposed with the reduction in the percent swell, its effect cannot be neglected because the shrinkage behaviour supported the suggestion that soil treated with CaLS should be compacted at MDUW/OMC to maximize its benefits.
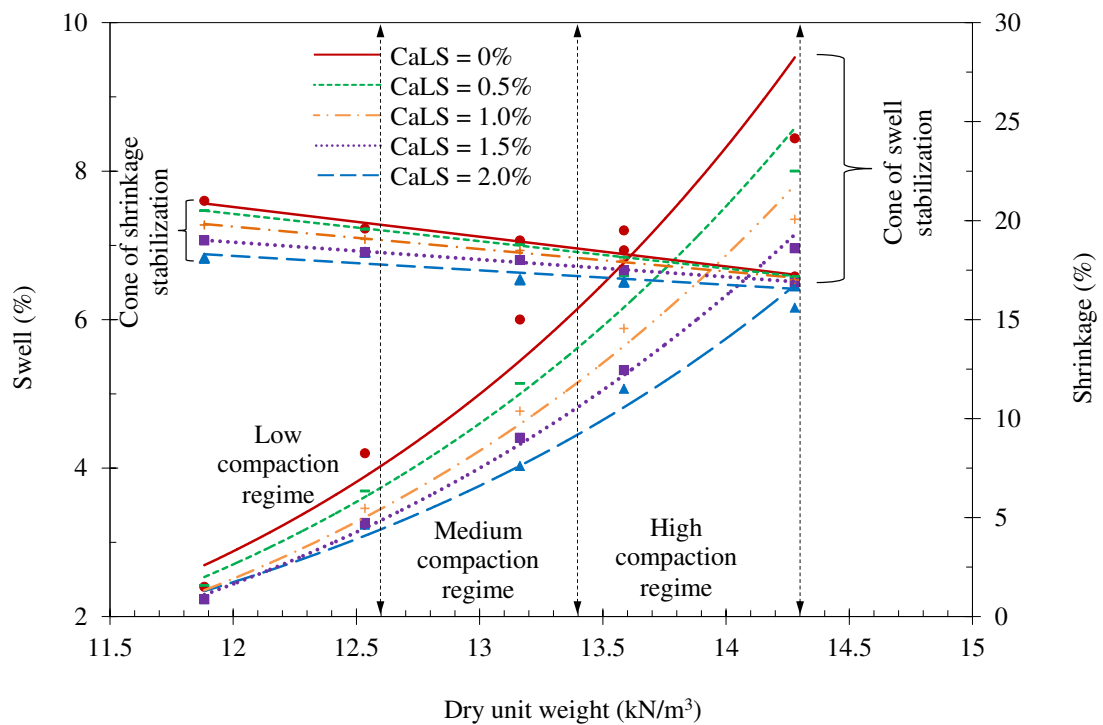
Figure 4.10: Effect of initial dry unit weight on shrink-swell behaviour of soil

4.4.4 *Effect of CaLS on the swell pressure of remoulded expansive soil*

The swelling pressure of the remoulded soil was 105kPa but it decreased to 84kPa after 2% of LS addition (Fig 4.9). In the sample treated with 2% cement the swelling pressure decreased to 80kPa. At this low dosage, the stabilizing effect of cement on the swell pressure of the remoulded soil was similar to using 2% CaLS admixture.

This suggested that CaLS could be a good alternative, considering its low cost and smaller environmental footprint, especially for stabilizing deposits of "low" expansive soil. The figure shows that within a surcharge pressure range of 80 to 280kPa, the treated samples compressed more than the untreated sample. This could be because untreated soil has a greater tendency towards swelling than the treated samples under the same surcharge pressure, but at surcharge pressure of about 300kPa, compression was the same for both untreated and chemically treated soil specimens.

The surcharge pressure at which the magnitude of compression of untreated sample equalled the chemically treated sample is referred to herein as the critical pressure, and this critical pressure is equal to the pressure beyond which the compressive behaviour of untreated and treated specimens does not change over time.
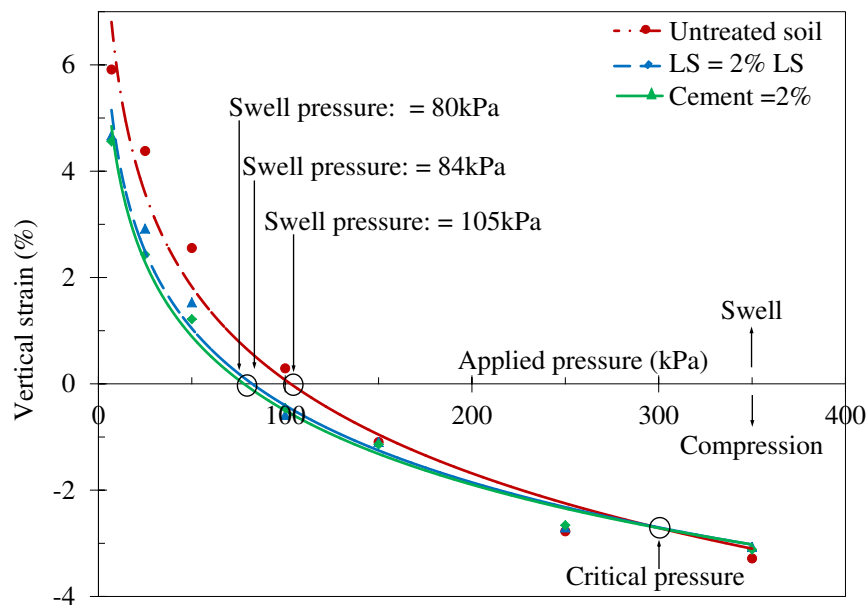
Figure 4.11: Wetting –after-loading test for swell pressure measurement of untreated chemically treated expansive soil

4.4.5   Effect of CaLS on soil shrinkage

4.4.5.1   Volumetric shrinkage

At the end of the one dimensional swell test, a shrinkage test was conducted on the specimens, as recommended by Briaud (1998). Immediately after the one

dimensional swell test the specimens were removed from oedometer, weighed, and the dimensions were measured and recorded. They were allowed to dry at room temperature while measurements were taken at regular intervals until they reached a constant mass, and then placed inside an oven set to 105^0C, after which their final weight and dimensions were measured and recorded. The data obtained from this procedure was used to determine the volumetric shrinkage of the specimens at various moisture contents (Fig 4.10). The slope of the fairly linear portions of the plots which Sarkar et al. (2000) referred to as the "shrink modulus" (E_w) was determined. The E_w value for untreated, 2% CaLS, and sample treated with 2% cement was 1.19, 1.41 and 1.48, respectively. Sarkar et al. (2000) posited that the higher the E_w in a soil, the narrower the range of volume change with changing in moisture content. Thus, samples treated with 2% CaLS and those treated with cement shrank less than the untreated sample with an equal change in the moisture content. The degree of soil shrinkage improved by 19% after 2% of CaLS addition, and there was a 24% improvement after 2% cement treatment.
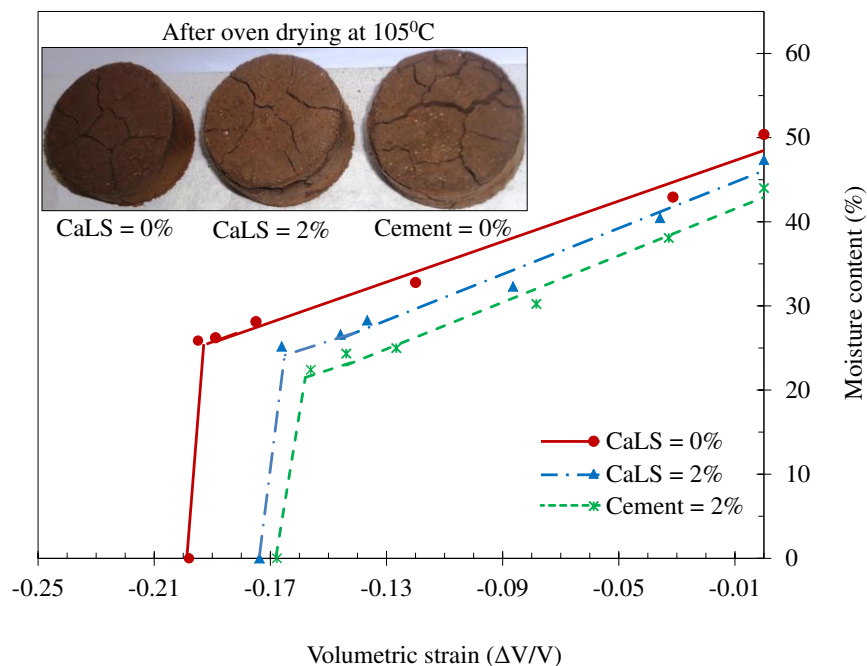
Figure 4.12: Effect of 2% CaLS and cement treatment on the volumetric strain of expansive soil

4.4.5.2   Linear shrinkage

The effect that the 2% CaLS admixture had on the linear shrinkage of the remoulded soil is illustrated in Fig 4.11, and although the effect was not significant, the admixture did increase the shrinkage limit from 9% to 11%, possibly due to moisture entrapped in the interlayers of clay minerals as the CaLS intercalated these inner layers. Moreover a visual observation of the test specimen after oven drying (Fig 4.11; inset) indicated significant textural variations and substantial cracking on the untreated and 2% cement treated specimens. The presence of CaLS reduced the formation of cracks quite significantly, which implied that the cohesive properties of the soil were only altered minimally. However, an addition of 2% cement admixture resulted in a loss of cohesiveness in the soil thus, the formation of prominent cracks, although the effect on the shrinkage limit was similar to the CaLS admixture. An addition of 2% cement increased the shrinkage limit from 9% to 12%. The hydration and cation exchange reactions were the likely reasons for this improvement.
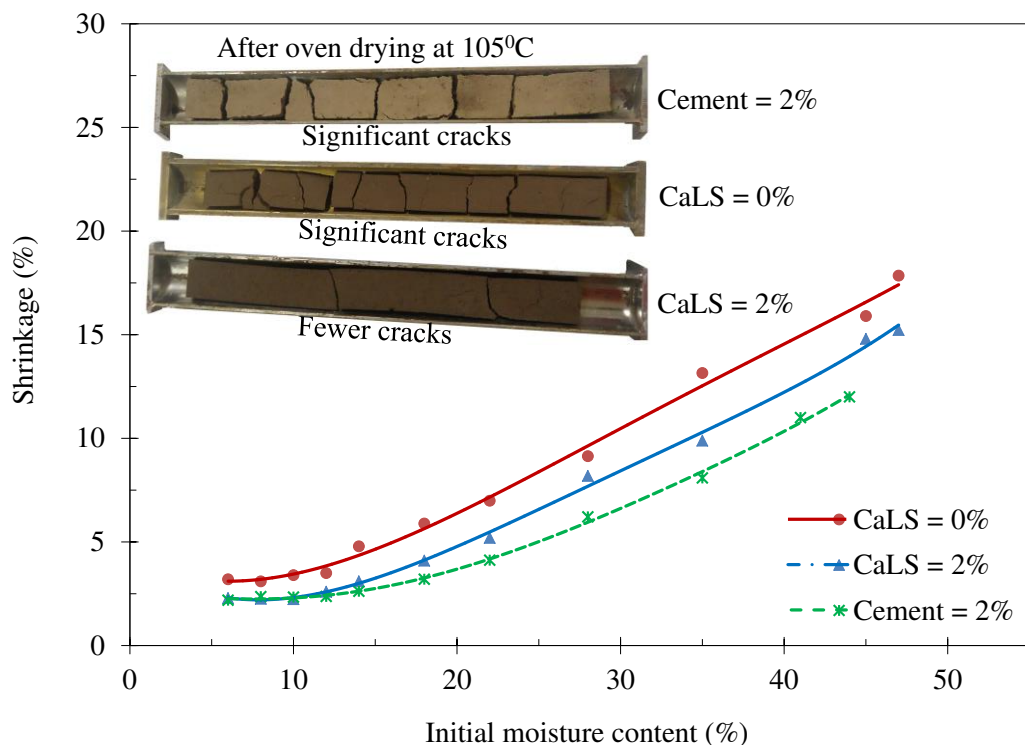
Figure 4.13: Effect of initial moisture content on shrink-swell behaviour of untreated and 2% CaLS treated expansive soil

4.5   CALCIUM   LIGNOSULFONATE   ADMIXTURE   AND   THE
ENGINEERING PROPERTIES OF REMOULDED EXPANSIVE SOIL

4.5.1   *Effect on Atterberg limits of the soil*

Fig 4.12 shows the variations in the liquid limit and plasticity characteristics based on the percentage of CaLS admixture. For a comparison, the effect that 2% of cement had on the consistency limits of the same soil is presented. The addition of CaLS decreased the liquid limit (LL) and slightly increased the plastic limit (PL; not shown). The net effect was a reduction in the plasticity index (PI) of the soil. With the addition of 2% CaLS, the LL decreased from 91% to 76% whereas, the PL increased from 40% to 44% which resulted in a decrease in soil PI from 51% to 32%. This could be attributed to the decrease in fine clay particles that contributed to plasticity. This observation was supported by a particle size analysis of untreated and 2% CaLS treated samples (Fig 4.13). The content of clay size particles decreased from 36% to 20% due to particle aggregation, which in turn decreased the plasticity of the soil, but an increase in the content of CaLS beyond the 2% threshold resulted in adverse soil characteristics. For example, at 4% the LL decreased to 80% only, with a corresponding decrease in the plastic limit to 41%, so the PI of soil treated with CaLS decreased from 51% to 39%, possibly due to CaLS acting as expanding polyelectrolytes. A t application rates exceeding the threshold value, the excess molecules of the polyelectrolyte (CaLS) expanded due to strong mutually repulsive forces between the charged sections of the stabilizer (Sarkanen and Ludwig, (1971). Although a reduction in LL from 91% to 80% occurred with 4% CaLS admixture, the optimum reduction in PI was attained at 2%, so 2% LS was considered as the optimum in this study.

The LL and PI decreased in soil treated with cement as the amount of cement increased. For example, when 7% cement was added the LL (91%) of untreated soil decreased to 60% while the plastic limit increased from 40% to 46%; this reduced the PI from 51% to 26%. This reduction in LL and increase in the PL of soil treated with CaLS and cement was similar to previous research studies. For example, Sarkar et al. (2012) attributed the decrease in LL to the fact that more water is required for the soil treated with cement to make it fluid while the increase in plastic limit was

attributed to the greater amount of water needed to change the soil from a plastic state to a semi-solid state. Although the PI of soil treated with cement was much lower than the sample treated with CaLS, CaLS prompted a 37% reduction in plasticity, thus CaLS could effectively improve the plasticity of a "low" expansive soil.
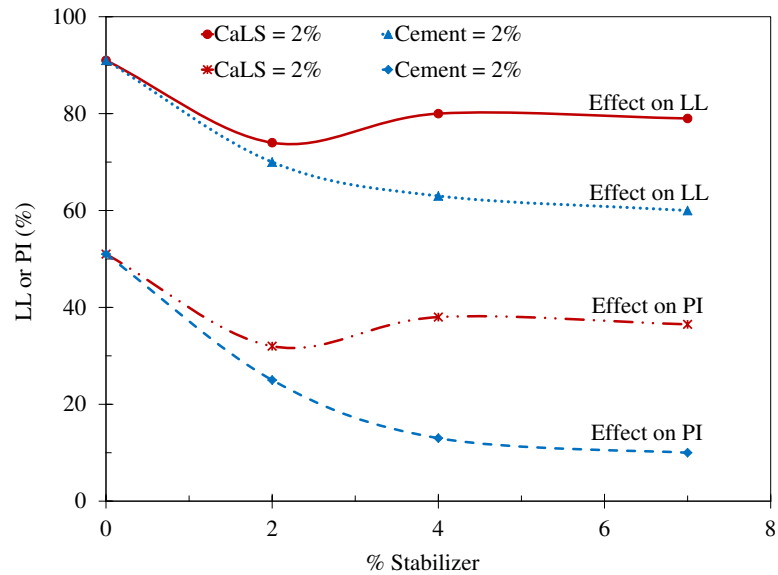
Figure 4.14: Effect of CaLS content on the consistency limits of a remoulded expansive soil
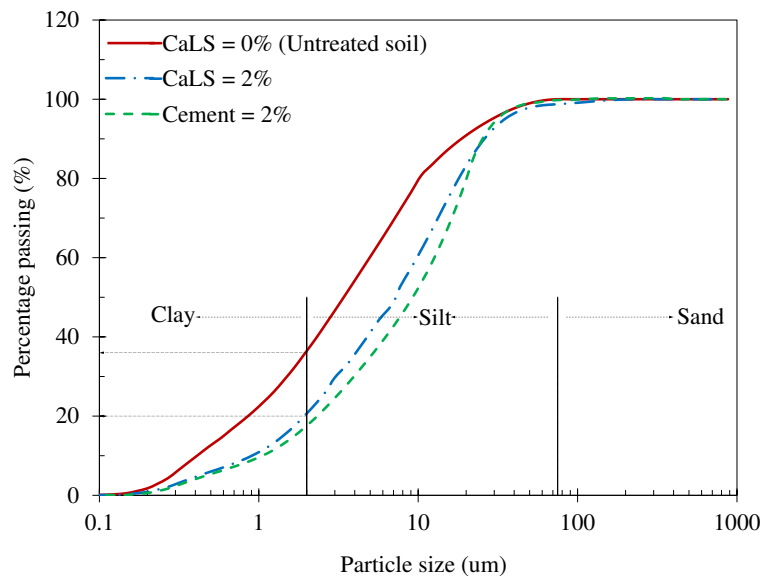
Figure 4.15: Particle size distribution of untreated and chemically treated expansive soil

141

The improvement in Atterberg limits after the addition of CaLS was similar to the work done by Bowders and Daniel (1987) on non-traditional soil stabilization. Bowders and Daniel mixed kaolinite and illite/chlorite with a acetic acid, which is a non-traditional stabilizer in various concentrations and observed similar characteristic changes in LL and PI. They believed that these changes were due to alterations in the chemistry of the soil solution which altered the inner and outer DDL of the clay particles. Sivapullaiah et al. (1996) opined that the addition of fly ash or lime-fly ash resulted in the (1) reduction in thickness of the DDL of clay particles, (2) flocculation of clay particles, and (3) an increase in content of coarse soil. In this investigation the XRD results indicated that CaLS permeated the DDL of the smectite minerals and altered the thickness leading to mineral aggregation. This observation was in accord with Sivapullaiah et al. (1996). Details of this are presented in section 5.2.1.

The moisture contents of soil specimens were determined at the end of the one dimensional swell tests, and the sample treated with 2% CaLS recorded 46.5% rather than 51% for untreated sample. It has been demonstrated in this study (section 5.2.7) that as CaLS intercalated the inner layers, the adsorbed moisture was displaced and the hydrophobic portion of the admixture restricted the treated soil from absorbing water. This is why the moisture content was less than the specimen of untreated soil.

4.5.2 *Effect on compaction characteristics of soil*

The densification of soil by mechanical compaction is one of the oldest and most common ground improvement techniques because fundamentally, compaction is a reduction in the volume of voids using mechanical energy. This study investigated the impact that the CaLS admixture had on the densification of a remoulded expansive soil. The moisture content-dry unit weight curves for the untreated soil and soil treated with 2% CaLS were determined using a Standard Proctor compaction effort of 590kJ/m^3 (AS 1289.5.1.1). Fig 4.14 shows how the admixture affected the compaction characteristics of the remoulded expansive soil. There was a slight tendency for the OMC and MDUW to decrease when CaLS was added, but given that some variation in the initial moisture content was unavoidable, coupled with possible variability introduced by the compaction effort, such a marginal reduction in

compaction characteristics could exist even without a soil additive. It is safe to surmise that comparing the compacted dry unit weights of the untreated sample with the treated sample, the addition of CaLS stabilizer had no appreciable effect on the density of the soil or improved the compaction moisture content. Nevertheless, the compaction curve for the soil treated with CaLS was determined after a weighted average of three Standard Proctor tests. Therefore, the marginal decrease in OMC and MDUW could be associated with the CaLS admixture which might have initiated the flocculation of soil particles through adsorption and cation exchange mechanisms. After treatment the lower MDUW implied that less effort was required to attain 95-100% compaction, while the reduced OMC in treated soil implied that less water will be needed to lubricate soil particles during compaction than untreated soil. This is in agreement with other workers; for example, Puppala and Hanchanloet (1999) mixed sulphuric acid and lignosulfonate chemicals (SA-44/LS-40, or DRP) to improve soft subgrade soil, and found that the variations of OMC and MDUW with treated soil changed slightly, which was attributed to cation exchange between the additives and expansive soil minerals that reduced the thickness of DDL and led to flocculation aggregation. In this study the MDUW and OMC for 2% CaLS treated sample was $12.9kN/m^3$ and 36%, respectively, as opposed to $13.1kN/m^3$ and 37% for untreated soil sample.
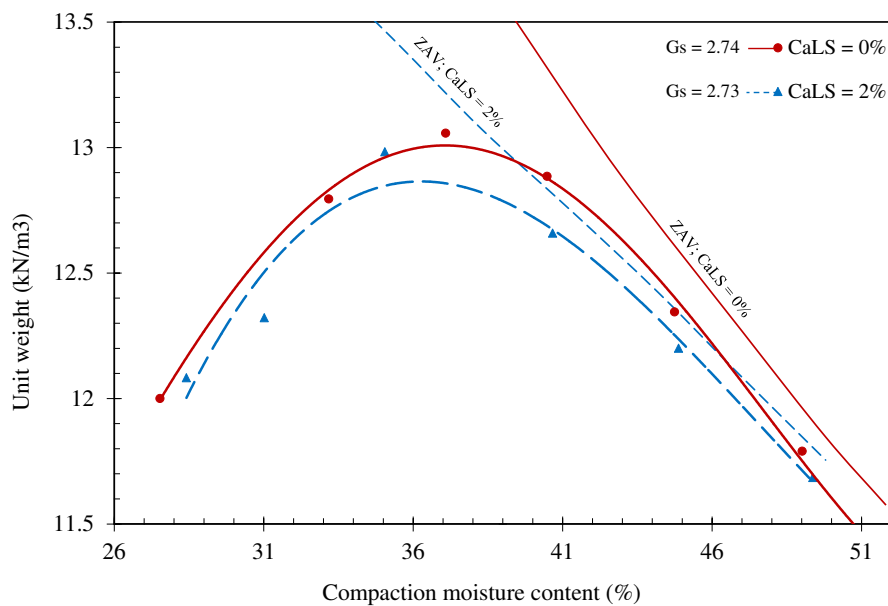
Figure 4.16: Effect of 2% CaLS on the Proctor compaction characteristics of the soil

4.5.3   *Effect on freeze-thaw durability of soil*

Freeze-thaw durability is the ability of a soil to resist the adverse effects of cycles of freezing and thawing resulting from changes in environmental conditions during a given time period. The durability of the untreated and chemically treated specimens was measured by the percentage of mass loss, the percentage of volumetric change and the percentage of moisture variation. The results of these tests are presented in Fig 4.15-17. All the specimens were prepared at OMC (standard Proctor) and compacted into a 105mm diameter by 115mm high plastic mould. After compaction, the specimens were cured for 7 days at a constant temperature prior to freeze-thaw testing. The freezing-and-thawing cycles consisted of freezing the specimens at -4^0C for 24hours and thawing them for 24hours at a room temperature of 20^0C and 98% humidity, indicating slight deviation from the ASTM D560 recommendations. Freezing a specimen for 24hours and thawing it for another 24hours represents one cycle. Samples were predetermined to undergo 12 cycles in 24 days.

During the freezing stage, as the temperature dropped below 0°C, moisture in the soil began to freeze and resulted in the formation of ice crystals which subjected the specimen to change its volume. Throughout the freeze–thaw tests for untreated and chemically treated specimens, both specimens developed cracks around the surfaces that caused parts of the specimen to break off at the upper and lower ends. As the test continued these cracks increased in size and became more widespread, resulting in significant spalling (Fig 4.15). All the specimens withstood 12 cycles of testing except the specimen stabilised with 2% cement; this specimen experienced the highest level of mass loss, so the durability test was stopped after 6 cycles (Fig 4.15). The number of cycles at which the specimens began to deteriorate was affected by the CaLS admixture. A visual inspection of the specimen treated with CaLS indicated there was less surface spalling from the 1st to the 12th freeze-thaw cycles, and there was a substantial improvement in resistance to temperature degradation. At the end of the 12th cycle, the untreated soil lost approximately 7% of its mass while the CaLS treated specimen only experienced a 3.4% loss in mass. Chamberlain *et al.* (1990) reported that a 10–15% loss of mass at the end of the 12th cycle of freezing and thawing does not affect the strength of a soil, and the specimen treated with 2%

CaLS was well below this percentage of mass loss so it may be tentatively concluded that the percentage of mass lost in soil with 2% CaLS subjected to 12 freeze-thaw cycles would have no significant effect on its strength. However, the soils stabilised with 2% cement exceeded this "mass loss" threshold; the specimen deteriorated rapidly, losing as much as 17.8% of its original mass at the end of the 6th cycle so the test was discontinued. This result suggested that the strength of soil stabilized with cement could be compromised due to seasonal variations in temperature.

In terms of change in the percentage of volume, the untreated specimen had a significant change in volume from the 1st to the 3rd cycle; the specimen treated with 2% cement experienced the least change in volume, while the specimen treated with 2% CaLS was in between these two extremes (Fig 4.16). The maximum change in volume for all the specimens occurred at the end of the 3rd cycle. For untreated soil the volume increased by almost 15.9% as opposed to 11.2% and 6% for specimens treated with CaLS and cement respectively. The change in volume in each subsequent cycle was less than the preceding cycle, and this trend continued until about the 9th cycle for the untreated and CaLS treated specimens. After the 9th cycle, repeated freezing and thawing did not change the volume which indicated that the specimens had reached their state of equilibrium. At this state, maximum expansion during thawing for untreated soil was 7.0% as opposed to 4.6% for the specimen treated with 2% CaLS. Chen (1988) referred to this progressive decrease in volume towards a state of equilibrium as the "fatigue" of volume change due to a gradual decrease in the dry density of soil with repeated freezing and thawing. He argued that when the decreasing dry density reaches the "critical dry density" (where swelling and shrinkage equalizes) a state of equilibrium is reached where swelling, shrinkage, and dry density become stable and thus the volume of soil is stable irrespective of changes in environmental conditions such as temperature.
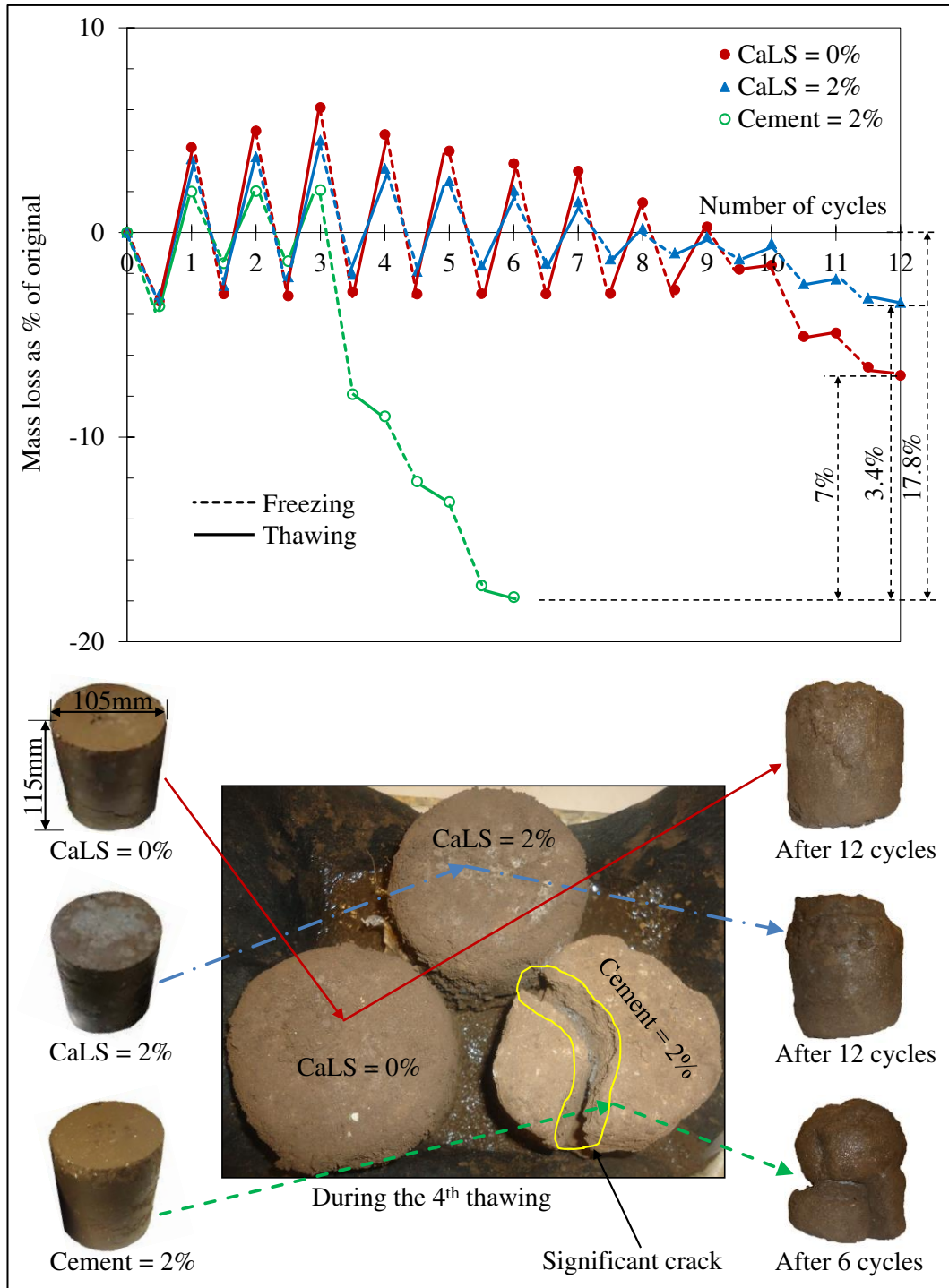
Figure 4.17: Effect of chemical treatment on percentage mass loss in freeze-thaw durability test for soil specimens

The freezing cycles had a minimal effect on the shrinkage of soil (Fig 4.16); shrinkage of untreated soil during the 1st cycle was 4.7% but it decreased to 3.8% at

the 9th cycle, whereas the soil treated with 2% CaLS decreased in shrinkage from 3.8 to 3%. Chen (1988) attributed this behaviour to the decreasing dry density of the soil. As the decreasing dry density reaches a critical value due to repeated wetting and drying, shrinkage in the soil is neutralized by the percent swell and hence further wetting and drying has no effect on shrinkage behaviour of the soil.
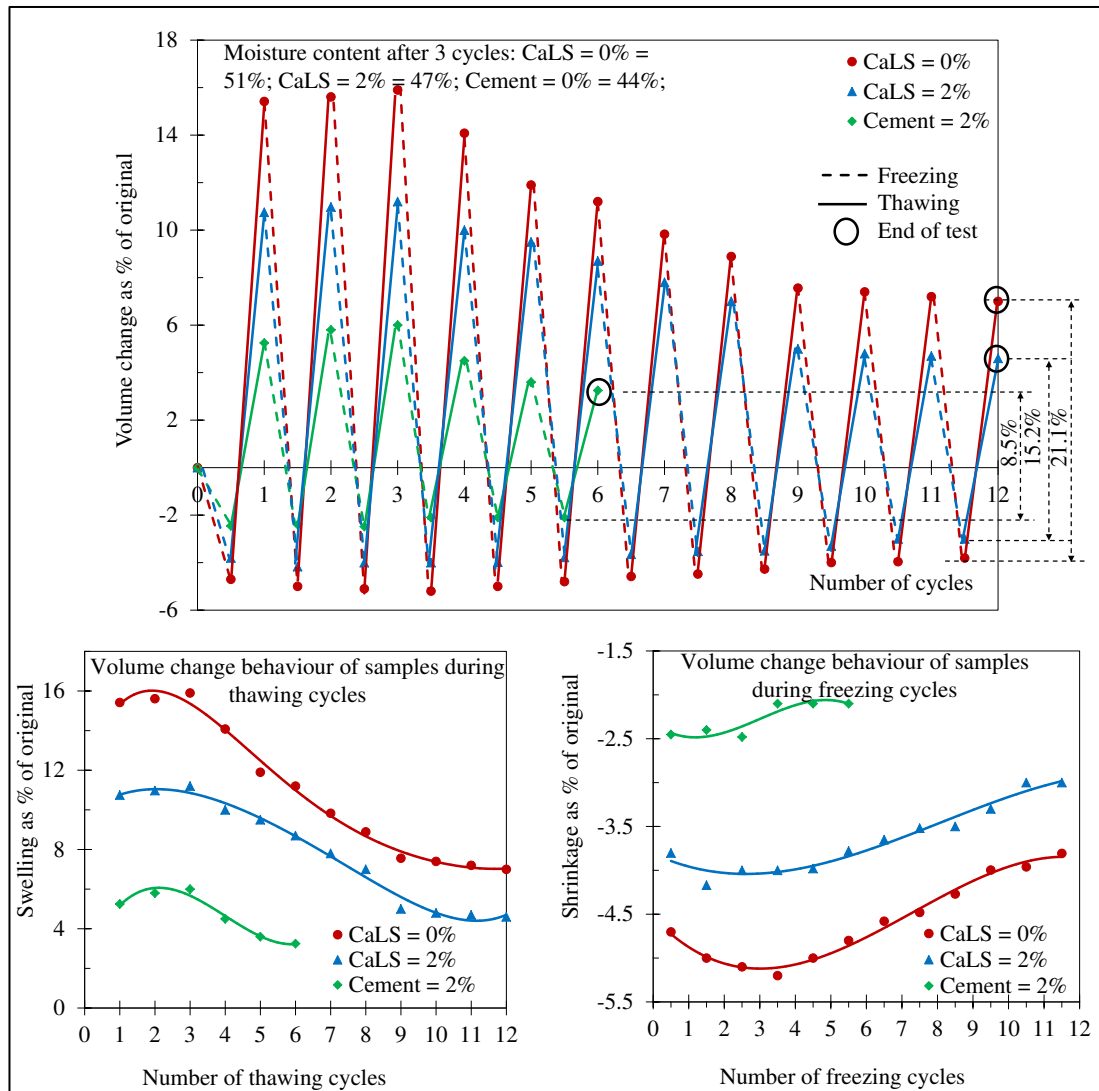
Figure 4.18: Effect of chemical treatment on volumetric strain in freeze-thaw durability test for soil samples

The moisture content at the end of each cycle was used to determine any variation in the moisture of the specimens. A unique relationship existed between variation in moisture content and change in volume in the specimens such that the change in

moisture content was proportional to the change in volume; that is, higher moisture content was synonymous with a higher volume change and vice-versa. Consequently, the adsorbed moisture content at the end of the 3rd cycle (where maximum swelling occurred) experienced the maximum moisture content in all specimens. The specimen treated with 2% cement exhibited the least variation in moisture content, followed by samples treated with 2% CaLS, and then the untreated specimen (Fig 4.17). The gravimetric moisture content at the end of the 3rd cycle was 51%, 47%, and 44% for untreated, 2% CaLS, and 2% cement treated specimens, respectively. For the CaLS treated sample, the hydrophobic component of the admixture probably inhibited the adsorption of moisture by clay minerals, hence the relatively low percent swell exhibited in this treated soil. For soil stabilised with 2% cement the reaction mechanisms of hydration and cation exchange altered the mineralogy of the soil, causing it to behave more or less like a silty soil, so the lower adsorbed moisture content was translated into the low percentage of swell of this treated soil. Similarly, the variation in moisture for untreated and CaLS treated soil attained a state of equilibrium at about the 9th cycle of freezing and thawing. Such a trend supported the unique relationship between the amount of adsorbed moisture and the percent swell of the expansive soil.
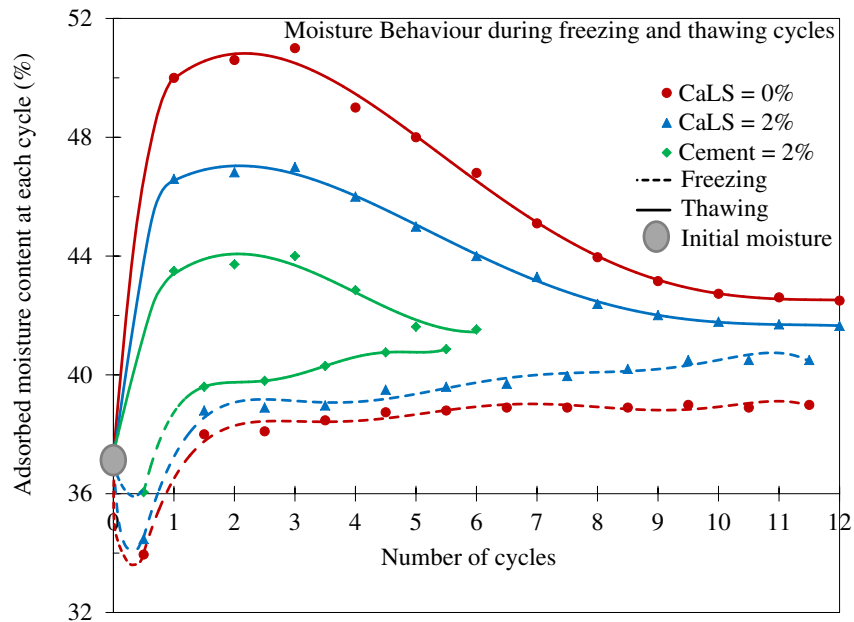
Figure 4.19: Effect of chemical treatment on moisture behaviour in freeze-thaw durability test for soil specimens

4.5.4 *Effect on wet-dry durability of soil*

The wet-dry durability test was used to measure the sustainability of the treated soil to repeated wetting and drying cycles in the laboratory in order to simulate environmental conditions. All the test specimens (105mm diameter x 115mm high) were prepared at OMC and statically compacted and cured for 7 days prior to the wetting and drying test. The test method used in this investigation deviated slightly from the Standard ASTM D559 in that the duration of wetting was reduced from 5 hours to 1 hour, as stipulated in the standard. This adjustment was necessary because none of the specimens could withstand 5hrs of continuous wetting. Moreover, after being dried in an oven for 42hrs, the samples were not stroked vertically with a wire brush because the materials had a low resistance to such pressure.

The durability of soil upon repeated wetting and drying depends primarily on the pore structure, tensile strength, inter-particle friction, and cohesion of the material. As water moves in and out of the pore network during wetting and dying, capillary pressure develops and acts on the walls of the pores such that the pore structure, tensile strength, inter-particle friction and cohesion of the material will then dictate how the soil will respond to this capillary pressure (Tripathy et al. 2002). In this investigation the untreated soil suffered a rapid loss of material during the 1st wetting phase so the test was stopped at the end of the second cycle owing to the level of disintegration experience by the untreated soil specimen (Fig 4.18). The attractive forces between the untreated soil particles were so weak (van der waal forces) that capillary pressure that developed on the walls of the pores cause the untreated sample to collapse. This behaviour changed after chemical admixtures were added. The specimen treated with 2% CaLS disintegrated substantially during the wetting phase of the 3rd cycle due to the chemical admixture in the soil; while the specimen treated with 2% cement withstood the 3rd cycle but disintegrated during the 4th wetting phase.

The ASTM D559 test standard recommended 12 cycles of wetting and drying but all the test specimens failed at the end of the 3rd cycle. This could be related to the fact that the standard was designed for soil-cement mixes and thus the time duration of wetting and dry may not apply to the type of specimens used in this investigation.

Although the wetting time was reduced to 1hour, it still might not be applicable. Due to these deviations from the ASTM D559 recommendations, a simple procedure was used to measure the loss of soil mass at the end of each cycle. This procedure involved measuring the mass of a specimen before the test and at the end of each cycle. Broken pieces of soil were carefully removed before measurements were taken. Data obtained from these measurements were used to graphically represent the degree of mass lost in each specimen (Fig 4.19).

According to AASHTO (1986), the maximum allowable soil-cement loss for base and sub-base material should be 14% at the end of the 12th cycle, but Fig 4.19 shows an unacceptable 33% loss of mass for untreated soil just after 1st cycle. During the 2nd wetting cycle of this specimen, about 71% of its mass was lost and after oven drying the soil completely collapsed, as shown in Fig 4.18. The addition of 2% CaLS increased the resistance of the soil to repeated wetting and drying such that at the end of the 1st cycle only 7.7% of mass was lost; this was a 76.7% improvement in the durability of the soil. However, at the end of the 2nd cycle, an unacceptable 32.4% of mass was lost. The untreated soil lost 98% of its mass at this stage, meaning that the addition of 2% CaLS improved the wet-dry durability of the soil at the end of the 2nd cycle by 66%. These very high losses in mass in the early stages of the tests clearly showed that the test standard was not suitable for the materials used in this investigation.

A comparison of the performance of the specimens indicated that soil treated with 2% cement experienced the least loss of mass under wet-dry conditions, with only 2.5% and 9.2% of mass lost at the end of the 1st and 2nd cycles, respectively. This specimen progressed to the 4th cycle but collapsed completely during the 4th wetting phase. It is most likely that the addition of cement increased its strength and aided the resistance offered by soil particles against the capillary pressure exerted on the pore walls. The specimen treated with 2% CaLS experienced a higher resistance to capillary pressure compared to the untreated soil specimen which could be attributed to the hydrophobic nature of the CaLS admixture. Subsequently, the volume of water adsorbed into the pores of CaLS treated soil was less, implying that less capillary

pressure developed within the pore walls so its ability to withstand repeated wetting and drying conditions increased.
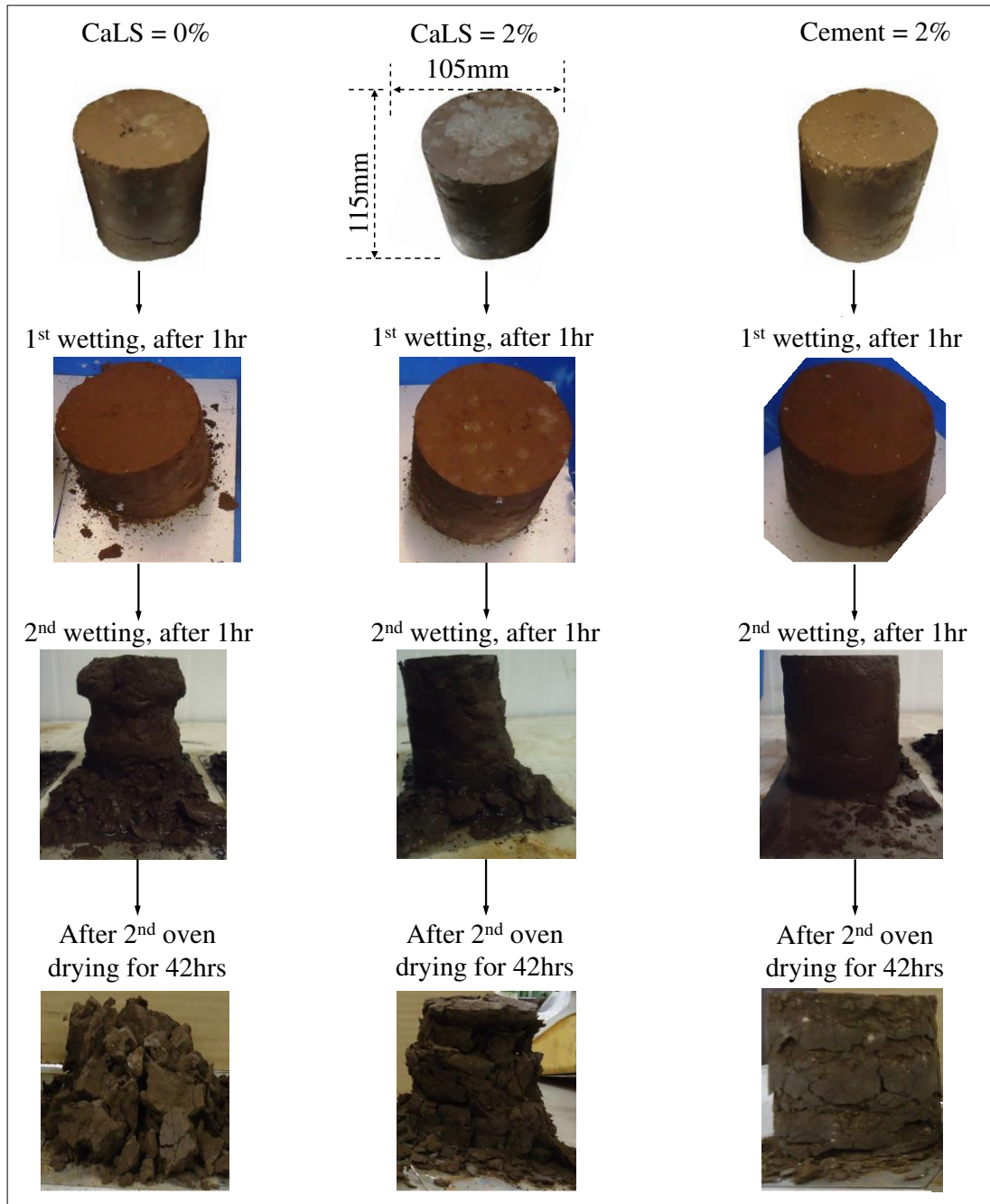
Figure 4.20: Pictorial illustration of the wetting and drying durability testing of untreated and chemically treated expansive soil
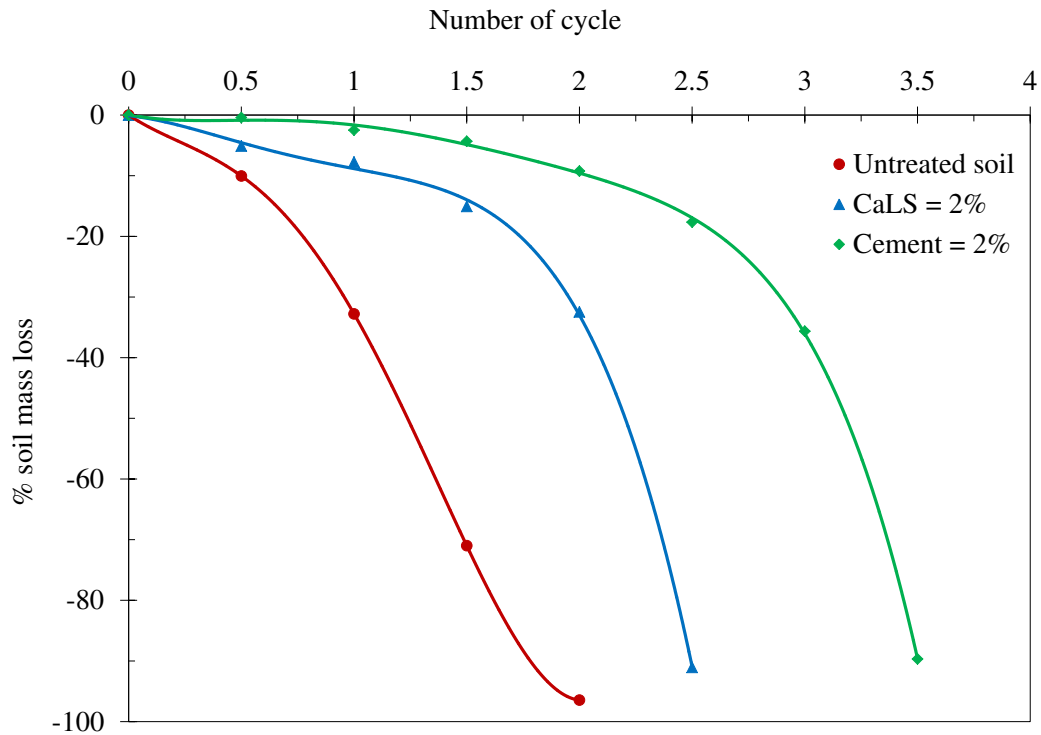
Figure 4.21: Graphical representation of weight loss in wet-dry durability testing of untreated and chemically treated expansive soil

4.5.5 *Effect on unconfined compressive strength (UCS) and soil failure mode*

The unconfined compressive strength (q_u) is the load per unit area at which a cylindrical specimen of a cohesive soil fails in compression. This test was carried out to determine the strength and failure mode of the untreated and 2% CaLS stabilized remoulded expansive soil. For the sake of comparison, identical specimens treated with 2% cement were prepared and tested accordingly. It was evident that the strength of soil improved after 2% CaLS was added (Fig 4.20), although not significantly (265kPa to 285kPa), accounting for 7.5%, but more importantly, the CaLS admixture did not change the ductility of the soil, unlike the cement admixture. A ductile mode of failure could be ascribed to CaLS treated sample as opposed to the brittle failure exhibited by sample treated with cement, which is less desirable in engineering practice. In terms of strength, the addition of 2% cement increased the strength of the soil from 265kPa to 293kPa, which is a 10.6% improvement. At higher rates (e.g. $6 - 10\%$) of cement additive, a significant gain in strength has been widely reported (e.g. Sariosseiri and Muhunthan 2009), but despite this improvement

in strength, soil engineers are faced with the inherent problem of brittle behaviour of soil treated with cement under cyclic loading. It is interesting to note that although the growth in strength for CaLS specimen was less than with the addition of 2% cement, the treated soil maintained the soil's ductility.
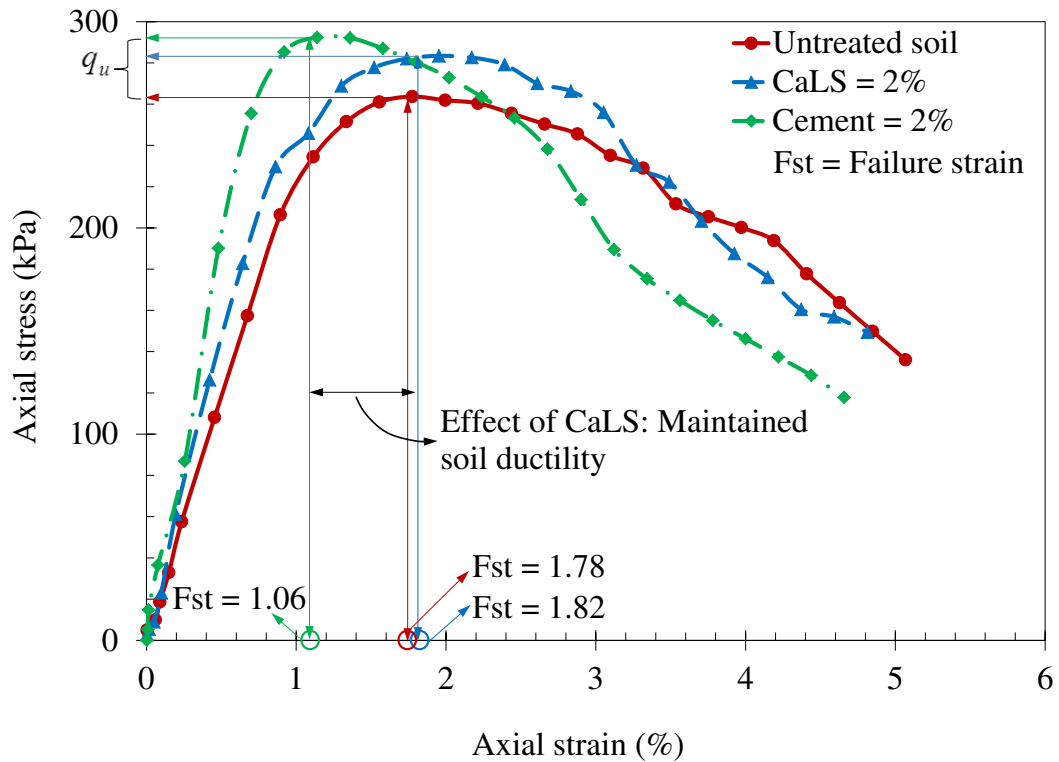
Figure 4.22: UCS behaviour and failure mode of untreated and chemically treated expansive soil

Axial strain at failure was 1.78% and 1.82% for untreated and 2% CaLS treated specimens whereas the ductility of the untreated soil was replaced by brittleness after cement was added. Strain at failure occurred at 1.06%. The ductile mode at failure exhibited by the CaLS treated soil could give improved "warning signs" prior to failure of engineering infrastructure. These different modes at failure could be the result of different mechanisms of stabilization in the CaLS and cement admixtures. Ola (1977) reported that the increase in strength and subsequent brittleness in traditionally treated soils may be due to bonding agents with cement particles to form large aggregates, making the soil behave as a coarse-grained, strongly bonded particulate matter. In this study a microscopic analysis of treated specimens revealed

that the stabilization mechanism of CaLS was mainly due to basal and peripheral adsorption, entrapment of moisture within the inner layers, and subsequent coating and binding of soil particles to form a more rigid soil mass.

4.5.6 *Effect on consolidation characteristics of soil*

Consolidation characteristics

The time-dependent settlement (expulsion of water) of saturated clayey soil subjected to a static, sustained load is referred to as consolidation, and the consolidation characteristics of soils are needed to predict the magnitude and rate of settlement. The data collected during the consolidation tests for untreated, 2% CaLS, and 2% cement treated soil in this study allowed for a determination of the coefficients of consolidation (C_v) and coefficient of compressibility (m_v) of the samples. To determine the coefficient of saturated soil permeability (k_w), the "Falling Head Permeability" test was conducted and the data obtained was used in equation 4.1.

$$k_w = 2.303 \frac{aL}{At} \log_{10} \frac{h_1}{h_2}$$

(4.1)

Where

k_w = coefficient of permeability, h_1 = initial head difference at $t = 0$, h_2 = final head difference at $t = t_F$, A = cross sectional area of the specimen, L = length of the specimen, and a = cross sectional area of the standpipe.

The C_v behaviour of the untreated and chemically treated soil samples at various consolidation pressures (Fig 4.21) indicated that the C_v generally decreases with increasing consolidation pressure, contrary to the anticipation of Terzaghi and Peck (1967, cited in Mitchell and Soga 2005). Terzaghi and co-workers envisaged that with increasing consolidation pressure (i.e. decreasing void ratio) both k_w and m_v will rapidly decrease i.e. the k_w/m_v ratio will be fairly constant and thus their

equation; $k_w = c_v m_v \rho_w g$ suggests that C_v will be constant within a wide range of consolidation pressure.

The decreasing C_v for samples in this study varied slightly from one another (Fig 4.21). For example, for CaLS and cement treatment, the specimens experienced a fairly rapid initial settlement due to a speedy dissipation of pore water pressure, but this initially rapid settlement was immediately replaced by a reasonable stability. So it may be anticipated that after an immediate settlement, the long term settlement of CaLS treated clay may be insignificant. This consolidation behaviour exhibited by the treated soil specimens is not typical of clayey soils, implying that the chemical admixtures altered the soil structure in such a way that its consolidation seemed to be more-or-less like silty material.

However, the typical consolidation behaviour of clayey soil was demonstrated by the untreated soil sample. From the literature, the C_v behaviour of a soft Bangkok clay was obtained and plotted in Fig 4.21 for the sake of clarity (Indraratna *et al.,* 1994). The untreated clayey soil did not experience immediate settlement initially, suggesting that the CaLS and cement admixtures altered the soil structure by aggregating particles. This observation was supported by a slight increase in the permeability of treated soil samples, as discussed in section 4.5.7. Following Terzaghi's (1925, cited in Mitchell and Soga 2005) time rate of consolidation theory (equation 4.2), the implication of the C_v behaviour of the CaLS treated soil sample was that less time will be required to complete 90% of consolidation compared to the untreated counterpart under the same conditions.

$$C_v = \frac{T_v H_{dr}^2}{t} \qquad (4.2)$$

It has been reported (e.g. Robinson and Allam 1998) that exchangeable cation could influence the C_v behaviour of expansive soils. It is most likely that the introduction of CaLS and cement admixtures changed the soil cation capacity and suppressed the diffuse double layer of clay particles leading to flocculation aggregation. It is noteworthy that the test soil in this study was a natural remoulded expansive soil, thus it is non-homoionic, and therefore quartz and kaolinite minerals for example

will not experience the collapse of diffuse double layer concept, a phenomenon described by Olson and Mesri (1970) as the physicochemical effect. It is rather anticipated that in this study, the non-expansive soil minerals might aggregate due to the mechanical properties of the solid grains and by the lubricating effect of the CaLS as consolidation pressure increased among other mechanisms identified and discussed in chapter 5. Overall, the soil aggregated to form larger effective pore sizes which allowed the pore fluid to dissipate faster than its dispersed soil counterpart, hence the initial rapid settlement after treatment.

Fig 4.22 illustrates the variation of m_v with consolidation pressure of untreated and 2% CaLS treated expansive soil. Conventional one dimensional consolidation tests were performed on specimens at full saturation with applied vertical stresses of 100, 200, 400, 800, 1500, 2500, and 3500kPa. For comparison, an identical specimen treated with 2% cement was also prepared and tested, and the result is shown in the same Fig 4.22. As expected, m_v decreased with increasing consolidation pressure for all samples, but this decrease in m_v was much more evident for the untreated specimen followed by the specimen treated with 2% CaLS, while the specimen treated with 2% cement experienced the lowest change in the value of m_v. The implication here is that soil treated with CaLS will offer greater resistance to compression than untreated soil under similar conditions.

This behavioural difference between the untreated and chemically stabilized sample was ascribed to the stabilizing effects of the chemical admixtures. CaLS and cement admixtures increased the strength of the soil by binding the soil particles together so they offered more resistance to volumetric compression. In the samples treated with CaLS, the collapse of the DDL of expandable minerals instigated flocculation agglomeration whereas externally adsorbed CaLS on non-expandable soil minerals (e.g. kaolinite, quartz) also contributed to the agglomeration and subsequent development in strength. Theng (1979) provided a theoretical description of the m_v of soil with an organic pore fluid by explaining that at a low dielectric constant of pure organic fluids, the diffuse double layer around the particles collapses resulting in particle aggregation and changes in the void ratio. It is believed that the organic

liquid CaLS, has similar effects on the DDL of clay minerals, as observed from the XRD test data.
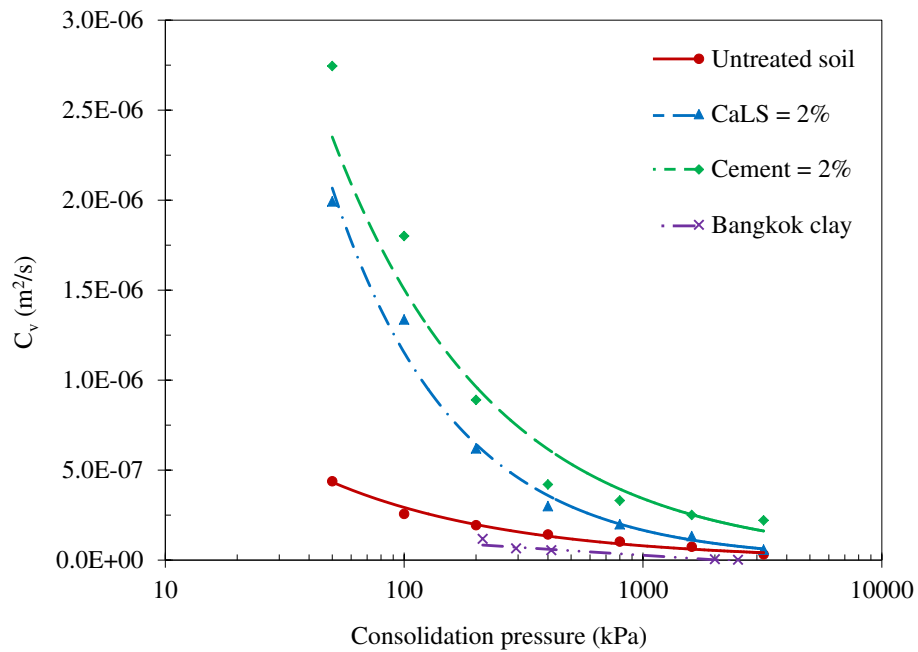
Figure 4.23: Variation of C_v with consolidation pressure for untreated, 2% CaLS and 2% cement treated expansive soil
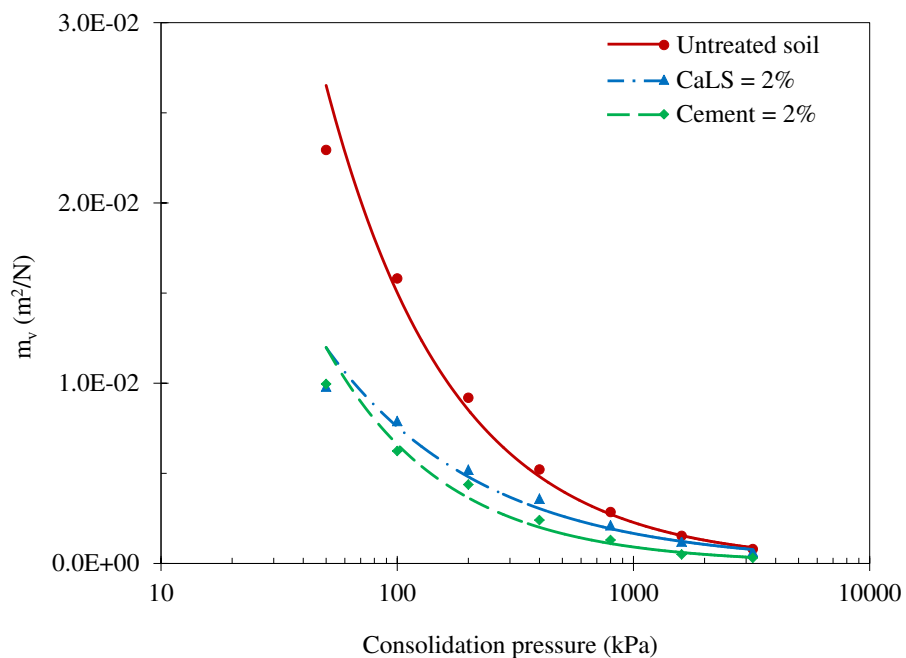
Figure 4.24: Variation of m_v with consolidation pressure for untreated, 2% CaLS and 2% cement treated expansive soil

4.5.7 *Effect on the permeability characteristics of soil*

Permeability is one of the most important soil properties of interest to geotechnical engineers because it has a direct relationship with the rate of heave in expansive soils. Fundamentally, the higher the permeability, the deeper moisture penetrates into the soil and hence the greater the differential soil surface movement. Fig 4.23 illustrates the change in soil permeability (k_w) due to a chemical admixture in the soil. As expected, the k_w of all the specimens decreased with increasing consolidation pressure simply because of the reduction in total void space, and the k_w did not change substantially with the addition of CaLS. Figure 4.23 shows there was a marginal increase in k_w at all consolidation pressure; for instance, with a consolidation pressure of 50kPa, the CaLS induced effect is such that it was 0.5 times more pervious than the untreated soil sample whereas the sample with 2% cement was almost 0.9 times more pervious. Moreover, the specimen treated with 2% CaLS reached the relatively stable permeating stage after 15hours as opposed to 18 hours for the untreated sample and 12 hours for specimen with 2% cement.

The size of the flow channels before and after chemical treatment, as a result of particle aggregation, is one reason for the differences in the k_w values. The untreated sample had the smallest particle size/least connected pore sizes but the increases in particle size after the addition of CaLS and cement, as evident in the SEM and SSA test data (see 5.22 and 5.2.9) means that the chemically stabilised soil had larger but fewer connected pores leading to a slight increase in permeability, especially with the cement admixture. The shape and orientation of clay particles could also dictate the geometry of the flow channel. Lambe (1953) opined that with flaky clay particles, the application of pressure under fully drained conditions would result in an orientation of the platelets normal to the direction of maximum principal stress which leads to an increasingly tortuous flow path in the direction of the applied pressure. This tortuosity was greater for particles with larger diameter to thickness ratios (Mitchell 1956). The increased diameter to thickness ratios in chemically treated soil, as seen in the SEM micrographs, could also have contributed to the slight increase in permeability, especially with the addition of 2% cement.

158

Furthermore, the coefficient of permeability of soil could have been affected by the chemistry of the permeating fluid. For example, Macey (1942) measured the coefficient of permeability of clays in water and non-polar fluids and reported that the rate of flow for the non-polar fluid (benzene) was 100,000 to 1,000,000 times greater than for water in the same clay. This significant increase in k_w for soil treated with benzene was attributed to an increase in particle size, particle spacing, particle arrangement, and interlayer swelling.
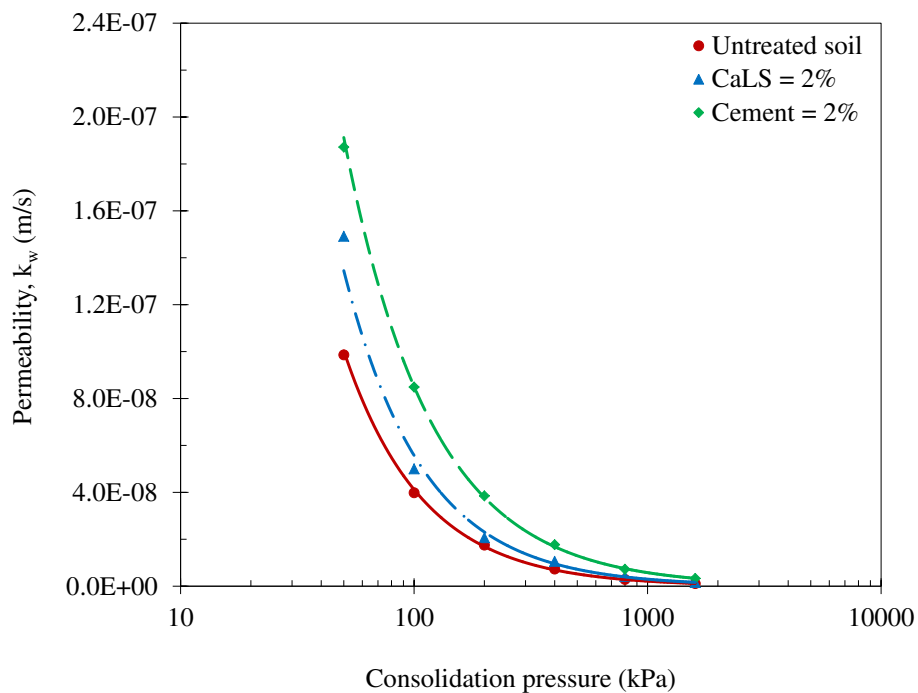
Figure 4.25: Effect of chemical admixtures on the permeability of remoulded expansive soil

4.5.8   Effect on soil pH

In this study, an Orion Star A325 portable pH meter was used to measure the pH of soil fluid in untreated, 2% CaLS, and 2% cement samples in accordance with AS 1289.4.3.1-1997. The pH meter was standardized using pH buffers (pH 7) prior to each use. The pH of the untreated and CaLS treated soil after 7 days of curing were measured and recorded. Four replicate pH measurements were obtained for each sample. The results were averaged and found to be 7.43, 7.17 and 9.65 for untreated, 2% CaLS and 2% cement treated samples, respectively. The pH of the soil after

CaLS treatment remained practically unchanged, possibly because the soil ions acted as an acid to form $H^+_{(aq)}$ with water, while the CaLS ions acted as a base to give $OH^-_{(aq)}$ with water, so they effectively neutralised each other. Moreover, the unchanging soil pH could also be ascribed to the very small amount of LS required to stabilize the soil (2% by dry weight of soil). High or low pH values could affect the underground water and could be detrimental to flora and fauna. High pH levels could also affect the longevity of reinforced concrete and steel frame structures, according to Perry, (1977). Traditional admixtures can increase the pH of treated soils. This increase in pH has contributed to the clamour for a sustainable alternative to traditional admixtures, which is why this research was carried out.

4.6 CALCIUM LIGNOSULFONATE ADMIXTURE APPLICATION CHART FOR EXPANSIVE SOIL

Extensive laboratory investigation on the efficacy of CaLS at controlling the swell behaviour of a remoulded expansive soil was conducted and results analysed at length. Additional artificial soils were also prepared by mixing bentonite with silt to form soils with geotechnical properties that were identical to Seed et al. (1962) expansive soil classification scheme (see Table 2.25). According to Seed and co-workers, the severity of the percent swell could be classified as low, medium, high, and very high. Five samples from each of these classes of soil were prepared by mixing predetermined amounts of bentonite and silt minerals leading to 20 soil samples with varying degrees of expansiveness. These soils were treated with 2% CaLS admixture and cured for 7 days prior to the conventional one dimensional swell test. Control specimens (specimens without the CaLS admixture) were also prepared and tested to give an insight into the effectiveness of the LS admixture. The numerous results were analysed and the outcome is presented in Fig 4.24, otherwise referred to as the "Calcium Lignosulfonate Application Chart" for the stabilization of expansive soils.

The green region of the chart shows that CaLS is very suitable for the treatment of such "low" expansive soils, but as the plasticity index of soil increases, LS will have

less and less effect on percent swell of soil. The yellow region illustrates the effectiveness of the admixture in such soil. A further increase in the plasticity index translates to increasing expansiveness of the soil thus, the efficacy of the LS admixture become more and more insignificant, as represented by the blue region. As the degree of expansion increases to the "high" class with a plasticity index exceeding 55%, and a swell pressure greater than 200kPa, it is recommended that the use of LS admixture in controlling the swell behaviour be avoided in such soils because the effect cannot be measured.
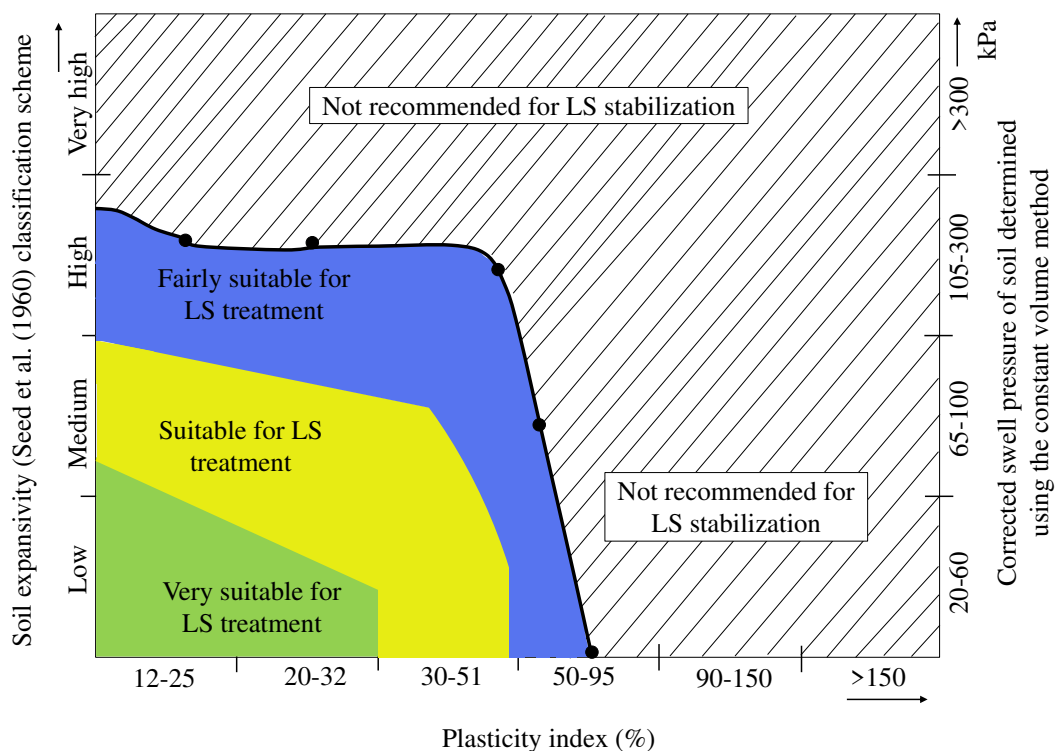
Figure 4.26: Calcium Lignosulfonate application chart

4.7 A SIMPLE MODEL FOR PREDICTING PERCENT SWELL FOR LS TREATED EXPANSIVE SOIL

From the laboratory test data, a correlation between the adsorbed moisture content (w) during one dimensional swell test (w) and applied pressure (σ) can be represented as shown in Fig 4.25. As expected, the amount of adsorbed moisture

which translated to the degree of heave, decreased with increasing surcharge pressure.
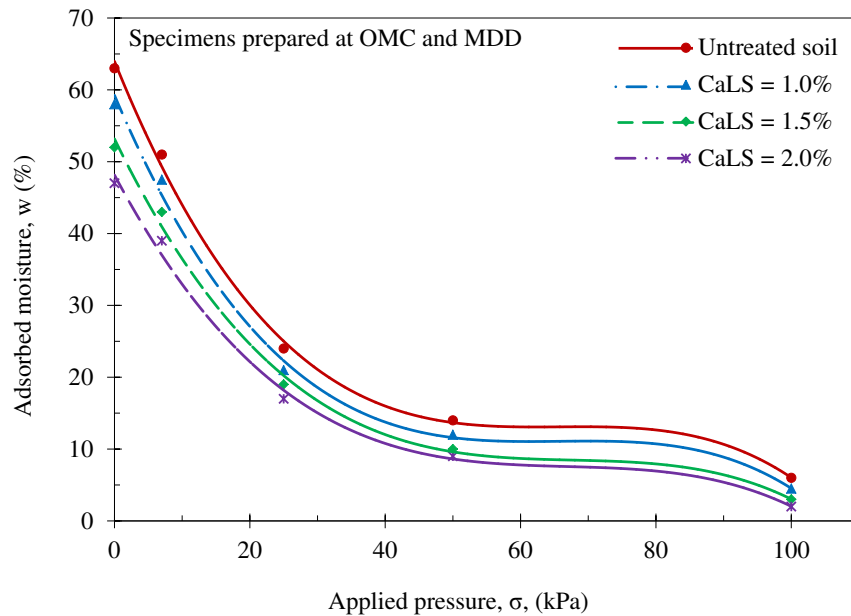
Figure 4.27: Relationship between adsorbed moisture content and applied pressure of a remoulded expansive soil during a one-dimensional swell test.

It was apparent that the relationship between adsorbed moisture and applied pressure could attain a common trend line if each value of "σ" is raised to a certain numerical number, otherwise known herein as the fitting parameter (α). The α values were chosen arbitrarily until a common trend line was achieved (Fig 4.26). Table 4.1 illustrates the numerical values of alpha (α).

Table 4:1: Alpha (α) values for soil specimens (fitting parameter)

S/No.	Soil description	Fitting parameter (α)
1	Untreated soil	0.98
2	CaLS = 1.0%	1.07
3	CaLS = 1.5%	1.2
4	CaLS = 2.0%	1.32
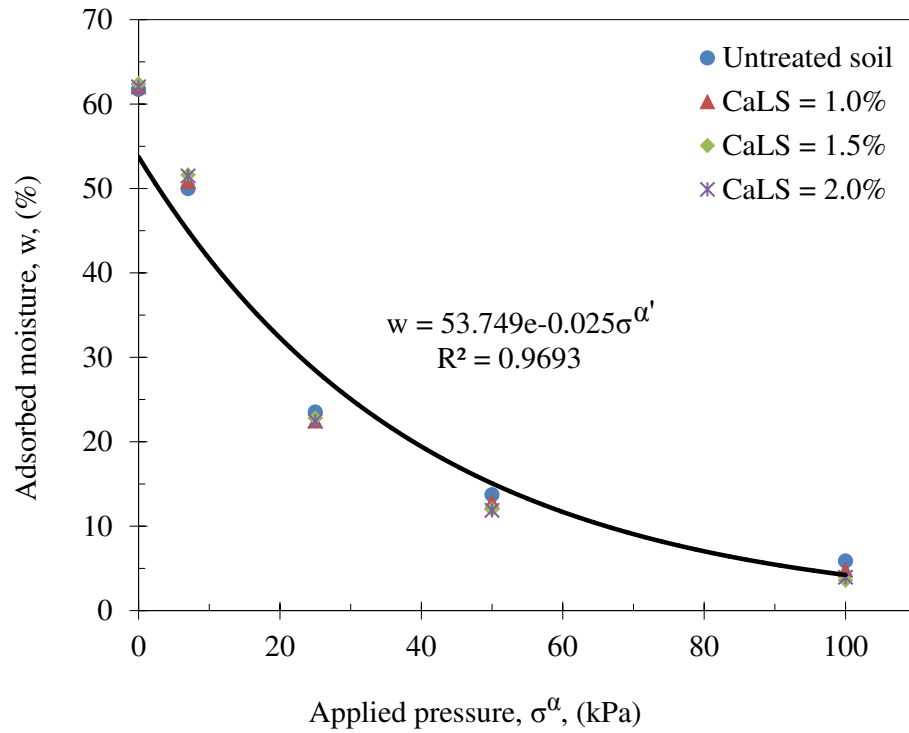
Figure 4.28: Adsorbed moisture and applied load relation with arbitrary selected α values as given in Table 4.1

It is rational to develop a simply empirical equation to predict likely "α" values of various types of soil instead of making arbitrary assumptions, so the fitting parameters (α) in Table 4.1were correlated with the plasticity index (PI) of the untreated and CaLS treated samples (Fig 4.27). This relationship shows that α was greatly influenced by the PI of the soil after CaLS addition. The soil samples exhibited decreasing α values with decreasing PI. This relationship could be represented mathematically by equation 4.3.

$$\alpha' = 12.266(PI)^{-0.641} \qquad (4.3)$$

Thus, equation (4.3) was used to back calculate the fitting parameters (α′) for the untreated and CaLS treated samples. The alpha (Table 4.2) values were in good agreement with the arbitrarily estimated alpha values.

$$\alpha = 12.266(PI)^{-0.641}$$
$$R^2 = 0.9971$$
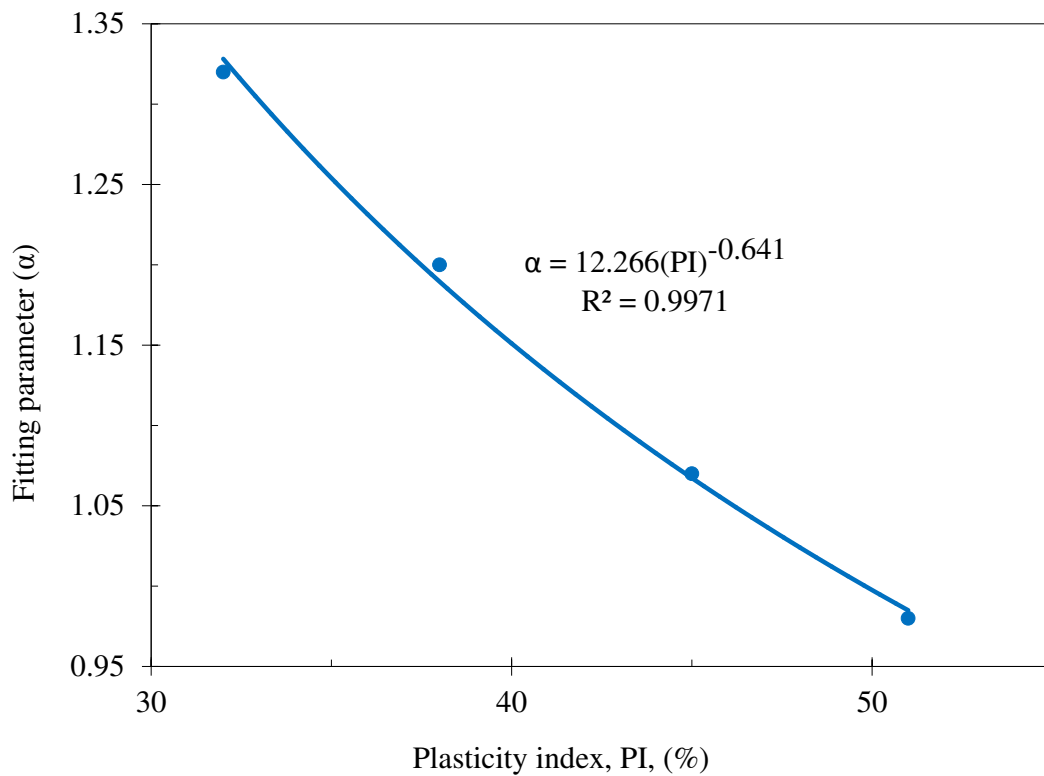
Figure 4.29: Relationship between fitting parameter and applied pressure.

Table 4:2: Calculated alpha dash values of soil samples using equation (4.3)

S/No.	Soil description	PI	Assumed (α)	Calculated (α')
1	Soil A: LS = 0%	51	0.98	0.9866
2	Soil A: LS = 2%	45	1.07	1.0690
3	Soil B: LS = 0%	38	1.2	1.1914
4	Soil B: LS = 2%	32	1.32	1.3302

The calculated α' values were then used to replot Fig 4.26. The result is shown in Fig 4.28. Both figures are identical, suggesting that the alpha predicting equation (equation 4.3) was very reasonable. Fig 4.28 could be represented mathematically as follows.
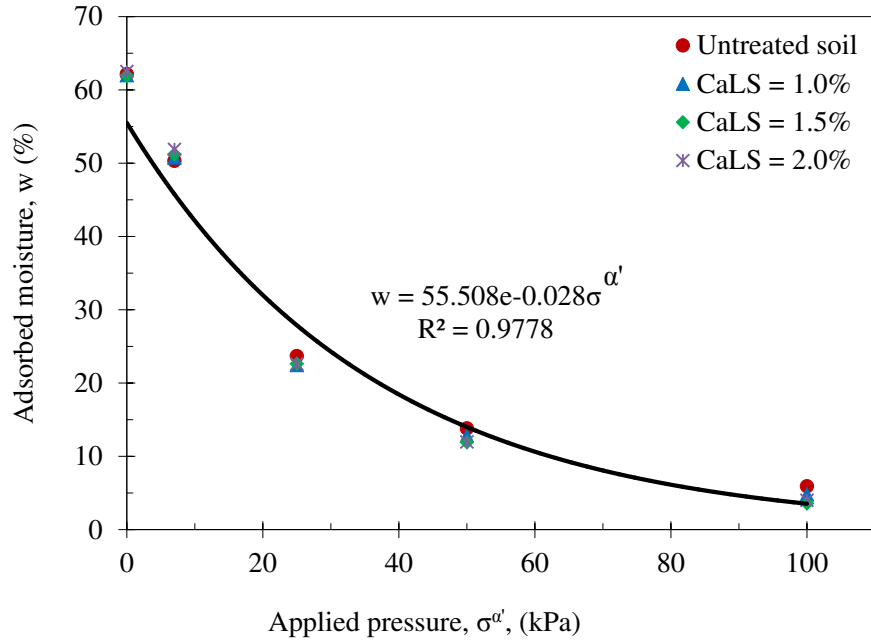
Figure 4.30: Depicts adsorbed moisture and applied load using calculated alpha (α')

$$w = 55.508e^{-0.028\sigma^{\alpha'}} \qquad (4.4)$$

However, the experimental data has shown (Fig 4.29) that the percent swell of a soil is a function of the adsorbed moisture content and a factor C_m. This relationship has been demonstrated previously by Seed et al. (1962) and Dhowian (1992).

$$S = C_m w \qquad (4.5)$$

Where,

S = percent swell, w = adsorbed moisture content, C_m = is a constant of proportionality and is equal to 1.4066 x 10^{-3}.

Now substituting equation (4.4) into (4.5) gives

$$S = C_m \left(55.508e^{-0.028\sigma^{\alpha'}} \right) \qquad (4.6)$$

$$S = 0.075e^{-0.028\sigma^{\alpha'}} \qquad (4.7)$$

165

Equation 4.7 is the simplified swell predictive model for CaLS treated expansive soil. The equation makes it possible to predict the percent swell of any given soil when the PI, the applied pressure (σ), and a fitting parameter (α') which could be calculated using equation 4.3, is known.
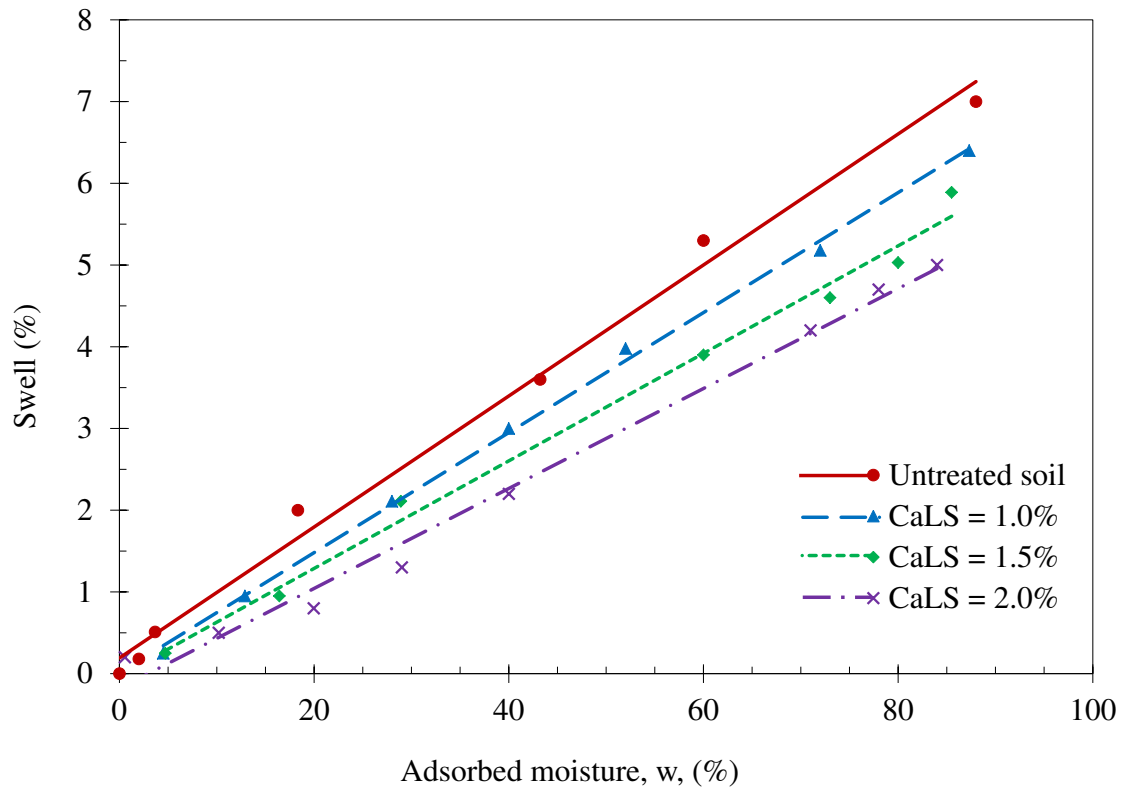
Figure 4.31: Relationship between percent swell and adsorbed moisture content of the remoulded expansive soil

4.7.1   Model verification

Equation 4.7 was verified by calculating the percentage of swell of the untreated and CaLS treated specimens under various surcharge pressures. Table 4.3 illustrates the initial test conditions and the calculated percentage of swell of the specimens. The calculated values were correlated with the experimental values with a reasonable fit (Fig 4.30), with a standard deviation of 0.246 and standard error (Se) $[Se = Standard\ deviation/\sqrt{n}]$ of 10%. The relatively high Se is due to the few data (n = 6) available for analysis.

Table 4:3: Swell predictive model verification data.

Soil type	Calculated α'	Applied pressure, σ, (kPa)	$\alpha' \times \sigma$	$e^{\left(-0.028\sigma^{\alpha'}\right)}$ A	Swell (%) = (0.0747*A)100
untreated	0.9866	0	0	1	7.45
CaLS = 1.0%	1.069	7	8.0059	0.7992	5.95
CaLS = 1.5%	1.1914	25	46.2920	0.2736	2.04
CaLS = 2.0%	1.3302	50	181.9575	0.0063	0.05

At low applied pressure the predictive model performed very well, but as the surcharge pressure increased the model under estimated the magnitude of the percent swell of the soil.
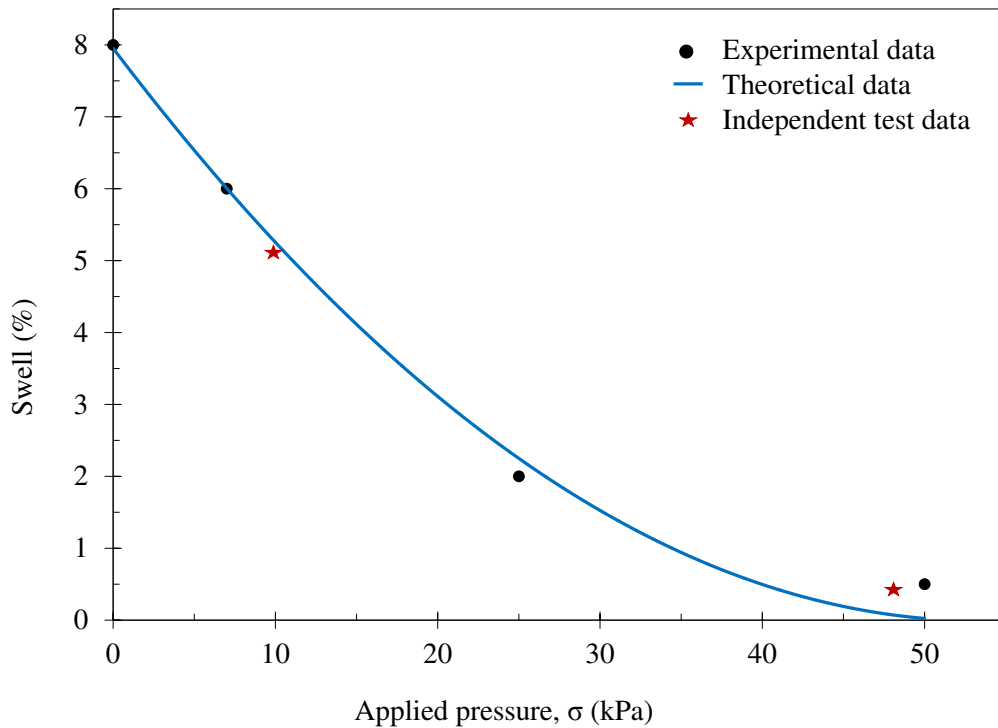
Figure 4.32: Experimental and theoretical correlation of test data

4.8 SUMMARY

In this study the efficacy of a non-traditional admixture (CaLS) was evaluated by performing standard geotechnical laboratory tests on the swell potential (i.e. percent swell and swell pressure), shrinkage, Atterberg limits (Liquid limit, plastic limit and plasticity index), soil durability, uniaxial compressive strength (UCS), compaction characteristics, consolidation characteristics, and the permeability of soil before and after treatment. In some instances identical test specimens were prepared using 2% cement admixture and tested accordingly for the sake of comparison. All the test specimens were prepared at OMC and MDUW unless stated otherwise. The test data suggested that various facets of the expansive soil treated with 2% CaLS could be explained by the interplay of a few underlying reaction mechanisms that are discussed in chapter 5. In general the results showed significant and consistent changes in the engineering properties of the test soils following 2% CaLS addition, so on the basis of the experimental data the nature of the coordinating cation in LS admixture played a vital role in its ability to control the swelling of expansive soil, but LS with monovalent coordinating cations were less effective than those with divalent cations such as calcium.

The addition of 2% CaLS caused a 22% reduction in the percent swell of the otherwise expansive soil. The reduction in the plasticity index of the treated soil translated to reducing swelling in the soil. Although the identical sample treated with 2% cement exhibited a 33% reduction in swell, it significantly increased the pH of the soil, which was in direct contrast with the CaLS admixture where the soil pH practical remained unchanged.

The presence of CaLS significantly improved the percentage weight loss compared to the sample treated with 2% cement under freezing and thawing conditions. Moreover, the ductility of remoulded soil was unaltered after treatment with CaLS admixture whereas the sample with 2% cement lost its ductility and exhibited brittleness at failure. Furthermore, the permeability of the CaLS treated soil sample remained practically unchanged. The admixture improved other engineering properties such as the consolidation parameters and shrinkage limit, and still retained

permeability integrity so any instability in the soil due to internal piping will be minimal compared to the soil treated with cement that showed a significant increase in permeability. With such significant increase in permeability of cement treated soil, the soil becomes erodible or dispersive in nature thus, it is in danger of surface and internal erosion (piping). In Australia, failures of small dams due to piping caused by erodible and dispersive soils have been documented (Philips 1977; Fell et al. 2003). It is therefore, important that the permeability of treated soil be maintained to avoid such problems on road/rail or dam embankments. It is interesting to note that CaLS maintained the permeability of the soil but improved other engineering properties.

5 THE STABILIZATION MECHANISMS OF A CALCIUM LIGNOSULFONATE ADMIXTURE ON A REMOULDED EXPANSIVE SOIL

5.1 INTRODUCTION

This chapter will investigate and identify the mechanisms by which a remoulded expansive soil was modified or altered by a CaLS admixture. To achieve this objective, untreated and CaLS treated samples of remoulded soil were studied microscopically using techniques such as x-ray diffraction (XRD), a scanning electron microscope coupled with energy dispersive spectroscopy (SEM/EDS), fourier transform infrared (FTIR), computed tomography (CT Scan), Cation exchange capacity (CEC), and the specific surface area (SSA). The idea was to identify and compare any physical/chemical changes between the untreated and treated samples and then propose the most likely reaction modes of the admixture with expansive soil minerals. This chapter presents the results of these experiments and elaborate detailed description of stabilization mechanisms of CaLS on the remoulded expansive soil.

5.2 MICROSTRUCTURAL CHARACTERIZATION OF STABILIZER MECHANISMS

The following analytical techniques were used to study the micro-fabrics of untreated and 2% CaLS treated expansive soil.

5.2.1 *XRD analysis:*

An X-ray diffractometer is essentially a camera that uses energetic x-rays to image crystalline materials rather than visible light. When an x-ray beam with a wavelength (λ) is incident on the lattice planes in a crystal at a given angle (θ), diffraction occurs

when the rays reflected from successful planes differ. By varying the angle of incidence (θ), Bragg's law is satisfied by different d-spacing (the distance between the atomic planes) in crystalline materials. A plot of θ and intensities of the resultant diffraction peaks produces a pattern that is unique to each mineral, and since these inter-atomic distances are unique to each mineral, the subsequent change in the d-spacing can be an indicator of mineralogical alteration. This was achieved using Bragg's law (equation 5.1).

$$n\lambda = 2d \sin\theta \qquad (5.1)$$

Where

d = inter-planar spacing distance (as function of θ), n = number of diffraction, θ = critical angle of incidence on the crystal plane, λ = wavelength of the x-rays.

XRD was used in this study to determine the arrangement and spacing of atoms within soil crystals, to identify clay minerals in the soil, to qualitatively verify clay minerals, and to assess changes in clay mineralogy due to 2% CaLS addition. Oriented specimens were prepared and analyzed using a GBC X-ray diffractometer. The tests were conducted at wavelength of Cu-$K\alpha$ (λ=1.54056 Å), an input voltage of 35.0kV, a current of 28.5mA, and a continuous scan mode from $2\theta = 2^0$ to 60^0 with a step size of 02^0 at a speed of 1^0/min in a laboratory with approximately 98% relative humidity. The diffractograms of the untreated and 2% CaLS treated samples of expansive soil contained smectite, illite, kaolinite, quartz groups, and layers of mixed minerals (Fig 5.1).

Changes in the refractive angle (2θ) which translate to changes in the d-spacing in soil minerals were determined by evaluating the d_{001} smectite peak at $2\theta = 5.78^0$ before and after treatment. There was a noticeable change in this d_{001} peak after the addition of CaLS such that the peak became much broader. Cullity (1979) attributed peak broadening to a decrease in the average size of crystallite in the reflecting minerals. According to Cullity (1979), large crystallites give sharp peaks but as they decrease in size, so does the width of the peak. Cullity also reported that amorphous samples display hump shaped peaks, so changes in the shape of the d_{001} smectite

peak after the addition of CaLS suggested that the amorphicity of the CaLS admixture played a significant role in the crystallographic alteration of the d_{001} smectite minerals. Although this "broadening" may have been caused by the orientation of the clay in the sample holder, it was only visible in the treated samples so it was concluded that the peaks broadened due to the CaLS admixture. The basal and peripheral coating of the smectite minerals by the CaLS admixture, a non-crystalline polymer, restricted diffraction from the characteristics atomic planes of the minerals thus, the the d_{001} smectite peak broadened after treatment.

The d_{001} smectite peak also shifted to the left on the 2θ axis. The shift in this peak from $2\theta = 5.78^0$ to 5.38^0 caused a corresponding initial increase in the d-spacing of the smectite minerals from 13.90 to 14.93Å (Bragg's law). This was due to the crystalline domains of the mineral lattices relaxing as the ion-carrier and cross-linking agent (CaLS) intruded, leading to initial expansion of the inner layer and subsequent moisture entrapment. These findings suggested that for soil treated with 2% CaLS, the layers of clay initially expanded as the admixture intercalated the space. This result is consistent with the mechanism of interlayer expansion with subsequent moisture entrapment, as proposed by Scholen (1991; 1995; Rauch et al. 1993; Tingle et al. 2007).

Note that the peaks of non-swelling soil minerals such as kaolinite and quartz did not shift along the 2θ axis in the specimen treated withCaLS and while the d-spacing of these minerals before and after treatment was practically the same, the intensities decreased significantly. This could be indicative of the inability of CaLS admixture to intercalate the inner layers of non-expansive soil minerals; instead they underwent peripheral adsorption which caused a decrease in the intensities of the minerals. Whittig and Allardice (1986) ascribed this reduced intensity in the diffractograms of minerals to a decrease in the concentration of particular mineral, which means the external adsorption of CaLS on these minerals tended to reduce the availability of the mineral crystals to reflect incident rays, resulting in a decrease in the peak intensities.
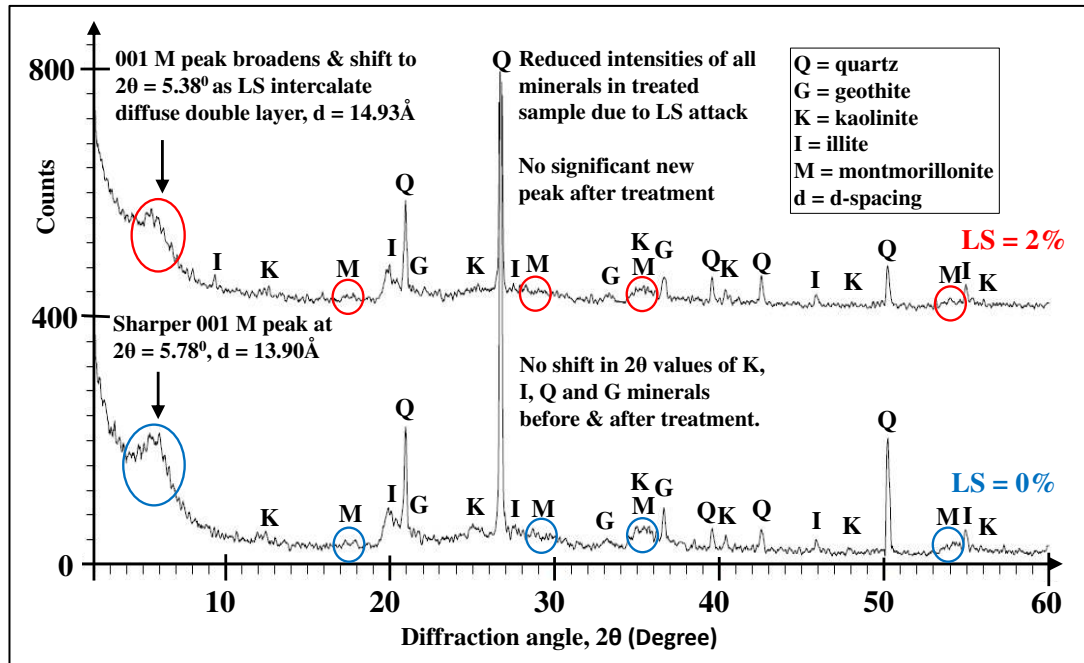
Figure 5.1: Difractograms of untreated and 2% CaLS treated expansive soil. Notice the decrease in peak heights after treatment and the slight shift of the 001 peak to the left upon treatment.

The absence of new peaks (minerals) in the XRD diffractogram of the treated soil coupled with the negligible change in their mineral ratios (e.g. Al:Si) (see Table 5.1) as obtained from an EDS analysis of samples before and after treatment suggested there were mainly inter-molecular interactions between the soil minerals and the CaLS admixture rather than major chemical reactions. Therefore, based on the XRD data, it could be surmised that CaLS altered the smectite minerals through basal and peripheral adsorption, whereas the non-expandable minerals only experienced peripheral adsorption, probably because the interlayer spacing of these minerals was very small compared to the relatively large molecular size of CaLS admixture.

5.2.2   SEM analysis:

A SEM is a microscope that uses electrons instead of light to form an image. The signals derived from interactions between electrons and the sample reveal information about the sample such as its external morphology (texture), crystalline structure, and particle orientation of a material. SEM can also qualitatively or semi-

quantitatively determine the elemental composition of materials using an energy dispersive x-ray spectrometer (EDS).

The morphological changes upon the addition of 2% CaLS were investigated using a JEOL JSM-6460LA SEM, equipped with a Minicup EDS. Compacted swell test specimens were broken and about 0.5g was collected and placed onto an uncoated aluminium stub sample holder that was then inserted into the SEM equipment for analysis. SEM micrographs of the untreated and treated samples taken at x2500 magnification (Fig 5.2) revealed that the fabric of the untreated sample consisted mainly of dense clay matrixes with little or no appearance of aggregations. The image exhibited a poorly open and/turbulent type of microstructure, with smectite lamelle in a fairly orderly arrangement toward the centre of the micrograph. The minimal appearance of the 'corn-flake' like clay minerals usually associated with the smectite group was attributed to the fact that the soil had been remoulded.
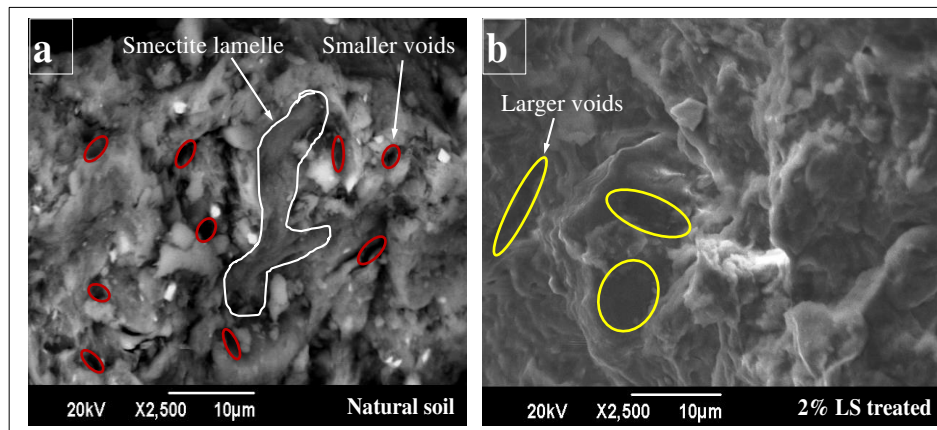
Figure 5.2: a) SEM micrographs of untreated soil, b) SEM micrograph of 2% CaLS treated soil

By comparison, the SEM micrographs indicated that the morphology of the soil had changed considerably after treatment with CaLS (Fig 5.2b). The figure shows the presence of flocculated particles with sharper edges. These morphological changes were ascribed to the adsorption/coating mechanisms and cation exchange processes between the soil and the CaLS complex. Fig 5.2b also shows how the clusters of clay particles were interspaced by larger but fewer pore spaces compared to the sample of untreated soil. This result implied that the sample treated with 2% CaLS had

flocculated more than the untreated counterpart so the ingress of water into the entire soil body would be restricted, resulting in a decrease in the magnitude of swell potential of this otherwise expansive soil.

5.2.3   EDS analysis:

An X-ray microanalysis in SEM is the process of using characteristic x-rays generated in a specimen by the electron beam to determine the elemental composition of a given material. The JOEL SEM is equipped with mini-cup energy dispersive spectroscopy (EDS) which automatically generates a qualitative and quantitative elemental composition of materials. When an incident x-ray strikes the detector it is converted into pulses that are sorted and counted by voltage. The energy as determined from the voltage measurement for each incident x-ray is used to identify the elements present in a specimen (i.e. peak response) whereas, the peak intensity (counts/sec) indicates the concentration of that particular element (Electroscan 1996).

The micrographs for the untreated and CaLS treated samples are presented in Fig 5.3, and reveal there was practically no difference in intensity in the EDS spectra of the untreated and CaLS treated specimens. This suggested that no substantial chemical reaction occurred between the sorbent (soil minerals) and the sorbate (CaLS admixture), although the treated sample shows minute traces of sulphur, possibly due to the presence of an unreactive sulphite group in the chemical admixture.

Meanwhile Table 5.1 quantitatively describes the elements present in each specimen of soil. The change in the ratio of elements following CaLS treatment was insignificant; for example the ratio of Al:Si varied by about 8.1%. These elements (Al and Si) were chosen because they form the basic units of clay minerals so if there was a significant decrease in the aluminium-silica ratio after treatment, this could have meant a structural change in the tetrahedral sheets due to octahedral Al^{3+} cations transferring to the admixture. Alternatively, if the Al:Si ratio had increased then silica was released from the clay minerals, just like a natural soil weathering process. The amounts of aluminium and silica in the untreated soil were 15.34g and 48.85g respectively, but after treatment the amount of aluminium was almost the

175

same (14.21g), and the same applied to the amount of silica (41.61g). The Al:Si ratio increased insignificantly from 0.3140 to 0.3415 after treatment (Table 5.1), which suggested that a negligible weathering effect occurred on the soil after the CaLS admixture was added. The results from EDS corroborated well with the XRD results that confirmed a minimal change in soil mineralogy but functioned through crystallographic alteration of the mineral lattices.

It is pertinent to keep in mind that data obtained from Al:Si analysis could be affected by the topography of the specimen, so conclusions drawn from this analysis must be treated with caution. To minimise this topographical effect on the test data, all the specimens tested in this study were prepared identically and it was assumed that the untreated and treated samples had a similar topography. Moreover, multiple samples (five) were analysed in each case and averaged to quantitatively determine their elemental compositions.

Table 5:1: Elemental composition of expansive soil before and after 2% CaLS treatment using EDS

Compound	Mass (%) LS = 2%	Mass (%) LS = 0%	Al:Si before treatment	Al:Si after treatment	% change Al:Si
Carbon	13.1	23.64			
Na_2O	0.19	0.14			
MgO	2.49	2.26			
Al_2O_3	15.34	14.21			
SiO_2	48.85	41.61			
SO_3	0.001	0.06	0.3140	0.3415	8.1%
K_2O	0.68	0.69			
CaO	1.83	3.82			
TiO_2	2.48	2.00			
FeO	15.02	11.56			
Total	100	100			
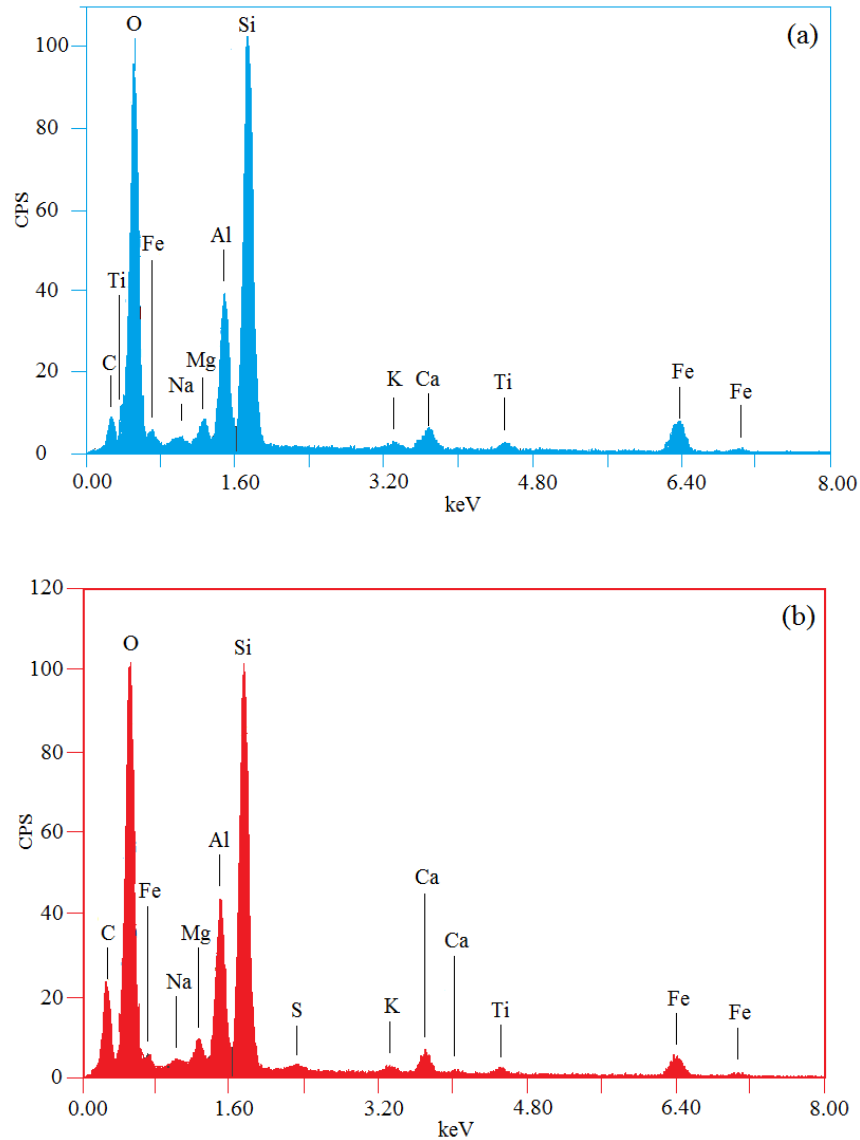
Figure 5.3: a) EDS spectrum of untreated soil, b) EDS spectrum of 2% CaLS treated soil.

5.2.4   CT scan:

Due to the very small specimen sizes commonly used in analytical techniques (e.g. XRD), the data may always not represent the bulk samples, so a non-destructive CT scan was used to reveal the overall internal structure of compacted specimens of untreated and 2% CaLS treated before and after the laboratory swell tests. In recent years the use of CT to describe physically complex pore spaces with respect to variables such as the bulk density of soil is not uncommon (Anderson et al. 1990;

Heitor et al. 2013). Fig 5.4 shows the 50mm diameter by 20mm high test specimens that were examined using this technique. The first column represents CT scan images of the untreated compacted specimens before and after one-dimensional swell tests while the second column denotes 2% CaLS treated specimens before and after one-dimensional swell tests.

Each pair of images was scaled to the same minimum and maximum grayscale and set to the same threshold to allow for a quantitative comparison of the partially saturated and fully saturated images. It is common knowledge that with high-resolution CT images, white/light grey represents the water phase, black denotes the air phase, and darker grey is the solid phase if taken on a black background. The images in Fig 5.4, although taken on a black background did not conform to this definition due to limitations in the scanner's resolution, so the structural changes in the soil were only evaluated in terms of macroscopic pores; the lighter shades in these images symbolise high macroscopic water saturation, while the darker spots represent less saturated phases. Therefore, the low resolution images only provided macroscopic information, i.e. they showed variations in the moisture content of samples but could not detect the geometry of the pore space.

It was very clear that the degree to which the specimen of expansive soil was saturated was undoubtedly affected by the CaLS admixture (2nd row; Fig 5.4). The adsorbed moisture content was much less in the sample treated with CaLS compared to the untreated sample. Indeed, a close examination of both micrographs after the swell test shows more prominent "black" (existence of air phase) spots in the treated than in the untreated samples. The presence of CaLS limited the adsorption of moisture by soil minerals into certain macro-pores in the treated sample. The hydrophobic component of CaLS might have hindered the ingress of such moisture into these pore spaces, and the intercalation of the admixture into the inner layers of the expansive minerals might have displaced water molecules from the soil body. This theory agrees with the gravimetric water content determined at the end of the swell test. Gravimetric moisture contents measured at the end of swell tests for untreated and 2% CaLS treated specimens' shows a decrease from 51% to 47%, respectively.
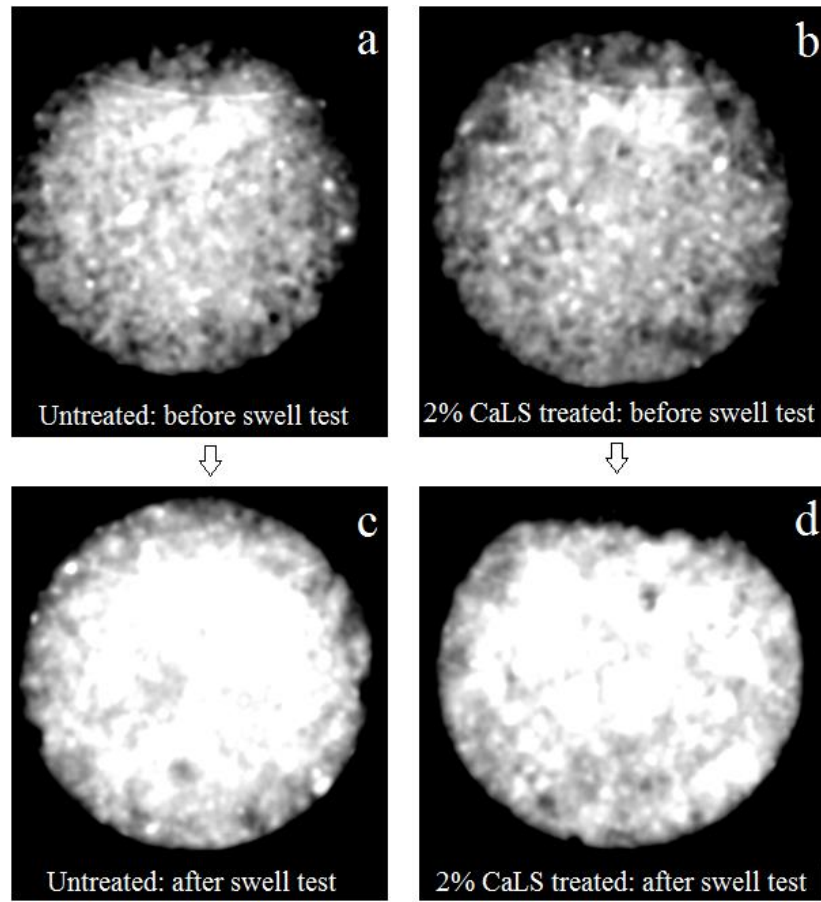
Figure 5.4: CT scan images of Φ50x20mm height specimens of untreated and 2% LS treated samples before and after swell test. (Top row: as compacted specimen & bottom row: after swell test. White represents the water phase; black is the air phase and grey is the solid phase in soil specimens).

5.2.5   FTIR:

Previous research on clays has shown that a complex system of interlayer water exists in smectite minerals (Russell and Farmer 1964). Russell and Farmer (1964) posited that interlayer water could be bounded to the interlayer surface, to interlayer cations, to other water molecules, and could be adsorbed in the grain surfaces. In this study the effect of admixture cations and/reactive groups on interlayer water molecules was analysed through FTIR spectroscopy from 400–7000cm^{-1}. This technique was carried out on untreated and 2% CaLS treated samples after 7 days of curing with a Shimadzu IRAffinity-1 C 8984 Model. By measuring the fundamental H_2O vibrations, combinations and overtones, Bishop (1994) observed correlations

179

between the cation-water behaviour. The rationale behind the use of this technique in this investigation was to examine the infrared spectral absorptions due to interlayer water in smectite and other minerals, and how cations in interlayers influence these absorptions.

5.2.6   *Spectrum of untreated soil:*

The FTIR technique was used to investigate the vibrational behaviour of the –OH, H-O-H, interlayer cations, tetrahedral silicate/aluminate anions, octahedral metal cations and as well as identify the soil mineralogy. The infrared spectra for each sample was recorded with 120 scans in the near-infrared (NIR) and mid-infrared (MIR) spectral regions in a transmission mode at $4cm^{-1}$ resolution.

Literature reveals that the absorption bands at the near-infrared (NIR) region of $6800\text{-}7000cm^{-1}$ are signature vibrations of water molecules (Fig 5.5). These adsorption bands result from the first overtone of the stretching vibrations of H-O-H molecules involved in strong hydrogen bonds (Bishop 1994). The band recognisable at $4520cm^{-1}$ was attributed to a combination of –OH stretching (3620 and $3694cm^{-1}$) linked to AlAlOH groups, while the $4624cm^{-1}$ band (915, 600 and $920cm^{-1}$; in the MIR region) is the deformation vibrations of AlAlOH groups. Bands at about 6984 and $5520cm^{-1}$ were also reported to be -OH vibration modes of water (Buijs and Choppin 1963). Petit et al. (1999) reported that the –OH stretching (ν_{OH}) and binding ($2\delta_{OH}$) combination ($\nu_{OH} + 2\delta_{OH}$) modes associated with inner-surface and inner hydroxyl groups were synonymous with bands at $5484cm^{-1}$ (($\nu_{OH} = 3694cm^{-1}$, $\delta_{OH} = 920cm^{-1}$) and at $5420cm^{-1}$ ($\nu_{OH} = 3620cm^{-1}$, $\delta_{OH} = 915cm^{-1}$), respectively. The subtle peaks at 6976 and $5250cm^{-1}$ corresponded to -OH bending overtone of FeFeOH and combinations involving inner sphere and surface H_2O molecules, respectively (Madejova 2003). A similar assignment was given to the band at $5065cm^{-1}$ by Cariati et al. (1983). Combinations of –OH stretching bands of kaolinite with lattice deformation vibrations were seen between $4300\text{-}4000cm^{-1}$. The spectra also showed common bands for all dioctahedral smectite. For example, the shoulder at $6852cm^{-1}$ was assigned to H-O-H molecules involved in strong hydrogen bonds ($2\nu_{\omega}$). The strong bands at 5253 and $5342cm^{-1}$ were caused by smectite minerals due to a

180

combination of the stretching (ν_{OH}) and bending (δ) vibrations of water and (ν_{OH} + δ_{AlFeOH}) combination modes, respectively (Komadel 1999).
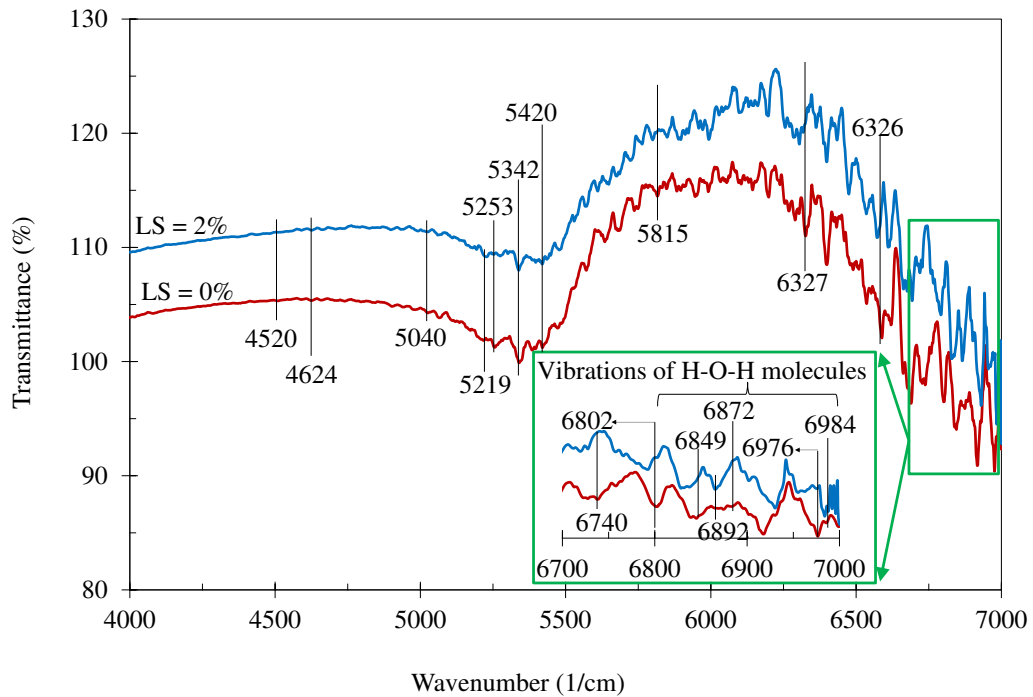
Figure 5.5: FTIR patterns of untreated and CaLS treated expansive soil (NIR)

In a detailed microstructural study, Russell and Fraser (1996) assigned absorption bands to soil minerals within the infrared region. They attributed the band at 2285cm^{-1} to the presence of illite minerals in a soil sample (Fig 5.6). The broad band at about 3000 – 3800cm^{-1} was exclusively associated to sorbed H-O-H with the –OH stretching vibration peak of water centred at 3365cm^{-1}. The shoulder at 3393cm^{-1} was assigned to –OH stretching of structural hydroxyl groups in smectite. They further ascribed the 3620cm^{-1} characteristic band to the inner -OH and the 3645-3697cm^{-1} bands to the vibrations of the external –OH. Bishop et al. 1994 assigned 1116cm^{-1} band to the –OH vibrational mode of the hydroxyl molecule in smectite and the band at 3610cm^{-1} was assigned to the –OH stretching mode of kaolinite group. Saikia and Parthasarathy (2010) assigned the symmetrical and anti-symmetrical stretch of C-H mode of –CH$_2$ group to the bands at 2920-2961cm^{-1} and 2850-2867cm^{-1}, respectively while the band at about 2960cm^{-1} was attributed to symmetric stretch of –CH$_3$ group of kaolinite by Bishop et al. (1994).

181
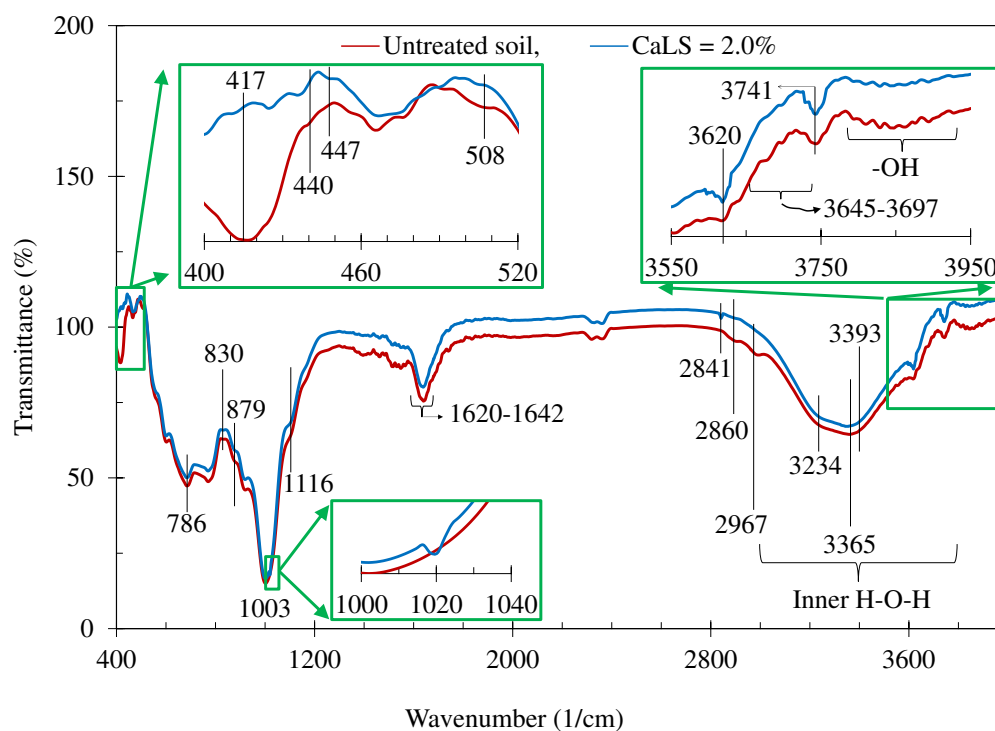
Figure 5.6: FTIR patterns of untreated and CaLS treated expansive soil (MIR)

The bands at 510 and 464cm^{-1} were due to Si-O-Al (where Al is an octahedral cation) and Si-O-Si bending vibrations, respectively (Komadel et al. 1999). However, a 505cm^{-1} band in soil was later attributed to the presence of Al-OH groups (Madejova 2003). The band at 786cm^{-1} and the weak shoulder at 795cm^{-1} represent quartz mineral in the soil, and this was confirmed by X-ray data. Bishop et al. (1994) assigned absorption bands of 918, 879cm^{-1} and 827cm^{-1} in clay to -OH bending vibrations of AlFeOH, (Al_2OH) and AlMgOH) minerals in smectite, respectively. The -OH bending vibrations at these wave numbers suggested that the Al octahedral was partially substituted by Fe and Mg. The 1003cm^{-1} band is a finger print vibration –OH deformation of gibbsite. The prominent absorption band at 1620-1642cm-1 is a signature of the -O-H bending of water in smectite whereas the multiple bands at 1364-1620cm^{-1} were associated with C-H, Na^+ and SiO_4 vibrations.

5.2.7 *Spectrum of soil treated with 2% CaLS:*

The NIR of 4000-7000cm^{-1} of the sorbent-sorbate complex (Fig 5.5) showed insignificant spectral differences to the sorbent spectrum, probably because the

adsorbed CaLS molecules did not adopt a regularly organized structure at the soil mineral surfaces. However, identifiable band shifts/deformations were seen after 2% CaLS was added. For example, the near disappearance of the bands at 6972, 6872, 6740, and 6802 cm^{-1} was associated with a decrease in the amount of interlayer water (Bishop et al. 1994). The bands (5040-5420cm^{-1}) assigned to a combination of stretching and bending vibrations of water decreased in intensity after the addition of CaLS, which suggested there was dehydration in the already collapsed inner layers of the expansive mineral lattices. These finding are in union with Bishop and co-workers (1994). They used the FTIR technique to investigate the spectrum of soil under dry and moist environments and reported weaker peaks in dry conditions at 5236cm^{-1} but very strong peaks at the same band position in the moist sample. Similar observations were made within the NIR range of 5040-5420cm^{-1} in this investigation.

Moreover, the spectrum of the 2% CaLS treated soil at 6892 and 5342cm^{-1} became sharper and more symmetrical, which indicated dehydrated conditions. Bishop and co-workers (1994) reported that under dehydrated conditions the interlayer water was bounded to cations or interlayer surface which caused the H-O-H stretching vibration bands to shift to lower wavelengths than similar absorptions under hydrated conditions. This was clearly seen in the bands associated with H-O-H vibrations at 6984, 6872, 6849, 6740, 6589, 6327, and 5815cm^{-1} in this investigation. Furthermore, the intensities of the bands at 5219 and 6500 – 6920cm^{-1} increased after the addition of CaLS. Farmer and Russell (1971) attributed this behaviour in ionic treated soils to water directly coordinated to the cations forming hydrogen bonds with surrounding H_2O molecules rather than the silicate lattice of the soil. In a similar study, Farmer and Mortland (1966) reported that polar organic molecules such as nitrobenzene readily displace water in outer spheres of coordination round monovalent and divalent cations, where they then form hydrogen bonds with water directly coordinated to cations.

The intensity of the shoulder bands corresponding to inter-lamellar water (3200–400cm^{-1} and 1640 cm^{-1}) indicates that most of its water was lost after the addition of CaLS, probably due to the displacement of water molecules as a consequence of

sorbate intercalation of the inter-lamellar space in the lattices of the expansive soil minerals (Fig 5.6). These perturbed water absorption bands shifted from 1640 to 1636 cm^{-1} and 3365cm^{-1} to 3353cm^{-1}, which also augmented a decrease in the inner layer water content theory after the addition of CaLS. The reduction in intensities and shifts associated with the above peaks suggested that CaLS underwent basal and peripheral adsorption on soil particles (Theng 1979). This reduction in band intensities could also mean that the few water molecules remaining at the inter-lamellar space were coordinated to CaLS molecules through a "water bridging" mechanism. It is also likely that some CaLS molecules displaced water to become directly coordinated with the cation, as a consequence of the high polarizing strength of the Ca^{2+} cation. This behavioural observation was similar to previous works in benzonitrile-montmorillonite (Serratosa, 1968) and nitrobenzene-montmorillonite (Parfitt and Mortland 1968) complexes.

It is common knowledge that the -OH stretching vibration shifts to a lower frequency when the hydrogen bonding interactions become stronger. The -OH vibration bands at 3700-3900, 3365, 508, 440, and 417cm^{-1} weakened considerably and/or shifted to lower wave numbers upon CaLS addition. Russell and Farmer (1964) have ascribed such behaviour of adsorption peaks to a reduction in the interlayer water in the soil samples. This created the right environment for CaLS to form direct bonds with adsorbed cations or coordinate directly with adsorbed moisture. Further spectra analysis within the MIR region (400 – 4000cm^{-1}) after chemical modification of the soil caused an increase in peak intensity at 1020cm^{-1}, which could then be correlated with the undissociated sulfonic acid group in the CaLS admixture in treated soil. Similarly, the appearance of a subtle band at 2841cm^{-1} assigned to C-H stretching suggested the presence of unreacted CaLS molecules in treated soil. The presence of sulphur molecules were also seen in the EDS spectrum of treated samples, which also supported the FTIR data.

The addition of 2% CaLS admixture produced an intense -OH band at approximately 3597 - 3630cm^{-1}. Russell and Farmer (1964) have attributed adsorption in this region to -OH molecules being strongly co-ordinated to Al^{3+} in the octahedral layer. The sample of CaLS modified soil also showed higher band intensity at 1116cm^{-1} and a

new peak at $447 cm^{-1}$. These bands suggested the formation of Si-O stretching vibrations for amorphous silica and implied that amorphous CaLS attacked silica mineral and deposited its footprint of amorphocity.

The intensity of the -OH bending vibrations at $830 cm^{-1}$ of AlMgOH and $879 cm^{-1}$ of AlFeOH decreased slightly after the admixture was added, indicating an alteration of the crystalline lattices of these minerals (Bishop et al. 1994). This decrease in intensities depicted a quantitative reduction of AlMgOH and AlFeOH. An important consequence of replacing inorganic with organic cations is that the surface of the clay becomes hydrophobic, which might have contributed to a reduction in the affinity for water by treated soil minerals, and hence a reduction in the swell potential of an otherwise expansive soil.

5.2.8 CEC:

The cation exchange capacity (CEC) of a soil is a relative reflection of the quantity of negatively charged sites on mineral surfaces that can retain positively charged ions (cations) through electrostatic forces. Cations retained electrostatically could easily be exchanged with cations in a soil solution, and thus the CEC of the remoulded expansive soil was determined before and after 2% CaLS addition. The rationale behind the CEC test is that any alteration in the CEC of treated soil will infer a mineralogical change within the soil.

Many researchers (Cokca and Birand 1993; Santamarina et al. 2002) have agreed that the methylene blue (MB) test is one of the most accurate and simplest methods to determine the CEC of soils. The test works on the basis that clay minerals have a large surface area with negative charges that could be exchanged by methylene blue cations (Santamarina et al. 2002). Methylene blue (MB) in an aqueous state is a cationic dye ($C_{16}H_{18}N_3ClS^+$) with a corresponding molecular weight (M_W) of 319.85 g/mol that can be adsorbed onto negatively charged clay surfaces. The "spot-test" method of the methylene blue dye test was used in this study to determine the CEC of untreated and 2% CaLS treated expansive soil.

The "Spot-Test" method was carried out in accordance with ASTM C837 with the assumption that methylene blue dye could attach itself to the exchange sites on the mineral surface by replacing the exchangeable cations. This procedure involved preparing a stuck solution of MB (1mL = 0.01meq)[3] and then adding 2.0g dry soil to 300mL of distilled water in a 600mL beaker and stir it to homogeneity. The pH of the soil-CaLS solution is then reduced to the $2.5 - 3.8$ range by adding appropriate drops of sulphuric acid (0.1N) while stirring continually. While the soil-water-acid solution was still on the mixer, 5mL of the MB solution was added in increments. After each addition of the MB solution, a drop of the soil-water-acid complex was taken with a glass road and placed on the edge of a Whitman No. 1 filter paper to observe the appearance of the drop on the filter paper. This procedure was repeated until the end point was reached which was indicated by the formation of a light blue halo around the drop (Fig 5.7).
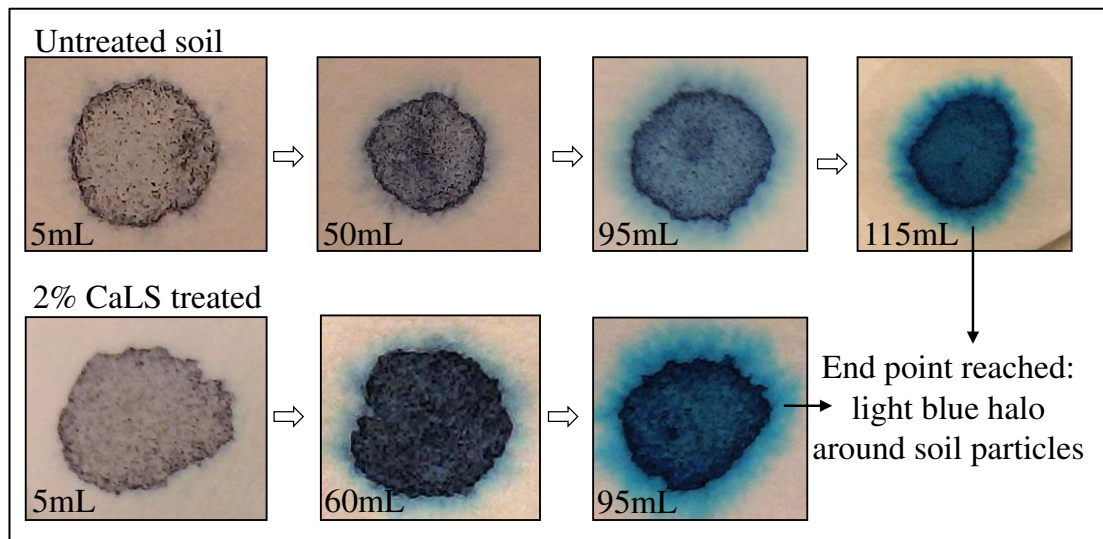
Figure 5.7: Determination of CEC of the untreated and 2% CaLS treated expansive soil showing the "end point" indicated by the light blue halo

The amount of adsorbed MB (methylene blue index; MBI: an estimate of CEC) which equal the CEC for each soil sample were calculated as follows (ASTM C837):

$$MBI = 0.5V \qquad (5.1)$$

Where

V = millilitres of MB solution required to reach the end point

For the untreated soil sample

$$MBI (CEC) = 0.5 \times 115 = 57.5 meq/100g$$

For the sample treated with 2% CaLS

$$MBI (CEC) = 0.5 \times 95 = 47.5 meq/100g$$

The CaLS admixture had virtually no effect on the CEC of the remoulded expansive soil. The untreated soil had a CEC of 57.5meq/100g but this decreased to 47.5meq/100g upon 2% CaLS addition, which is a paltry 17% of the ion exchange mechanism. It was most likely that the large molecular size (201,300.00g/mol; Fredheim et al. 2002) of the CaLS polymer resulted in a "cover-up-effect" leading to an incomplete cation exchange mechanism between the soil minerals and the admixture. Hendricks (1941) reported that small organic molecules quantitatively replaced exchangeable cations on montmorillonite mineral surfaces but incomplete cation exchange mechanisms were observed for polymers with larger molecular sizes. In addition, Theng (1979) reported that LS with monovalent coordinating cations largely serve as charge-balancing species so monovalent cations are more or less completely dissociated from the polymer matrix in an aqueous medium. However, Theng opined that LS with coordinating polyvalent cations are tightly bonded to the polymer matrix through coordination and/or chelation, involving sulphonic and hydroxyl groups and these cations are not easily dissociated in an aqueous medium. This non-dissociation of polyvalent cations from LS structure is believed to have aided the aforementioned "cover-up-effect". The LS used in this investigation had a coordinating polyvalent cation (Ca^{2+}). As Ca^{2+} tends to exchange monovalent cations (e.g. Li^+, Na^+), or Mg^{2+} ions on soil mineral surfaces, the LS structure accompanies the exchange process and tends to cover-up exchangeable sites leading to an incomplete cation exchange mechanism. This was the most likely reason why the exchange capacity measured after CaLS treatment was only 17%.

Determining the CEC of a soil using the MB technique is easy and quick compared to the Standard Determination of CEC with Ammonium Acetate, as proposed by

Chapman (1965). However, from personal experience, the current MB test ("spot-test") technique contains operator related errors such as the ability to judge the test's end point. It is difficult to make discrete judgements on how "light" the "light blue halo" should be at the end point, so the current MB test is not well suited for routinely determining the CEC of soil and any data obtained should be treated with caution. No doubt further standardization of the MB technique is required.

5.2.9 Specific surface area (SSA):

The same assumption made in the CEC test was made for determining the SSA of untreated and 2% CaLS treated soil. MB dye is a heterocyclic aromatic chemical compound ($C_{16}H_{18}N_3ClS$) that ionizes as a cationic dye ($C_{16}H_{18}N_3ClS^+$) in an aqueous solution, enabling it to be adsorbed on negatively charged clay surfaces by displacing cations such as Na^+, Mg^{2+}, K^+, and Ca^{2+} located on the surfaces of soil particles. The quantity of adsorbed MB enabled the SSA of the soil specimens to be estimated. The SSA of the untreated and 2% CaLS treated samples were calculated using equation (5.2) proposed by Hang and Brindley (1970). From the maximum amounts of adsorbed MB, and by assuming that the area covered by one molecule of MB equals $130Å^2$, which corresponds to the molecules lying flat on the clay mineral surfaces (Santamarina et al. 2002):

$$SSA = MBI \times A_{MB} \times 0.01 \quad (5.2)$$

Where

MBI = methylene blue index for the clay in meq/100g clay (an estimate of soil CEC), AMB = surface area of methylene blue molecule (130Å; 1Å = 0.1nm), 0.01 = normality of MB i.e. the concentration of the MB solution used.

Therefore the SSA of the untreated soil sample was given as:

$$SSA = 57.5 \text{ x } 130 \text{ x } 0.01 = 74.75 m^2/g$$

And the SSA of the 2% CaLS treated soil sample was given as:

$$SSA = 57.5 \text{ x } 130 \text{ x } 0.01 = 61.75 m^2/g$$

The calculated SSA vales of untreated and 2% CaLS treated samples were 74.75m^2/g and 61.75m^2/g, respectively, a result that suggested that CaLS admixture through the cation exchange mechanism caused the soil particles to agglomerate by 17%. Assuming that the difference between the two SSA values of samples (74.75-61.75m^2/g = 13.0m^2/g) represented the area of MB dye in actual contact with the soil minerals, as suggested by Ramachandran et al. (1962), 13.0m^2/g suggests that the actual contact area of Ca^{2+} with the soil minerals was probably very small. This might be the likely reason for the "cover-up-effect" earlier mentioned. The SSA data also supported the findings that there were no significant chemical reactions involved in the CaLS stabilization mechanisms of expansive soil, but the crystallography of soil mineral were altered mainly through chemo-adsorption (hydrogen bonding), and/or ionic bonding of CaLS molecules to form direct bonds with cations and hydroxyl groups on soil mineral surfaces and a minimal cation exchange mechanism.

In this investigation the methylene test method was the preferred choice, rather than the famous nitrogen (N$_2$) BET analysis technique, when dealing with expansive soils. It has been reported that the BET adsorption method can only measure the external surface area of particles due to the inability of N$_2$ molecules to intercalate the inner layer of dry expansive soil lattices, and therefore the BET SSA values usually give lower estimates (Ramachandran et al. 1962). This limitation was overcome by choosing the MB method. The MB test was conducted on a soil-water suspension where the innerlayers of the weakly bonded silica sheets of smectite are easily intercalated by water or MB ions to enable the internal and external surface layers to be measured. The corresponding areas determined by the N$_2$ BET adsorption method for the same samples were 62.45m^2/g and 49.85m^2/g for untreated and 2% CaLS treatment, respectively.

5.3 PROPOSED STABILIZATION MECHANISMS OF CALCIUM LIGNOSULFONATE TREATED EXPANSIVE SOIL BASED ON MICRO-CHEMICAL ANALYSIS

The micro-characterization study and subsequent identification of the stabilization mechanisms of CaLS treated expansive soil was achieved through a number of instrumental analytical techniques as discussed above. The physico-chemical changes before and after CaLS addition was evaluated and compared to gain an insight into the possible stabilizing mechanisms of the admixture on the remoulded expansive soil.

The findings from this study suggested that the primary stabilizing mechanisms of CaLS admixture was via adsorption onto the surfaces of soil minerals through electrostatic interactions, hydrogen bonding, covalent bonding, and as well as cation exchange mechanisms with subsequent smearing, and agglomeration of soil particles (Fig 5.8). When CaLS was added to a remoulded expansive soil, it intercalated the inner layer of expandable clay minerals and became adsorbed through mechanisms such as water bridging, hydrogen bonding, covalent bonding, and cation exchange mechanisms. However, for non-expandable minerals such as quartz, the adsorption of CaLS was limited to the surface alone, probably due to the relatively larger molecular size of the polymer compared to the tightly held basal spaces of these minerals. The mechanism of adsorption of CaLS by soil minerals as the principle stabilizing mechanism is fully supported by data obtained from the analytical techniques (e.g. XRD, FTIR). For instance, the appearance of a new peak at 470cm^{-1} suggested that amorphous CaLS attacked the silica minerals and deposited its footprint of amorphocity.

The intercalation of CaLS into the lattices of the expandable minerals displaced water at the outer spheres of coordinating monovalent and divalent cations, where they then formed direct hydrogen bonds with the coordinated water or else developed covalent bonds in adsorbed cations in the soil. The intercalation of CaLS and subsequent adsorption on inner surfaces was accompanied by an initial expansion of the clay mineral lattices with subsequent moisture entrapment, as observed from the

190

XRD micrographs. The adsorptions of CaLS by soil minerals through hydrogen bonding led to the encapsulation of soil minerals with subsequent flocculation-agglomeration of the soil particles, as supported by the SEM micrographs and reduced specific surface area of soil samples.

Besides the adsorption mechanisms of CaLS on soil particles, another mechanism is the ability of the cationic end of the admixture replacing the negative surface of the charged soil particles to prompt particle flocculation and decrease the soil's affinity for water. Moreover, the thin coating of soil particles by the organic cationic compound exposed its hydrophobic end, so the particles were essentially waterproofed which in turn reduced the swell magnitude of an otherwise expansive soil. In summary, the stabilization mechanisms consist of the exchange of interlayer cations (though not significant due to "cover-up-effect"), basal, and peripheral adsorption onto soil minerals through hydrogen bonding (water bridging), initial inner layer expansion with moisture entrapment, and covalent bonding (directly bonding to adsorbed cations) leading to the soil particles being smeared, and with a subsequent reduction in the soil's affinity for water.

The absence of significant new peaks (minerals) after treatment coupled with the negligible change in the soil mineral ratios (e.g. Al:Si) as obtained from EDS analysis of samples, suggested mainly inter-molecular interactions between soil minerals and the CaLS admixture rather than major chemical reactions. These mechanisms of the non-standard admixture collaborate well with Scholen (1992; 1995) proposed mechanisms for non-traditional admixtures.
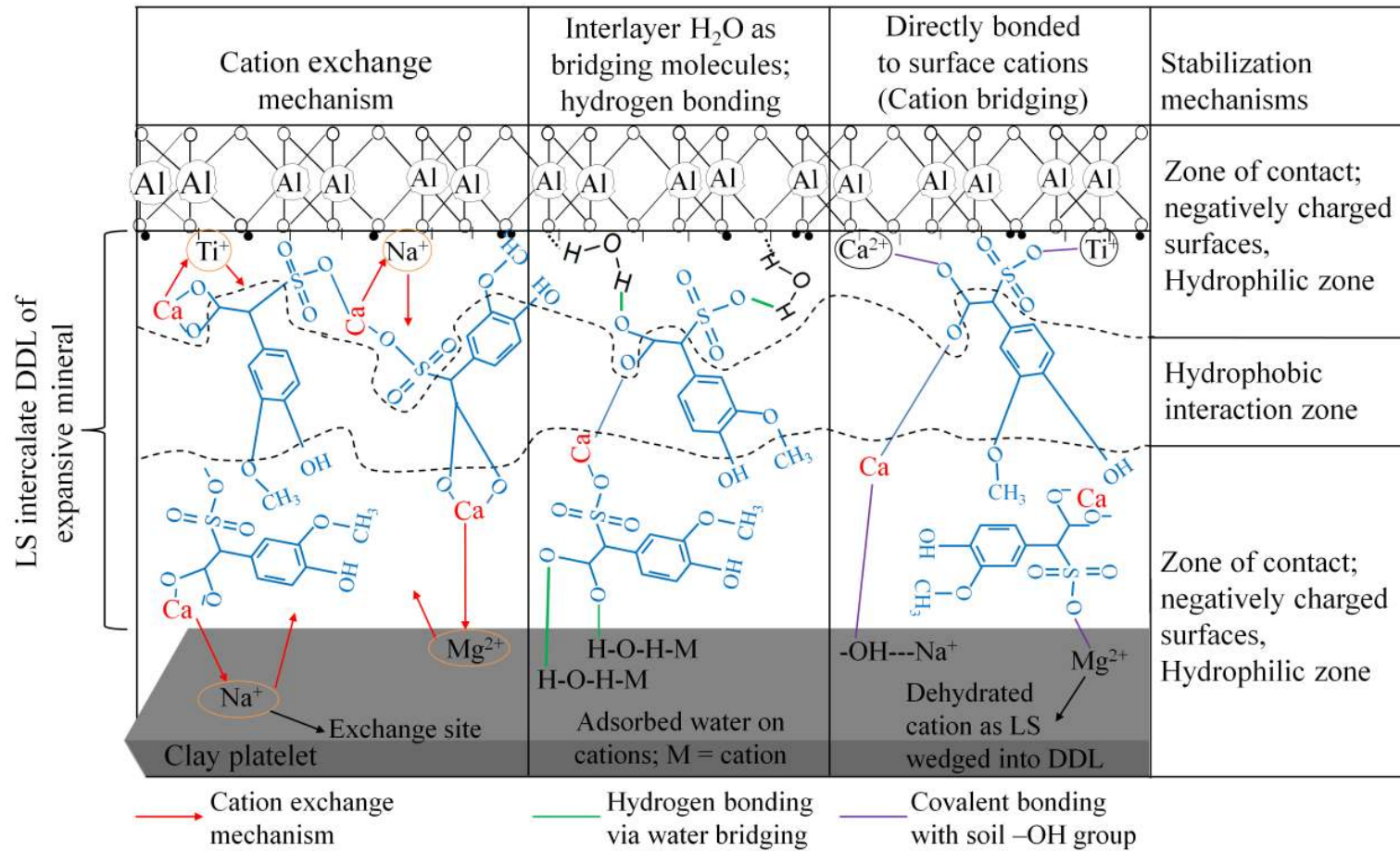
Figure 5.8: Schematic illustration of the stabilization mechanisms of CaLS on a remoulded expansive soil

5.4   SUMMARY

In their reviews, (Rauch et al. 2003; Chen 1988; Bolander 1999; Jones and Vantura 2003; Newman and Tingle 2004; Chen and Indraratna 2014, 15; Scholen 1992 and 1995) emphasized the importance of understanding the stabilizing mechanism of non-traditional admixtures. To a large measure, research into identifying these mechanisms in non-traditional admixtures has not been intense because the focus has always been on improving the strength of the soil. This is due partly to the lack of interest within this research area by geotechnical engineers, but what about the consequences? In light of the above, this research was conducted to identify the mechanisms by which CaLS, a non-traditional waste by-product, stabilized a remoulded expansive soil.

Various analytical techniques were used to achieve this aim. The chemical admixture and the remoulded untreated expansive soil were characterized to establish their reactive products/baseline properties. The physical/chemical properties of the soil following CaLS treatment were then compared with untreated samples to determine whether the admixture prompted any changes. The results of this investigation revealed some important observations regarding the CaLS admixture mechanisms. On addition of CaLS, the organic molecules wedged into the structural sheets of the expansive clay minerals displaced water and caused an initial increase in d-spacing. The intercalated admixture was then adsorption through hydrogen bonding (water bridges), and/or bonded directly with the dehydrated cations. Moreover, this investigation also revealed that the admixture experienced cation exchange between Ca^{2+} in the admixture and soil cations (Na^+, Ti^+, Mg^{2+}) which altered the clay's mineral lattices.

For non-expanding clay minerals, only surface adsorption was observed (XRD). Furthermore, based on XRD data, significant chemical changes in clay mineralogy were not apparent, but changes in the crystalline nature of the adsorbent due to basal and peripheral adsorption of CaLS were observed. The EDS data showed minimal change in the Al:Si ratio, which was expected if the interaction of an admixture and

soil was more by physical rather than chemical means. This was in union with the XRD data. SEM studies visualized the formation of e CaLS films on the soil surface whereas the FTIR studies indicated participation by the surface sites of the sorbent in the adsorption mechanisms. Scholen (1992; 1995) suggested that non-traditional admixtures could stabilize soil by aggregation of soil particles, basal, and peripheral adsorption onto clay lattices to prevent water absorption, or interlayer expansion with subsequent moisture entrapment. In this investigation the stabilizing mechanism was mainly adsorption of the admixture through hydrogen bonding, direct bonding between the CaLS and dehydrated cations in the inner layers, and partial cation exchange mechanisms. These findings were concordant with Scholen's reported mechanisms of non-traditional admixtures.

CHAPTER 6

6 A MATHEMATICAL MODEL FOR THE PREDICTION OF THE SWELLING BEHAVIOUR OF LS TREATED EXPANSIVE SOIL

6.1   INTRODUCTION

Expansive soil formations are characterised by substantial volume increase upon inundation primarily due to the presence of smectite mineral group. This volume change affect structures founded on such soils to damages ranging from minor cracking of pavements and buildings to irreparable displacements of structures. Therefore, it is very important to control their potential to swell in an appropriate, cost-effective and sustainable manner. Traditional chemical admixtures such as lime and cement are often used for stabilizing such soils globally. But despite the global acceptance of this technique, geotechnical engineers in Australia are disinclined in specifying their use because of stringent occupational health and safety concerns. Thus, numerous studies have been carried out to investigate the applicability of non-traditional admixtures in soil stabilization (e.g Mashiri et al. 2013; Indraratna et al. 2008, Sarkar et al. 2000; Vinod et al. 2010; Athukorala et al. 2013; Chen and Indraratna 2015). The traditional additives increase soil and groundwater alkalinity, which often affect flora and fauna, or create corrosion problems in concrete reinforcements and steel frame structures (e.g. Rollings et al. 1999). Moreover, traditionally treated soils often exhibit excessive brittle behaviour that affect the stability of structures (e.g. Sariosseiri and Muhunthan 2009). Most importantly, traditional admixtures perform poorly in reducing the swell potential of sulfate rich expansive soils due to ettringite mineral formation (Harris et al 2006; Pappula et al. 2004). To overcome these problems, a sustainable alternative admixture is imperative.

A lignin-based chemical known as lignosulfonate (LS) with an estimated annual production of over 50 million tons (Gandini and Belgacem, 2008) from the paper

manufacturing industry has demonstrated its potential as an alternative admixture for problematic soils (Tingle et al. 2007; Puppala and Hanchanloet 1999; Chen et al. 2014; Indraratna et al. 2009; Chen and Indraratna 2014). These studies have elaborately dealt with strength and erosion behaviours of LS treated soils. However, currently there is no theoretical swell predictive model for lignosulfonate treated expansive soils. Indraratna et al. (2009) proposed an analytical model to simulate the erosion behaviour of silty sand by capturing its tensile behaviour based on the law of conservation of energy. The model showed that erosion rate of soil could be determined if the tensile force-deformation characteristics, mean particle diameter, dry density, and mean flow velocity were known. It was reported that LS admixtures increased the resistance to erosion. The validation of the theoretical model using the experimental results indicated that the model was capable of capturing the erosion processes accurately for a wide range of hydraulic shear stresses.

Mitchell (1980) developed a theoretical model to simulate soil surface movement in expansive soils. The model was based on the fact that the movement of an expansive soil is a function of the rate of moisture diffusion through the soil and the soil type. The model predicted soil suction profiles with depth and time for natural expansive soils under various initial and boundary conditions. Once the suction state was determined, the seasonal shrinkage or swell was estimated using an equation proposed by Aitchison 1970. In a similar study, Dhowian (1992) developed a soil-suction-potential model based on suction-water-content relationships. In this model, the soil suction was obtained as a function of depth, time and percent swell. The analytical solution was based on a linear swell-suction relationship. The predicted solution values were in close proximity with the laboratory measured values.

Although numerous theoretical models have been developed for LS treated soil (Athukorala 2013; Indraratna et al. 2014; Chen et al. 2014), these studies either modelled the shear strength or erosion behaviour of treated soils. Moreover, theoretical swell models in the literature have been developed for untreated expansive soils, which differ structurally with the LS treated soil (Fig 1), thus these models might not be adopted for LS treated swell behaviour. Within the authors' knowledge, research into this area is understandably limited. Addressed herein is the

effect of LS admixture on the vertical differential movement of soil under certain boundary conditions. The main objective of this paper is to develop an analytical model to capture the percent swell behaviour of LS treated expansive soil by incorporating common geotechnical soil parameters.

In this study, a theoretical approach capable of representing the soil suction potential of CaLS treated expansive soil is presented. The model incorporated the effect of the admixture through a permeability parameter derived from experimental data. This was done to account for changes in the permeability of the soil upon treatment. The procedures (tasks) followed for the development of the suction and hence, swell predictive model is as follows:

- o **Task 1**: Development of a relationship between percent swell and soil suction based on experimental data.

- o **Task 2**: Derivation of unsaturated coefficient of permeability for CaLS treated expansive soil based on experimental data.

- o **Task 3**: Theoretical derivation of moisture diffusion (soil suction) equation for CaLS treated expansive soil.

- o **Task 4**: Solutions to the suction equation at various time frames.

- o **Task 5**: Using the theoretically obtained suction data with the earlier developed swell equation in task 1 as a tool for predicting the swell behaviour of the CaLS treated soil.

6.2 RELATIONSHIP BETWEEN PERCENT SWELL AND SUCTION BASED ON LABORATORY TEST DATA FOR CALS TREATED EXPANSIVE SOIL

In this study, it is proposed that swelling characteristics of CaLS treated expansive soil could be predicted by considering the suction change behaviour of the soil. McDowell, (1956) reported that within typical soil suction range (30-3000kPa), the

soil water characteristic curve could be approximated by a straight line. Evaluated experimental data shows a reasonable evidence of such correlation between soil suction and adsorbed water content (Fig 6.1).

This moisture-suction relation for each soil specimen could be represented mathematically. However, it will be more rationale to represent these relationships by a common model. Therefore, both axes were normalized using maximum values of adsorbed moisture content and suction (Fig 6.2).
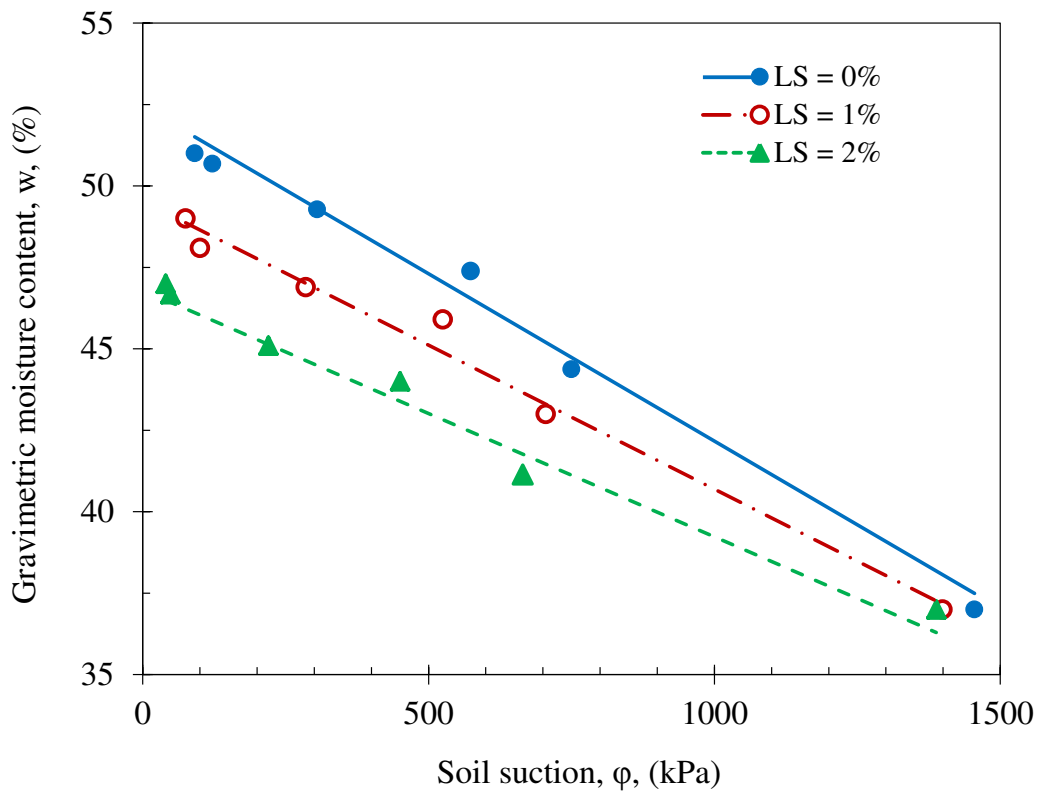
Figure 6.1: Adsorbed moisture and suction relation for a remoulded expansive soil
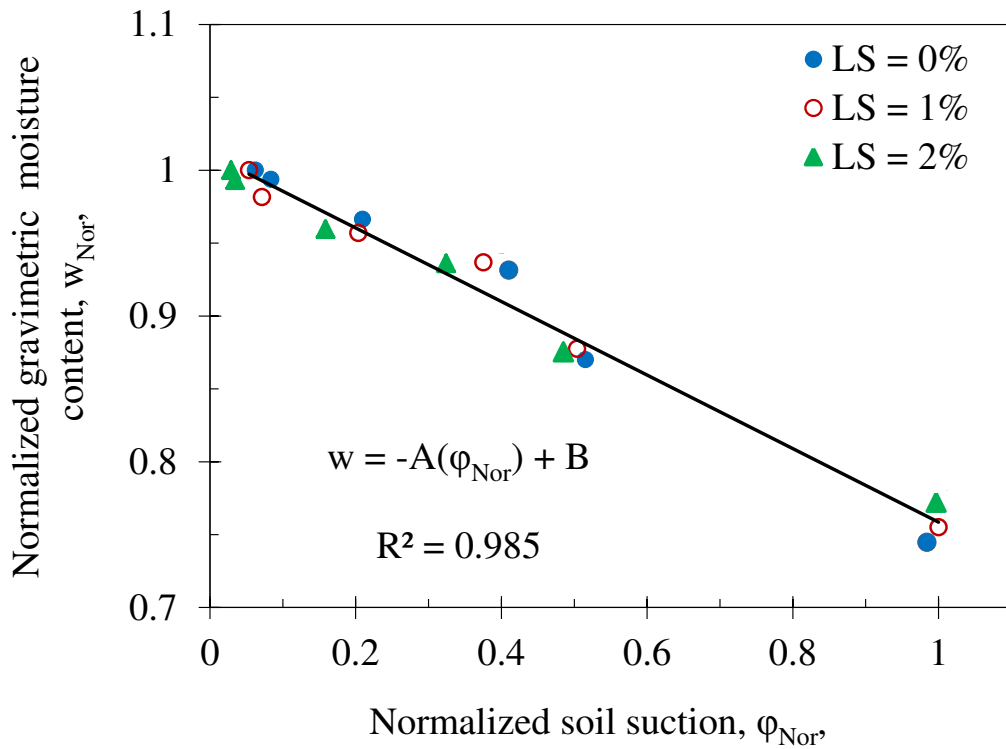
Figure 6.2: Normalized relationship of adsorbed moisture content and suction of soil specimens

According to Seed et al. (1962); Dhowain (1992), the magnitude of percent swell in an expansive soil could be estimated with a simple relation of the form (Equation 6.1):

$$S = C_w W \qquad (6.1)$$

Where, S = percent swell, W = gravimetric moisture content, C_w = coefficient depending on soil type.

Therefore, considering equation (6.1) and Fig (6.2), the percent swell (S) of the untreated and CaLS treated soil specimens could be estimated by a common mathematical relation of the form (equation 6.2).

$$S = C_w\left[-A(\varphi_{Nor}) + B\right] \qquad (6.2)$$

$w_{nor} = w/w_{max}$, and $\varphi_{nor} = \varphi/\varphi_{max}$, A and B are fitting parameters equal to - 1.99 and 0.81, respectively.

Equation (6.2) is the basic swell predictive model for the untreated and CaLS treated expansive soil.

The coefficient (C_w) depends on soil type and it changes with time (i.e. moisture content). The C_w was back calculated from swelling test results at different times and plotted against product of normalized moisture content (w_{nor}) and normalized time (t_{nor}) as shown in Fig 6.3. This relation could be represented mathematically by Equation (6.3) in quadratic form.
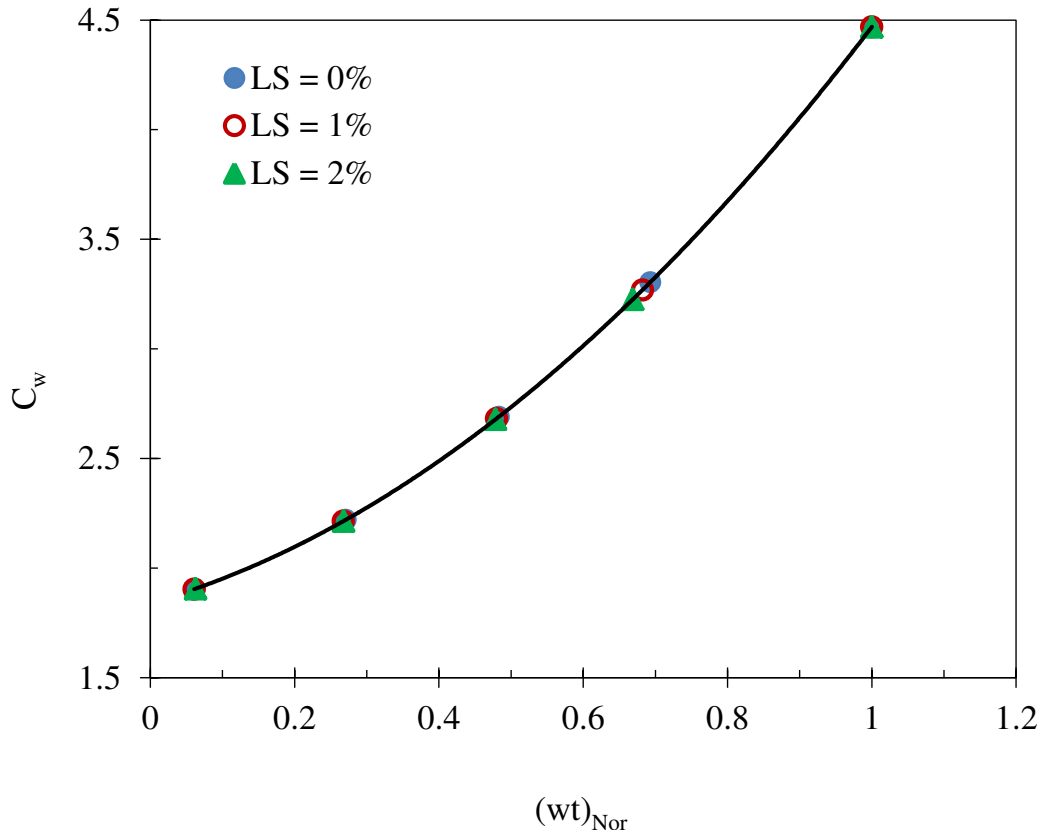
Figure 6.3: Relationship between coefficient C_w and adsorbed moisture and time

$$C_w = a\left(w_{nor} \times t_{nor}\right)^2 + b\left(w_{nor} \times t_{nor}\right) + c \qquad (6.3)$$

200

Where

$$t_{nor} = t/t_{max}$$ (t_{max} is time at which secondary swelling is observed), a, b, and c are fitting parameters, which equals 1.68, 0.95, and 1.84, respectively. In this case, time was normalized by the time at which the secondary swell began, i.e. the value of time corresponding to the horizontal portion of the swell-time plot. The application of equation (3) requires knowledge of suction (β) behaviour of a soil sample. A theoretical approach was developed herein to estimate the changing suction of soil specimens with time under continues wetting condition. But to develop this theoretical suction model, knowledge of the unsaturated permeability of the soil is important hence, a permeability model for the unsaturated LS treated soil is developed as follows:

6.3   DETERMINATION OF THE UNSATURATED PERMEABILITY FOR CALS TREATED EXPANSIVE SOIL

The addition of CaLS admixture changes the fabric of the remoulded soil from discrete soil particles to a more aggregated structure with visible connectors and larger but fewer pores (Fig 6.4a and b). These changes will cause variability in permeability in untreated and treated soil samples.

6.4   DERIVATION OF THE UNSATURATED PERMEABILITY FOR CALCIUM LIGNOSULFONATE TREATED EXPANSIVE SOIL

6.4.1   Soil-water retention curve using the axis-translation apparatus

The soil from the field was oven dried at 105^0C to constant mass, pulverized and sieved through a 1.18mm sieve. A predetermined mass of soil passing the 1.18mm sieve, appropriate water content, and CaLS (2% dry of weight of soil) admixture were collected and mixed thoroughly and allowed to mellow for 24hrs for equilibration in a humidity control room. Then the test specimens were prepared by statically compacting predetermined soil mass into a 50mm diameter x 20mm height

mould at 1mm/min until the desired maximum dry unit weight (MDUW) was reached.
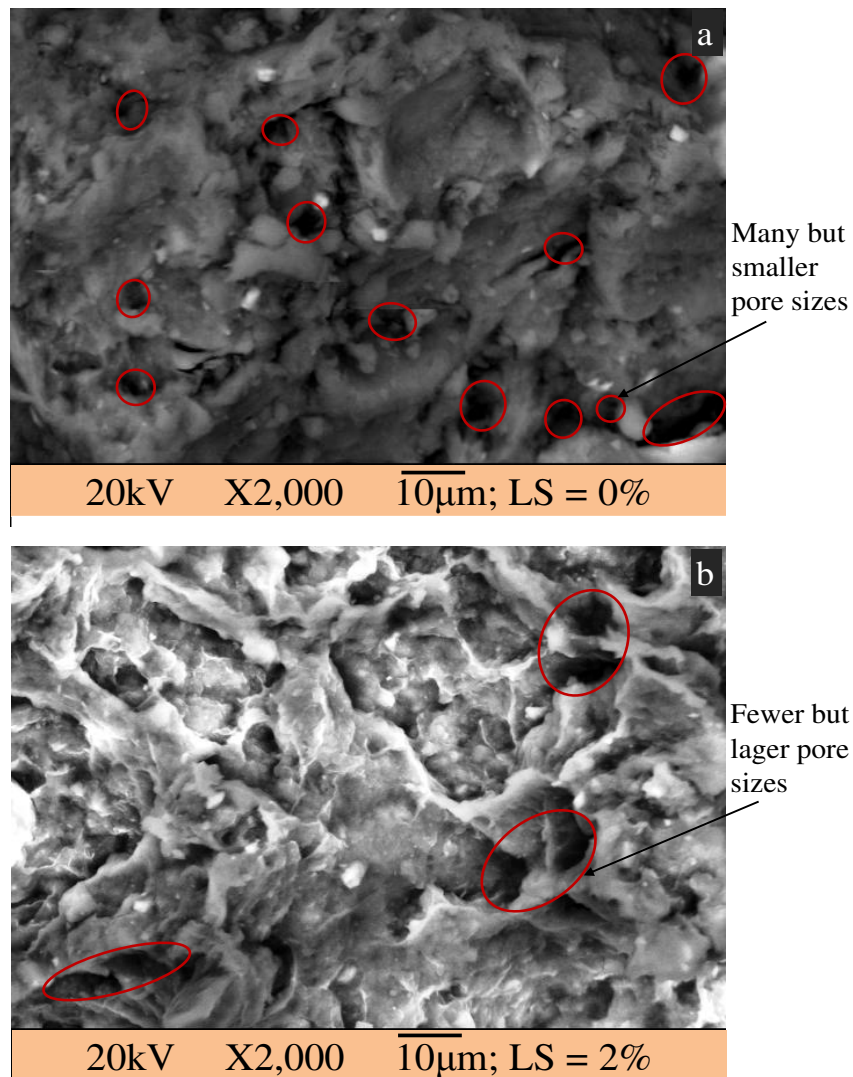
Figure 6.4: a) Microstructure of remoulded expansive soil, b) 2% LS treated expansive soil

All specimens were prepared at MDUW and OMC and compacted in a single layer. Compacted specimens were then cured for 7 days prior to soil-water retention curve test. To saturate soil specimens for this test, specimens were carefully placed into the conventional oedometer equipment with a nominal seating pressure of 7kPa and inundated with distilled water and allowed to saturate for 12 days. The degree of saturation of the specimens was checked with a dummy specimen and was found to

be about 98% degree of saturation. These saturated specimens were used to obtain data for the soil-water retention curve in accordance with ASTM D6836.

Fig 6.5 shows the normalized soil water retention curve for untreated and CaLS treated soil specimens from which the unsaturated soil parameters such as air entry value $(u_a - u_b)_b$, residual degree of saturation (S_r), pore size distribution index (λ), and the effective degree of saturation (S_e) were estimated. These parameters were ultimately used to determine the unsaturated coefficient of permeability of the soil samples.
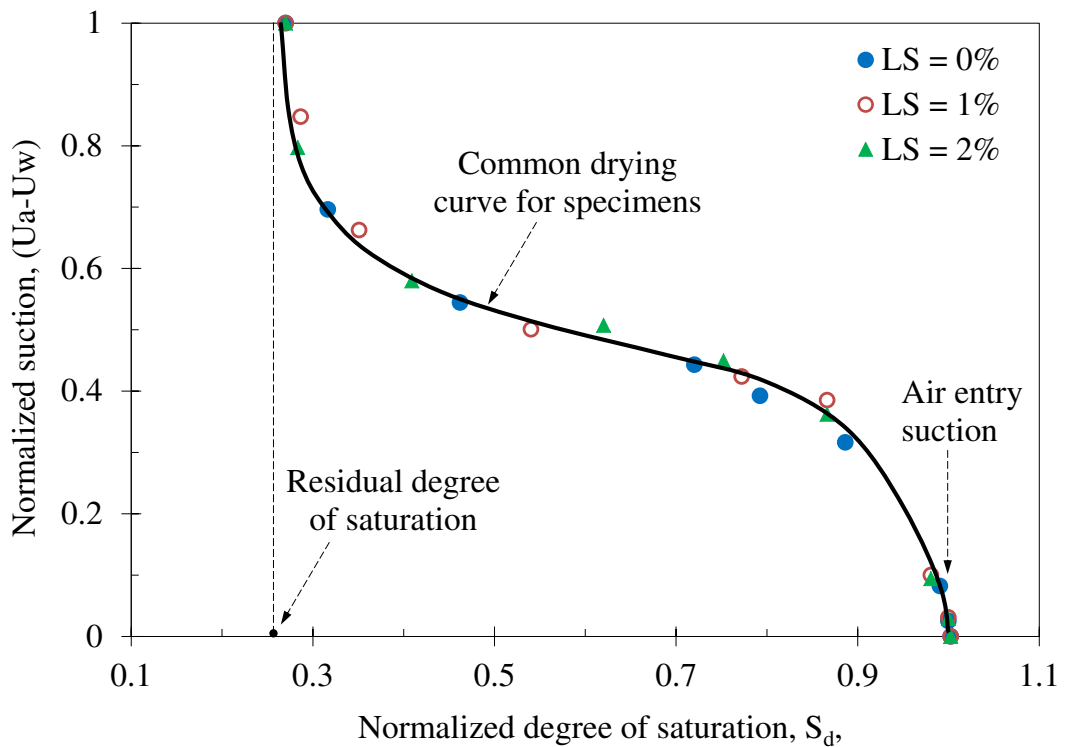
Figure 6.5: Normalized soil-water retention curves for the remoulded expansive soil, obtained via drying process for specimens prepared at OMC and MDUW.

The estimated residual degree of saturation (S_r = 26%) was used in Brooks and Corey (1964) equation (eqn. 6.4) to determine the effective degree of saturation (S_e) as follows.

$$S_e = \frac{S - S_r}{1 - S_r} \qquad (6.4)$$

203

Where, S = degree of saturation.

The calculated values of S_e from equation (6.4) were plotted against soil suction (Fig 6.6). At higher suction values, the relationship attains a common trend. The pore size distribution index (λ) was then estimated as the slope of the straight line portion of the relation (Course Hero, 2011).
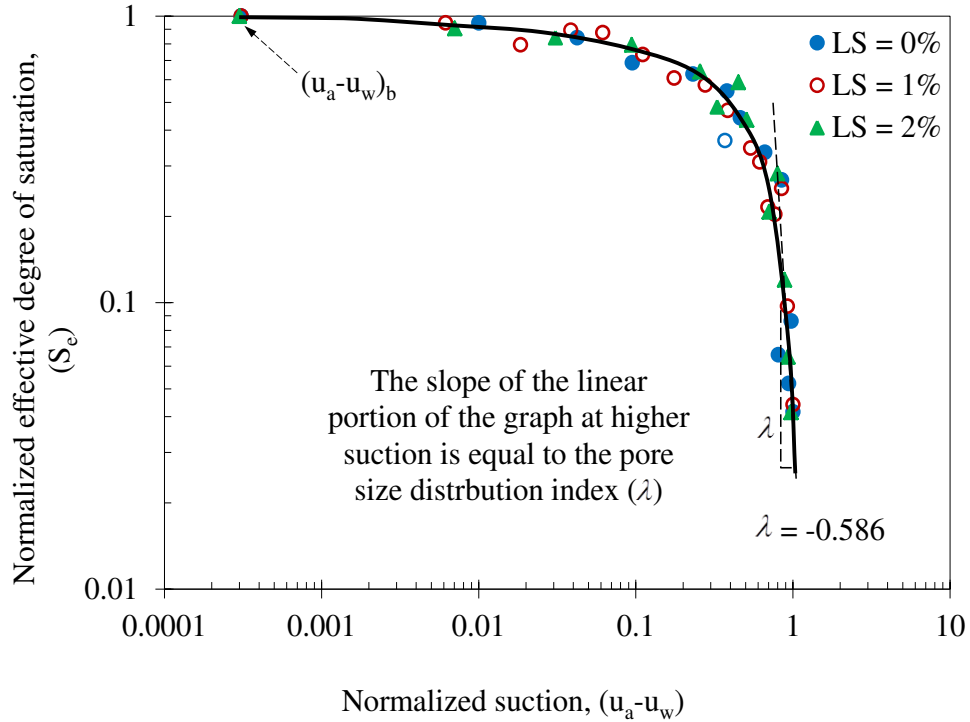
Figure 6.6: Determination of the pore size distribution index (λ) for the soil.

From the above, the effective degree of saturation (S_e) could be correlated with air entry value $(u_a - u_b)_b$, pore size distribution index (λ), and soil suction. According to Course Hero, (2011), this relationship could take the following form:

$$S_e = \left\{ \frac{(u_a - u_w)_b}{u_a - u_w} \right\}^{\lambda} \qquad \text{for } (u_a - u_w) > (u_a - u_w)_b \qquad (6.5)$$

Several relationships have been developed between effective degree of saturation (S_e), coefficient of permeability for saturated soil (k_s) and the coefficient of

permeability for unsaturated soil (k_w). One of such studies was undertaken by Brooks and Corey (1964). They proposed the following relationship:

$$k_w = k_s S_e S_e^\delta \tag{6.6}$$

Where,

$$\delta = \frac{2 + 3\lambda}{\lambda}$$

Thus, k_w values were calculated using equation (6.6), but k_w and k_s could be related to the relative permeability (k_{rw}) of the soil as follows:

$$k_{rw} = \frac{k_w(100)}{k_s} \tag{6.7}$$

The relative permeability (k_{rw}) of the untreated and CaLS treated soil samples were calculated using equation (6.7) and plotted against the degree of saturation (S_d) (Fig 6.7).
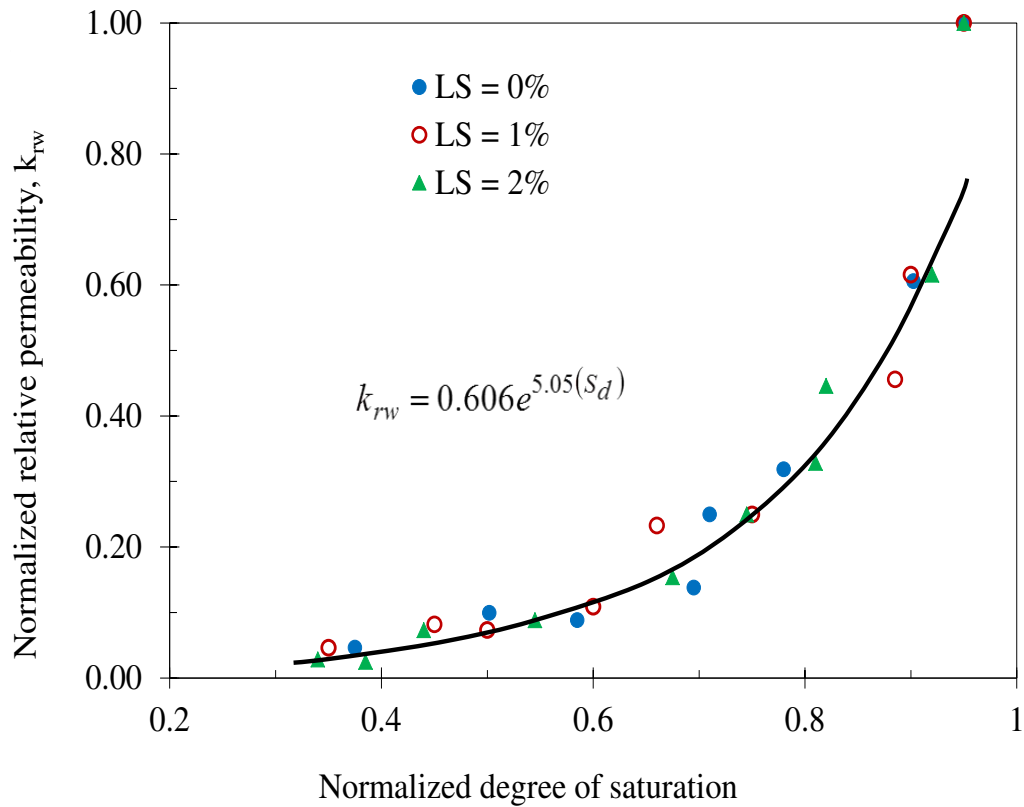
Figure 6.7: Relationship between relative permeability and degree of saturation of the 2% CaLS treated expansive soil

Thus, the unsaturated permeability behaviour of the untreated and CaLS treated expansive soil samples could be represented by:

$$\frac{k_w}{k_s} = 0.06e^{5.05(S_d)}$$

$$k_w = k_s\left[0.06e^{5.05(S_d)}\right] \qquad (6.8)$$

Equation (6.8) is the permeability equation for untreated and CaLS treated expansive soil and it's dependent on the degree of saturation which in turn depends on the suction behaviour of the soil.

6.5   MODEL DEVELOPMENT

The swell characteristics of CaLS treated expansive soil could be predicted using equation (6.2) if suction change within the soil layer is known. The vertical strain of a soil is a function of the rate of moisture diffusion into the interlayers and inter-particle pores of clay minerals. But, this flow of moisture in unsaturated soils depends on suction variation. Thus, to measure soil suction in the soil samples, the rate of moisture diffusion into the soil was theoretically developed. If the moisture flow through a soil body is determined, the suction could be mathematically estimated using modified Darcy's law (Lytton 1977).

6.5.1   Derivation of moisture diffusion equation for soil samples

Consider a soil body subjected to moisture flow as shown in Fig 6.8. The corresponding suction can be determined using Darcy's law.

Equation 6.9 is the famous Darcy's Law.

$$v = K_{sat} \frac{\partial \varphi}{\partial y} \qquad (6.9)$$

But for unsaturated soils, the permeability is not a constant, but depends on the degree of saturation (equation 6.8). Thus, the saturated coefficient of permeability (k_{sat}) in equation (6.9) is replaced by the unsaturated coefficient of permeability (k_w) (equation 6.8) of the CaLS treated expansive soil (Philip 1972). Hence, equation (6.9) becomes

$$v = -K_{sat} \left[0.06 e^{5.05(S_d)} \right] \left(\frac{\partial \varphi}{\partial y} \right)$$
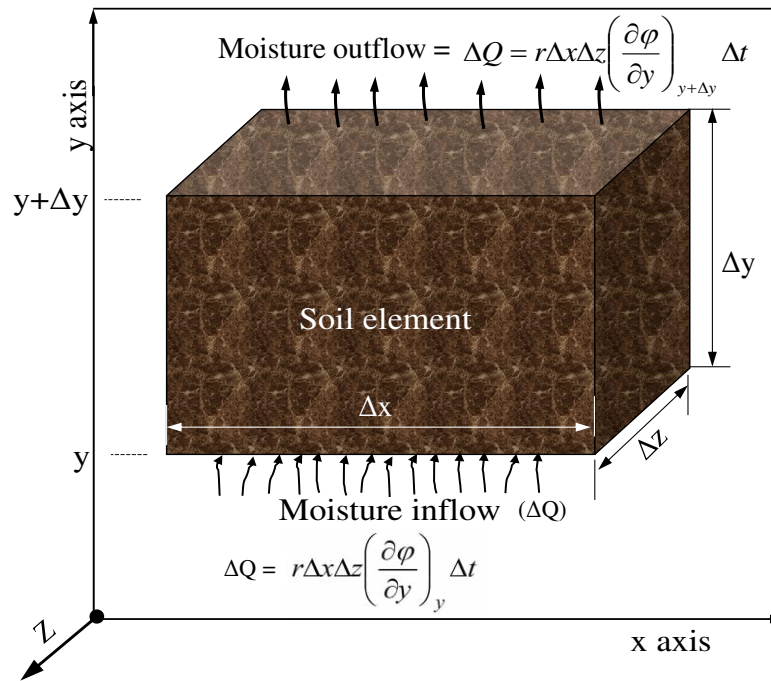
Figure 6.8: Schematic representation of moisture diffusion in unsaturated soil

But let

$$r = -K_{sat} \left[0.06 e^{5.05(S_d)} \right]$$

Thus,

$$v = r \frac{\partial \varphi}{\partial y} \qquad (6.10)$$

Note that the *"r"* in equation (6.10) represents the unsaturated permeability (k_w) of the CaLS treated expansive soil.

From the literature, correlations between adsorbed moisture content in expansive soils and percent swell shows a linear relationship (e.g. Dhowian 1992; Chen 1988; Mitchell 1980). Mitchell (1980) demonstrated that the quantity of moisture flow into an expansive soil equal the quantity stored in the soil (law of conservation of mass). Now considering Fig 6.8 and equation (6.10):

The quantity of moisture flow into the expansive soil body = Quantity of moisture stored in the soil

Therefore,

Moisture inflow:

$$\Delta Q = r\Delta x\Delta z \left(\frac{\partial \varphi}{\partial y}\right)_{y+\Delta y} \Delta t - r\Delta x\Delta z \left(\frac{\partial \varphi}{\partial y}\right)_{y} \Delta t$$

$$\Delta Q = r\Delta x\Delta z\Delta y \frac{\left(\frac{\partial \varphi}{\partial y}\right)_{y+\Delta y} - \left(\frac{\partial \varphi}{\partial y}\right)_{y}}{\Delta y} \Delta t \qquad (6.11)$$

$$\Delta y \to 0 \quad r\Delta x\Delta z\Delta y\Delta t \left(\frac{\partial^2 \varphi}{\partial y^2}\right) \qquad (6.12)$$

Stored moisture:

The stored moisture in soil is dependent on prevailing suction (Morris and Gray 1976). The established relationship between the stored moisture and soil suction is termed moisture characteristics (C). Morris and Gray (1976) defined C, as the amount of moisture (Δmc) a soil gains or losses due to a unit change in soil suction $(\Delta\varphi)$ (equation 6.13) expressed in pF unit.

$$C = \frac{\Delta mc}{\Delta \varphi} \qquad \Delta mc = C\Delta \varphi \qquad\qquad (6.13)$$

But $\Delta mc = \dfrac{w_w}{w_s} = \dfrac{\Delta w_w}{V\gamma_d}$ Thus, $\Delta w_w = \Delta y \Delta x \Delta z \gamma_d C \Delta \varphi$ (6.14)

Where,

w_w = weight of water, w_s = weight of soil solids, γ_d = dry unit weight of soil, V = volume of soil.

Thus, the quantity of soil moisture stored is

$$\Delta Q = \Delta y \Delta x \Delta z \gamma_d C \Delta \varphi \qquad\qquad (6.15)$$

Recall;

Moisture inflow = Moisture stored i.e. equating equations (6.12) and (6.15)

$$r\Delta x \Delta z \Delta y \Delta t \left(\frac{\partial^2 \varphi}{\partial y^2} \right) = \Delta y \Delta x \Delta z \gamma_d C \Delta \varphi$$

As Δy, Δx, Δz, and $\Delta t \to 0$

$$\frac{\partial \varphi}{\partial t} = \beta \frac{\partial^2 \varphi}{\partial y^2} \qquad\qquad (6.16)$$

Mitchell (1980) referred to the term; β, as the diffusion coefficient of soil, whose magnitude defines the rate of moisture diffusion with change in soil suction. β is therefore, equal to;

$$\beta = \frac{K_{sat}\left[0.06e^{5.05(S_d)} \right]}{r_d C} \qquad\qquad (6.17)$$

209

β, account for the effect of CaLS admixture on the diffusion coefficient of the expansive soil. The parameter; β is similar to the famous coefficient of consolidation (c_v) of soil and the magnitude of β defines the rate of diffusion of moisture with changes in soil suction.

Equation (6.16) is the governing moisture diffusion equation for CaLS treated soil. The equation is solved using Laplace Transform as shown below with initial and boundary conditions. The solution of this equation defines the distribution of soil suction within the CaLS treated soil.

Solution of the moisture diffusion equation

In order to solve equation (6.16) analytically, initial and boundary conditions were prescribed as follows. NOTE: The full details of the solution are presented in appendix A.

$$\text{\textit{Initial condition:}} \lim_{t \to 0} \varphi(y,t) = \eta \qquad (6.18a)$$

Where; η is a constant representing the initial soil suction value of CaLS treated soil

Boundary condition: Assuming a constant watering of soil surface without groundwater infiltration into treated soil body, e.g. ponding. The boundary conditions are:

$$\lim_{y \to 0} \varphi(y,t) = \eta \qquad (6.18b)$$

$$\lim_{y \to L} \varphi(y,t) = \rho \qquad (6.18c)$$

Where,

ρ = new suction state in which soil boundary is exposed to liquid of known suction.

Using the Laplace Transform on both sides with time t, the boundary value problem can be solved as follows:

$$F(s) = \ell\{f(t)\} = \int_0^\infty e^{-st} f(t)\, dt \qquad \textit{Fundamental Laplace Transform equation}$$

$$\ell\left\{ \frac{\partial \varphi}{\partial t} - \beta \frac{\partial^2}{\partial y^2} \right\} = \ell\{0\}$$

$$\ell\{f(t)\} = \int_0^\infty \left(\frac{\partial \varphi}{\partial t} - \beta \frac{\partial^2 \varphi}{\partial y^2} \right) e^{-st}\, dt = \underbrace{\int_0^\infty \frac{\partial \varphi}{\partial t} e^{-st}\, dt}_{\text{Part I}} - \underbrace{\int_0^\infty \beta \frac{\partial^2 \varphi}{\partial y^2} e^{-st}\, dt}_{\text{Part II}} \qquad (6.19)$$

Using integration by parts: $\int uv'\, dt = uv - \int vu'\, dt$) for part I and II

$$\int_0^\infty \left(\frac{\partial \varphi}{\partial t} - \beta \frac{\partial^2 \varphi}{\partial y^2} \right) e^{-st}\, dt = \left[\varphi e^{-st} \right]_{=0}^{t=\infty} + s\,\overline{\varphi}(y,s) - \beta \frac{\partial^2 \,\overline{\varphi}(y,s)}{\partial y^2} = 0$$

$$\left[\varphi(y,t) e^{-st} \right]_{=0}^{t=\infty} + s\,\overline{\varphi}(y,s) - \beta \frac{\partial^2 \,\overline{\varphi}(y,s)}{\partial y^2} = 0 \qquad (6.20)$$

$$s\,\overline{\varphi}(y,s) - \eta = \beta \frac{\partial^2 \overline{\varphi}(y,s)}{\partial y^2} \qquad (6.21)$$

In order to solve equation (6.21), the boundary conditions for φ must undergo Laplace Transform (equations 16b and c) i.e. $\overline{\varphi} = \ell(\varphi)$.

$$\lim_{y \to 0} \overline{\varphi}(s, y) = unknown \qquad\qquad \lim_{y \to L} \overline{\varphi}(s, y) = unknown$$

$$\lim_{y \to 0} \overline{\varphi}(s, y) = \lim_{y \to 0} \int_{t=o}^{t=\infty} \varphi(y,t) e^{-st}\, dt = \int_{t=0}^{t=\infty} \lim_{y \to 0} \varphi(y,t) e^{-st}\, dt = \int_{t=0}^{t=\infty} \eta e^{-st}\, dt = \left[\eta \frac{1}{s} e^{-st} \right]_{t=0}^{t=\infty} = \frac{\eta}{s}(1-0) = \frac{\eta}{s}$$
(6.22)

$$\lim_{y \to L} \overline{\varphi}(s, y) = \lim_{y \to L} \int_{t=o}^{t=\infty} \varphi(y,t) e^{-st}\, dt = \int_{t=0}^{t=\infty} \lim_{y \to 0} \varphi(y,t) e^{-st}\, dt = \int_{t=0}^{t=\infty} \rho e^{-st}\, dt = \left[\rho \frac{1}{s} e^{-st} \right]_{t=0}^{t=\infty} = \frac{\rho}{s}(1-0) = \frac{\rho}{s}$$
(6.23)

Substituting equation (21) into the general solution equation for "real different roots" for homogeneous equation and solving simultaneously gives

$$\bar{\varphi}(s, y) = \frac{\rho - \eta}{s} \frac{1}{\sinh\left(\sqrt{\frac{s}{\beta}}L\right)} \left(\sinh\left(\sqrt{\frac{s}{\beta}}y\right)\right) + \frac{\eta}{s} \quad \text{But}$$

$$\csc hx = (\sinh x)^{-1}$$

$$\bar{\varphi}(s, y) = \frac{\rho - \eta}{s} \csc h\left(\sqrt{\frac{s}{\beta}}L\right)\left(\sinh\left(\sqrt{\frac{s}{\beta}}y\right)\right) + \frac{\eta}{s} \quad (6.24)$$

The aim is to determine $\varphi(y,t)$, and not $\bar{\varphi}(s, y)$ therefore, we have to find the inverse Laplace Transform of equation (6.24). Using Oberhettinger and Badii (1973) tables of Laplace Transform (attached).

From equation (6.24), let;

$$a = \frac{L}{\sqrt{\beta}} \qquad\qquad b = \frac{y}{\sqrt{\beta}}$$

$$0 \le y \le L$$

$$\bar{\varphi}(s, y) = \frac{\rho - \eta}{s} \sinh\left(\sqrt{s}b\right)\csc h\left(\sqrt{s}a\right) + \frac{\eta}{s} \text{, this conforms to Oberhettinger and}$$

Badii's Laplace (1973) Inverse Transform equation in page 296, equation 8.62. Thus, the Inverse Laplace Transform of equation (6.24) and further manipulation (page 422 of Oberhettinger and Badii (1973) tables of Laplace Transforms, see Q_3) of the equation yields

$$\varphi(y|t) = \frac{\rho - \eta}{a} \int_a^{a+b} Q_3\left(\frac{1}{2a}u \left| \frac{t}{a^2}\right.\right) du \quad (6.25)$$

$$= 1 + 2\sum_{n=1}^{\infty} e^{\left(\frac{-\pi^2 n^2 t}{a^2}\right)} \cos\left(\frac{\pi n}{a}u\right)$$

212

$$= (\rho - \eta)\left(\frac{b}{a}\right) + 2(\rho - \lambda)\left(\frac{1}{a}\right)\sum_{n=1}^{\infty} e^{\left(-\frac{\pi^2 n^2 t}{a^2}\right)}\left[\frac{\sin\left(\frac{\pi n}{a}u\right)}{\frac{n\pi}{a}}\right]_a^{a+b}$$

$$\varphi(t, y) = (\rho - \eta)\left(\frac{b}{a}\right) + 2(\rho - \eta)\left(\frac{1}{a}\right)\sum_{n=1}^{\infty}(-1)^n e^{\left(-\frac{\pi^2 n^2 t}{a^2}\right)}\frac{a}{\pi n}\sin\left(\frac{b}{a}\pi n\right) \quad (6.26)$$

But,

$$\sin\left(\frac{b}{a}\pi n + \pi n\right) = (-1)^n \sin\left(\frac{b}{a}\pi n\right) \text{ and } a = \frac{L}{\sqrt{\beta}}, \ b = \frac{y}{\sqrt{\beta}}$$

Hence,

$$\boxed{\varphi(t, y) = (\rho - \eta)\left(\frac{y}{L}\right) + \left(\frac{2(\rho - \eta)}{\pi}\right)\sum_{n=1}^{\infty}\frac{(-1)^n}{n}e^{\left(-\frac{\pi^2 n^2 \beta}{L^2}t\right)}\sin\left(\frac{y}{L}\pi n\right)} \quad (6.27)$$

Equation (6.27) is a simple suction behaviour model of CaLS treated expansive soil and it is governed by a single constant β. With knowledge of β and with known initial values of η and ρ the suction behaviour of a laboratory soil specimen could be estimated at any times.

6.5.2 *Theoretical soil suction*

If the degree of saturation at a particular time is known, then equation (6.27) could be used to estimate the soil suction at any time using appropriate boundary conditions. With assumed initial boundary, boundary conditions, and varying values of β depending on the degree of saturation (S_d) the suction behaviour with time was calculated for the soil samples. For instance, at 42, 70, 95, 97, and 100% degrees of soil saturation with corresponding times (0, 1000, 7000, 12800, and 14000mins) the normalized suction of the soil sample was theoretically computed using equation (6.27) and presented in Table 6.1.

Table 6:1: Measured and calculated suction values

Time (min)	Measured suction, φ, (kPa): (Fig 6.9); normalized			Calculated Suction, φ, (kPa): Using equation (6.27); normalized		
	Surcharge pressure = 7kPa			Surcharge pressure = 7kPa		
	LS = 0%	LS = 1%	LS = 2%	LS = 0%	LS = 1%	LS = 2%
0	1	1	1	1	1	1
1000	0.500	0.540	0.529	0.498	0.514	0.540
7000	0.309	0.226	0.261	0.267	0.273	0.226
12740	0.034	0.081	0.080	0.102	0.071	0.081
14000	0.150	0.070	0.033	0.041	0.054	0.070

The degree of accuracy was tested by plotting the experimentally determined suction values with the calculated values (Fig 6.10). A good correlation is observed especially with the optimally (2% by dry weight of soil) treated soil specimen. The correlation decreases with decreasing amount of CaLS thus, predicted and measured suction values varied maximally in untreated soil specimens.
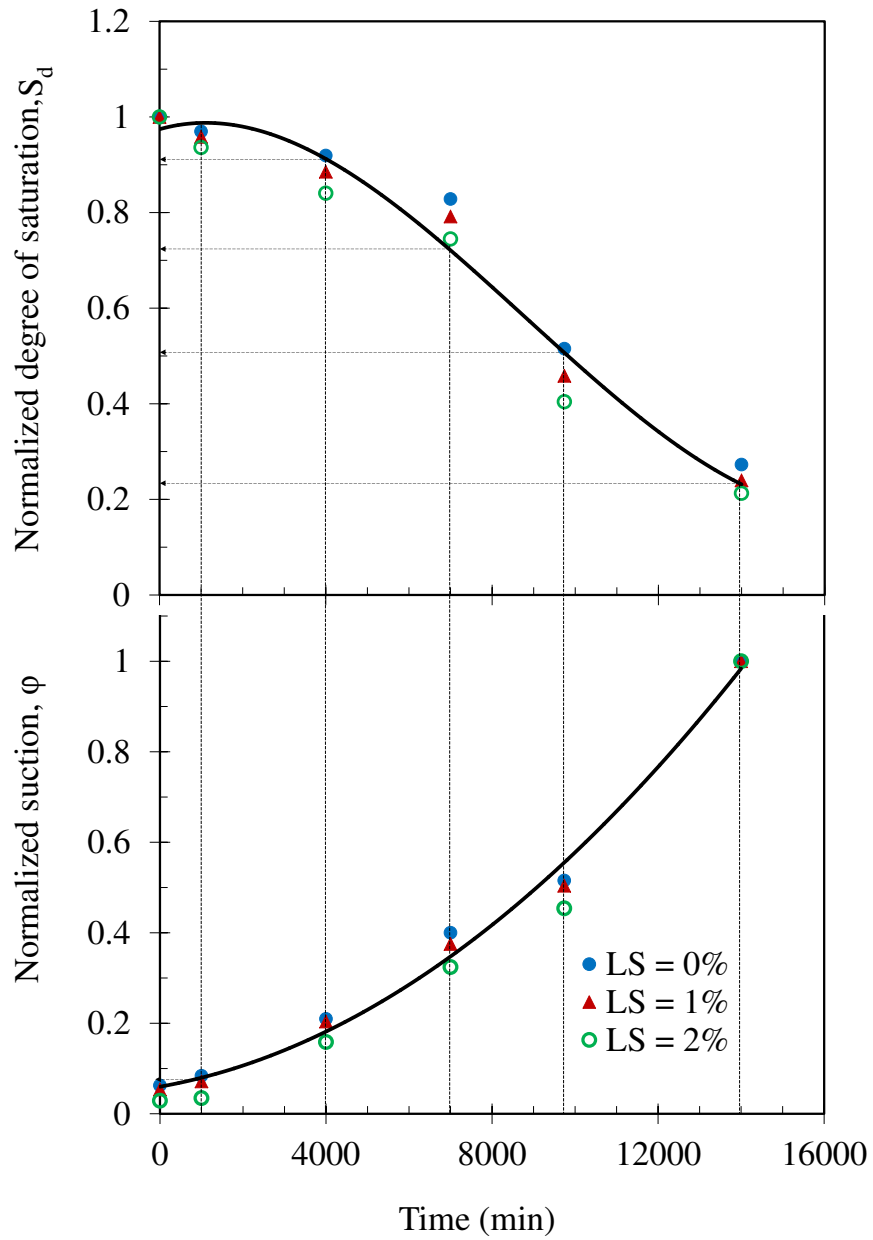
Figure 6.9: Experimentally determined suction data and degree of saturation with time for CaLS treated expansive soil
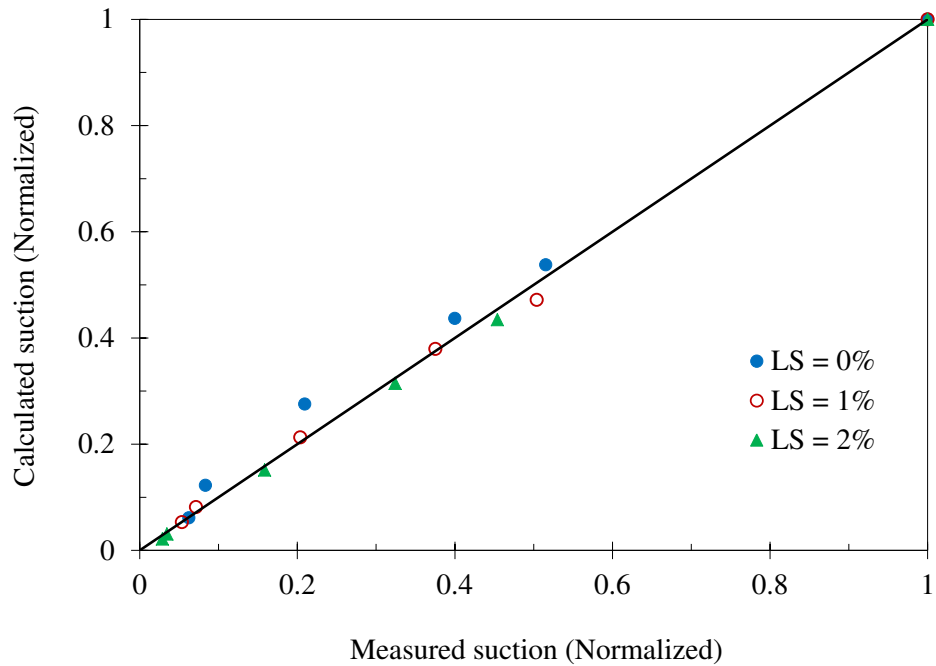
Figure 6.10: Correlation of measured and calculated soil suction values

The implication of Fig 6.10 is that the percent swell of the untreated and CaLS treated soil could be estimated using equations (6.2 and 6.27). Table 6.2 shows such data with calculated and measured swell behaviour of the remoulded expansive soil, which is graphically represented in Fig 11.

Reasonable correlation exists between predicted and measured swell values of both untreated and CaLS treated expansive soil. However, the calculated percent swell values are slightly higher than the corresponding measured values. In addition, at the secondary swelling regime, the percent swell of the soil specimens are underestimated. A more efficient prediction was observed towards the midpoint of the swell-time relation. It is also observed that the accuracy of the predicted swell values decreased with decreasing CaLS content thus, the values for the untreated soil is least accurate while the predicted percent swell of the 2% CaLS treated soil specimens tends to mimic the measured values closely.

216

Time (min)	Measured suction, φ, (kPa)							Calculated Suction, φ, (kPa): Using equation (19)					
	LS = 0%	LS = 0%, Nr	LS = 1%	LS = 1%, Nr	LS = 2%	LS = 2%, Nr		LS = 0%	LS = 0%, Nr	LS = 1%	LS = 1%, Nr	LS = 2%	LS = 2%, Nr
0	91	0.0625	75	0.0536	40	0.0288		98	0.0612	63	0.0532	30	0.0214
1000	122	0.0835	100	0.07148	48	0.0346		182	0.1223	115	0.0816	43	0.0307
4000	305	0.2096	285	0.2037	220	0.1585		410	0.2755	300	0.2128	212	0.1512
7000	582	0.4000	525	0.3753	450	0.3242		650	0.4368	535	0.3794	441	0.3146
9740	750	0.5155	705	0.5039	630	0.4539		800	0.5376	665	0.4716	469	0.3345
14000	1455	1	1399	1	1388	1		1488	1	1410	1	1402	1

NOTE: Swell (%) = $S = C_w\left[-0.86(\varphi_{Nor}) + 0.93\right]$, where, $C_w = a(wt)_{Nor}^2 + b(wt)_{Nor} + c$, a, b, and c = fitting parameters, w =

adsorbed moisture content, and w is the corresponding time.
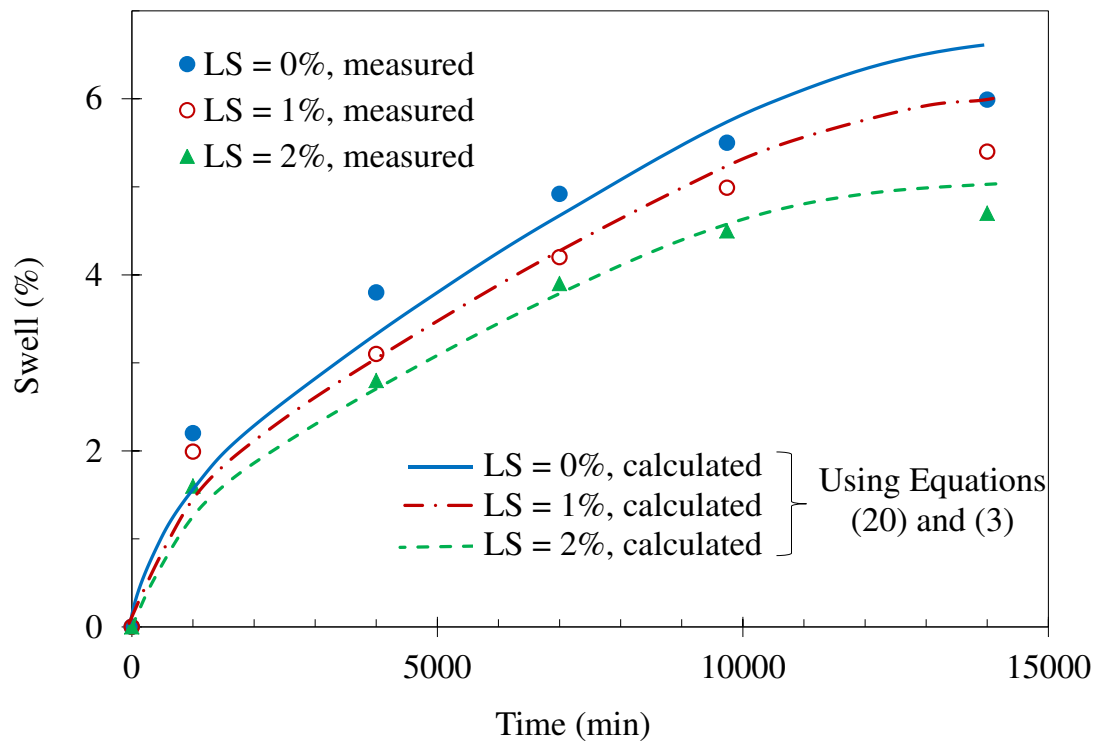
Figure 6.11: Measured and predicted swell behaviour of 2% CaLS treated expansive soil.

6.6   SUMMARY

This chapter presented the development of a theoretical model for predicting suction behaviour and ultimately the swell characteristics of LS treated expansive soil. The model estimated the suction behaviour with time and it is governed mainly by a single parameter; β, which depends on the permeability of the treated unsaturated soil that is controlled by the degree of saturation. Thus, if the degree of saturation for a LS treated soil is known with time, β could be estimated and hence, the suction behaviour could be modelled with time and used in estimating the swell behaviour (equation 2) of LS treated expansive soil. In unsaturated soil, the permeability is not a constant but depends on the changing suction. For this reason, an empirical permeability model based on experimental data was developed for the treated soil. This expression was then used in the model to predict the suction behaviour of the soil.

In validating the suction and swell models, the suction behaviour of soil with and without LS admixture was experimental determined using the axis translation technique in the laboratory. In addition, the same soil samples were measured for swell behaviour using the conventional one-dimensional swell test. The experimental data obtained from these tests were correlated with theoretically determined values. It was found that the proposed suction model could closely represent the soil suction behaviour of the expansive soil treated with LS hence, a good correlation existed between measured and calculated percent swell of the soil specimens.

This proposed suction/swell predictive models can be used by practicing engineers to assess heave-related problems. At times structures are inevitably built on expansive soil deposits, and therefore, the solution is to adopt effective and sustainable techniques in reducing soil heaving. In this context, LS has proven to be an effective chemical treatment method. The proposed equations (2 and 27) could be used to obtain a swell-time relation thus, helping practicing engineers to forecast the likely swell magnitude a structure may undergo at any given time in LS treated soil. Such information could assist engineers during the design phase and throughout the life span of a structure founded on such soil.

CHAPTER 7

7 CONCLUSIONS AND RECOMMENDATIONS

7.1 INTRODUCTION

In this research the potential use of LS admixture in controlling the swell behaviour of a remoulded expansive soil was studied in detail. In addition, the efficacy of the admixture in altering other engineering properties (e.g. Atterberg limit, free/thaw and wet dry durability, strength behaviour, compaction characteristics, consolidation parameters, permeability and soil pH) of the remoulded soil were investigated and reported. Furthermore, the stabilizing mechanisms of the admixture were investigated and identified using analytical techniques (e.g. XRD, FTIR, SEM/EDS). The theoretical aspect of this investigation involved developing a mathematical model capable of predicting the suction behaviour of the LS treated expansive soil and hence, predict the percent swell behaviour of the treated soil. The measured and calculated values were in very good accord.

7.2 CONCLUSION

A large number of laboratory geotechnical experiments were conducted with and without LS treatment. The results of these investigations indicated that LS solution could be a resourceful admixture in controlling the swell potential and other engineering properties of an expansive soil. Based on the data collected from laboratory tests, the major contributions of this study are as follows:

➢ The ligand (coordinating cation) within a LS structure plays a vital role in controlling the swell behaviour of an expansive soil. For instance, with calcium as a coordinating cation, the effect is more significant than monovalent cations such as sodium or potassium forming a LS-ligand. This is because the valency of exchangeable cations controls the thickness of the

DDL of soils. The higher the valency of the cation the thinner the DDL of the expansive soil minerals, which reduces the tendency to swelling.

➢ The amount of CaLS required to effectively reduce the swell potential of the remoulded expansive soil is about 2% by dry weight of soil, a value that seems to be related to the stabilising mechanisms of the LS admixture. The percent swell decreased from $\approx$ 6.0% to 4.7%, which accounted for a 22% reduction over the untreated soil sample after 7 days of curing. The LS admixture decreased the swell pressure at an average of 20% over the untreated soil, i.e. from 105kPa to 84kPa, while the volumetric shrinkage decreased from -19.0% to -16.8% and with an increase in the shrinkage limit from 9% to 11%.

➢ The rate of percent swell for 2% LS treated soil decreased with increasing curing time under laboratory conditions, implying that the stabilizing mechanisms of the admixture continued beyond 7 days, and thus could have long term benefits.

➢ A microstructural analysis showed that variations in the moisture content of reconstituted soil after treatment were primarily accompanied by changes in the volume of inter-aggregate and intra-aggregate pores. Flocculation of the soil material occurs upon treatment thus, the reduced swell-shrink potential of the soil as water infiltration was restricted.

On the basis of the effect of LS admixture on other engineering properties of the remoulded expansive soil, the main conclusions based on standard laboratory tests results are as follows:

➢ The soil pH did not change with the addition of LS (7.43 to 7.17) which was in direct contrast to the cement admixture which increased the pH of the treated soil from 7.43 to 9.65 at 2% dosage. Such a pH value could lead to serious corrosion problems on founded steel infrastructure.

➢ With 2% addition of LS it was noted that the LL decreased from 91% to 76%, with a corresponding decrease in the plasticity index (PI) from 51% to 32%.

221

As PI is a good indicator of the swelling behaviour of soils, the reduced PI helped to decrease the swell potential of treated soil. Similar trends occurred in the sample treated with 2% cement where the LL decreased from 91% to 70% with a corresponding reduction in PI from 52% to 24%

➤ The sample stabilised with LS exhibited a significant improvement in terms of percentage weight loss under freezing and thawing durability compared to the sample treated with 2% cement. In fact soil stabilised with cement disintegrated up to 17.8% of its original mass after just 6 cycles of freezing and thawing, while the sample treated with LS only lost 3.4% of its original mass after 12 cycles, as opposed to 7.0% for the untreated sample. This implies that expansive soil treated with LS under the same freeze-thaw conditions could be regarded as a reasonable soil admixture. However, the samples treated with 2% cement were more durable under wetting and drying conditions because they only disintegrated during the wetting phase of the 4th cycle, whereas the specimen treated with 2% LS disintegrated completely during the 3rd wetting phase. With the untreated sample, during the 2nd wetting stage, about 71% of its mass was lost and collapsed completely during the 2nd drying phase.

➤ The particle size distribution curve for LS treated soil shifted slightly towards the coarse side compared to the untreated soil. This shift in direction showed a decrease in the percentage of soil passing sieve apertures, which substantiated the effect that the admixture had on increasing the particle size due to flocculation aggregation. Treated (2% LS) soil sample became more ductile at failure than the sample treated with 2% cement. This result implied there was no loss of cohesion in the soil with the addition of LS, whereas cohesion was lost in samples treated with cement, hence they were brittle at failure.

➤ The addition of LS admixture did not result in appreciable improvement on soil density nor on the compaction moisture content. However, there was a marginal decrease in the MDD (13.1 to 12.9kN/m^3) and OMC (37 to 36%) in

the treated sample implying that less quantity of water/energy is needed to attain optimum compaction conditions.

➢ The coefficient of permeability for the sample treated with LS remained practically unchanged. This implies that problems with internal erosion in treated soils will be less significant than the sample treated with cement which experienced a significant increase in permeability. The c_v behaviour of the remoulded expansive soil after the addition of LS deviated from the typical characteristics of clay soils. The sample experienced a fairly rapid initial settlement due to the rapid dissipation of pore water pressure, followed by a reasonably stable rate of settlement. This type of consolidation by the treated soil sample was not typical of clayey soils, which implied that the chemical admixtures altered the structure of the soil such that its consolidation seemed to be more-or-less like silty material. This behaviour occurred because the admixture suppressed the diffuse double layer of clay minerals. The m_v for untreated and chemically treated samples decreased with increasing consolidation pressure, and this decrease is more evident for untreated, 2% LS, and 2% cement treated specimens, respectively. The implication here is that the soil treated with LS will offer greater resistance to compression than untreated soil under similar conditions. This difference in behaviour between the untreated and chemically stabilised samples was ascribed to the stabilising effects of the chemical admixtures.

In spite of the potential advantages offered by LS admixtures this technique is yet to gain world attention, due in part to the lack of documented research on its stabilising mechanisms. On the basis of the mineralogical and microstructural analyses with XRD, SEM/EDS, FTIR, NMR, CT scan, SSA, and CEC for untreated and 2% LS treated samples, this study successfully described the mechanisms by which an LS admixture altered the remoulded expansive soil. The following conclusions could be drawn.

➢ The micro-characterization study suggest that LS modified the soil through adsorption mechanisms [i.e. basal, and/or peripheral adsorptions via hydrogen

bonding (water bridging), directly bonding with dehydrated cations] and cation exchange mechanism with subsequent smearing, and agglomeration of soil particles. These mechanisms reduced the specific surface area of the treated soil and prevented the adsorption of water. These adsorption mechanisms also exposed the hydrophobic structure of the admixture, and thus the waterproofing effect on soil particles which ultimately reduced the swell potential of the soil.

➤ The supporting evidence for these proposed mechanisms is revealed in the XRD diffractograms where upon treatment, the smectite peaks either shifted towards a lesser $2\theta^0$ or in some cases disappeared completely as a result of admixture adsorption into the inner and outer layers of soil minerals and subsequent smearing of the mineral lattices. There was no peak shift for the non-swelling minerals, which suggested that the admixture did not intercalate the inner layers of these minerals probably because of the tightly held lattices in these minerals compared to the relatively large molecular size of the admixture. Moreover, the absence of new peaks (minerals) in the XRD diffractogram of the treated soil coupled with the negligible change in the mineral ratios (e.g. Al:Si) as obtained from EDS analysis of the samples before and after treatment, suggested mainly inter-molecular interactions between the minerals and the LS admixture as opposed to major chemical reactions.

➤ Further analysis of the XRD patterns showed that the treated diffractogram mimicked that of the untreated, implying that no significant chemical reaction occurred in the treated soil. The XRD diffractograms of treated samples showed a convincing change in d-spacing for smectite minerals after treatment that could be related to the intercalation of the admixture into the inner layers of the smectite minerals, leading to an initial expansion of the clay layer and subsequent moisture entrapment. This intercalation of the admixture into the inner layers of smectite minerals readily displaced water molecules in the inner spheres of such minerals and thus, water molecules in

the dehydrated inner layers formed hydrogen bonds of "water bridge" with oxygen of the organic molecules present.

➤ The FTIR patterns supported the LS adsorption theory with an increase in peak intensity at 1116cm^{-1} and the presence of a new peak at 470cm^{-1} which was related to Si-O stretching vibrations for amorphous silica. This suggested that the amorphous LS attacked silica minerals and deposited its footprint of amorphocity. The FTIR band of adsorbed H-O-H and structural -OH before and after the addition of LS differed significantly, which supports one of the proposed mechanisms of hydrogen bonding through "water bridging".

➤ The CEC data also postulated the possibility that the cationic end of LS would replace the negative surface of the charged clay particles to prompt particle flocculation and reduce the soil's affinity for water. Moreover, the thin coating of soil particles by the organic cationic compound (LS) exposed its hydrophobic end, so the particles were essentially waterproofed and led to a reduction in the percentage of swell in an otherwise expansive soil.

➤ In summary, the stabilization mechanisms consisted of an exchange of interlayer cations (albeit not significant due to the "cover-up-effect"), basal, and peripheral adsorption on mineral surfaces through hydrogen bonding (water bridging), water entrapment, and direct bonding to the adsorbed dehydrated cations with a subsequent formation of flocculation-aggregates that changed the crystallographic characteristics of the soil. This reduced the shrink-swell behaviour of the remoulded expansive soil.

The development of a robust mathematical model capable of predicting the suction behaviour and hence, the percent swell of expansive soil treated with LS was justified after reviewing the existing literature. Accordingly, this research formulated a simplified mathematical model based on laboratory test data.

➤ Mathematical relationships were proposed to estimate the suction behaviour of soil treated with LS based on laboratory test data that was obtained experimentally. Suction behaviour was governed by a single constant β which

depends on a variable; degree of saturation. The accuracy of the predicted suction behaviour depends largely on how accurately the above input parameter was determined. The suction obtained theoretically at varying time intervals were used in the percent swell equation to predict the swell behaviour of the laboratory soil specimen. A reasonable correlation was found between the experimentally determined percent swell and the predicted values.

7.3 RECOMMENDATIONS

Below are some recommendations for the beneficial use of this novel stabilization technique, including the additional tests required for the effective use of the LS admixture.

Analysis of laboratory data revealed that LS could be a resourceful alternative in controlling the swell behaviour of expansive soil because it can reduce the affinity soil minerals have for water. However, for this technique to gain worldwide attention, the following should be considered:

➤ Construction industries interested in using this waste by-product should collaborate with LS manufacturers to ensure that at least a poly-valent coordinating cation such as Ca^{2+}, Mg^{2+}, Fe^{3+} or Cr^{3+} is used as a ligand rather than monovalent cations such as Na^+, K^+ or Li^+.

➤ As noted in chapter 3, the actual structure of LS is unknown because pure lignin cannot be extracted from wood; the source of the lignin is complex (i.e. tree type), and due to the manufacturing method. Consequently, the chemical compositions of similar LS's such as calcium lignosulfonate from different manufacturers might contain varying functional groups, so it is recommended that standard laboratory tests be conducted prior to field applications, to prove how affective the treatment would be on a particular type of soil.

➤ This research project was only accomplished in the laboratory. The use of LS as a non-traditional stabilization product for expansive soil treatment seems to

be a viable solution in terms of waste management and green construction,, but the significant reduction in swell behaviour achieved in the laboratory may not be achieved in field applications where conditions are much more complex. Therefore, field testing and monitoring will be needed to build confidence in this novel treatment technique.

➢ In order to simulate field conditions where soil behaviour is highly controlled by confining pressure and moisture content, the shear strength of expansive soils treated with LS should be studied using triaxial testing apparatus. Moreover, considering the relevance of the resilient modulus in pavement design and other design tools, the resilient modulus should be tested on expansive clays stabilised with LS.

7.4 RECOMMENDATIONS FOR FUTURE RESEARCH

For a non-traditional soil additive such as LS to achieve global recognition, further research on this admixture is inevitable. Based on the reviewed literature and findings from this investigation, it is recommended that the following areas of the waste by-product be investigated:

➢ A comparison of cost implications between traditional admixtures (e.g. lime or cement) and the LS admixture on specific projects such as field trial sections of unpaved low volume roads.

➢ Laboratory and field measurements should be conducted on the leaching characteristics of the LS admixture and its potential environmental impact on groundwater. Trials should be carried out on the possibility of administering LS through a non-destructive means such as injection. If a positive outcome is achieved through a non-destructive application, this could be an additional bonus for the LS option of stabilization.

➢ One of the major concerns for using traditional admixtures in soil stabilization is the quantity required and the associated cost of transporting large quantities of admixture to site. It is therefore recommended that a study

of soil stabilization using a combination of LS with lime or cement be conducted. This study should develop protocols on how best to formulate a binary admixture of LS and traditional admixtures for various types of soil. This study should also bear in mind the disadvantages of using traditional additives when formulating a binary admixture but at the same time preserve the benefits of traditional admixtures.

➢ The LS admixture significantly improved the properties of soil, so a study should be carried out to assess the longevity of this improvement. Because the lifespan of a road is long and general approval for new and non-traditional stabilization agents would require that well-documented, long term field trials be conducted and reported, these independent reports will build confidence in this novel stabilization technique and increase our knowledge of the limitations and benefits of the LS admixture.

➢ LS for instance, have revealed water proofing characteristics on treated soil in the course of this investigation. In a research project by Santoni et al. (2002), the optimum amount of 5% LS proved to give good water protection properties in silty sand. Additional research work could be performed on the use of this additive to minimise the ingress of water into fractured rock joints, which is a major concern in the mining and construction industries. However, in order that it might be used for this purpose, additional admixtures such as lime or cement might be added which would hasten dehydration without adding greatly to the cost.

Clearly, a non-traditional admixture such as LS has the potential to become technically and economically competitive alternatives in the stabilization of expansive soil. However, quite a lot more research is needed to gain world attention. The end-results of these future research projects will serve as a knowledge bank to better understand the cost benefits, environmental sustainability, and long-term effectiveness in treating expansive soil deposits.

The sustainable use of LS as a resourceful soil admixture could be an alternative solution to the cost of its disposal, and with over 50 million tons of annual

production, the successful use of LS admixture as a new stabilization material for expansive soil would align with positive efforts towards climate warming under the context of sustainable development and green construction, as well as saving on disposal problems within the paper manufacturing industry.

REFERENCES

AASHTO, (1986). standard Specifications for Transportation Materials and Methods of Sampling and Testing, American Association of State Highway and Transportation Officials, Washington, DC, 14th Ed.

Abduljauwad, S.N. (1995). "Improvement of Plasticity and Swelling Potential of Calcareous Expansive Clays", *Geotechnical Engineering Journal,* Southeast Asian Geotechnical Society, SEAGS, (26): 1, 3-16.

ACI 230.1R-90. (1990). "State-of-the-Art report on soil Cement", *ACI Material Journal,* 87 (4).

Adams, J.W. (1988). Environmental Effects of Applying Lignosulfonate to Roads, Daishowa chemicals Incorporated.

Addo, J.Q., Sanders, T.G., and Chenard, M. 2004. Road Dust Suppression: Effect on Maintenance Stability, Safety, and the Environment Phases 1–3.

Albino, V., Dangelico, R.M., Natalicchio, A., and Yazen, D.M., (2011). Alternative Energy Sources in Cement Manufacturing: A systematic review of the body of knowledge, Network for Bussiness Sustainability, University of Western Ontario, Ontario, Canada.

Al-Rawas A.A., and Goosen MFA (2006) *Expansive soils: Recent advances in characterization and treatment.* Taylor and Francis, London, UK.

Åhnberg, H., Johansson, S.E., Retelius, A., Ljungkrantz, C., Holmqvist, L., and Holm, G. (2005). Cement and lime for deep stabilization of soil. Swedish Geotechnical Institute, Report No. 48. *(In Swedish).*

Anderson, S.H., Peyton, R.L., Gantzer, C.J., (1990). Evaluation of constructed and natural soil macropores using x-ray computed tomography, Transport of water and solutes in macropores, Geoderma 46, 13–29.

Arioz, O., Kilinc, K., Karasu, B., Kaya, G., Arslan, G., Tuncan, M., Tuncan, A., Korkut, M., and Kivrak, S. (2008). "A Preliminary Research On The Properties of Lightweight Expanded Clay Aggregate", *Journal of Australian Ceramic Soceity, 44 [1], 23-30.*

Australian Standard 1289-(1992): Methods for Testing Soils for Engineering Purposes: Method 7.1.1: "Determination of the Shrinkage Index of a Soil; Shrink Swell Index".

Australian Standard 1289-(2002): Methods for Testing Soils for Engineering Purposes: Method 3.9.1: "Soil classification tests-Determination of the cone liquid limit of a soil".

Australian Standard 1289-(2003): Methods for Testing Soils for Engineering Purposes: Method 5.1.1: "Soil Compaction and Density Tests-Determination of the Dry Density/Moisture Content Relation of a Soil Using Standard Compactive Efforts".

Australian Standard 5101-(2008): Methods for Preparing and Testing of Stabilized Materials: Method 4: "Unconfined Compressive Strength of Compacted Materials".

Australian Standard 1289-(2009): Methods for Testing Soils for Engineering Purposes: Method 3.2.1: "Soil classification tests-Determination of the plastic limit of a soil".

AS 2870 (2011). Residential slabs and footings-Construction, *Standards Australia*.

ASTM (2003) D559. Standard Test Methods for Wetting and Drying Compacted Soil-Cement Mixtures, West Conshoshocken, PA, USA.

ASTM (2003) D560. Standard Test Methods for Freezing and Thawing Compacted Soil-Cement Mixtures, West Conshoshocken, PA, USA.

ASTM (2008) D6836. Standard test Method for the Determination of the Soil Water Characteristics Curve for Desorption Using a Hanging Column, Pressure Extractor, Chilled Mirror Hygrometer, and/or Centrifuge, West Conshoshocken, PA, USA.

ASTM (2008) D4546. Standard test Method for One-Dimensional Swell or Collapse of Cohesive Soils, West Conshoshocken, PA, USA.

ASTM (2011) D653. Standard Terminology Relating to Soil, Rock, and Contained Fluids, West Conshoshocken, PA, USA.

ASTM (2014) C837. Standard Test Method for Methylene Blue Index of Clay, West Conshoshocken, PA, USA.

Athukorala, R., Indraratna, B. & Vinod, J. S. (2013). Modeling the internal erosion behavior of lignosulfonate treated soil. In C. L. Meehan, D. Pradel, M. A. Pando & J. F. Labuz (Eds.), Geo-Congress 2013 (1872-1881). United States: American Society of Civil Engineers

Attom, M., Abu-Zreig, M., and Obaidat, M. (2001). "Changes in Clay Swelling and Shear Strength Properties with Different Sample Preparation Techniques". Geotechnical Testing Journal, (23) 157-163.

Bank, R.G., (1995). Soil landscapes of the Curlewis 1:100 000 sheet (Breeza, Caroona, Pine Ridge, Colly Blue, Goran Lake), Sydney : Dept. of Conservation and Land Management, vi, ill., maps ; 30 cm. + 1 col. fold. map.

Bergado, D.T., Anderson, L.R., Miura, N., and Balasubramaniam, A.S., (1996). *"Soft Ground Improvement: In lowland and other environments"*, ASCE Press, New York.

Bhattacharja, S., Bhatty, J.I., and Todres, H.A. (2003). Stabilization of clay soils by Portland cement or lime – a critical review of literature, Portland Cement Association: PCA R&D Serial No. 2066.

Bishop, J.L., Pieters, C.M., and Edwards, J.O. (1994). "Infrared spectroscopic analyses on the nature of water in montmorillonite", *Clays and Clay Minerals*, 42, 701.715.

Bolander, P. (1999). Laboratory testing of nontraditional additives for stabilization of roads and trail surfaces. Transportation Research Record 1652, 24-31.

Borchardt, G. (1989). Smectites: in Minerals in Soil Environments: 2nd ed., J. B. Dixon and S. B. Weed, eds., Soil Sci. Soc. Am., Madison, Wisconsin, 675-727.

Bowders, J., and Daniel, D.E. (1987). "Hydraulic conductivity of compacted clay to dilute organic chemicals". Journal of Geotechnical Engineering. (113): 12, 1432-1448.

Briaud, J.L. (1998). Shrink Test for Predicting Heave and Shrink Movements. *Proceedings, ASCE Texas   Section Fall Meeting*, Dallas, Texas.

Brierley, J.A., Stonehouse, H.B., and Mermut, A.R. (2001). "Vertisolic soils of Canada: Genesis, distribution, and classification", *Canadian Journal of Soil Sciences,* 91: 903-916.

Brooks, R.H., and Corey, A.T. (1964). Hydraulic properties of porous media, Colorado State University Hydrology Paper, (3): 27.

Buijs, K., and Choppin, G.R. (1963). Near-infrared studies of the structure of water. I. Pure water. *Journal of Chemical Physics* 39: 2035-2041.

Buol, S.W., Hole, F.G., McCracken, R.J., and Southard, R.J. (1997). *Soil genesis and classification*, 4th edition. Iowa St. Univ. Press, Ames.

Buzzi, O. (2010). "On the use of dimensional analysis to predict soil swelling", *Engineering Geology*, 116, 149-156.

Cameron, D.A., and Walsh, P.F. (1984). Damage to Buildings on Clay soils, Australian Council of National Trusts, Victoria, Australia.

Cameron, D.A., Walsh, P.F. and Richards, B. G. (1987). Australian Approach to the Problem of Expansive Soils, *Proceedings, 9th Regional Conference for Africa on Soil Mechanics and Foundation Engineering*, Lagos, Nigeria, 977-989.

Cameron, D. A. (2001). The extent of soil desiccation near trees in a semi-arid environment, Footings Group, IE Aust SA. 17.

Cariati, F., Erre, L., Gessa, C., Micera, G., and Piu, P. (1983). "Effects of charge on the near-infrared spectra of water molecules in smectites and vermiculites. *Clays & Clay Minerals,* 31: 447--449.

Cerato, A.B., and Miller, G.A. (2014). Important Aspects of Chemical Stabilization of Fine-Grained Soils, Southern Plains Transportation Center, SPTC Seminar Series, April 24, University of Oklahoma, Oklahoma City.

Chamberlain, E.J, Iskander, I., and Hunsiker, S.E. (1990). Effect of freeze-thaw on the permeability and macrostructure of soils. *Proceedings International Symposium on Frozen Soil Impacts on Agriculture*, Range, and Forest Lands. Special Report 90 – 1: 145–155.

Chapman, H.D. (1965). Cation-exchange capacity. In *Methods of Soil Analysis. Part 2. Chemical and Microbiological Properties,* Black C.A. et al. ed. American Society of Agronomy, 9, 891-901.

Chen, F.H. (1988). *Foundations on expansive soils*. Elsevier Science Publishers, Amsterdam, The Netherlands.

Chin R.K.H., and Fredlund, D.G. (1984). A Small Saskatchewan town copes with swelling clay problems. *Proceedings, 5th International Conference on Expansive Soils,* Adelaide, Australia, 306-310.

Coates, J. (2002). *Interpretation of the Infrared Spectra, A Practical Approach*, In Encyclopedia of Analytical Chemistry, R.A. Meyers (Ed.), 10815-10837, Willy, Chichester.

Coduto, D.P. (2001). *"Foundation Design: Principles and Practices",* 2nd Edition, Prentice Hall Inc., Englewood Cliffs, New Jersey.

Çokca, E., and Birand, A.A. (1993). "Determination of cation exchange capacity of clayey soils by the methylene blue test", *Geotechnical Testing Journal,* 16 (4): 518-524.

Cokca, E. and Birand, A.A. (2000). Suction-Swelling Relations. Geotechnical Special Publications No. 99 on Advances in Unsaturated Geotechnics: 379-392.

Considine, M. (1984). Soils shrink, trees drink, and houses crack, *ECOS Magazine* 41, 13-15.

Cornell University, College of Engineering. (1951). Soil solidification research, Cornell University, 1946 to 1951: Final Report, Ithaca, New York.

Course Hero. (2011). "Civil Engineering 7004" Online Class Note, Spring 2011, Boğaziçi University, viewed July 11 2015.

Cullity, B.D. (1979). *Elements of X-Ray Diffraction*", 2nd edition, Addison-Wesley Publishing, London.

Das, M.B. (1997). *Principles of geotechnical engineering*. PWS Publishing, Boston, MA.

Day, R.W. (1994). "Swell–shrink behaviour of compacted clay". *Journal of Geotechnical Engineering* 120 (3): 618–623.

Dhowian, A.W., Erol, A.O., and Youssef, A. (1990). Evaluation of expansive soils and foundation methodology in the Kingdon of Saudi Arabia, Final Report, King Abdulaziz City for Science and Technology, KACST, AT-5-88.

Dixon, J.B. 1989. Kaolin and serpentine group minerals. p.467-525. *In* J.B. Dixon and S.B. Weed (ed.) Minerals in soil environments. 2nd ed. Soil Sci. Soc. Am. Book Ser. No. 1. Madison, WI.

Donaldson, G.W. (1969). The Occurrence of Problems of Heave and the Factors Affecting its Nature, *Proceedings, 2nd International Research and Engineering Conference on Expansive Clay Soils,* Texas A&M University, College Station, 25-36.

ElectroScan Corporation, (1996). *Environmental Scanning Electron Microscopy: An Introduction to ESEM®.* Robert Johnson Associates, Wilmington, Massachusetts.

El-Sohby, M.S., and Rabba, E.A. (1981), "Some factors affecting swelling of clayey soils", *Geotechnical engineering,* (12): 19 – 39.

Entwisle, D., and Kemp, S. (2003). Specific surface area: an aid to identify some problem soils. *An International Conference on Problematic Soils,* Nottingham, UK, 28-30th July, CI-Premier, Singapore 235-266.

Eswaran, H. (1979). "The alteration of plagioclases and augites under differing pedo-environmental conditions", *Journal of the Soil Society of America,* (30):547-555.

Farmer, V. C., and Mortland, M.M. (1966). An infrared study of the coordination of pyridine and water to exchangeable cations in montmorillonite and saponite: *Journal of chemical Society of America,* 344-351.

Farmer, V.C., and Russell, J.D. (1971). "Interlayer complexes in layer silicates; the structure of water in lamellar ionic solutions": *Transaction of Faraday Society,* 67, 2737-2749.

Fanning, D.S., Keramidas, V.Z., and El-Desoky, M.A. (1989). Micas. p. 551-634. *In* J.B. Dixon and S.B. Weed (ed.) Minerals in soil environments. 2nd ed. Soil Sci. Soc. Am. Book Ser. No. 1. Madison, WI.

Fell, R., Wan, C., Cyganiewicz, J., and Foster, M. (2003). "Time for Development of Internal Erosion and piping in Embankment Dams." Journal of geotechnical and geoenvironmental engineering 129 (4): 307 – 314.

Fityus, S.G., Smith, D.W. (1998). A simple model for the prediction of free surface movements in swelling clay profiles, Proceedings, 2nd international Conference on Unsaturated Soils, Beijing, 743-478.

Fityus, S.G., Smith, D.W., and Allman, M.A., (2004). "Expansive soil test site near Newcastle", *Journal of Geotechnical and Geoenvironemntal Engineering,* (130): 7, 686-695.

Fityus, S. G., Cameron, D. A., and Walsh, P. F. (2009). "The Shrink Swell Test." *Geotechnical Testing Journal,* Vol. 28 (1): 92 – 101.

Fredheim, G.E., Braaten, S.M., Christensen, B.E. (2002). "Molecular weight determination of lignosulfonates by size-exclusion chromatography and multi-angle laser light scattering", *Journal of Chromatography A,* 942:191–199.

Fredlund, D.G. (1983). Prediction of ground movements in swelling clays. *31st Annual Soil Mechanics and Foundation Engineering Conference,* Minneapolis, Minn.

Fredlund, D.G., and Rahardjo, H. (1993). *Soil mechanics for unsaturated soils*, Wiley, New York.

Furtado, N. (2010). Situational analysis of the soil map of Brazil. Federal Institute of Education, Science and Technology Goiano: Rio Verde, Brazil.

Gargulak, J.D., Lebo, S.E. (2000). Commercial use of lignin-based materials. *ACS Symposium Series*, 742, 304.

Gandini, A., Belgacem, M. (2008). Lignin as Components of Macromolecular Materials. In *Monomers, Polymers, and Composites from Renewable Resources*; Eds.; Elsevier: Oxford, UK, 243–273.

Gourley, C. S., Newill, D., and Schreiner, H. D. (1993). "Expansive Soils: TRL's research strategy." *In: Proceedings of the First International Symposium on Engineering Characteristics of Arid Soils,* City University, London.

Gow, A.J., Davidson, D.T., and Sheeler, J. B. (1961). Relative effects of chlorides, lignosulfonates and molasses on properties of a soil-aggregate mix. *Highway ResearchBoard Bulletin 282.*

Grim, R. F. (1968). *Clay mineralogy*, McGraw Hill, New York, 2nd edn, ch. 4 and 7.

Hamilton, J.J. (1965). Shallow foundations on swelling clays in Western Canada. Proceesings, International Research and Engineering Conference on Expansive Clay Soils. College Station, TX.

Harkin, J. M. (1966). Lignin Production and Detection in Wood, Forest Product Laboratory Note, Forest Service U.S. Department of Agriculture, university of Wisconsin, FPL–0148.

Harkin, J. (1969). Lignin and its uses, For. Prod. Lab. Rept. 0206. Madison, Wisconsin.

Harris, P., Von, H., J., Sebasta, S., and Scullion, T. (2006). Recommendations for stabilization of high-sulfate soils in Texas. Report for the Texas Department of Transportation and the Federal Highway Administration. Report $0 - 4240 - 3$, Project Number $0 - 4240,$

Heitner, C., Dimmer, D., Schmidt, J. A. (2010). *Lignin and Lignans: Advances in Chemistry*; CRC Press: Boca Raton, FL, 686.

Heitor, A., Indraratna, B. and Rujikiatkamjorn, C. (2013). "Laboratory study of small strain behaviour of a compacted silty sand". *Canadian Geotechnical Journal,* 50 (2): 179-188.

Hendricks, S.B. (1941). "Base-exchange of the clay mineral montmorillonite for organic cations and its dependence upon adsorption due to van der Waals forces": *Journal of Physical Chemistry* (45), 65-81.

Holtz, W.G., and Gibbs, H.J. (1956). "Engineering Properties of Expansive Clays". *Transactions of the American Society of Civil Engineers*, 121, 641-663.

Huang, E.Y. (1954). Selected bibliography on soil stabilization. Ann Arbor : University of Michigan; Engineering Research Institute, LCCN: 56-62661.

Hubble, G.D. (1972). The swelling clay soils. Physical aspects of swelling clay soils. Res. Symposium University of New England, Armidale, New South Wales, Australia.

Indraratna, B., Gasson, I. and Chowdhury, R. N. (1994b). Utilization of Compacted Coal Tailings as a Structural Fill. *Canadian Geotechnical Journal*, 31(5), 614-623.

Indraratna, B., Muttuvel, T., Khabbaz, H., and Armstrong, R. (2008). "Predicting the Erosion Rate of Chemically Treated Soil using a Process Simulated Apparatus for Internal Crack Erosion." *Journal of Geotechnical and Geoenvironmental Engineering,* ASCE, 134 (6): 837–844.

Indraratna, B., Mahamud, M., Vinod, J.S., and Wijeyakulasuriya, V. (2010). Stabilization of an erodible soil using a chemical admixtures, In Bouassida, M, Hamdi, E & Said, I (eds), ICGE'10: *Proceedings, 2nd International Conference on Geotechnical Engineering*: 45-54.

Indraratna, B., Athukorala, R. and Vinod, J.S. (2013). "Estimating the rate of erosion of a silty sand treated with lignosulfonate", *Journal of Geotechnical and Geoenvironmental Engineering,* 139 (5), 701-714.

ILI, (1992). Web site of the International Lignin Institute, available at http://www.ili-lignin.com. Accessed on July 15 2015.

Israelachvili, J. (1991). *Intermolecular and Surface Forces*, 2nd edition, Academic Press, Carlifornia, USA.

Jackson, M.L., and Sherman, G.D. (1953). Chemical weathering of minerals in soils. Adv. Agron., 5:219-318.

Jackson, M.L. (1965). Clay transformations in soil genesis during the Quaternary. Soil Science, (99):15-22.

JECFA (Joint FAO/WHO Expert Committee on Food Additives), (2008). New specifications prepared at the 69th JECFA (2008), published in FAO JECFA Monographs 5. Available at:http://www.fao.org/ag/agn/jecfa-additives/details.html?id=927, accessed July 15 2015.

Johnson, L.D., and Snethan, D.R. (1978). "Prediction of potential heave in swelling soils". Journal of the Geotechechnical Testing, 1 (3): 117-124.

Jones, D.E. and Holtz, W.G. (1973). "Expansive Soils - the hidden disaster", *Civil Engineering – ASCE,* (43): 8 49-51.

Jones, D.E. (1981). Perspectives on needs for an availability of scientific and technical information, Department of Housing and Urban Development, presented at 1st meeting of Committee on Emergency Management, Commission on Sociotechnical Systems, Nation Research Council, Washington, D.C.

Jones, D., and Ventura, D.F.C. (2003). The Development of a research protocol and fit-for-purpose certification for road additives-Phases I-III. Pretoria: CSIR Transportek, (Report; CT-2003/34).

Jones, L.D., and Hobbs, P.R.N. (2004). The Shrinkage and Swelling Behaviour of UK Soils: Clays of the Lambeth Group. British Geological Survey Research Report RR/04/01

Jones, L.D., and Jefferson, I., (2012). "Expansive soils", Institution of Civil Engineers Manuals Series, ICE Publishing, 1 - 46.

Kapitzke, J., and Reeves, I., (2000). Paving Materials and Type Cross Sections for Roads on Expansive Soils in Western Queensland, Technical Note WQ35, Main Roads, 1-6.

Kassiff, G., and Wiseman, G., (1966). "Control of moisture and volume change in clay subgrades by subdrainage, *Highway Res. Board Rec.* 111:1 − 11.

Katti, R.K. (1978). Search for solution to problems in black cotton soils, *First IGS Annual Lecture* at I.I.T, Delhi.

Kelm, R.P.E., and Wylie, N.P.E. (2008). Which Way Is It Moving? Guidelines for Diagnosing Heave, Subsidence and Settlement, Forensic Engineering INC, available at www.forensicengineersinc.com, accessed on May 20 2015.

Khalil, S.M., and Ward, M.A. (1973). Influence of a Lignin Based Admixture of the Hydration of Portland Cements. Cement Concrete Res. (3): 677-688.

Klute, A. (1986). Methods of soil analysis, part 1, physical and mineralogical methods (2nd edition), Madison: Soil Science Society of America, Wisconsin,

Knappett, J.A., and Craig, R.F. (2012). *Craig's Soil Mechanics,* 8th edition, Spon Press, Abingdon, RN, 3-14.

Komadel, P., Madejova´, J., and Stucki, J.W. (1999). "Partial stabilization of Fe(II) in reduced ferruginous smectite by Li fixation", *Clays and Clay Minerals*, **47**, 458-465.

Komine, H., and Ogata, N. (1996). "Prediction for swelling characteristics of compacted bentonite", *Canadian Geotechnical Journal,* 33: 11-22.

Kota, P.B.V.S., Hazlett, D., and Perrin, L. (1996). "Sulfate-Bearing Soils: Problems withCalcium-Based Stabilizers." *Transportation Research Record 1546,* TRB, National Research Council, Washington, D. C., 62-69.

Krohn, J.P., and Slosson, J.E., (1980). Assessment of Expansive Soils in the United States. *Proceedings, 4th International Conference on Expansive Soils,* Denver, CO, (1): 596-608.

Lambe, T.W. (1953). The structure of inorganic soil, *Proceedings of the American Society of Civil Engineers,* 79 (315): 1-49.

Lebo Jr., S.E., Gargulak, J.D., McNally, T.J. (2002). *Encyclopedia of Polymer Science and Technology*; Wiley: Hoboken, New Jersey, 100–124.

Lytton, R.L. (1977). Foundations in expansive soils. In: Desai, C.S., Christian, J.T. (Eds.), *Numerical methods in Geotechnical Engineering*. McGraw-Hill.

Madejova, J. (2003). "FTIR techniques in clay mineral studies", *Journal of Vibrational Spectroscopy 31*, 1–10

Macey, H.H. (1942). "Clay-water relationship and the internal mechanism of drying": *Transaction of British Ceramic Society,* 41, 73-121.

McBride, M.B. (1989) Surface chemistry of soil minerals. In *Minerals in Soil Environments (2nd edition),* J.B. Dixon and S.B. Weed, eds., *Soil Science Society of America,* Madison, Wisconsin, 35-88.

McKenzie, D.C., and Anderson, A.N. (1998). SOILpak pocket notes: a summary of "SOILpak for cotton growers, 3rd edition" for use in the field. Information series (Queensland. Department of Primary Industries) QI 98013. Agfacts (NSW Agriculture); Agfact AC 10.

McManus, K J 1983, 'Lightly Loaded Structures on Expansive clay soils' 75th Anniversary Professional Engineering Update Seminar, Swinburne Institute of Tech-nology, Faculty of Engineering, Hawthorn, Australia, 1983,

McManus, K J & De Marco, S 1996, 'Variability of Expansive Nature of Clay on a site' 7th Australia New Zealand Conference on Geomechanics : Geomechanics on a changing world, Adelaide, Australia, 1-5July,1996, The institute of Engi-neers Australia, Canberra

McManus, K. J., Lopes, D., Osman, N. Y., (2004). The effect of Thornthwaite Moisture Index Changes in Ground movement predictions in Australian Soils, *Proceedings 9th Australia New Zealand Conference on Geomechanics*, 2, 555-561.

Meier, J.N., Fyles, J.W., MacKenzie, A.F., O'Halloran, I.P. (1993). "Effects of lignosulfonate fertilizer applications on soil respiration and nitrogen dynamics". *Journal of Canadian Soil Sciences,* 73, 233.

Mitchell, J.K., and Soga, K., (2005). *Fundamentals of soil behaviour,* 3rd edition, Wiley, Hoboken, New Jersey, USA.

Mitchell, J.K. (1956). The Fabric of Natural Clays and Its Relation to Engineering Properties, *Proceedings, Highway Research Record*, (35), 693-713.

Mitchell, P.W., (1980). The structural analysis of footings on expansive soil. Kenneth W.G, and Smith & Associates Research Report No. 1, 2nd Edition.

Morris, P O., and Gray, W J. (1976). Moisture conditions under roads in the Australian environment, *Australian Road Research Board,* ARR No. 69, 39.

Murty, V., and Praveen, G., (2008). "Use of Chemically Stabilized Soil as Cushion Material below Light Weight Structures Founded on Expansive Soils." *Journal of Materials and Civil Engineering*, 20 (5), 392–400.

Nayak, N.V., and Christensen, R.W. (1971). "Swelling Characteristics of compacted, expansive soils." *Journal of Clay and Clay Minerals,* 19: 251 – 261.

Nelson, J.D., and Miller, D.J., (1992). *Expansive soils, problems and practice in foundation and pavement engineering*, Wiley, USA.

Newman, K. and Tingle, J.S. (2004). Stabilization of silty sand using polymer emulsions. Transportation Research Record, Annual Meeting CD-ROM paper no 04-3108, 11-13.

Nicholls, R.L., and Davidson, D.T. (1958). Polyacids and lignin used with large organic cations for soil stabilization, Highway Research Board Proceedings, 37, 517-537.

Oberhettinger, F., and Badii, L., (1973). *Table of Laplace Transforms*. Springer Varlag, Berlin, Germany.

Ola, S.A. (1977). "The potencial of lime stabilization of lateritic soils", *Engineering Geology 11,* 305-317.

Ola, S. A., and Omange, G.N. (1987). Nature and properties of expansive soils in Nigeria. 6th International Conference on expansive soils, New Delhi, India. 11-16.

Oloo, S., Schreiner, H.D., and Burland, J.B. (1987). Identification and classification of expansive soils. *6th International Conference on Expansive Soils*, New Delhi, India, Imperial College of Science and Technology, London, 23-29.

Olson, R.E. (1964). "Discussion of paper- Effective stress theory of soil compaction". *Journal of the American Society of Civil Engineers'*, Soil Mechanics and Foundations Division, (90), SM2: 171-189.

Olson, R.E., Mesri, G. (1970). "Mechanism controlling compressibility of clays", *Journal of the SMFE Division ASCE,* 6 (11): 1863–1878

Orszulik, S.T. (2013). Environmental Technology in the Oil Industry, Springer Science and Business Media, Netherlands, Also available at https://books.google.com.au/books?id=QDjpCAAAQBAJ, accessed on May 21 2015.

Palmer, J.T., Edgar, T.V., and Boresi, A.P. (1995). Strength and density modification of unpaved road soils due to chemical additives, Mountain-Plains Consortium (MPC) Report No. 95–39, Fargo, ND.

Parfitt, R.L., and Mortland, M.M. (1968) Ketone adsorption on montmorillonite, *Proceedings of Soil Science Society of America,* 32, 355 363.

Parfitt, R.L., and Greenland, D.J. (1970). "The adsortpion of poly(ethylene glycols) on clay minerals", *Clay Minerals* 8, 305–315.

Pearl, I. A. (1967). "The Chemistry of Lignin". Publisher; Marcel Dekker, INC., New York.

Perry, J.P. (1977). "Lime treatment of dams constructed with dispersive clay soils", *Soil and Water Division, Transactions of the ASAE,* 1093-1099.

Philip, J.R. (1972). Steady Infiltration from Buried, Surface, and Perched Point and Line Sources in Heterogeneous Soils: I. Analysis. Soil Science Society of America Proceedings 36: 268-273.

Puech, P.A., Boussel, L., Belfkih, S., Lemaitre, L., Douek, P., and Beuscart, R. (2007). "DicomWorks: Software for Reviewing DICOM studies and promoting low-cost releradiology", *Journal of Digital Imaging,* 20 (2): 122-130.

Puppala, A.J., and Hanchanloet, S. (1999). Evaluation of a new chemical (SA-44/LS-40) treatment method on strength and resilient properties of a cohesive soil." *Transport Research Board, 78th Annual Meeting*, January 10 – 14, 1999, Washington, D.C., Paper No. 990389.

Puppala, A.J., Wattanasantichatoen E., Intharasombat L., Hoyos L.R. (2003). "Studies to Understand Soil Compositional and Environmental Variables Effects on Sulfate Heave Problems," 12th Panamerican Conference on Soil Mechanics and Geotechnical Engineering.

Puppala, A.J., Griffin, J.A., Hoyos, L.R., and Chomtid, S. (2004). "Studies on Sulfate-Resistant Cement Stabilization Methods to Address Sulfate-Induced Soil Heave." *Journal of Geotechnical and Geoenvironmental Engineering,* (130): 391-402.

Ramachandran, V.S., Kacker, K.P., and Patwardhan, N.K. (1962). Adsorption of dyes by clay minerals, The American mineralogist, 47.

Rankin, G., and Fairweather, S. (1978). Expansive soil clays, *Seminar on foundations in expansive clay soils*, Resource materials centre, DDIAE, Darling Downs, 2-4.

Rauch, A.F, Harmon, J.S., Katz, L.E., and Liljestrand, H.M. (2003). An Analysis of the Mechanisms and Efficacy of Three Liquid Chemical Soil Stabilizers, Federal Highway Administration, Report no. FHWA/TX 03/1993–1, (1), Austin, TX.

Reeves, I. (2001). Risk Management – Materials [presented at Road System and Engineering Technology Forum 2001], Road System and Engineering Group, Queensland Department of Main Roads.

Reid, D.A., Graham, R.C., Douglas, L.A., and Amrhein, C. (1996). "Smectite mineralogy and charge characteristics along an arid geomorphic transect". *Journal of the Soil Society of America,* (60):1602-1611.

Richards, B.G., Peter, P., and Emerson, W.W., (1983). "The effects of vegetation on the swelling and shrinking of soils in Australia", *Geotechnique,* 33 (2): 127-139.

Richards, B. G., (1990), "Footings for small and domestic structures", Linn Education and Training Services, Brisbane, Australia.

Robinson, R.G., and Allam, M.A. (1998). "Effect of clay mineralogy on coefficient of consolidation", *Clays and Clay Minerals*, 46(5), 596–600.

Rollings, R.S., and Burkes, M.P. (1999) "Sulfate Attack on Cement-Stabilized Sand", *Journal of Geotechnical and Geoevnironmental Engineering,* ASCE, 125 (5): 364-372.

Rosauer, E.A., Handy, R.L., and Demirel, T. (1961). "X-Ray Diffraction Studies of Organic Cation Stabilized Bentonite", *Clays and Clay Minerals,* National Academy of Science - National Research Council, 10 (1961), 235-243.

Russell, J.D., and Farmer, V.C. (1964). "Infared spectroscopic study of the dehydration of montmorillonite and saponite": *Clay Minerals Bulletin,* 5, 443-464.

Russell, J.D., and Fraser, A.R. (1996). Infrared methods. In *Clay Mineralogy: Spectroscopic and Chemical Determinative Methods,* MJ. Wilson, ed., Chapman and Hall, London, 11-64.

Saikia, B.J., and Parthasarathy, G. (2010). "Fourier Transform Infrared Spectroscopic characterization of kaolinite from Assam and Meghalaya, Northeastern India", *Journal of Modern Physics,* 1, 206-210.

Santagata, M., Bobet, A., Johnston, C.T., and Hwang, J. (2008). "One-Dimensional Compression Behaviour of a Soil with High Organic Matter Content", *Journal of Geotechnical and Geoenvironmental Engineering* © ASCE, 134(1):1-13.

Santamarina, J.C., Klein, K.A., Wang, Y.H., and Prencke, E. (2002). "Specific surface: determination and relevance", *Canadian Geotechnical Journal*, 39, 233-241.

Santoni, R.L., Tingle, J.S., and Webster, S.L. (2002). Nontraditional Stabilization of Silty-Sand. *81st Transportation Research Board Annual Meeting,* Paper no. 02-3756, Washing- ton, D.C.

Saride, S., Puppala, A.J., and Chikyala, S.R. (2013). "Swell-shrink and strength behaviours of lime and cement stabilized expansive organic clays", *Applied Clay Science*, (85), 39-45.

Sariosseiri, F., and Muhunthan, B. (2009). "Effect of cement treatment on geotechnical properties of some Washington State soils", *Engineering Geology,* 104 (1-2): 119-125.

Sarkanen, K.V., Ludwig, C.H. (1971). *Lignins Occurrence, Formation, Structure and Reactions*, Wiley-Interscience, New York, 285-290.

Sarkar, S., Herbert, B., and Scharlin, R. (2000). "Injection Stabilization of Expansive Clays Using a Hydrogen Ion Exchange Chemical", *Advances in Unsaturated Geotechnics*: 487-516.

Sarkar G, Islam R, Alamgir M and Rokonuzzaman (2012) Study on the Geotechnical Properties of Cement based Composite Fine-grained Soil, *International Journal of Advanced Structures and Geotechnical Engineering,* 1(2): 42-49.

Scholen, D. E. (1992). Non-Standard Stabilizers. Report No. FHWA-FLP-92-011, FHWA, Washington, D. C.

Scholen, D.E. (1995). Stabilizer Mechanisms in Nonstandard Stabilizers, *Proceedings of 6th International Conference on Low-Volume Roads,* 2, TRB, National Academy Press, Washington, D. C., 252-260.

Seed, H.B., and Chan, C.K. (1959). "Structure and Strength Characteristics of Clay", *Journal, Soil Mechanics and Foundations Division*, American Society of Civil Engineers, (85): SM5, 87-128.

Seed, H.B., Woodard, R.J., & Lundgren, R. (1962). "Prediction of swelling potential for compacted clays". *Journal of American Society of Civil Engineers, Soil Mechanics and Foundations Division,* 88(SM3), 53– 87.

Serratosa, J.M. (1968). Infrared study of benzonitrile (C6H5-CN)-montmorillonite complexes. *Am Mineral* 53:1244-1251.

Sinha, S.P., Davidson, D.T., and Hoover, J.M. (1957). Lignins as Stabilizing Agents for Northeastern Iowa Loess. *Proceedings of the Iowa Academy of Science*, 69th Session, Iowa.

Sivapullaiah, P.V., Prashanth, J.P., Sridharan, A. (1996). "Effect of fly ash on index properties of black cotton soil", *Soils Foundation,* 36 (1): 97–103.

Skempton, A.W. (1953). The colloidal activity of clays. *Proc. 3rd. Int. Conf. on SoilMechanics*, (1), 57-61.

Snethan, D.R., Townsend, F.C., Johnson, L.D., Patrick, D.M., and Vedros, P.J. (1975). A Review of Engineering Experiences with Expansive Soils in Highway Subgrades, Report No. FHWA-RD-75-48, U.S., Army Engineer Waterways Experiment Station, Vicksburg, Miss., USA.

Snethan, D.R., Johnson, L.D., and Patrick, D.M. (1977). An Evaluation of Expedient Methodology for Identification of Potential Expansive Soils. Report FHWA-RD-77-94 for the Federal Highway Administration. Vicksburg, Miss., U.S. Army Waterways Experiment Station.

Snethen, D.R., (1986). Expansive Soils: Where Are We?, in Ground Failure, No.3, Nat. Res. Council Comm. On Ground Failure Hazards, 12-16.

Sridharan, A., Jayadeva, M.S. (1982). "Double layer theory and compressibility of clays". *Geotechnique* (London) 32:133-144.

Steinberg, M.L. (1998). *Geomembranes and the control of expansive soils in construction*, McGraw-Hill, New York, U.S.A.

Sulphite Pulp Manufacturers Research League, (1963). A Bulletin about Spent Sulphite Liquor, Appleton, Wisconsin, USA.

Teng, T.C.P., Mattox, R.M., and Clisby, M.B., (1972). A study of active clays as related to highway design, Research and development division, Mississippi State Highway Dept., Engineering and Industrial Research Station, Mississippi State University, MSHD-RD-72-045.

Tingle, J.S., and Santoni, R.L. (2003). Stabilization of Clay Soils with Nontraditional Additives. In Transportation Research Record: *Journal of the Transportation Research Board*, No. 1819, Vol. 2, Transportation Research Board of the National Academies, Washington, D.C., 72–84.

Tingle, J.S., Newman, J.K., Larson, S.L., Weiss, C.A., and Rushing J.F. (2007). "Stabilization mechanisms of non-traditional additives", *Transportation Research Record: Journal of the Transportation Research Board,* No. 1989, 2, Transportation Research Board of the National Academics, Washington, D.C., 59 – 67.

Theng, B.K.G. (1979). *Formation and properties of clay-polymer complexes,* Eksevier Scientific Publishing Company, Amsterdam, The Netherlands.

Tripathy, K.S., Subba Rao, K.S., and Fredlund, D.G.(2002). "Water content – void ratio swell shrink paths of compacted expensive soils", *Journal of Canadian Geotechnics,* (39): 938–959.

U.S. Department of the Interior Bureau of Reclamation (1998). *Earth Manual*, Part 1, Third edition. Colorado: United States Government Printing Office.

Vanapalli, S.K., Fredlund, D.G., and Pufahl, D.E. (1999). "The influence of soil structure and stress historyon the soil-water characteristics of a compacted till". *Geotechnique* 49 (2), 143-159.

Van der Merwe, D H. (1964). "The prediction of heave from the plasticity index and percentage clay fraction of soils". *Transaction of the South African Institution of CivilEngineers*, 6, 103-107.

Van Olphen, H., (1977). *An Introduction to Clay Colloid Chemistry*, Wiley, New York, USA, 318.

Vinod, J.S., Indraratna, B., and Mahamud M.A.A. (2010). "Stabilization of an erodible soil using a chemical admixture." *Journal of Ground Improvement,* Vol. 163: 43 – 51.

Walsh, P.F., Fityus, S., and Kleeman, P. (1998). A Note on the Depth of Design Suction Change for Clays in whiSouth Western Australia and South Eastern Queensland. *Australian Geomechanics,* 33**,** 37-40.

WEC, 1995. Efficient Use of Energy Utilizing High Technology: An Assessment of Energy Use in Industry and Buildings, World Energy Council, London, United Kingdom.

Whittig, L.D., and Allardice, W.R. (1986). X-ray diffraction techniques. p. 331–362 *In* A. Klute (ed.) *Methods of soil analysis*. Part 1. 2nd ed. Agron. Monogr. 9. ASA and SSSA, Madison, WI.

Williams, A.A.B., Pidgeon, J.T. and Day, P. (1985). Problem Soils in South Africa - State-of-the-Art: Expansive Soils. *The Civil Engineer in South Africa*, 367-377.

Wray, W.K. (1995). So your home is built on Expansive Soils: A discussion of how Soils affect Buildings, *American Society of Civil Engineers*, USA.

Xie, M., Moog, H.C., and Kolditz, O. (2007). Geochemical Effects on Swelling Pressure of Highly Compacted Bentonite: Experiments and Model Analysis, Theoretical and Numerical Unsaturated Soil Mechanics, Springer Proceedings in Physics 113 (113): 93-100.

Yong, R.N., and Warkentin, B.P. (1966). *Introduction to Soil Behaviour,* Macmillan, New York.

Yong, R.N., and Warkentin, B.P. (1975). *Soil Properties and Behaviour*. Elsevier, Amsterdam, The Netherlands.

APPENDIX A. THE SOLUTION OF THE MOISTURE DIFFUSION EQUATION

Refer to the moisture diffusion equation; chapter 6, equation 6.14.

$$\frac{\partial \varphi}{\partial t} = \beta \frac{\partial^2 \varphi}{\partial y^2} \qquad \text{(A.1)}$$

Where, β = diffusion coefficient of soil, whose magnitude defines the rate of moisture diffusion with change in soil suction (Mitchell 1980). It is the governing moisture diffusion equation for LS treated soil.

$$\beta = \frac{K_{sat}\left(0.06e^{5.05(S_d)}\right)}{r_d C}$$

Which account for the effect of LS admixture on the diffusion coefficient of the expansive soil, S_d = degree of saturation.

Equation (A.1) is solved using Laplace Transform as shown below with initial and boundary conditions. The solution of this equation defines the suction behaviour of the laboratory soil specimen with time.

Solution of the Moisture Diffusion Equation

In order to solve equation (A.1) analytically, we prescribe initial and boundary conditions as follows:

$$\textit{Initial condition: } \lim_{t \to 0} \varphi(y,t) = \eta \qquad \text{(A.2)}$$

Where, η is a constant representing the initial soil suction value of CaLS treated soil

Boundary condition: Assuming groundwater does not infiltrate treated soil but only surface water does e.g. rain. The boundary conditions are:

$$\lim_{y \to 0} \varphi(y,t) = \eta \qquad \text{(A.3)}$$

$$\lim_{y \to L} \varphi(y,t) = \rho \qquad (A.4)$$

Where, ρ = a constant suction by watering at soil surface.

Using the Laplace Transform on both sides with time t, the boundary value problem can be solved as follows:

$$F(s) = \ell\{f(t)\} = \int_0^\infty e^{-st} f(t) dt \quad \text{Fundamental} \qquad \text{Laplace} \qquad \text{Transform}$$

equation

$$\ell\left\{\frac{\partial \varphi}{\partial t} - \beta \frac{\partial^2}{\partial y^2}\right\} = \ell\{0\}$$

$$\int_0^\infty \left(\frac{\partial \varphi}{\partial t} - \beta \frac{\partial^2 \varphi}{\partial y^2}\right) e^{-st} dt = \underbrace{\int_0^\infty \frac{\partial \varphi}{\partial t} e^{-st} dt}_{\text{Part I}} - \underbrace{\int_0^\infty \beta \frac{\partial^2 \varphi}{\partial y^2} e^{-st} dt}_{\text{Part II}} \qquad (A.5)$$

Part I   Part II

Considering Part I: *using integration by parts* (i.e. $\int uv' dt = uv - \int vu' dt$)

$$u = e^{-st} \qquad\qquad u' = -se^{-st} \qquad v = \varphi$$

$$\int_0^\infty \frac{\partial \varphi}{\partial t} e^{-st} dt = uv - \int u' v dt = \left[\varphi e^{-st}\right]_{t=0}^{t=\infty} - \int \left(-se^{-st}\right) \varphi dt$$

$$= \left[\varphi e^{-st}\right]_{t=0}^{t=\infty} + s \int \varphi e^{-st} dt \qquad (A.6)$$

Considering Part II: *using integration by parts*

$$\int_0^\infty \beta \frac{\partial^2 \varphi}{\partial y^2} e^{-st} dt = \beta \frac{\partial^2}{\partial y^2}\left(\int_0^\infty \varphi e^{-st} dt\right) \qquad (A.7)$$

Now we define:

$$\bar{\varphi}(y,s) = \int_0^\infty \varphi e^{-st} dt \qquad (A.8)$$

Substituting equation (A.8) into (A.6)

$$\int_0^\infty \frac{\partial \varphi}{\partial t} e^{-st} dt = \left[\varphi e^{-st} \right]_{t=0}^{t=\infty} - s\bar{\varphi}(y,s) \tag{A.9}$$

Substituting equation (A.8) into (A.7)

$$\int_0^\infty \beta \frac{\partial^2 \varphi}{\partial y^2} e^{-st} dt = \beta \frac{\partial^2 \bar{\varphi}(y,s)}{\partial y^2} \tag{A.10}$$

Now substituting equations (A.9) and (A.10) into (A.5)

$$\int_0^\infty \left(\frac{\partial \varphi}{\partial t} - \beta \frac{\partial^2 \varphi}{\partial y^2} \right) e^{-st} dt = \left[\varphi e^{-st} \right]_{t=0}^{t=\infty} + s\bar{\varphi}(y,s) - \beta \frac{\partial^2 \bar{\varphi}(y,s)}{\partial y^2}$$

$$\left[\varphi(y,t) e^{-st} \right]_{t=0}^{t=\infty} + s\bar{\varphi}(y,s) - \beta \frac{\partial^2 \bar{\varphi}(y,s)}{\partial y^2} = 0 \tag{A.11}$$

Inserting equation (A.2) into (A.11)

$$\left[\varphi(y,t) e^{-st} \right]_{t=0}^{t=\infty} = 0 - \eta \tag{A.12}$$

Inserting equation (A.12) into (A.11)

$$-\eta + s\bar{\varphi}(y,s) - \beta \frac{\partial^2 \bar{\varphi}(y,s)}{\partial y^2} = 0$$

$$s\bar{\varphi}(y,s) - \eta = \beta \frac{\partial^2 \bar{\varphi}(y,s)}{\partial y^2} \tag{A.13}$$

In order to solve equation (A.13), the boundary conditions for φ must undergo Laplace Transform (equations A.3 and A.4c) i.e. $\bar{\varphi} = \ell(\varphi)$.

$$\lim_{y \to 0} \bar{\varphi}(s,y) = unknown \qquad\qquad \lim_{y \to L} \bar{\varphi}(s,y) = unknown$$

249

$$\lim_{y \to 0} \overline{\varphi}(s, y) = \lim_{y \to 0} \int_{t=o}^{t=\infty} \varphi(y,t)e^{-st}dt = \int_{t=0}^{t=\infty} \lim_{y \to 0} \varphi(y,t)e^{-st}dt = \int_{t=0}^{t=\infty} \eta e^{-st}dt = \left[\eta \frac{1}{s}e^{-st} \right]_{t=0}^{t=\infty} = \frac{\eta}{s}(1-0) = \frac{\eta}{s}$$

(A.14)

$$\lim_{y \to L} \overline{\phi}(s, y) = \lim_{y \to L} \int_{t=o}^{t=\infty} \varphi(y,t)e^{-st}dt = \int_{t=0}^{t=\infty} \lim_{y \to L} \varphi(y,t)e^{-st}dt = \int_{t=0}^{t=\infty} \rho e^{-st}dt = \left[\rho \frac{1}{s}e^{-st} \right]_{t=0}^{t=\infty} = \frac{\rho}{s}(1-0) = \frac{\rho}{s}$$

(A.15)

Now, to solve equation (A.10): First, solve the homogeneous equation using Laplace Transform

$$\beta \frac{\partial^2 \overline{\varphi}(s, y)}{\partial y^2} - \eta - s\overline{\varphi}(s, y) = 0 \qquad\qquad \Rightarrow \beta \frac{\partial^2 \overline{\varphi}}{\partial y^2} = s\overline{\varphi}$$

$$\beta.\xi^2 = s \qquad\qquad \Rightarrow \xi_{1,2} = \pm\sqrt{\frac{s}{\beta}} \qquad\qquad (A.16)$$

Substituting equation (A.13) into the general solution equation for "real different roots" for homogeneous equation

$$\overline{\varphi}(s, y) = Ae^{\xi_1 y} + Be^{\xi_2 y} = Ae^{-\sqrt{\frac{s}{\beta}}y} + Be^{\sqrt{\frac{s}{\beta}}y} \qquad\qquad (A.17)$$

From equation (A.13), assuming $\overline{\varphi} = \text{constant} = c$, then:

$$sc - \eta = \beta \frac{\partial^2 c}{\partial y^2} \qquad\qquad \text{Thus,} \quad c = \frac{\eta}{s}$$

Therefore, the solution of equation (A.13); inhomogeneous equation is

$$\overline{\varphi}(s, y) = Ae^{-\sqrt{\frac{s}{\beta}}y} + Be^{\sqrt{\frac{s}{\beta}}y} + c$$

Where, c is a particular integral and substituting c gives;

$$\overline{\varphi}(s, y) = Ae^{-\sqrt{\frac{s}{\beta}}y} + Be^{\sqrt{\frac{s}{\beta}}y} + \frac{\eta}{s} \qquad\qquad (A.18)$$

To solve for A and B in equation (28)

$$\lim_{y \to 0} \overline{\varphi}(s, y) = A + B + \frac{\eta}{s} = \frac{\eta}{s} \tag{A.19}$$

$$\lim_{y \to L} \overline{\varphi}(s, y) = \frac{\eta}{s} + Ae^{-\sqrt{\frac{s}{\beta}}L} + Be^{\sqrt{\frac{s}{\beta}}L} = \frac{\eta}{s} \Rightarrow Ae^{-\sqrt{\frac{s}{\beta}}L} + Be^{\sqrt{\frac{s}{\beta}}L} = \frac{\rho}{s} - \frac{\eta}{s} = \frac{\rho - \eta}{s} \tag{A.20}$$

Solving equations (A.19) and (A.20) simultaneously;

From equation (A.19)

$$B = -A \tag{A.21}$$

Substituting equation (A.21) into (A.20)

$$Ae^{-\sqrt{\frac{s}{\beta}}L} - Ae^{\sqrt{\frac{s}{\beta}}L} = \frac{\rho - \eta}{s}$$

$$A\left[e^{-\sqrt{\frac{s}{\beta}}L} - e^{\sqrt{\frac{s}{\beta}}L}\right] = \frac{\rho - \eta}{s}$$

$$A = \frac{\rho - \eta}{s\left[e^{-\sqrt{\frac{s}{\beta}}L} - e^{\sqrt{\frac{s}{\beta}}L}\right]} \tag{A.22}$$

Substituting equation (A.22) into (A.21)

$$B = -\frac{\rho - \eta}{s\left[e^{-\sqrt{\frac{s}{\beta}}L} - e^{\sqrt{\frac{s}{\beta}}L}\right]} \tag{A.23}$$

Now substituting equations (A.22) and (A.23) into (A.18)

251

$$\overline{\varphi}(s,y) = \left[\frac{\rho - \eta}{s\left(e^{-\sqrt{\frac{s}{\beta}}L} - e^{\sqrt{\frac{s}{\beta}}L}\right)} \right] e^{-\sqrt{\frac{s}{\beta}}y} - \left[\frac{\rho - \eta}{s\left(e^{-\sqrt{\frac{s}{\beta}}L} - e^{\sqrt{\frac{s}{\beta}}L}\right)} \right] e^{\sqrt{\frac{s}{\beta}}y} + \frac{\eta}{s} \quad \text{(A.24)}$$

$$\overline{\varphi}(s,y) = \left[\frac{\rho - \eta}{s\left(e^{-\sqrt{\frac{s}{\beta}}L} - e^{\sqrt{\frac{s}{\beta}}L}\right)} \right] \left(e^{-\sqrt{\frac{s}{\beta}}y} - e^{\sqrt{\frac{s}{\beta}}y} \right) + \frac{\eta}{s} \qquad \text{But;} \qquad Sinhx = \frac{e^x - e^{-x}}{2}$$

$$\overline{\varphi}(s,y) = \frac{\rho - \eta}{s} \frac{1}{-2\sinh\left(\sqrt{\frac{s}{\beta}}L\right)} \left(-2\sinh\left(\sqrt{\frac{s}{\beta}}y\right) \right) + \frac{\eta}{s}$$

$$\overline{\varphi}(s,y) = \frac{\rho - \eta}{s} \frac{1}{\sinh\left(\sqrt{\frac{s}{\beta}}L\right)} \left(\sinh\left(\sqrt{\frac{s}{\beta}}y\right) \right) + \frac{\eta}{s} \qquad \text{But}$$

$$\csc hx = (\sinh x)^{-1}$$

$$\overline{\varphi}(s,y) = \frac{\rho - \eta}{s} \csc h\left(\sqrt{\frac{s}{\beta}}L\right) \left(\sinh\left(\sqrt{\frac{s}{\beta}}y\right) \right) + \frac{\eta}{s} \qquad \text{(A.25)}$$

The aim is to determine $\varphi(y,t)$, and not $\overline{\varphi}(s,y)$ therefore, we have to find the inverse Laplace Transform of equation (A.25). Using Oberhettinger and Badii (1973) tables of Laplace Transform (attached).

From equation (A.25), let;

$$a = \frac{L}{\sqrt{\beta}} \qquad\qquad b = \frac{y}{\sqrt{\beta}}$$

(A.26)

$$0 \le y \le L$$

252

$$\bar{\varphi}(s,y) = \frac{\rho - \eta}{s} \sinh(\sqrt{s}b) \operatorname{csc} h(\sqrt{s}a) + \frac{\eta}{s},$$ this conforms to Oberhettinger and Badii's Laplace Inverse Transform equation in page 296, equation 8.62. Thus, the Inverse Laplace Transform of equation (A.25) could be written as

$$\varphi(y|t) = \frac{\rho - \eta}{a} \int_a^{a+b} Q_3\left(\frac{1}{2a}u \middle| \frac{t}{a^2}\right) du \tag{A.27}$$

But, page 422 of Oberhettinger and Badii (1973) tables of Laplace Transforms, Q_3 is given as follows

$$Q_3(y/t) = \sum_{n=0}^{\infty} \varepsilon_n e^{\left(-\pi^2 t n^2\right)} \cos(2\pi n z)$$

$$Q_3\left(\frac{1}{2a}u \middle| \frac{t}{a^2}\right) = \sum_{n=0}^{\infty} \varepsilon_n e^{\left(-\pi^2 t \frac{1}{a^2} n^2\right)} \cos\left(2\pi n \frac{1}{2a}u\right)$$

$$= \sum_{n=0}^{\infty} \varepsilon_n e^{\left(\frac{-\pi^2 n^2 t}{a^2}\right)} \cos\left(\frac{\pi n}{a}u\right) \tag{A.28}$$

$$= 1 + 2 \sum_{n=1}^{\infty} e^{\left(\frac{-\pi^2 n^2 t}{a^2}\right)} \cos\left(\frac{\pi n}{a}u\right)$$

Now from equation (A.27)

$$\varphi(t,y) = \left(\frac{\rho - \eta}{a}\right) \int_a^{a+b} Q_3\left(\frac{1}{2a}u \middle| \frac{t}{a^2}\right) du$$

$$= \left(\frac{\rho - \eta}{a}\right) \int_a^{a+b} \left[\sum_{n=0}^{\infty} \varepsilon_n e^{\left(-\frac{\pi^2 n^2 t}{a^2}\right)} \cos\left(\frac{\pi n}{a}u\right)\right] du$$

$$= \left(\frac{\rho - \eta}{a}\right) \int_a^{a+b} \left[1 + 2 \sum_{n=1}^{\infty} e^{\left(-\frac{\pi^2 n^2 t}{a^2}\right)} \cos\left(\frac{\pi n}{a}u\right)\right] du$$

$$= \left(\frac{\rho - \eta}{a}\right)\int_a^{a+b} du + \frac{\rho - \lambda}{a}\int_a^{a+b} 2\sum_{n=1}^{\infty} e^{\left(-\frac{\pi^2 n^2 t}{a^2}\right)} \cos\left(\frac{\pi n}{a} u\right) du$$

$$= (\rho - \eta)\left(\frac{b}{a}\right) + \frac{\rho - \lambda}{a}\left(\frac{1}{a}\right)2\sum_{n=1}^{\infty} e^{\left(-\frac{\pi^2 n^2 t}{a^2}\right)}\int_a^{a+b} \cos\left(\frac{\pi n}{a} u\right) du$$

$$= (\rho - \eta)\left(\frac{b}{a}\right) + 2(\rho - \lambda)\left(\frac{1}{a}\right)\sum_{n=1}^{\infty} e^{\left(-\frac{\pi^2 n^2 t}{a^2}\right)}\left[\frac{\sin\left(\frac{\pi n}{a} u\right)}{\frac{n\pi}{a}}\right]_a^{a+b}$$

$$= (\rho - \eta)\left(\frac{b}{a}\right) + 2(\rho - \eta)\left(\frac{1}{a}\right)\sum_{n=1}^{\infty} e^{\left(-\frac{\pi^2 n^2 t}{a^2}\right)}\frac{a}{\pi n}\left[\sin\left(\frac{b}{a}\pi n + \pi n\right) - \sin(\pi n)\right]$$

$$= (\rho - \eta)\left(\frac{b}{a}\right) + 2(\rho - \eta)\left(\frac{1}{a}\right)\sum_{n=1}^{\infty} e^{\left(-\frac{\pi^2 n^2 t}{a^2}\right)}\frac{a}{\pi n}\left[(-1)^n \sin\left(\frac{b}{a}\pi n\right) - 0\right]$$

$$\varphi(t, y) = (\rho - \eta)\left(\frac{b}{a}\right) + 2(\rho - \eta)\left(\frac{1}{a}\right)\sum_{n=1}^{\infty}(-1)^n e^{\left(-\frac{\pi^2 n^2 t}{a^2}\right)}\frac{a}{\pi n}\sin\left(\frac{b}{a}\pi n\right) \qquad \text{(A.29)}$$

NOTE:

$$\sin\left(\frac{b}{a}\pi n + \pi n\right)$$

$$n = 0 \Rightarrow \qquad \sin\left(\frac{b}{a}\pi.0\right) = 0$$

$$n = 1 \Rightarrow \qquad \sin\left(\frac{b}{a}\pi n + \pi\right) = -\sin\left(\frac{b}{a}ny\right)$$

$$n = 2 \Rightarrow \qquad \sin\left(\frac{b}{a}\pi n + 2\pi\right) = \sin\left(\frac{b}{a}ny\right)$$

$$\downarrow \qquad\qquad \downarrow$$

Therefore: $\quad \sin\left(\dfrac{b}{a}\pi n + \pi n\right) = (-1)^n \sin\left(\dfrac{b}{a}\pi n\right)$

Now recall;

$$a = \dfrac{L}{\sqrt{\beta}} \qquad\qquad b = \dfrac{y}{\sqrt{\beta}}$$

Substituting 'a' and 'b' into equation (A.29)

$$\varphi(t,y) = (\rho - \eta)\left(\dfrac{y}{L}\right) + \left(\dfrac{2(\rho - \eta)}{\pi}\right)\sum_{n=1}^{\infty}\dfrac{(-1)^n}{n}\, e^{\left(-\dfrac{\pi^2 n^2 \beta}{L^2}t\right)} \sin\left(\dfrac{y}{L}\pi n\right) \quad \text{(A.30)}$$

Equation (A.30) is the governing moisture diffusion equation for CaLS treated soil. The equation is solved using Laplace Transform as shown below with initial and boundary conditions. The solution of this equation defines the distribution of soil suction within the CaLS treated soil with time. It is a simple suction behaviour model that is governed by a single constant β.